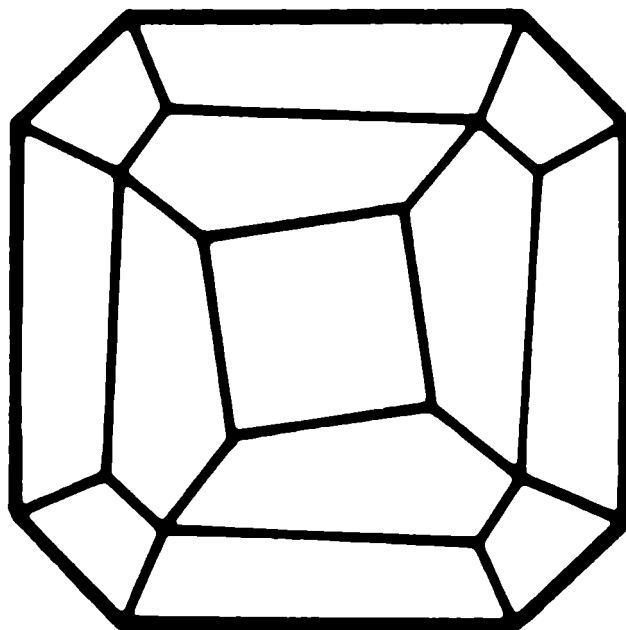


Mitteilungen der Österreichischen Mineralogischen Gesellschaft



Band 159

2013

Herausgegeben von der Österreichischen Mineralogischen Gesellschaft
für das Vereinsjahr 2012
Eigenverlag

Österreichische Mineralogische Gesellschaft

Sekretariat: Naturhistorisches Museum,
Mineralogisch-Petrographische Abteilung, Burgring 7, A-1010 Wien

Sehr geehrtes Mitglied der ÖMG, bitte überweisen sie
ihren Mitgliedsbeitrag auf folgendes Bankkonto:

Österreichische Postsparkasse (BAWAG P.S.K.)
Adresse: Georg-Coch-Platz 2, 1018 Wien
BLZ: 60.000 Kto.: 7.807.220
BIC: OPSKATWW IBAN: AT31 6000 0000 0780 7220
lautend auf: Österreichische Mineralogische Gesellschaft

Mitgliedsbeitrag 2013: 30 € €
Mitgliedsbeitrag für Studenten: 10 € €

Ausstände aus früheren Jahren:

2012 €
2011 €
2010 €

Summe €

Spende 2013 €

**Bitte vergessen sie nicht, ihren Namen bei der
Überweisung anzugeben; wir können sonst die
Einzahlung nicht zuordnen.**

DANKE und Glück Auf!

Mitteilungen der Österreichischen Mineralogischen Gesellschaft

Band 159

2013



Vereinsjahr 2012

Impressum:

Eigentümer, Herausgeber und Verleger: Österreichische Mineralogische Gesellschaft
p.A. Mineralogisch-Petrographische Abteilung, Naturhistorisches Museum Wien

Burgring 7, A-1014 Wien

Homepage: <http://www.univie.ac.at/Mineralogie/Oemg.htm>

ISSN 1609-0144

Redaktion:

Friedrich Koller, Institut für Geologische Wissenschaften, Universität Wien
Geozentrum, Althanstraße 14, A-1090 Wien

Anton Beran, Institut für Mineralogie & Kristallographie, Universität Wien
Geozentrum, Althanstraße 14, A-1090 Wien

Richard Tessadri, Institut für Mineralogie & Petrographie, Universität Innsbruck
Innrain 52, A-6020 Innsbruck

Gestaltung und Layout:

R. Tessadri (Innsbruck)

Für den Inhalt sind die Autoren selbst verantwortlich.

Druck: Anton Riegelnik, Piaristengasse 19, A-1080 Wien

Printed in Austria

**INHALT
CONTENT**

MinPet2013 - Key Note Lectures

Cesare B.. Melt inclusions in migmatites and granulites	S. 15
Krüger H.. Layered structures: Examples of disorder	S. 19
Miletich R.. In very tight places! – structural transformations of minerals under extreme conditions	S. 21
Molnár F. Orogenic gold deposits in Finland	S. 22
Postl W. Über Gesteine und Mineralvorkommen der Koralpe [Public Lecture]	S. 27
Schmahl, W.W., Grießhaber E., Jordan G., Ziegler A., Kelm K. & Maier B.. Mechanical functionalization of minerals by organisms	S. 28

MinPet2013 - Abstracts (Talks and Posters)

Abart R. & Jerabek P. Element partitioning at a propagating reaction front: Experiment and theory	S. 31
Abu-Alam T.S., Hassan M., Stüwe K. & Kadi K.. Multistage tectonism during Gondwana collision: Baladiyah Complex, Saudi Arabia	S. 32
Artac A., Pippinger T., Nestola F., Redhammer G. & Miletich R.. Pressure-induced phase-transformation in LiAlGe ₂ O ₆ and LiCrGe ₂ O ₆ clinopyroxenes	S. 33
Aßbichler D. & Poyer A.. Evidence for bimetasomatism between eclogite and adjacent rocks from the Tauern Window, Austria	S. 34
Azimzadeh A.M., Ghorbani M., Hosseinzadeh G. & Moayyed M.. Mineralogical investigation of sulfide-oxide mineralization in the Misho mafic-ultramafic complex (NW Iran)	S. 35
Baldermann A., Warr I.N., Grathoff G.H. & Dietzel M.. The rate and mechanism of deep sea glauconite formation	S. 36
Bauer C., Rollinger B., Krumpel G., Hoad O., Pascual J., Rogers N. & Krenn K.. ZrO ₂ in refractory products: Characterization methods	S. 37
Bechtold A. & Wildner M.. Crystal chemistry of kieserite-cobaltkieserite solid solutions, Mg _{1-x} Co _x (SO ₄)·H ₂ O	S. 38
Benkó Zs., Molnár F., Mogessie A., Poulson S., Archart G., Severson M., Hauck S. & Raič S.. Sulphur isotope variation of sulfide ores in function of footwall-magma contamination within the Bathtub intrusion, Duluth Complex, USA	S. 39
Berninger U.-N., Jordan G., Schott J. & Oelkers E.H.. Assessing dolomite reactivity by hydrothermal atomic force microscopy	S. 40
Beukes J.J. & Gauert C.D.K.. Investigation of hangingwall norites of the Merensky Reef Unit at Two Rivers Platinum Mine, Eastern Bushveld	S. 41

Blümel A., Ntaflos T., Ashchepkov I., Prikhodko V.S. & Gregoire M.. Low temperature earth mantle xenoliths from Sikhote-Alin. Far East Russia	S. 42
Böttcher M.E.. Barium, manganese, iron and sulfur authigenesis in modern euxinic basins: The state of the art	S. 43
Bojar II.-P., Bojar A.-V., Ilalas S. & Wojtowicz A.. K-Ar geochronology of igneous amphibole macrocrystals of Miocene to Pliocene volcaniclastics. Styrian Basin, Austria	S. 44
Bourgin N., Petrakakis K. & Abart R.. Symplectites in high pressure granulites from the Gföhl Unit (Dunkelsteinerwald, NÖ)	S. 45
Brandl M., Haubzenberger C., Postl W. & Trnka G.. New Approaches for chert source provenance studies	S. 46
Brandstätter F., Konzett J., Koeberl C., Ferrière L. & Mader D.. The Ischgl Meteorite: Finding circumstances, mineralogy and bulk chemistry	S. 47
Čopjaková R., Škoda R. & Vašinová Galiová M.. Scandium and REE-rich tourmaline from the Kracovice pegmatite (Bohemian Massif) and its breakdown to allanite	S. 48
Doppler G., Bakker R. & Baumgartner M.. The effect of the α - β -quartz transition boundary in re-equilibration experiments	S. 49
Đorđević T.. Mineral-like arsenates: crystal structure of $\text{Sr}_2\text{Mg}(\text{AsO}_4)_2 \cdot 2\text{H}_2\text{O}$ with kröhnkite-type chains	S. 50
Eberlei T., Habler G., Thöni M. & Schuster R.. New Rb-Sr data from Permian meta-pegmatites in the Austroalpine Matsch Unit	S. 51
Effenberger H., Miletich R. & Libowitzky E.. On the true space-group symmetry of Norsethite, $\text{BaMg}(\text{CO}_3)_2$	S. 52
Ertl A., Vereshchagin O.S., Giester G., Meyer H.-P., Ludwig T., Rozhdestvenskaya I.V. & Frank-Kamenetskaya O.V.. Structural and chemical investigation of a zoned synthetic Cu-rich tourmaline	S. 53
Frei D.. U-Pb microgeochronology by laser ablation ICP-MS: Applications, limitations and future developments	S. 54
Gasteiger P., Tropper P., Haefeker U. & Tessadri R.. Petrographie und Mineralchemie von Betafit aus dem Pollestal (Ötztal-Stubai Kristallin)	S. 55
Girtler D., Tropper P. & Hauzenberger C.. Androsite-(Ce) and ferriandrosite-(Ce) as indicator for low-grade REE mobility in the Veitsch Mn deposit (Styria)	S. 56
Grengg C., Mittermayr F., Baldermann A., Böttcher M.E., Leis A. & Dietzel M.. Bacteriogenically induced sulfuric acid attack on concrete in an Austrian sewer system	S. 57
Grom N., Rečnik A., Samardžija Z., Vrhovnik P., Daneu N. & Dolenc T.. Zonation and Bi-rich inclusions in andradite crystals from Kope skarn deposit, Slovenia	S. 58
Haefeker U., Kaindl R. & Tropper P.. The effect of Class 1 H_2O on a Raman active T_2 stretching mode in Mg-Cordierite	S. 59
Haefeker U., Kaindl R., Tropper P. & Konzett J.. Raman spectroscopy of N_2 in natural cordierite and beryl single crystals	S. 60
Haefeker U., Kaindl R., Tropper P., Krüger H., Kahlenberg V. & Orlova M.. Structural and Raman-spectroscopic investigations of synthetic hexagonal and orthorhombic Fe-cordierite	S. 61
Haslinger E., Williams C.T., Fröschl H., Koller F., Gier S. & Ottner F.. Mineralogy and geochemistry of soils of the Alnö Carbonatite Complex, Sweden	S. 62
Hauzenberger C.A., Konzett J., Khoi N.N., Hoang N. & Auzinger T.. Petrology of mantle xenoliths from central and south Vietnam	S. 63

Heinisch M., Micheuz P., Krenn K., Hoinkes G. & Tropper P. Garnet zoning and garnet isopleths geothermobarometry at the transition between the Ötztal-Bundschuh nappe system and the Koralpe-Wölz high-pressure nappe system west of the Tauern Window	S. 64
Hejny C. & Konzett J.. Cr-incorporation into kyanite: A high pressure experimental and crystallographic study	S. 65
Höller D., Klammer D., Letofsky-Papst I. & Dietzel M.. Tailoring of a Hierarchically Structured Material from diatomite	S. 66
Höller D., Schubernig M., Aldrian A., Czyzykiewicz P., Sarc R., Pomberger R. & Raith J.G.. Mineralogy and leachability of iron and steel work slags	S. 67
Houzar S., Irazdil V. & Toman J.. Dravite-schorl evolution in tourmalinite from Oparno crystalline complex. Saxothuringicum	S. 68
Janisch A., Mundl A. & Ntaflos T. Mantle xenoliths from Bondoró volcanic complex	S. 69
Kaindl R., Pichler J., Fischer R., Jakopic G. & Waldhauser W. Graphene- and graphite-like thin films from amorphous carbon coatings	S. 70
Kis A., Váczí T., Weiszburg T.G. & Buda Gy. Textural position and structural state of zoned zircons from Mórággy, Hungary and Rastenberg, Austria	S. 71
Klemd R., Meyer M., Hegner E. & Konopelko D.. Eclogite-facies mafic oceanic and continental crustal rocks from the Aktyuz and Makbal complexes, Tianshan Mountains (Kazakhstan & Kyrgyzstan): Geodynamic implications	S. 72
Klötzli U. & Kovaleva E.. Plastic deformation of zircon: A high-T deformation dating tool?	S. 73
Kolitsch U. & Giester G.. The crystal structure of a new secondary zinc mineral from Lavrion, Greece: $Zn_9(SO_4)_2(OH)_{12}Cl_2 \cdot 6H_2O$	S. 74
Kolitsch U., Ciriotti M.E. & Blaß G.. Preliminary data on a new natural Ca-Ce ⁴⁺ -arsenate and its crystal structure	S. 75
Kolosova-Satlberger O., Ntaflos T. & Bjerg E.. Metasomatism in the lithospheric mantle beneath southern Patagonia, Argentina	S. 76
Konrad F., Stalder R. & Tessadri R.. Quantitative phase analysis of lateritic bauxite with NIR-spectroscopy	S. 77
Konrad L., Hauzenberger C.A. & Konzett J.. Evidence for mantle metasomatism in selected samples from the Styrian basin	S. 78
Konzett J., Schneider T., Melcher F., Hauzenberger C., Mundl R. & Fügenschuh B.. Magmatic staurolite in a pegmatite from the Texel Complex, Southern Tyrol - Evidence for anatetic formation of beryl-coltan pegmatites in the Austroalpine basement of the Eastern Alps	S. 79
Kovaleva E. & Klötzli U.. Zircon plastic deformation examples from the Tauern Window	S. 80
Kozlik M. & Raith J.. Geochemical aspects of the mineralised early carboniferous K1-K3 orthogneiss in the Felbertal scheelite deposit (Austria)	S. 81
Krismer M. & Tropper P. Fe-Ni-Co-Pb-Zn bearing copper ores in the Mauken Area (Radfeld-Brixlegg, North Tyrol, Austria): Implications for the provenance of Bronze Age „Fahlore-Copper“ metal artefacts in the Eastern Alps	S. 82
Krismer M. & Tropper P. Copper ore survey in South Tyrol: Possible ore sources for the Late Bronze Age (Laugen Culture) smelting site Fennhals/Kurtatsch (South Tyrol, Italy)	S. 83
Krüger H., Tropper P., Haefeker U., Kahlenberg V., Többens D., Fuchs M.R., Olieric V. & Troitzsch U.. Single-crystal structure and Raman spectroscopy of synthetic CaAlSiO ₄ F	S. 84
Krüger H., Tropper P., Haefeker U., Tribus M., Kahlenberg V., Wikete C., Fuchs M.R. & Olieric V. Mn ₃₃ (Si ₂ O ₅) ₁₄ (OH) ₃₈ : A new manganese phyllosilicate mineral from the Tyrol	S. 85

Kuleci H., Abart R. & Schmidt C.: The hydration of periclase to brucite: An experimental study	S. 86
Leitner T., Raith J.G. & Paar W.H.: Gold in the historic copper deposits at Flatschach, Styria	S. 87
Lenz C. & Nasdala L.: Potential estimation of radiaton-induced structural disorder with RFL ³⁺ -luminescence spectroscopy	S. 88
Maier M., Kahnenberg V. & Thome V.: Mineralogical investigations on melting products from incinerator bottom ashes	S. 89
Mair P., Hauzenberger C.A. & Konzett J.: Metasomatic titanites associated with Cl-rich amphibole and phlogopite in multiply metasomized peridotites from Letseng-la-Teræ, Lesotho	S. 90
Mandi M., Hauzenberger C.A., Konzett J., Jumanne R., Gobba J. & Nguyen H.: Characterization of the subcontinental lithospheric mantle beneath the Tanzania craton based on garnet xenocrysts	S. 91
Manninger T. & Kahnenberg V.: Synthesis and crystal structures of new alkali-REE-fluorosilicates	S. 92
Michálek M., Putíš M. & Hauzenberger C.A.: Petrology of eclogites and associated gneisses of the Polinik structural complex (Kreuzegg Mountains, Eastern Alps)	S. 93
Micheuz P., Krenn K., Fritz H. & Kurz W.: Fluid inclusions from blueschist-facies boudin structures within the phyllite-quartzite unit of the external Hellenides, Greece	S. 94
Mirwald P.W.: Decomposition of clathrate hydrates as indicator of anomalous PVT-behaviour of water	S. 95
Mirwald P.W., Miletich R. & Loerting T.: Anomalous compression behaviour of cordierite	S. 96
Mittermayr F., Baldermann A., Klammer D., Leis A. & Dietzel M.: Concrete deterioration-reaction mechanisms revealed by a multiproxy approach	S. 97
Müller T., Dohmen R. & Chakraborty S.: Experimental determination of Fe-Mg interdiffusion rates in clinopyroxene and implications for geothermometry involving ferromagnesian minerals	S. 98
Mundl A., Ntallos T., Bjerg E.A., Hauzenberger C.A. & Ackerman I.: Lithospheric mantle heterogeneities beneath southern Patagonia	S. 99
Nantasin P., Hauzenberger C., Richoz S., Abu-Alam T.S. & Wathanakul P.: Contact aureole of the Sri Sawat granite, Kanchanaburi province, western Thailand	S. 100
Nasdala L., Kostrovitsky S., Kennedy A.K. & Zeug M.: Retention of radiation damage in zircon xenocrysts from kimberlites, northern Yakutia	S. 101
Nickel C. & Warr L.N.: Experimental alteration studies at the bentonite-cement interface	S. 102
Novák M., Kadlec T. & Gadas P.: Tourmaline (schorl-dravite) from granitic pegmatites in Vlastějovice, Czech Republic: An indicator of fractionation and in-situ contamination	S. 103
Ntaflos T., Aschchepkov I., Koutsovitis P., Hauzenberger C. & Asseva A.: Delaminated lithospheric mantle from far east Russia affected by exotic metasomatism	S. 104
Oberwandler L., Pristacz H., Kolitsch U. & Lengauer C.L.: Structural characterization of lannomite from Anna Mine, Alsdorf, Germany	S. 105
Österle J., Palzer M. & Klötzli U.: New constraints on the timing of the Mae-Ping core-complex (NW-Thailand)	S. 106
Onuk P. & Dietzel M.: Formation of helectite in the cave Dragon Belly (Sardinia, Italy)	S. 107
Onuk P., Mogessie A., Bjerg E. & Krenn K.: Mineralization of the mafic-ultramafic rocks of the Las Aguilas-Las Higueras areas, San Luis Province, Argentina	S. 108

Ormándi S. & Dódony I.: Synthesis and structural examinations on LTA-type zeolite	S. 109
Palzer M., Österle J. & Klötzli U.: New constraints on the Mae Ping core-complex, NW-Thailand: Is it an Indosian relict?	S. 110
Papadopoulou M., Ntaflos T., Bjerg E. & Gregoire M.: Petrological and geochemical studies of mantle xenoliths from Rio Negro Province, Argentina	S. 111
Pertlik F. & Zirbs W.: Kristallographische Kuriositäten	S. 112
Petrichcheva E., Abart R. & Schaeffer A.-K.: Anisotropic diffusion in alkali feldspar: Reconstruction of the composition-dependent diffusion coefficients	S. 113
Pfingstl S., Hauzenberger C., Kurz W. & Schuster R.: Evolution of the Seckau crystalline basement (Seckau Mountains, Eastern Alps): Implications for pre-alpine magmatism and alpine metamorphism	S. 114
Praschl S., Leis A., Benischke R., Schramm M., Böttcher M.E., Daxner G. & Dietzel M.: Mineralogical, geochemical and isotopic characterisation of evaporites from the „Hallstätter Salzberg“	S. 115
Pristacz H., Giester G., Rieck B. & Lengauer C.L.: Thermal behaviour of the new mineral cairncrossite, $\text{Sr}_2\text{Ca}_7(\text{Si}_4\text{O}_{10})(\text{OH})_2 \cdot 15\text{H}_2\text{O}$	S. 116
Prokop J., Losos Z., Karásek J. & Čopjaková R.: Mineralogy and genesis of pegmatite-like veins in serpentinite eluvium at Nová Ves near Oslavany (Czech Republic)	S. 117
Pühr B., Hoinkes G., Schuster R. & Proyer A.: Metamorphic evolution of the Koralpe-Wölz high P/T-nappe pile east of the Tauern Window (Eastern Alps): Record from siliceous dolomitic marbles and scapolite-bearing calcsilicate rocks	S. 118
Purgstaller B., Niedermayr A. & Dietzel M.: Carbonate formation at alkaline conditions	S. 119
Raič S., Mogessie A., Benkó Z., Molnár F., Hauck S. & Severson M.: Arsenic-enriched Cu-Ni-PGE mineralization in Wetlegs, Duluth Complex, Minnesota, USA	S. 120
Rauschenbach J., Köhler S.J., McCleaf P., Höllen D. & Dietzel M.: Calcium carbonate formation in fluidized bed pellet reactors to reduce Ca, U, and DOC in drinking water (Uppsala, Sweden)	S. 121
Redhammer G.J. & Tippelt G.: The $C2/c$ - $P2_1/c$ phase transition within the synthetic clinopyroxene-series $\text{NaFeGe}_2\text{O}_6$ - $\text{LiFeGe}_2\text{O}_6$	S. 122
Redhammer G.J., Senyshyn A., Roth G. & Tippelt G.: Crystal and magmatic spin structure of germanium-hedenbergite, $\text{CaFeGe}_2\text{O}_6$	S. 123
Rinder T. & Dietzel M.: Mixing of aqueous solutions – impact on dissolution and precipitation of calcium carbonate	S. 124
Schaeffer A.-K., Petrichcheva E., Habler G., Abart R., Rhede D. & Zaefllerer S.: Na-K interdiffusion in alkali feldspar – composition dependence, anisotropy and chemically induced stress	S. 125
Schön W., Dietzel M. & Leis A.: Chemical and isotopic composition of soil solutions from Cambisols (Austria) – Field study and experiments	S. 126
Schuster R., Abart R. & Schafler E.: Torsional deformation of calcite	S. 127
Škoda R., Čopjaková R. & Novák M.: Influence of non-analyzed light elements on results of electron microprobe	S. 128
Stalder R. & Neuser R.D.: OH-defects in detrital quartz grains	S. 129
Stickler C.P., Deditius A.P., Baldermann A., Leis A. & Dietzel M.: Geochemistry and structure of dolomite and calcite at Oker (Germany)	S. 130

Švecová E., Čopjaková R., Losos Z. & Cicha J.. Chemistry of xenotime-(Y) from beryl-columbite pegmatites of the Pisek Region (Czech Republic)	S. 131
Talla D., Wildner M., Beran A., Škoda R. & Losos Z.. On the presence of hydrous defects in differently coloured wulfenites ($PbMoO_4$): An infrared and optical spectroscopic study	S. 132
Taferner II., Ilauzenberger C.A. & Konzett J.. Mineral chemistry and petrology of chromium-bearing kyanites in eclogites from the Pohorje Mountains, Slovenia	S. 133
Tessadri R., Kahlenberg V., Schmidmair D. & Haefeker U.. $Ca_2Mg(NO_3)_6 \cdot 12H_2O$ – first results on a new compound retrieved from chimney deposits of a combined heat and power plant	S. 134
Thaller D., Mittermayr F., Baldermann A., Fischer R., Leis A. & Dietzel M.. Concrete deterioration – formation conditions traced by crystal water of sulfate minerals	S. 135
Tribus M., Pomella II., Tropper P. & Linner M.. Compositional variation of Ba-rich white micas from two different geological settings	S. 136
Tropper P.. Thermodynamic modelling of in-situ eclogitization of metapelites from Val Savenca (Sesia Zone, Western Alps)	S. 137
Tropper P.. Der Zusammenbruch von Stauolith und Kyanit im westlichen Austroalpin als Monitor für den Grad der eo-alpinen Metamorphose	S. 138
Tropper P. & Hauenberger C.. How do experiments and calculations compare? Experiments versus pseudosections: A test from high- <i>P</i> high- <i>T</i> granulites and the role of Ti and F in biotite	S. 139
Tropper P. & Spielmann M.. Experimentelle Untersuchungen zur Knochen-Gesteinswechselwirkung in Brandopferplätzen	S. 140
Tropper P., Haefeker U. & Wyhlidal S.. Raman-spectroscopy of cordierites from Na-in-cordierite experiments: Chemical vs. structural equilibrium	S. 141
Tropper P., Haefeker U., Schneider P., Braunhofer D. & Pupp M.. Hot hotter hottest: Extreme cases of anthropogenic pyrometamorphism	S. 142
Tropper P., Pupp M. & Tessadri R.. Der Zusammenbruch von Zirkon in Trinititen	S. 143
Tropper P., Trauner S. & Töchterle U.. Petrographische Untersuchungen prähistorischer (End-Neolithikum-Spätbronzezeit) Keramik vom Kiechlberg	S. 144
Tropper P., Volgger A., Pasker J. & Fickert L.. Mineralogie und Petrologie experimentell erzeugter Pseudofulgurite	S. 145
Vrhovnik P., Rogan Šmuc N., Dolenc T., Serafimovski T., Tasev G. & Dolenc M.. Content of chalcophile elements in Lake Kalimanci surface sediments (Republic of Macedonia)	S. 146
Walter F. & Bojar H.-P.. Joanneumite, $Cu(C_3N_3O_3H_2)_2(NH_3)_2$, a new mineral species with ammine and isocyanurate groups	S. 147
Wittwer A., Nasdala L., Wildner M., Wanthanachaisaeng B., Bunnang N. & Giester G.. Colour enhancement of Ratanakiri (Cambodia) gem zircon	S. 148
Wyhlidal S. & Tropper P.. Experimental constraints on the Permian contact metamorphic event in metapelites from the southern rim of the Brixen granodiorite (South Tyrol, Italy)	S. 149
Zöll K., Tropper P. & Haefeker U.. REE-Karbonate in der dioritischen Intrusionsbrekzie bei Schrammbach (Südtirol/Italien): Indikator für tieftemperierte REE Mobilisation	S. 150
Alphabetical listing of contributors	S. 151
Sponsors of MinPet 2013	S. 158

Originalarbeiten - Original Contributions

- Dutzler D. & Tropper P.: Anwendung des Zr-in-Rutil Geothermometers in Pyropquarziten
des UHP Dora Maira Massives (Piemont, Italien) S. 161
- Pertlik F.: Johann Fibig (*~1720 †1792) Edition seiner mineralogisch orientierten Druckschrift
„Studium der Naturgeschichte“ und Kommentare zu seinem „Handbuch der Mineralogie“ S. 171
- Tribus M. & Tropper P.: Der Einfluss des Titanit-Aktivitätsmodells auf die Lage von Titanit-
involvierenden Mineralreaktionen aus den Metabasiten des Spronsertales (Südtirol, Italien) S. 187

Diplom/Masterarbeiten und Dissertationen von österreichischen Universitäten

Diploma/Master/Phd Thesis of Austrian Universities S. 199

Vereinsnachrichten - Society News

- Tätigkeitsbericht über das Vereinsjahr 2012 S. 201

Autorenhinweise - Guidelines for Authors

S. 213

Anzeigen - Adverdisments

S. 214

Anzeigen von Sponsoren - Advertisments of Sponsors (Band 159 / Volume 159)

BRUKER Austria GmbH (Wien)

<http://www.brukter.com>

Gebr. LEUBE KG (St. Leonhard)

<http://www.lcube.at>

JEOL (Germany) GmbH (Eching bei München)

<http://www.jeol.de>

OLYMPUS Austria GmbH (Wien)

<http://www.olympus.at>

PANALYTICAL B.V. - Branch Austria (Wien)

<http://www.panalytical.com>

RHI AG (Leoben)

<http://www.rhi-ag.at>

STOE & CIE GmbH (Darmstadt)

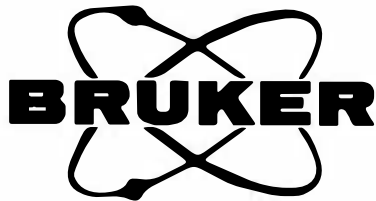
<http://www.stoe.com>

D. SWAROVSKI KG (Wattens)

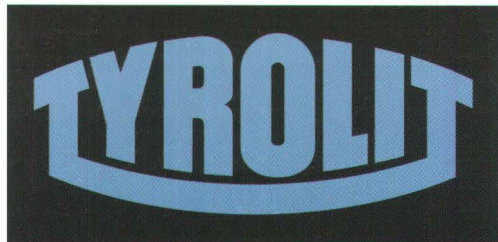
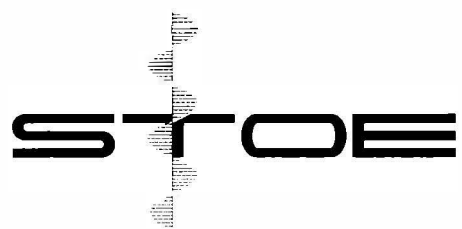
<http://www.swarovski.com> + <http://www.swarovski-gems.at>

TYROLIT - Schleifmittelwerke Swarovski K.G. (Schwaz)

<http://www.tyrolit.at>



JEOL



RHI

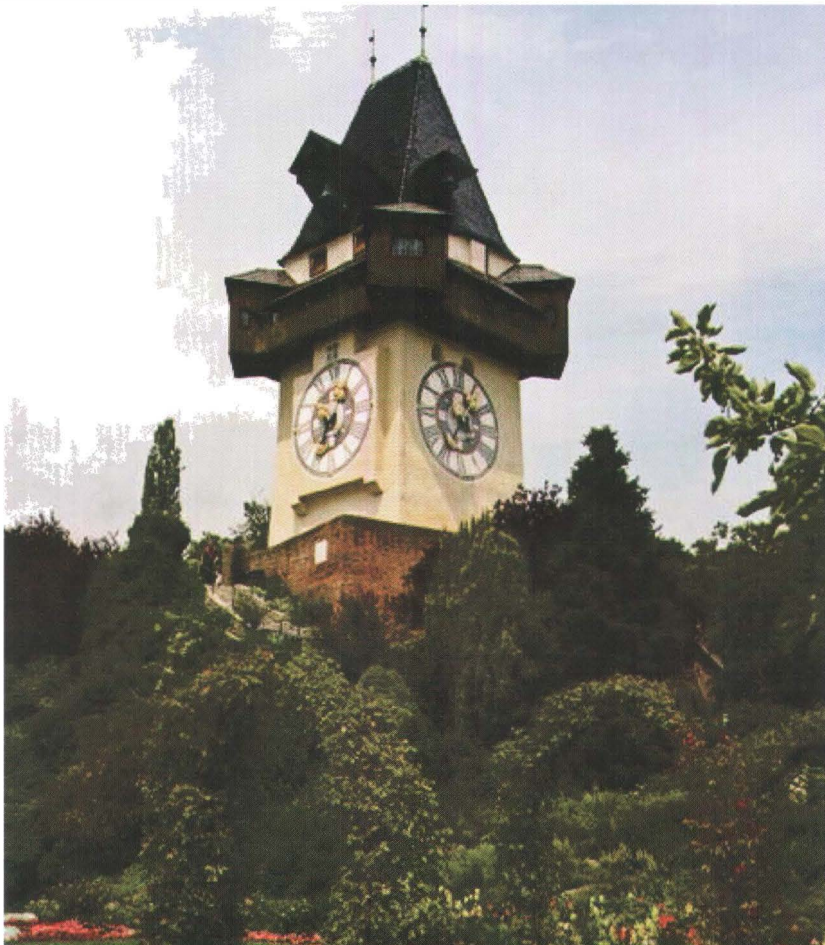
OLYMPUS

SWAROVSKI GEMS™

MINPET 2013

GRAZ / AUSTRIA
SEPTEMBER, 19th - 23th

PREFACE AND KEY NOTE LECTURES



MELT INCLUSIONS IN MIGMATITES AND GRANULITES

by

Bernardo Cesare

Dipartimento di Geoscienze, Università di Padova
Via Gradenigo 6, 35131 Padova, Italy
e-mail: bernardo.cesare@unipd.it

The study of melt inclusions is a recent, small-scale approach to a better understanding of melting in the continental crust. It builds on the discovery of glassy inclusions (CESARE et al., 1997) and their crystallized counterparts (“*nanogranites*”, CESARE et al., 2009) in garnet and other host minerals from anatetic crustal enclaves in lavas and from regional migmatites.

By producing a melt of broadly granitic composition and a silica-poor solid residue, crustal anatexis is of paramount importance in shaping the continental lithosphere: on one hand it determines the geochemical differentiation of the crust; on the other it allows easier and faster deformation of the crust, with important tectonic and geodynamic implications. Among the several aspects of crustal melting that are still poorly known to scientists, one is the composition of the *natural* melts produced during anatexis, as both leucosomes in migmatites and allochthonous crustal granites aren’t representative of primary melts.

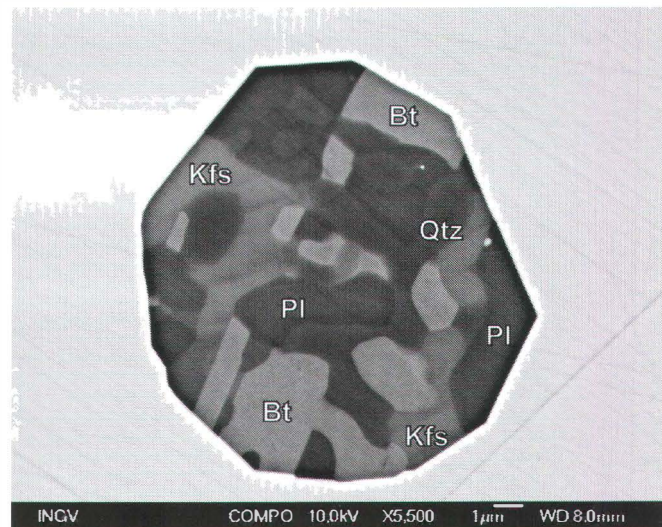
Such gap of knowledge has led to a new approach to characterize the composition of natural crustal melts: the study of melt inclusions. Building on the extensive work and literature on fluid and melt inclusions in mafic rocks, we realised that tiny droplets of the melt phase produced during crustal anatexis can be trapped by, and preserved within, those minerals that grow simultaneously with the melt, i.e. the *peritectic* phases produced during incongruent melting. For example, a garnet crystal that forms during the incongruent melting of biotite has the potential of trapping *primary* inclusions of the melt that is in contact with. Albeit straightforward, this perspective has found little application to migmatites and granulites in the past, until our first works in the crustal enclaves and xenoliths from El Hoyazo, SE Spain (CESARE et al., 1997). In these fragments of crustal rocks entrained in lavas that rapidly ascended, extruded and cooled on the Earth surface, the inclusions of anatetic melt could solidify to, and be preserved as, rhyolitic glass. The mineralogical and chemical composition of these rocks is comparable to that of residual melanosomes in migmatites, but here abundant glass is present, particularly as melt inclusions in all the minerals.

Glass inclusions were studied in particular in garnet and plagioclase (ACOSTA-VIGIL et al., 2007, 2010, 2012). They range in size between 5 and 50 µm, have a primary texture, contain fresh and undevitrified glass, and show very little evidence of melt crystallization upon cooling.

The peraluminous leucogranitic and close-to-eutectic compositions of glasses support the conclusion that they represent natural anatexic melts. Zircon and monazite saturation temperatures of 665–750°C suggest that melts were produced by muscovite breakdown melting early in a process of rapid anatexis, and mostly under H₂O-undersaturated conditions. The analysis of trace elements in the glass inclusions also allowed the first precise evaluation of the extent of chemical equilibrium between felsic melt and crystalline residuum during the anatexis of metasediments in a natural context.

Crustal enclaves such as at El Hoyazo are extremely unusual and rare. Nonetheless, they boosted an important development of melt inclusion studies by raising the question: “*Why shouldn't inclusions formed by the same process occur also in “normal” migmatites and granulites?*”

We (re)examined migmatite and granulite localities worldwide looking for garnet-producing incongruent reactions, until the first occurrence of melt inclusions was found in the slowly cooled granulites of the Kerala Khondalite Belt (KKB), India (CESARE et al., 2009). There, the inclusions are hosted within garnet: those in the range of 15–25 µm are fully crystallized to a cryptocrystalline aggregate of quartz, alkali feldspar, biotite and plagioclase (Fig. 1), locally showing micrographic intergrowths of quartz and feldspars. Inclusions generally have a negative crystal shape, and grain-size of crystals ranges from hundreds of nm to a few µm. Given the microstructural and chemical features, the cryptocrystalline aggregate found within these inclusions was named “nanogranite”



Another exceptional and intriguing discovery was that, despite the very slow cooling rate of the host rock, some inclusions <15 µm are still completely glassy. This has been explained by inhibition of nucleation in the inclusions with the smallest volumes, by analogy with the behavior of aqueous solutions in sediments or of glass in films and pores of contact meta-morphic rocks. Since the first finding, nanogranite and glassy inclusions have been identified also in regional metamorphic migmatites from other geological settings of various P-T conditions, such as the Ivrea Zone and the Ulten Zone (Italy), Ronda (Spain), the Barun Gneiss (Nepal), the Kaligandaki valley (Tibet), and south-central Massachusetts (U.S.A.).

Inclusions are hosted in garnet at all these localities, and also in ilmenite at Ronda. Their peculiar microstructural features (FERRERO et al., 2012) make nanogranites one of the most reliable indicators for the former presence of melt in a rock. Moreover, their appropriate characterization and analysis can provide the missing information on the composition of natural anatetic melts before these undergo modification processes. But while glassy inclusions can be directly analysed with minimal sample preparation, nanogranites need to be remelted to a homogeneous liquid and then quenched: to prevent the decrepitation of inclusions and loss of volatiles, remelting is achieved in a piston cylinder apparatus (BARTOLI et al., 2013a).

EMP, Raman and nanoSIMS analysis of major elements and H_2O contents of remelted nanogranites shows that despite being all leucogranitic, compositions of natural anatetic melts generally plot away from those of minimum melts, and display systematic differences among samples, particularly concerning Qtz-Ab-Or relationships (Fig. 2).

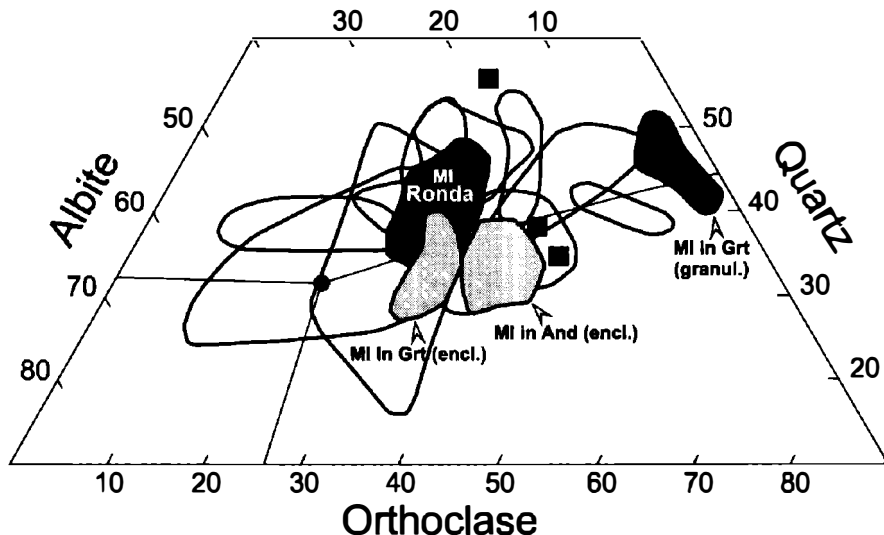


Figure 2:
Composition of remelted nanogranites (dark grey fields), of melt inclusions (MI) in garnet (Grt) and andalusite (And) from Spanish enclaves (encl.; light grey fields), and of experimental melts produced from metasedimentary starting materials (white fields), plotted in the CIPW Q-Ab-Or diagram. Gray squares are leucosomes in the migmatite from Ronda. Black dot and lines show the eutectic point and cotectic lines for the subaluminous haplogranite system at 5 kbar and $a_{H_2O} = 1$.

Redrawn after BARTOLI et al. (2013b), where details of the sources of data of experimental melts can be found.

The analysis of H_2O in the rehomogenized inclusions demonstrates that nanogranites preserve the primary fluid contents and that melts produced at Ronda were mainly H_2O -undersaturated even at low degree of melting (BARTOLI et al., 2013b). Since H_2O is one of the main parameters determining melt viscosities and, in turn, the strength of partially melted rocks, our characterization of the fluid contents of nanogranites is key for obtaining more realistic constraints to the rheological behaviour of the deep crust, and to the timescales of melt extraction from it.

Melt inclusions should be targeted in the most chemically inert and mechanically strong mineral hosts (e.g., spinel, ilmenite, zircon) from the least deformed rock domains. A major problem associated with this research is analytical and relates to the small size of the objects of study, enhancing the possibility of contamination by the host phase and loss of alkalis (in particular Na) due to the use of focused beams during analysis. Another problem is methodological and resides in the necessity of determining, case by case, the extent to which inclusions preserve their primary features, including the degree of chemical interaction with the host and the degree of crystallization upon cooling.

Because the composition of anatetic melts can now be analysed rather than assumed, we foresee that our investigation will stimulate further research on melt inclusions in migmatites and granulites. With extension to melting of mafic protoliths and to HP to UHP conditions of anatexis, our approach promises important impacts on a wide spectrum of disciplines including petrology, geochemistry, mineralogy, volcanology and geodynamics. As many occurrences of melt inclusions have been overlooked because they simply were not searched for, they will be uncovered by careful re-investigation of migmatite and granulite samples worldwide. In addition, the small size of inclusions (often <10 µm) and crystals within nanogranite (often <1 µm) offers new challenges and applications for cutting-edge micro-analytical techniques such as field emission gun-based SEM and EMP, LA-ICP-MS, nanoSIMS, synchrotron-based micro-XRF and micro-XRD. The fast technological development is likely to eliminate all analytical obstacles in a few years.

- ACOSTA-VIGIL, A., CESARE, B., LONDON, D., MORGAN VI, G.B. (2007): *Chem. Geology*, 237, 450-465.
- ACOSTA-VIGIL, A., BUICK, I., HERMANN, J., CESARE, B., RUBATTO, D., LONDON, D., MORGAN VI, G.B. (2010): *Journal of Petrology*, 51, 785-821.
- ACOSTA-VIGIL, A., BUICK, I., CESARE, B., LONDON, D., MORGAN VI, G.B. (2012): *Journal of Petrology*, 53, 1319-1356.
- BARTOLI, O., CESARE, B., POLI, S., ACOSTA-VIGIL, A., ESPOSITO, R., TURINA, A., BODNAR, R.J., ANGEL, R.J., HUNTER, J. (2013a): Nanogranite inclusions in migmatitic garnet: behavior during piston-cylinder remelting experiments. *Geofluids* (in press)
- BARTOLI, O., CESARE, B., POLI, S., BODNAR, R.J., ACOSTA-VIGIL, A., FREZZOTTI, M.L., MELI, S. (2013b): *Geology*, 41:115-118.
- CESARE, B., SALVIOLI MARIANI, E., VENTURELLI, G. (1997): *Mineralogical Magazine*, 61, 15-27.
- CESARE, B., FERRERO, S., SALVIOLI-MARIANI, E., PEDRON, D., CAVALLO, A., (2009): *Geology*, 37, 627-630.
- FERRERO, S., BARTOLI, O., CESARE, B., SALVIOLI-MARIANI, E., ACOSTA-VIGIL, A., CAVALLO, A., GROOPPO, C., BATTISTON, S. (2012): *Journal of Metamorphic Geology*, 30, 303-322.
- HOLNESS, M.B., CESARE, B., SAWYER, E.W. (2011): *Elements*, 7, 245-250.

LAYERED STRUCTURES: EXAMPLE OF DISORDER

by

Hannes Krüger

Institute of Mineralogy and Petrography
University of Innsbruck, Innrain 52, 6020 Innsbruck, Austria
e-mail: hannes.krueger@uibk.ac.at

Three examples of layered structures from the authors recent work will be presented. All structures show disorder due to stacking fault mechanisms.

The first example, is the *layered brownmillerite* $\text{Ca}_4\text{Fe}_2\text{Mn}_{0.5}\text{Ti}_{0.5}\text{O}_9$. This material shows strong one-dimensional diffuse scattering (Fig. 1). A simulation study revealed the stacking fault mechanism and using high-resolution transmission electron microscopy the faults could be imaged (KRÜGER et al., 2011).

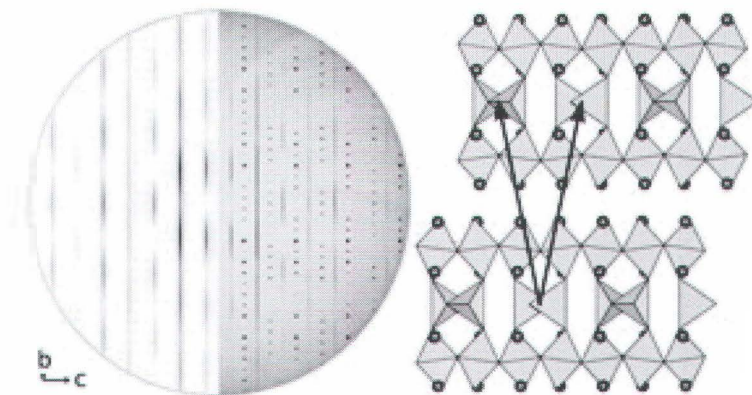


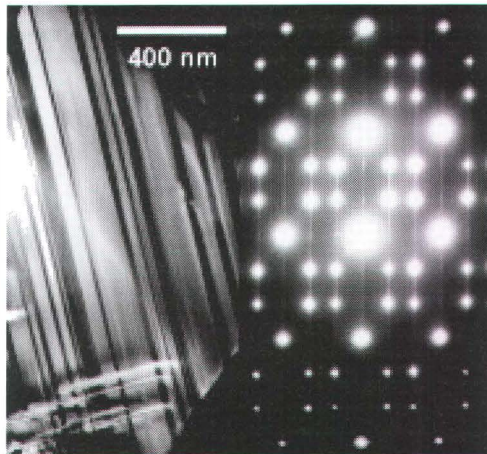
Figure 1:

Left side: a combination of calculated (left, Bragg scattering neglected) and observed (right) diffraction patterns ($3kl$) is shown. The right side shows two brownmillerite layers with alternative stacking vectors.

Potassium aluminate $\text{KAl}_9\text{O}_{14}$ exhibits a mullite-type structure. In single crystals grown from a vapour phase, we found a monoclinic superstructure which causes a complex nano- and micro-structure due to multiple twinning and stacking faults (Fig. 2, LAZIĆ et al., 2013).

Figure 2:

TEM of monoclinic KAl_9O_{14} : electron micrograph (left) showing the nano-sized twin domains, and electron diffraction pattern [010] (right) with superstructure reflections and diffuse scattering.



The third example highlights an interesting case of stacking faults in an ordered aluminosilicate framework structure: the monoclinic kalsilite phase $KAlSiO_4$ -O1 (KREMENOVIC et al., 2013). Our recent results revealed that the stacking faults are related to non-stoichiometry with silicon excess and potassium vacancies according to $K_{1-x}Al_{1-x}Si_{1+x}$. The proposed stacking faults do not break the framework, however, its topology is modified at the fault planes. Pseudo-hexagonal twinning causes a complex diffuse scattering pattern (Fig. 3).

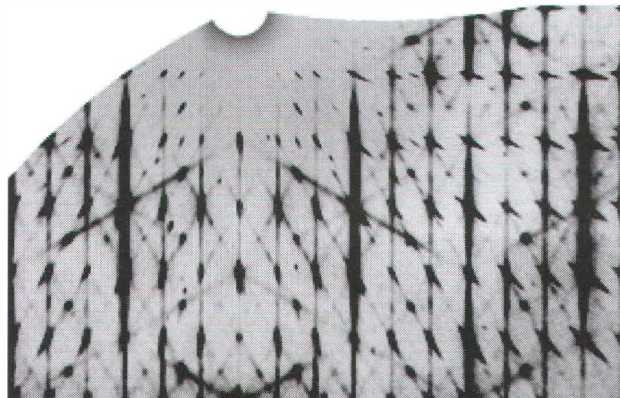


Figure 3:

Reciprocal space section $h00$ of non-stoichiometric $KAlSiO_4$ -O1. Strong one-dimensional diffuse scattering with twin-related additional directions.

KREMENOVIC, A., LAZIĆ, B., KRÜGER, H., TRIBUS, M., VULIĆ, P. (2013): Acta Crystallographica, C69, 334-336.

KRÜGER, H., STÖBER, S., WELBERRY, T.R., WITHERS, R.L., FITZ GERALD, J.D. (2011): Acta Crystallographica, B67, 476-485.

LAZIĆ, B., KRÜGER, H., KAINDL, R., PERFLER, L., KREMENOVIC, A., CVETKOVIĆ, V., WITHERS, R.L. (2013): Chemistry of Materials, 25, 496-502.

IN VERY TIGHT PLACES! – STRUCTURAL TRANSFORMATIONS OF MINERALS UNDER EXTREME CONDITIONS

Miletich, R.

Institut für Mineralogie und Kristallographie, Universität Wien, Althanstrasse 14, 1090 Wien, Österreich
e-mail: ronald.miletich-pawliczek@univie.ac.at

Extremes of pressure and temperature shape our planets and extraterrestrial bodies, turn everyday gases and liquids within the interior of gas giants into condensed solids, form unexpected compounds, and densify any matter (including our Earth's geomaterials) exposed to that kind of non-ambient conditions. Densification of crystalline solids follows the given freedom as determined by simple geometry aspects in stereochemistry, changes in electronic structures and chemical bonding, but also as controlled by symmetry and energetics related to the long-range order of the crystal structure. In many cases structural transformations in the sense of rapid transitions between long-lived structural states are the consequence of dynamically changed conditions.

Mineral transformations are in the focus of interest for mineral physics, as they control e.g. geochemical element distribution, considering the formation of new host phases, or account for anomalies in seismic wave propagation, seismic discontinuities, and related geophysical heterogeneities at our planets deep interior. Our current knowledge about mineral transformations is the result of experimental and computational advances of the past decades. In particular in-situ techniques, such as the diamond-anvil cell, nowadays allow to directly probe materials exposed to pressure, temperature, to electric and magnetic fields, radiation, and combinations of them.

Access to advanced in-situ characterization tools, including diffraction, scattering, spectroscopy, microscopy, and imaging is provided through dedicated large-scale facilities. In this context the newest technical developments including the advances made for in-situ high-pressure high-temperature experiments will be demonstrated, and an outlook for upcoming technical developments will be provided. A particular focus is dedicated to single-crystal techniques, which most currently started to experience a renaissance owing to the demand for very small sample sizes on approaching multi-megabar pressures at temperatures relevant to the Earth interior. Examples of selected mineral transformation are supposed to illustrate the recent activities in experimental crystallography and extreme-condition research, the application if developed techniques, and the efforts to use synchrotron radiation for in-situ investigations. Case studies encompass investigations of geologically relevant transitions in carbonate phases (transformation of calcite polymorphs, the pressure-induced transformation in dolomite-type norsethite).

OROGENIC GOLD DEPOSITS IN FINLAND

by

Ferenc Molnár

Geological Survey of Finland
P.O. Box 96, FI-02151, Espoo, Finland
e-mail:ferenc.molnat@gtk.fi

Introduction: general characteristics of orogenic gold deposits

Orogenic gold deposits are typical metallogenic features in moderate to high temperature - low to moderate pressure metamorphic belts of convergent plate margins (GROVES et al., 2003). They formed in large scale metamorphic fluid dominated fluid flow systems at 3-20 km depths, along compressional-transpressional shear zones in accreted terrains during the late stages of orogenies. Their host rocks most typically consist of mafic metavolcanic and metasedimentary sequences which also often host felsic (porphyry) and lamprophyre dikes and granitoid intrusions and thus magmatic input into the fluid flow system cannot be ruled out in some deposits. Location of ore is controlled by brittle-ductile shear zones and it is also influenced by competency contrasts among host rock lithologies as well as by superimposition of shear zones on each other or on fold structures. The mineralization forms disseminations, stockworks and veins. Gold enrichments are usually associated with elevated concentrations of Ag, Bi, Sb, As, Te, W. The base metal content of the ore is usually low; exceptions are the orogenic gold deposits with atypical metal associations. Epizonal (3-6 km depth) deposits may be enriched in Sb and Hg whereas concentration of As and Te is more typical to meso- and hypozonal (6-10 and >10 km depths, respectively) deposits. Native gold most commonly associates with pyrite and/or pyrrhotite, arsenopyrite and telluride minerals in car-bonate-quartz veins. Hydrothermally altered host rocks are characterised by enrichments of K, Na, Ca, Fe, Mg, CO₂, B and S. Thus albite, K-feldspar, K-micas, biotite, phlogopite, amphibole, tourmaline, carbonates and Fe-sulphides are the typical alteration minerals. Parent fluids of mineralisation are dilute (<6.8 NaCl equiv wt%) H₂O-NaCl-CO₂ (\pm CH₄ \pm N₂) type fluids. These reduced, near-neutral fluids transport gold in sulphur complexes and precipitation of gold is triggered by phase separation as a consequence of pressure fluctuation, removal of sulphur by sulphurisation of Fe-rich silicate/oxide minerals in the wall rocks and changes in the oxidation state by mixing with more reductive/oxidative fluids or carbonatisation of wall rocks. Most of the giant (>250t Au) and world class (>100t Au) deposits were formed in relation to Archean and Paleoproterozoic supercontinent cycles at around 2.6-2.7 and 1.8-1.9 Ga, as well as during the Phanerozoic, modern-style orogenic cycles between 600 and 50 Ma (GOLDFARB et al., 2001). Therefore it is especially interesting to study this kind of deposits on the Fennoscandian shield where the Archean cratonic nuclei are surrounded by Proterozoic and Phanerozoic orogenic belts (Fig.1).

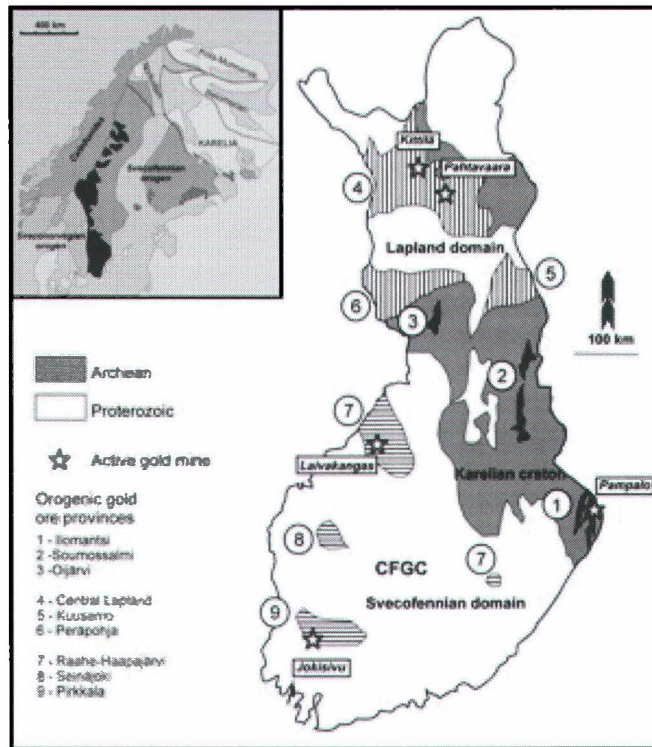


Figure 1: orogenic gold provinces in Finland.

Archean greenstone belts of the Karelian craton

The northerly trending, up to 200 km long, narrow greenstone belts with greenschist-amphibolite facies metasedimentary and metavolcanic units are surrounded by granite-gneiss complexes on the Karelian craton (Fig.1). The most important deposits are located in the Hattu schist belt (HSB) in the eastern part of the Ilosti. Similar deposits are also known in the Soumussalmi belt and in the Oijärvi belt. These latter belts have comparable geology to the Ilomantsi greenstone belt. However, rocks and related cumulates are more widespread in relation to sedimentary rocks. The currently known cumulative ore resource of gold deposits in the HSB is 4.8208 Mt. The Pampalo mine has 1.6488 Mt resources with 4.3 g/t Au grade. In the HSB, the deposits are located along the major N-S trending shear zones which cut folded, sedimentary and volcanic units. Pre- and syn-deformation emplacement of tonalitic granite plutons and felsic porphyry dikes took place between 2.75 and 2.72 Ga. Amphibolite facies peak metamorphic conditions were established at around 2.72 Ga (VAASJOKI et al., 1993). According to SORJONEN-WARD (1993), formation of the gold deposits took place before the peak of metamorphism, but STEIN et al. (1998) reported a 2.72 Ga Re-Os isochron age for pyrite associated to gold and suggested syn- to post peak timing of gold ore deposition.

Results of Pb-isotope studies on galena, altaite and hydrothermal K-feldspar, sulphur isotope data for sulphides from the Pampalo mine and regional boron-isotope studies on tourmaline in the HSB suggest that an early stage ore formation was synchronous with emplacement of granitoids and the hydrothermal circulation included magmatic fluids. Occurrences of high salinity (30-40 NaCl equiv wt.%) high temperature (min. 300-350°C) carbonic-aqueous fluid inclusions in addition to the dilute CO₂-CH₄-NaCl-H₂O type ones in some deposits of the HSB (and in the Suomussalmi belt; POUTAINEN & PARTAMIES (2003) probably also indicate this input of magmatic fluids. The gold mineralisation consists of disseminated-stockwork, locally vein type ore which is enveloped by sericite-chlorite alteration zones with tourmaline in the host metasedimentary units and felsic dikes. Gold is associated with pyrrhotite, pyrite, arsenopyrite and various telluride minerals. The ore of the Pampalo mine is slightly different due to the presence of more widespread K-feldspar alteration zones and almost total absence of pyrrhotite and arsenopyrite. At ca. 1.85-1.7 Ga, tectonothermal processes affected the western parts of the Karelian craton due to overthrust of the up to 5-6 km thick east-verging Svecofennian nappe complex. (KONTINEN et al., 1992; O'BRIEN et al., 1993). Pb-isotope and fluid inclusion data from the Pampalo mine indicate local re-mobilisation of ore and overprinting wall rock alteration during interaction of carbonic-aqueous dilute (5-12 NaCl equiv. wt.%, 350-400°C temperature) fluids with the Archean mineralisation. Pb-isotope and fluid inclusions data also record an even more younger and lower temperature (200-250°C) saline (up to around 20 NaCl equiv. wt.%) fluid flow and ore remobilisation event.

Orogenic gold provinces of the Lapland domain

The Lapland domain (Fig.1) contains three orogenic gold provinces: the Central Lapland greenstone belt (CLGB), the Kuusamo belt (KS) and the Peräpohja belt (PB). One of the largest gold producer of Europe, the Kittilä mine (Suurikusikko deposit, 59 Mt total resources + reserves with 4.18 g/t average gold grade) is located in the CLGB. Pahtavaara (5.5 Mt total resources and reserves with 2.65 g/t average grade) is another active mine in this belt. In addition to these active mines, several other orogenic gold deposits and occurrences are known in the CLGB and KS. The PB is underexplored but the current discovery of extremely high grade (over 1000 g/t Au) showings in the northern part of this province highlights further exploration potential. The host rocks of gold deposits in these belts deposited during the elongated (2.45-2.0 Ga) intracontinental rifting of the Karelian craton. The early stage rifting produced bimodal komatiitic and felsic volcanic accumulations which are covered by quartzite, carbonate, BIF, turbidite, and graphitic schist bearing metasedimentary sequences with intercalations of tholeiitic basalts and repeated emplacement of mafic dikes and sills (LAHTINEN et al., 2005). The KS and PB represent failed rift zones but a narrow oceanic basin was developed in the zone of CLGB at around 1.97-1.95 Ga. SW oriented subduction and final collision took place between 1.93-1.91 Ga. Metamorphism and synorogenic plutonism between 1.96-1.88 Ga and repeated deformation events with development of ore controlling shear zones between 1.92 and 1.77 Ga established the final geological architecture of the Lapland domain. The common feature of the CLGB and KS is that the zones of ore deposits along the major shear zones and connected second to fourth order structures show low grade (greenschist facies) metamorphism whereas the metamorphic grade is increasing apart from these zones (HÖLTTÄ et al., 2007).

The peculiar feature of the mineralised zones is the presence of pre-ore albite-carbonate (\pm scapolite) alteration which resulted in formation of competent massive albitites. This alteration most likely indicates mobilisation of formation brines during the early stages of the development of crustal scale fault structures (VANHANNEN, 2001). The same structures were reactivated during the development of major ore controlling shears and competency differences between albitites and the metasedimentary-metavolcanic units supported development of favourable conditions for ore deposition. The Fe-rich composition of mafic metavolcanic host rocks also supported precipitation of gold by extraction of sulphur from hydrothermal fluids. The most common Fe-minerals in association to gold are pyrite, pyrrhotite, arsenopyrite and löllingite. In the Suurikusikko deposit, most of the gold is refractory and is hosted by arsenopyrite and pyrite. Typical wall rock alteration assemblages around ore veins and stockwork zones contain quartz, carbonate, sericite/fuchsite, biotite, chlorite and feldspars. Another interesting feature of the CLGB and KS is that about half of the orogenic gold deposits have atypical metal associations with possible economic concentrations of cobalt (gersdorffite) and enrichments of Cu, Ni, Mo, U, Se, Ba and LREE (EILU et al., 2003). This specific geochemistry of ore may be connected to remobilisation of these metals by saline fluids from the Paleoproterozoic basin sequences. Age of formation of orogenic gold deposits in the Lapland domain is not well established; Pb-isotopic data from galena suggest 1.84-1.80 Ga ages (MÄNTTÄRI, 1995). Lead isotopes data also indicate Caledonian reactivation of ore controlling structures and local redistribution of metals.

Orogenic gold provinces in the Svecofennian domain

Orogenic gold provinces in the Svecofennian domain are located in collision zones surrounding the Central Finland granitoid complex (CFGc; Fig. 1). Gold is currently mined at Laivakangas (22Mt@ 2.03 g/t Au) in the southern Ostrobothnia part of the Raahe-Haapajärvi province and at Jokisivu (1.9 Mt@ 5.8 g/t Au) in the Pirkkala province. The basement of the CFGC, the Keitele microcontinent with a ca. 2.0 Ga old continental crust (LAHTINEN et al., 2005) formed the upper plate in those subduction zones which were developed along its eastern, western and southern boundaries between 1.92-1.89 Ga. Subduction related volcanism and plutonism, then metamorphism and deformation of accreted domains took place between 1.9 and 1.87 Ga. Formation of orogenic gold deposits post dated the mid to upper amphibolite facies metamorphism: results of studies by SAALMAN et al. (2010) support 1.83-1.80 Ga age for ore deposition in the Jokisivu deposit. The mineralized shear zones have NW-SE most typical orientation in the Svecofennian domain. They are mostly located in intrusive-volcanic complexes in Ostrobothnia: these host rocks also contain earlier formed porphyry-Cu type ore at some places. In the Seinäjoki and Pikkala province, turbiditic rocks are also common hosts of orogenic gold deposits. In the Seinäjoki province, and subordinately in the Pirkkala province (Jokisivu deposit) composition of ore is characterised by enrichments of antimony (aurostibnite, native antimony). The deposits usually contain free gold in association to pyrite, pyrrhotite, löllingite, arsenopyrite and Bi-Te minerals.

Conclusions

Orogenic gold deposits in Finland were formed at around 2.7 Ga and 1.8 Ga in correlation with the Archean and Paleoproterozoic global crustal growth cycles. This feature and their comparable mineralogical, petrological, geochemical and structural peculiarities with orogenic gold deposits on other shield areas highlight the exploration and mining potential in the metallogenic provinces introduced in this brief summary.

- EILU, P., SORJONEN-WARD, P., NURMI, P., NIIRANEN, T. (2003): *Econ. Geol.*, 98, 1329-1353.
- GOLDFARB, R.J., GROVES, D.I., GARDOLL, S. (2001): *Ore Geol. Rev.*, 18, 1-75.
- GROVES, D.I., GOLDFARB, R.J., ROBERT, F., HART, C.J.R. (2003): *Econ. Geol.*, 98, 1-29.
- HÖLTTÄ, P., VÄISÄNEN, M., VÄÄNÄNEN, J., MANNINEN, T. (2007): *Geol. Surv. Finland Spec. Paper*, 44, 7-56.
- KONTINEN A., PAAVOLA, J., LUKKARINEN, H. (1992): *Geol. Surv. Finland Bull.*, 365, 1-31.
- LAHTINEN, R., KORJA, A., NIRONEN, M. (2005): in LEHTINEN, M., NURMI, P., RAMÖ, O.T. (eds). *Precambrian geology of Finland – Key to the evolution of the Fennoscandian shield*. Elsevier, 481-532.
- MÄNTTARI, I. (1995): *Geol. Surv. Finland Bull.*, 381, 70p.
- O'BRIEN, H., NURMI, P., KARHU, J.A. (1993): *Geol. Surv. Finland, Spec. Paper* 17, 291-306.
- POUTIAINEN, M., PARTAMIES, S. (2003): *Econ. Geol.*, 98, 1355-1369.
- SAALMAN, K., MÄNTTÄRI, I., PELTONEN, P., WITHEHOUSE, M.J., GRÖNHOLM, P., TALIKKA, M. (2010): *Geol. Mag.* 147, 551-569.
- SORJONEN-WARD, P. (1993): *Geol. Surv. Finland, Spec. Paper* 17, 9-102.
- STEIN, H., SUNDBLAD, K., MARKEY, R.J., MORGAN, J.W., MOTUZA, G. (1998): *Min. Dep.*, 33, 329-345.
- VAASJOKI, M., SORJONEN-WARD, P., LAVIKAINEN, S. (1993): *Geol. Surv. Finl., Spec. Pap.* 17, 103-132
- VANHANNEN, E. (2001): *Geol. Surv. Finland Bull.*, 399, 229p.

ÜBER GESTEINE UND MINERALVORKOMMEN DER KORALPE

Postl, W

c/o Mineralogie – Studienzentrum Naturkunde, Universalmuseum Joanneum,
Weinzötlstraße 16, 8045 Graz, Österreich
e-mail: walter.postl@gmx.at

Der am Ostrand der Alpen gelegene Gebirgszug der Koralpe gehört innerhalb der Austroalpinen Einheit (Ostalpin) zum Koralpe-Wölz-Deckensystem und wird aus einer Tausende Meter mächtigen Abfolge von Gneisen und Glimmerschiefern aufgebaut. Der durch Scherbewegungen in der Erdkruste „ausgewalzte“ Plattengneis spielt unter den verschiedenen Gneistypen eine Hauptrolle und bildet einen für die Koralpe typischen und markanten Bewegungshorizont. Ebenso charakteristisch sind die weithin verbreiteten Disthen-Paramorphosenschiefer. In diese Gneis-Glimmerschiefer-Abfolge sind Amphibolite, Eklogite, Gabbros, Pegmatite, Marmore und Kalksilikatgesteine eingeschaltet. An den Gesteinen sind zumindest zwei Metamorphosen erkennbar. Die letzte eoalpine Metamorphose, mit ihrem Maximum vor rund 90 Millionen Jahren, war sehr druckbetont und hat zur Eklogitbildung geführt (siehe MILLER et al., 2005, cum lit.). Eine Besonderheit der Koralpe ist es, dass der im Perm gebildete Gabbro an einigen wenigen Vorkommen nur gering verändert erhalten geblieben ist. Übergänge von Gabbro zu Eklogit im Dezimeterbereich sind petrologische Leckerbissen (HERITSCH, 1973; PROYER & POSTL, 2010). Schließlich können verschiedene, permisch gebildete Pegmatit-Typen unterschieden werden. Dazu gehört das Vorkommen von Spodumenpegmatit nahe der Weinebene, das als größte Lithium-Lagerstätte Europas gilt (GÖD, 1989), aber auch jene, oft nur einige cm-dicke Pegmatitmylonit-Lagen im Plattengneis, die sich durch die Führung von beachtlich großen Schörl-Kristallen auszeichnen. Tonnenschwere, anpolierte Blöcke aller in der Koralpe auftretenden Gesteine, u.a. herausragende Exemplare mit Gabbro-Eklogit-Übergängen, werden seit 2001 im Geopark Glashütten einer breiten Öffentlichkeit präsentiert (POSTL, 2009). Eine ähnliche Open-Air-Einrichtung ist kürzlich am neuen Dorfplatz von Wielfresen entstanden.

Nur beispielhaft werden der typische Mineralbestand einiger Koralpen-Gesteine, aber auch in diesen auftretende Kluftmineralbildungen vorgestellt. Noch vor wenigen Jahrzehnten war man der Auffassung, dass im Kristallin der Koralpe keine alpinen Kluftmineralisationen größeren Ausmaßes auftreten. Seit dem Fund der bedeutendsten Kluftmineralisation der Steiermark in einem nahe Deutschlandsberg temporär betriebenen Amphibolit-Steinbruch Anfang der 1970er-Jahre, mit bis 90 kg schweren Bergkristallen und den größten Titanitkristallen der Alpen (ALKER, 1975), sind weitere beachtenswerte Funde gefolgt.

ALKER, A. (1975): Mitt. Naturwiss. Ver Steiermark, 105, 21-24.

GÖD, R. (1989): Mineralium Deposita, 24, 270-278.

HERITSCH (1973): TMPM Tschermaks Min. Petr. Mitt., 19, 213-271.

MILLER, Ch., THÖNI, M., KONZETZ, J., KURZ, W SCHUSTER, R. (2005): Mitt. Österr. Min. Ges., 150, 227-263.

POSTL, W (2009): Geopark Glashütten. Ein Führer durch die Gesteinswelt der Koralpe. Geologische Bundesanstalt, 89 Seiten.

PROYER, A., POSTL, W (2010): Mitt. Naturwiss. Ver. Steiermark, 140, 45-67

MECHANICAL FUNCTIONALIZATION OF MINERALS BY ORGANISMS

Schmahl, W W¹, Grießhaber, E.¹, Jordan, G.¹, Ziegler, A.², Kelm, K.³ & Maier B.¹

¹Dept. of Earth & Environm. Sci., GeoBioCenter, LMU Munich, Theresienstraße 41, D-80333 Munich

²Central Facility for Electron Microscopy, Universität Ulm, Albert-Einstein-Allee 11, D-89069 Ulm

³DLR, Institute of Materials Research, Linder Höhe 2, D-51147 Köln-Porz

e-mail: wolfgang.schmahl@lrz.uni-muenchen.de

Despite the brittleness of Ca-carbonate and –phosphate minerals, these substances are found almost ubiquitously in skeletons or teeth of organisms (LOWENSTAM, 1981). However, unlike inorganic minerals, biominerals are always hybrid composites which include intra- and intercrystalline organic matrix. This matrix controls the structure from the nanofabric to the macroscopic morphology, and the resulting hierarchical composite has dramatically improved mechanical strength, hardness, and, most importantly, fracture toughness (DUNLOP & FRATZL, 2010). With our increasing inventory of detailed investigations by electron back-scatter diffraction (EBSD), TEM, AFM, and X-ray microdiffraction, we can now establish systematics of biomineral hierarchical architectures. Bioapatite, the main biomineral in vertebrates, always occurs in the form of nanocrystals embedded in organic matrix. With the possible exception of protozoa, the biocarbonate crystals also consist of primary particles in the 20–80 nm range. However, these particles are crystallographically co-oriented and constitute sub-micro- to-micrometer sized *mesocrystals* (SCHMAHL et al., 2012a, b), which are separated by organic membranes. The bioaragonite of corals (PRZENIOSŁO et al., 2008) and the nacre layers of mollusc shells (GRIESSHABER et al., 2013) consist of such poly-*mesocrystals* with a strong axial crystallographic texture. Biocalcite occurs in this form e.g. in the hard layer of brachiopod shells (GOETZ et al., 2011). More frequently in molluscs and brachiopods the calcite forms long *mesocrystal* fibres, columns, or prisms; and morphologically similar *mesocrystals* are sometimes combined to submillimeter-to-millimeter-sized *hybrid composite crystals*, in which the mesocrystal subunits are separated by organic membranes but are crystallographically co-oriented (KELM et al., 2012, SCHMAHL et al., 2012a, b). If *mesocrystal* subunits of different sizes and shapes are combined and display a “single-crystal”-like 3D crystallographic co-orientation, a *multiplex composite crystal* architecture (SCHMAHL et al., 2012b) is present, e.g. in sea urchin teeth where this architecture is essential for precise and reproducible self-sharpening of the tooth.

DUNLOP, J. W. C., FRATZL, P. (2010): Annual Review of Materials Research, 40, 1-24.

GOETZ, A. J., STEINMETZ, D. R., GRIESSHABER, E., ZAEFFERER, S., RAABE, D., KELM, K., IRSEN, S., SEHRBROCK, A., SCHMAHL, W W (2011): Acta Biomat., 7, 2237-2243.

GRIESSHABER, E., SCHMAHL, W W., UBHI, H.S., HUBER, J., NINDIYASARI, F. MAIER, B., ZIEGLER, A. (2013): Acta Biomaterialia, in press.

KELM K, GOETZ A, SEHRBROCK A, IRSEN S, HOFFMANN R, SCHMAHL WW, GRIESSHABER E (2012): Zeitschr. Kristallogr., 227, 758–765.

LOWENSTAM, H.A. (1981): Science, 211, 1126-1131

PRZENIOSŁO, R., STOLARSKI, J., MAZUR, M., BRUNELLI, M. (2008): J. Struct. Biol., 161, 74-82.

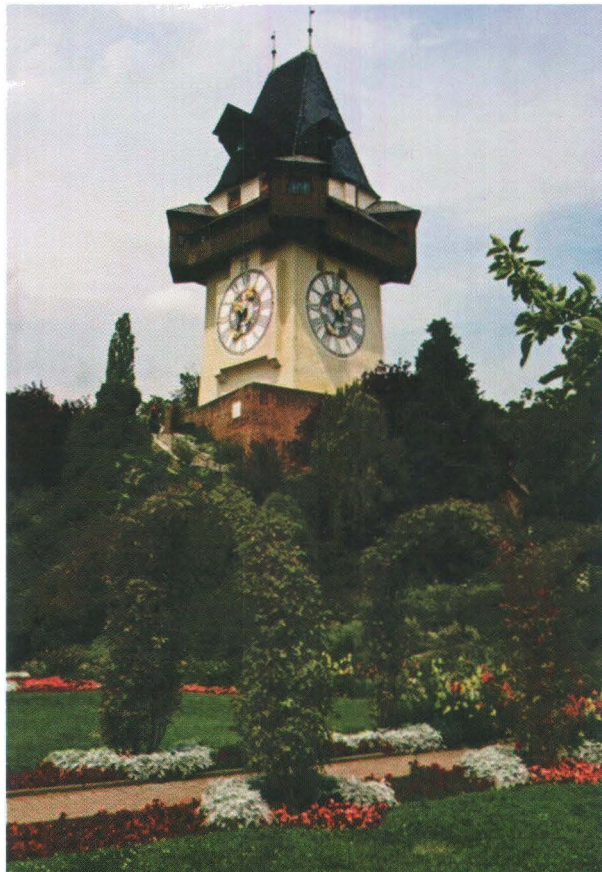
SCHMAHL WW, GRIESSHABER E, KELM K, GOETZ A, JORDAN G, BALL A, XU D, MERKEL C, BRAND U (2012a): Zeitschr. Kristallogr., 227, 793–804.

SCHMAHL WW, GRIESSHABER, E, KELM K, BALL, A, GOETZ, A, XU DY, KREITMEIER, L, JORDAN, G (2012b): Zeitschr. Kristallogr.. 227. 604-611.

MINPET 2013

GRAZ / AUSTRIA
SEPTEMBER, 19th - 23th

ABSTRACTS



**ELEMENT PARTITIONING AT A PROPAGATING REACTION FRONT:
EXPERIMENT AND THEORY**

Abart, R.¹ & Jerabek P²

¹University of Vienna, Department of lithospheric research, Althanstraße 14, 1090 Vienna, Austria

e-mail: rainer.abart@univie.ac.at

²Charles University Prague, Institute of Petrology and Structural geology,

Albertov 6, 12843 Prague, Czech Republic

e-mail: jerabek.petr@gmail.com

Equilibrium element partitioning between phases is the basis for many applications in petrology and geochemistry. We investigated Mg/Al partitioning by growing magnesio-aluminate spinel ($MgAl_2O_4$) at periclase (MgO) - corundum (Al_2O_3) contacts. Experimental conditions were 1 bar confining pressure and 1350 °C, at run durations of 5 to 160 h. The spinel forms polycrystalline reaction rims, which grow by the interdiffusion of Al^{3+} and Mg^{2+} . In accordance with the phase diagram, spinel is close to stoichiometric with X_{Al} (atomic $Al/(Mg+Al)$ ratio) of about 0.66 at the periclase-spinel contact and it becomes successively more aluminium-rich towards the corundum. Interestingly, at the spinel-corundum interface, the X_{Al} increases with increasing run duration. It is 0.66 in short time runs (5 h), and it is 0.69 after 160 h. This reflects a successive approach towards local equilibrium and corresponds to a decrease of the jumps in the Al_2O_3 and MgO chemical potentials across the propagating reaction interface. This evolution is due to the finite mobility of the spinel-corundum interface. A local driving force is required for interface motion. In this case it is provided by the free energy jumps of the MgO and Al_2O_3 components associated with their transfer across the reaction interface. This effect is pronounced during the initial, interface reaction controlled stages of the reaction and diminishes at later stages, when the reaction becomes diffusion controlled. From this observation the interface mobility, a key parameter in kinetic modelling, can be quantified.

MULTISTAGE TECTONISM DURING GONDWANA COLLISION: BALADIYAH COMPLEX, SAUDI ARABIA

Abu-Alam, T.S.¹, Hassan, M.¹, Stüwe, K.¹ & Kadi, K.²

¹Institut für Erdwissenschaften, Universität Graz, Universitätsplatz 2, A-8010 Graz, Austria

²Saudi Geological Survey, Medina Road, P.O. Box 54141, Jeddah 21514, Saudi Arabia

e-mail: tamer.abu-alam@uni-graz.at

The formation of orogens is a complex process often involving multiple stages of compression and extension. Field evidence from the Baladiyah complex in the northern part of the Arabian-Nubian Shield of Saudi Arabia shows that several erosional unconformities separate different high grade metasedimentary rocks within the complex. This indicates that the collision between East- and West-Gondwana involved several cycles of exhumation and burial. Mineral equilibria approach and thermodynamic modeling are used to place constraints on the formation conditions of each of these stages. It is shown that the complex is characterised by three regional metamorphic events followed by a fourth event of contact metamorphism due to the intrusion of post-tectonic granites. The first metamorphic event experienced peak metamorphism around 705 – 715 °C and 5.2 – 5.6 kbar and subsequent isothermal decompression to the Earth's surface. The second metamorphic events attained peak conditions of 635 – 670 °C and 4.2 – 5 kbar followed by exhumation, erosion and deposition of molasse sediments. The rocks were buried for a third time and metamorphosed to greenschist facies metamorphic conditions (330 ± 30 °C and 3.6 – 4.6 kbar) under the load of the molasse sediments. Post-tectonic granites intruded at a depth of 12 km during the final Pan-African exhumation causing the fourth metamorphic event (700 ± 25 °C). Correlation of this metamorphic evolution with the deformation history shows that the first and the second metamorphic events occurred in a compression regime (D_1 and D_2), interpreted to be related to the collision between East- and West-Gondwana. While the third deformation phase began as compression regime causing the third metamorphic event, and then turned into an oblique transpressive regime which led to form escape tectonics and development of a large scale strike-slip shear zone “the Najd Fault System”. This tectonic evolution accompanied several cycles of exhumation and burial indicates multistage crustal flexure during Gondwana Collision.

PRESSURE-INDUCED PHASE-TRANSFORMATIONS IN $\text{LiAlGe}_2\text{O}_6$ AND $\text{LiCrGe}_2\text{O}_6$ CLINOPYROXENES

Artac, A.¹, Pippinger, T¹, Nestola, F², Redhammer, G.³ & Miletich, R.¹

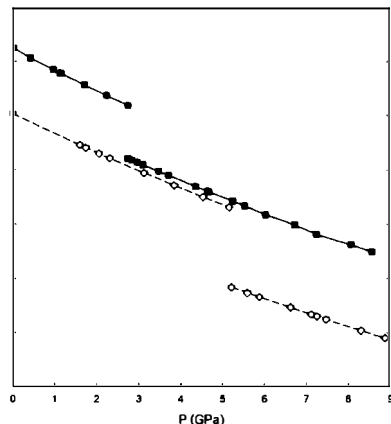
Institut für Mineralogie und Kristallographie, Universität Wien, Althanstraße 14, 1090 Vienna, Austria

²Dipartimento di Geoscienze, Università di Padova, Via Gradenigo 6, 35131 Padova, Italy

³Department of Materials Engineering and Physics, Division of Mineralogy, University of Salzburg
Hellbrunnerstraße 34, 5020 Salzburg, Austria

e-mail: andreas.artac@univie.ac.at

Clinopyroxenes and their synthetic analogues are in the focus of extensive experimental studies in mineral physics as the knowledge of elastic properties and the transformation behaviour depending on chemical variations is discussed for the geophysics under conditions in Earth's upper mantle. Among a series of analogue phases the two selected Li-ianate compounds $\text{LiAlGe}_2\text{O}_6$ (LAG, space group $P2_1/n$, REDHAMMER et al. 2012) and $\text{LiCrGe}_2\text{O}_6$ (LCG, space group $P2_1/c$, REDHAMMER et al. 2008) have been subject of experimental in-situ investigations at high pressures, carried out by means of single-crystal X-ray diffraction in a diamond anvil cell. Unit-cell parameters of hydrostatically pressurized single crystals were determined up to approximately 9 GPa. Both samples show a first-order phase transition (see Fig. 1).



The equations of state (EOS) were determined for the high-pressure (HP) and low-pressure (LP) polymorphs of both compounds, and fits of the P–V data to a Birch–Murnaghan EOS yield the parameters: $K_0 = 112.7(5)$ and $123.1(1.6)$ GPa for LP– and HP-LAG. The equivalent fits give $K_0 = 106(2)$ and $114.5(7)$ GPa for LP-LCG and HP-LCG, respectively. The observed reflection conditions suggest P-lattices for both high-pressure polymorphs. Structure investigations will shed light on the mechanisms of structural transformation.

Figure 1 Pressure dependent changes in the unit-cell volume of LAG (closed symbol) and LCG (open symbol). The solid line represents the fit of a 3rd-order Birch-Murnaghan EOS, the dashed line represents the fit of a 2nd-order Birch-Murnaghan EOS.

REDHAMMER, GJ., ROTH, G., AMTHAUER, G. (2008): Acta Crystallographica Section C, Volume C64, i97-i99.

REDHAMMER, GJ., NESTOLA, F., MILETICH, R. (2012): American Mineralogist, Volume 97, 1213-1218.

EVIDENCE FOR BIMETASOMATISM BETWEEN ECLOGITE AND ADJACENT ROCKS FROM THE TAUERN WINDOW, AUSTRIA

Aßbichler, D.^{1,2} & Proyer, A.^{1,3}

¹Institute of Earth Sciences, University of Graz, Universitätsplatz 2, A-8010 Graz, Austria

²now at: Department of Geo- and Environmental Sciences, LMU Munich, Theresienstraße 41, 80333 Munich, Germany

³now at: Department of Geology, University of Botswana, Private Bag UB 00704, Gaborone, Botswana
e-mail: dassbichler@lmu.de

The Eclogite Zone (Austria) is characterized by the occurrence of eclogite interbedded with other rocks, mainly metapelites and minor marbles, metapsammites and talc schists. According to geothermobarometry, PT-conditions of at least 26 kbar and about 580 °C were achieved. An open question is whether fluid-mediated compositional changes occurred between the interlayers during subduction zone metamorphism. Therefore, the mineralogy and geochemistry of the contacts eclogite–metapelite and eclogite–talc schists were investigated.

The eclogite in contact to the metapelite shows almost no change in volume, with minor gain of Si, Ca and Na and loss of Mg. The metapelite, however, exposes 30 % volume loss, mainly as Si and Ca, coupled with enrichment of K, Mg, Fe and Na; the latter two stem from external source. Trace element changes are less spectacular but corroborate changes in the major elements (Sr goes with Ca, Ba with K, etc.).

The eclogite in contact to the talc schist also underwent no significant change in volume, with minor enrichment in Mg and depletion in Na. The talc schist is ultrabasic in composition and of uncertain origin. It experienced more than 30 % volume loss towards the contact, where Mg, Fe, Si, Na and Ti are depleted and no major element is enriched.

These changes in bulk composition are expressed in mineralogical, textural and mineral chemical changes of considerable complexity. There is clear evidence that it is not caused by retrograde interactions. The compositional changes are too systematic and complex to be explained as primary (volcano-) sedimentary layering or mixing of clays and ashes. As the lithological boundaries are planar over distances of tens of metres at least, the volume loss are not induced by folding but rather by (pure or general) shear. Some composition changes cannot be explained by material exchange between the two lithologies (bimetasomatism) alone but must have been caused by advection parallel to the lithological boundaries. Rare garnets and epidotes with oscillatory zoning patterns near the contact indicate the effect of locally abundant fluids.

**MINERALOGICAL INVESTIGATION OF SULFIDE-OXIDE MINERALIZATION
IN THE MISHO MAFIC-ULTRAMAFIC COMPLEX (NW IRAN)**

Azimzadeh, A. M.¹, Ghorbani, M.², Hosseinzadeh, G.² & Moayyed, M.²

¹University of Leoben, Department of Applied Geosciences and Geophysics, Peter Tunner Str. 5,
8700 Leoben, Austria

²University of Tabriz, Faculty of Natural Sciences, Department of Geology, 5166616471 Tabriz, Iran
e-mail: amir.azimzadeh@unileoben.ac.at

The mafic-ultramafic complex of Misho is exposed in the north-western part of Iran. The Misho mountains are part of the Central Iran domain which consists of a Precambrian crystalline basement, Paleozoic platform sediments, Cambrian to Triassic sedimentary and magmatic rocks representing Gondwana marginal terranes (STÖCKLIN, 1968; ALAVI, 1991).

The ore mineralization is hosted in the mafic portion (gabbro) of Misho complex. Two different types of mineralization, sulphides and oxides, were identified. The sulphide ore bodies are mainly composed of pyrrhotite accompanied by chalcopyrite, pentlandite, sphalerite, pyrite and troilite. Representative texture shows the typical sulfide-silicate relationships as net-textured sulfides enclosing silicate. The oxides mineralization consists of ilmenite (< 5%) and with small amounts of magnetite as solid inclusions in pyrrhotite. Primary sulfide was replaced by pyrite, marcasite and violarite during alteration states.

Selected samples of sulphides were investigated at the E. F. Stumpf microprobe laboratory (University of Leoben, Austria). Pyrrhotite as a main sulfide phase contains 59.50 - 64.05 % Fe, 0.01 - 0.32 % Ni, 0.0 - 0.07 % As and 0.0 % of Co. Whole rocks analyses show that the total platinum-group element concentrations in sulfide rich gabbro are very low.

Chemical composition of the sulfide minerals and their texture suggest that they were formed in a magmatic immiscible sulfide Fe-Ni-Cu system. The early crystallization phases consisted of gabbro without associated Fe-Ni-Cu sulphide mineralization. This was followed by later progressive crystallization which depleted silicate-oxide phases from residual magma. The last stage of crystallization formed predominantly of sulfide minerals by accumulation of immiscible magmatic sulfide droplets. Thermometry investigation based on exsolution texture of chalcopyrite-sphalerite and chalcopyrite-pyrrhotite suggests that the sulfide zone probably formed at temperatures about 400 °C.

ALAVI, M. (1991): Geol. Soc. Am. Bull., 103, 983-992.
STÖCKLIN, J. (1968): Bull. Am. Assoc. Pet. Geol., 52, 1229-1258.

THE RATE AND MECHANISM OF DEEP SEA GLAUCONITE FORMATION

Baldermann, A.¹, Warr, L.N.², Grathoff, G.H.² & Dietzel, M.¹

¹Institute of Applied Geosciences, Graz University of Technology, Rechbauerstraße 12, 8010 Graz, Austria

²Department for Economic Geology and Mineralogy, Ernst-Moritz-Arndt University Greifswald, Friedrich-Ludwig-Jahn-Straße 17A, 17487 Greifswald, Germany

e-mail: baldermann@tugraz.at

The conditions and mechanism of glauconitization in shallow shelf environments (< 300 m water depth and 15–25 °C) are generally well understood, whereby glauconite formation takes place close to the seawater-sediment interface. In contrast, the key factors controlling the rate and mechanism of deep-water glauconitization are still poorly constrained.

Cores from the Ivory Coast-Ghana Marginal Ridge (ODP Site 959) were recovered in 2100 m water depth and related 3–6 °C seawater temperature. Sediments from Hole 959C comprise of foraminifera and nannofossil oozes mixed with detrital silicates and authigenic green grains. This sedimentary record was found to be without large hiatuses since the Miocene. In order to identify the process and rate limiting factors for recent deep sea glauconitization, green grains were collected from 0.16, 11.69, and 24.91 meter below sea floor, corresponding to sediment ages of ~10, ~900, and ~2500 ky. Mineralogical and chemical changes within the green grains were studied by X-ray diffraction and various electron microscopic methods, together with the burial-related changes in bulk sediment composition and interstitial solution chemistry. Our results reveal that the green clay was formed mainly in foraminifera tests, which provided the post-depositional conditions ideal for glauconitization. Within these tests, an early micro-environment was generated, wherein microbial biofilm with incorporated gels containing Fe, Mg, Al, and silica were formed. Fe-smectite precipitated from these gels (~10 ky), supported by microbial activity and cation supply from the interstitial solution. With increasing burial (~900 ky), the Fe-smectite reacted to form mixed-layered glauconite-smectite (Gl-S) and finally almost pure glauconite developed (~2500 ky), without any miscibility gaps between the Fe-smectite and glaucony group. This burial-related glauconitization process is controlled mainly by the interstitial solution chemistry, which strongly depends on early diagenetic oxidation of organic matter, microbial sulfate reduction, silicate alteration and carbonate dissolution, and in particular Fe redox reactions. As evident by progressively more glauconite layers in Gl-S, ongoing with a notably higher Fe_2O_3 content in Gl-S with increasing state of early marine diagenesis, it is the availability of Fe which may be the rate limiting factor for glauconitization. This explains the greening of the grain colour with depth and the various states of green grain maturity within the samples. The glauconitization rate is given by $\% \text{Gl}_{\text{sed}} = 22.6 \log(\text{age}_{\text{sed}}) + 1.6$, where Gl_{sed} is the state of overall glauconitization of the sediment and age_{sed} is the sediment's age (in ky) (BALDERMANN et al., 2013). The rate of deep-water glauconite formation at this site is 5-times less than that in shallow shelf regions, probably reflecting the lower temperatures and limited cation supply within deep sea environments.

ZrO₂ IN REFRACtORY PRODUCTS: CHARACTERIZATION METHODS

Bauer, C.¹, Rollinger, B.¹, Krumpel, G.¹, Hoad, O.¹, Pascual, J.¹, Rogers, N.¹ & Krenn, K.²

¹RHI-AG, Magnesitstraße 2, 8700 Leoben, Austria

²Institute of Earth Sciences, Karl-Franzens-University of Graz, Universitätsplatz 2, 8010 Graz, Austria

e-mail: christoph.bauer@rhi-ag.com

In the process of continuous steel casting, isostatically pressed products are commonly used for flow control. By the combination of an alumina graphite main body material grade and a zirconia graphite slag band grade, thermal shock resistance is combined with enhanced chemical resistance. Thermo-mechanical properties as well as chemical corrosion performance must be currently optimized. It is therefore of paramount importance to characterize the used raw materials. Microstructural information combined with an understanding of the crystallo-graphic phase transformations of zirconia provide predictive capabilities pertaining to the material performance. We present characterization methods for Ca-partially stabilized zirconia, including the in-situ trace element analysis of grains in combination with the characterization of the physical properties of zirconia-bearing materials. The application of electron backscatter diffraction (EBSD) and Raman spectroscopy allows deep insights in micro-scale phase transformations. The crystallographic transformation of the zirconia grains during operation is described by elemental distribution mappings. Recrystallization and exsolution phenomena are fundamental and also limiting factors regarding thermal shock resistance; and the chemical wear resistance changes with ongoing recrystallization. Structural modifications accompanied by chemical processes within the affected material are crucial to a better under-standing of refractory materials.

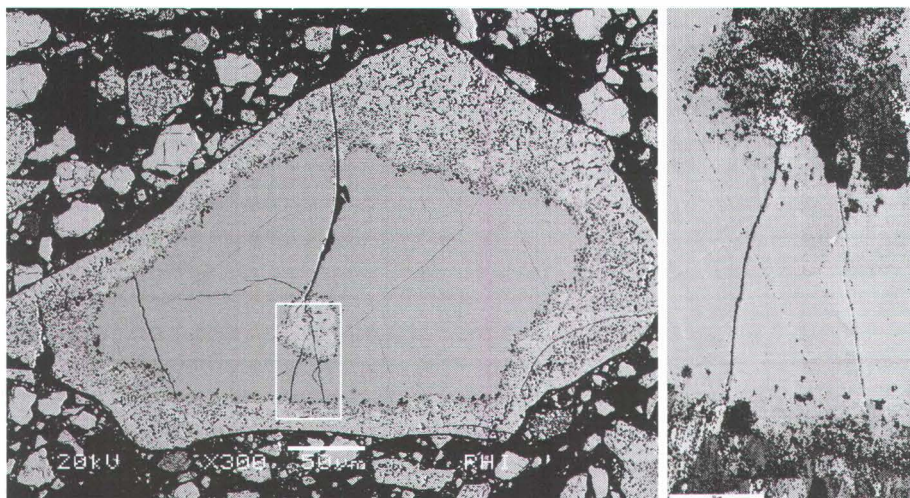


Figure 1. Left: BSE-image of Ca-partially stabilized zirconia showing a recrystallized rim. Scale bar is 50 μm . Right: Crystal orientation map for cubic zirconia. Scale bar is 15 μm .

CRYSTAL CHEMISTRY OF KIESERITE-COBALTKIESERITE SOLID SOLUTIONS, $Mg_{1-x}Co_x(SO_4) \cdot H_2O$

Bechtold, A. & Wildner, M.

Institut für Mineralogie und Kristallographie, Universität Wien, Althanstraße 14, 1090 Wien, Österreich
e-mail: manfred.wildner@univie.ac.at

The formation of solid solutions, i.e. the complete or partial replacement of crystal chemical related elements along joins of isotopic endmember structures, is a very common phenomenon in mineralogy. In rock-forming minerals in particular, the mutual substitution of Mg \vee Fe $^{2+}$ is one of the most important and best investigated replacement mechanisms, e.g. in the olivine solid solution system. Studies of solid solution systems of Mg with divalent 3 configurated transitions metal cations other than Fe $^{2+}$ are comparatively rare, but e.g. synthetic 'olivines' ($Mg,Co_2(SiO_4)$) attracted attention (e.g. MÜLLER-SOMMER et al., 1995 and references therein); as to be expected, the slightly larger ionic radius (SHANNON, 1971) of octahedral Co $^{2+}$ ($r = 0.745 \text{ \AA}$) vs. Mg ($r = 0.720 \text{ \AA}$) results in an increase of octahedral bond lengths and unit cell parameters with Co $^{2+}$ content.

However, for some groups of isotopic compounds a larger unit cell volume was surprisingly observed for the Mg representative compared to the respective Co $^{2+}$ endmember, in spite longer Co–O bond distances, among them the kieserite-type compounds $Me^{2+}(XO_4) \cdot H_2O$ (WILDNER & GIESTER, 1991, GIESTER & WILDNER, 1992).

Hence, in our present investigation we aim to synthesise representatives along the kieserite cobaltkieserite solid solution series, $Mg_{1-x}Co_x(SO_4) \cdot H_2O$, and to characterise them in detail by single crystal X-ray diffraction methods, in order to (i) check for complete miscibility along the solid solution series, (ii) check for possible cation ordering effects reducing symmetry and especially to (iii) thoroughly characterise the type and extent of the subtle structural changes governing the contradictory behaviour of polyhedral vs. unit cell dimensions.

First results confirm the above mentioned inconsistencies for the endmember phases [$V_{\text{kies}} = 355.53(20)$, $V_{\text{Co-kies}} = 354.77(14) \text{ \AA}^3$, but $\langle \text{Mg–O} \rangle = 2.077(1)$, $\langle \text{Co–O} \rangle = 2.097(1)$], and also indicate that complete miscibility along the solid solution series actually exists. Judging from the presently still limited number of X-ray data sets for mixed compositions, Vegard-type or at least approximate Vegard-type behaviour seems to prevail for most of the structural changes along the join. Further syntheses and X-ray diffraction experiments are in progress to fill compositional gaps and corroborate our preliminary results.

- GIESTER, G., WILDNER, M. (1992): N. Jb. Miner. Monatsh., 1992, 135-144.
MÜLLER-SOMMER, M., HOCK, R., KIRFEL, A. (1997): Phys. Chem. Minerals, 24, 17-23.
SHANNON, R.D. (1976): Acta Cryst., A32, 751-767.
WILDNER, M., GIESTER, G. (1991): N. Jb. Miner. Monatsh., 1991, 296-306.

SULPHUR ISOTOPE VARIATION OF SULFIDE ORES IN FUNCTION OF
FOOTWALL-MAGMA CONTAMINATION WITHIN THE BATHTUB INTRUSION,
DULUTH COMPLEX, USA

Benkó, Zs.¹, Molnár, F.², Mogessie, A.¹, Poulson, S.³, Arehart, G.³,
Severson, M.⁴, Hauck, S.⁴ & Raič, S.¹

¹ Karl-Franzens University Graz, Universitätsplatz 2, 8010 Graz, Austria

² Geological Survey of Finland, Betonimiehenkuja 4, 02151 Espoo, Finland

³ University of Nevada, Reno, 1664 N Virginia St, 89557 NV, Reno, USA

⁴ NRRI, University of Minnesota, 5013 Miller Trunk Highway, 55811 MN, Duluth, USA

e-mail: zsolt.benko@uni-graz.at

The 1.1 Ga old Duluth Complex (DC), is composed of multiple, discrete mafic intrusions. Intrusive rocks are emplaced between the Archean granitic and Paleoproterozoic metasedimentary footwall and co-genetic volcanic hanging wall rocks. The mineralized, troctolitic Bathtub Intrusion (BTI) contains particularly in the bottom part scattered bodies of hornfelsed metasedimentary footwall inclusions, granophyric textured felsic veins and hybrid rocks as a sign of the footwall-intrusion interaction. Mineralization is mainly disseminated but towards the intrusion-footwall contact locally semi-massive pods and veins also occur. Cubanite, chalcopyrite and pentlandite occur interstitially between cumulate phases, whereas a more fractionated sulfide melt composed of chalcopyrite and bornite form veins and disseminations within the silicate phases.

The average $\delta^{34}\text{S}$ values of sulfides in the troctolite are around +5 ‰. Irrespective of the stratigraphic height, melanocratic rocks have lower values (2.3-4.8 ‰), whereas samples of, or from the vicinity of metasedimentary footwall inclusions, quartz-bearing hybrid rocks, as well as felsic veins (all of them interpreted as derivate of the footwall) are enriched in heavy sulfur (8.6-16.7 ‰). With increasing contamination in the bottom 100 m thick part of the intrusion, sulfur isotope values increase abruptly towards the contact. Samples from the metasedimentary footwall have, however, slightly lower sulfur isotope signature (11.7-11.9 ‰) than samples in the lower, contaminated, inclusion-rich zone of the intrusion (11.0-16.7 ‰).

Although a large dataset is available for sulfur isotopes from the BTI (RIPLEY & ALAWI, 1986), our new data suggest that the grade of mineralization and the deviation of sulfur isotope value from the magmatic composition (~ 0 ‰) of a certain sample is exclusively the function of the distance of the sample from the metasedimentary footwall or from a footwall inclusion. Presence of mineralization along with heavy sulfur signatures at various levels, even at the top of the intrusion suggests that not only the bottom, but any part of the intrusion could be in direct contact with the heavy sulfur (0.2-25.8 ‰) bearing metasedimentary footwall rocks. In our model the BTI is composed of a series of horizontal sills that repeatedly intruded the metasedimentary footwall and the pre-existing sills. Therefore, contrary to other mineralized intrusions the metasedimentary rocks form not only the footwall but the hanging wall of the intrusion, as well.

ASSESSING DOLOMITE REACTIVITY BY HYDROTHERMAL ATOMIC FORCE MICROSCOPY

Berninger, U.-N.^{1,2}, Jordan, G.², Schott, J.¹ & Oelkers, E.H.¹

¹GET, CNRS, UMR 5563, Avenue Edouard Belin 14. 31400 Toulouse, France

²Department für Geo- und Umweltwissenschaften, LMU, Theresienstr. 41, 80333 Munich, Germany
e-mail: berninger@gec.obs-mip.fr

Dolomite reactivity is perplexing. Surface seawater is strongly oversaturated with respect to dolomite but there is no evidence of dolomite precipitation in modern marine depositional environments (ARVIDSON & MACKENZIE, 1999). The ancient sedimentary records however often contain dolomite. Laboratory preparation of synthetic dolomite generally requires hydrothermal conditions (KESSELS et al., 2000). Commonly this is interpreted as a kinetic limitation that inhibits dolomite formation at lower temperatures (HIGGINS & HU, 2005).

This study was designed to investigate dolomite reactivity on the (104) surface at elevated temperatures by applying hydrothermal atomic force microscopy. Experiments were conducted at temperatures up to 120 °C, pH ranging from 4-8 and pressures up to 5 bars.

All dissolution experiments produced crystallographically well defined etch pits which indicate stoichiometric release of ordered lattice cations. Most of the growth experiments however lead to the growth of two layers of a carbonate (~3 angstroms thick) which morphologically reproduced the initial surface features, resembling a template effect. Growth after these layers was strongly inhibited and does not show preferred crystallographic features.

In summary, the results show that, while dissolution proceeded uninhibited, growth kinematics were clearly self-limiting

ARVIDSON, R.S., MACKENZIE, F.T. (1999): Am. J. Sci.. 299, 257-288.

HIGGINS, S.R., HU, X.M. (2005): Geochim. Cosmochim. Acta, 69, 2085-2094.

KESSELS, L.A., SIBLEY, D.F., NORDENG, S.H. (2000): Sedimentology, 47, 173-186.

INVESTIGATION OF HANGINGWALL NORITES OF THE MERENSKY REEF UNIT AT TWO RIVERS PLATINUM MINE, EASTERN BUSHVELD

Beukes, J.J. & Gauert, C.D.K.

Dept. of Geology, University of the Free State, P.O. Box 339, Bloemfontein, South Africa
e-mail: Jarlenb7@gmail.com

This research study focuses on the enigmatic occurrence of noritic lenses (termed “brown sugar norite” by mine geologists), within the feldspathic pyroxenite of the Merensky Reef as well as the hangingwall at Two Rivers Platinum Mine which is situated on the southern sector of the eastern limb of the Bushveld Complex. The primary purpose of this study is to determine the origin of the noritic lenses (later on referred to as BSN) and their influence on PGE distribution of the Merensky Reef as well as to characterise the cumulate rocks associated with the Merensky Reef unit by the use of geochemistry and mineralogy from the different genetic facies types.

Underground samples were taken of different Merensky Reef profiles and studied petrographically. These samples are compared to hangingwall leuconorites and mesonorites of Merensky Reef units found north of the Steelpoort fault. The BSN are fine-grained and appear to only occur where the upper chromite stringer is present.

From petrography it is observed that orthopyroxene is the dominant cumulate phase in both the BSN and feldspathic pyroxenite followed by interstitial plagioclase. Both rock types contain a relatively high concentration of biotite, pyroxene exsolution lamellae and poikilitic textured clinopyroxene. Clinopyroxene may also occur as intermittent rims around orthopyroxene which could be attributed to a decrease in temperature and compositional change of the melt. Clinopyroxene inclusions are found in some of the well-rounded chromite grains present in the pyroxenite indicating possible magma erosion. Preliminary geochemical results of the BSN postulate that they are different from the melanorites which constitutes the HW of Merensky reef of the farms north of the Steelpoort Fault. Geochemical and petrographic evidence show that the BSN are in fact felspathic pyroxenites. EMPA results show cryptic vertical variation of incompatible and compatible elements in orthopyroxenes which indicates fractionation and replenishment of magma. A general negative trend of the Mg# with stratigraphic height in the Merensky reef profile where the BSN occurs which is caused by fractionation of the magma. The difference in texture as well as composition suggests a different or late-stage magmatic origin of the BSN. The fine grained texture of the BSN may suggest that a change in temperature of the magma occurred most likely due to an injection of a new cooler magma resulting in rapid cooling of the resident magma and thus a finer grained pyroxenite.

LOW TEMPERATURE EARTH MANTLE XENOLITHS FROM SIKHOTE-ALIN, FAR EAST RUSSIA

Blümel, A.¹, Ntaflos, T¹, Ashchepkov, I.², Prikhodko, V.S.³ & Gregoire, M.⁴

¹University of Vienna, Department of Lithospheric Research, Althanstraße 14, 1090 Vienna, Austria

²Institute of Geology and Mineralogy, SB RAS, Ac. Koptyuga ave. 6, 630090 Novosibirsk, Russian Federation

³Institute of Tectonics and Geophysics, Far-East Branch RAS, Kim Yu Chen Street 65, 680000 Khabarovsk, Russian Federation

⁴Géosciences Environnement Toulouse, Observatoire Midi Pyrénées, Université de Toulouse, Toulouse, France
e-mail: andrea.bluemel@hotmail.com

The study area, located in the Sikhote-Alin fold belt, comprises mantle xenoliths from Tuttochi, a locality close to Khabarovsk. The xenoliths are spinel lherzolites, their sizes vary from 3 to 8 cm in diameter and they are exceptional fresh. The most striking feature is the fact that part of the xenoliths show heavy infiltration of melts. These melts, undersaturated but rich in alkalis, circulate intergranular and react with the neighbor minerals creating veinlets with variable thickness consisting of glass and new forming minerals such as hydroxylapatite, apatite and ilmenite. According to their modal composition the xenoliths are fertile spinel lherzolites as also can be inferred from the compositions of their constituent minerals. Olivine is forsteritic with Fo varying from 89.3 to 90.0. The Mg# of orthopyroxene and clinopyroxene vary from 0.895-0.904 and 0.904-0.915, respectively and the Cr# of spinel varies around 0.100, indicating equilibrium conditions.

Model calculations have shown that the lithospheric mantle in this area has experienced 1-5 % batch melting. Also the calculated equilibrium temperatures for the xenoliths at 1.5 GPa are relative low and range from 780 to 940 °C. According to the REE abundances in cpx the spinel peridotites could be divided into three groups; group 1 with $(\text{La}/\text{Sm})_{\text{N}} = 0.11-0.53$, group 2 with $(\text{La}/\text{Sm})_{\text{N}} = 0.64-1.05$ and group 3 with $(\text{La}/\text{Sm})_{\text{N}} = 1.85$. While the chondrite normalized LREE abundances in cpx demonstrate variable enrichments and depletions, the HREE do not show significant differences among the three groups. Their overall $(\text{Dy}/\text{Yb})_{\text{N}}$ ratios vary from 1.05-1.16.

BARIUM, MANGANESE, IRON AND SULFUR AUTHIGENESIS IN MODERN EUXINIC BASINS: THE STATE OF THE ART

Böttcher, M.E.

Geochemistry & Isotope Geochemistry Group, Leibniz-Institute for Baltic Sea Research, IOW;
Seestrasse 15, 18119 Warnemünde, Germany)
e-mail: michael.boettcher@io-warnemuende.de

The deeps of the Baltic Sea provide ideal places to follow (trans)formations of barium, manganese and sulfur-bearing minerals in Holocene sediments under changing environmental and diagenetic conditions. The modern brackish conditions allow for the development of steep compositional pore water gradients already in surface sediments, leading to physico-chemical dis-equilibrium conditions that may trigger the authigenic formation and destruction of minerals. The Baltic Sea deeps are in particular well known for the occurrence of authigenic manganese(II)-calcium carbonate solid-solutions, manganese(II)sulfide, and different iron sulfides. Anoxic basins of the Baltic Sea, for instance, are the only known localities worldwide where authigenic MnS has been identified. Very recently, evidence for the formation of a previously unrecognized low-temperature BaMn double carbonate was found (BÖTTCHER et al., 2012). For a proper mechanistic relation of compositional and textural mineral occurrences to environmental conditions, experimental calibrations and physico-chemical interpretations are mandatory.

We present results from different studies on authigenic mineral (trans)-formation in the Baltic Sea system. Sediment cores were retrieved from sediments deposited during brackish and freshwater stages. Besides chemical and phase analytical compositions, the stable isotopic composition of sulfur was analyzed as a function of depth with high resolution. Brackish and freshwater stages during sediment formation can be separated, for instance, by the contents and stable isotope composition of organic carbon and sedimentary sulfur. Microbial reactions associated with the oxidation of organic matter result in the formation of characteristic (thermodynamically stable and metastable) carbonate, sulfide and sulfate mineral assemblages. The limnic pre-Litorina sediments are a place where downward diffusing species lead to a superimposition of original geochemical signatures by diagenetic mineral (trans)formations. Textural and (isotope) geochemical characteristics will be discussed.

Besides trace elements (BÖTTCHER & DIETZEL, 2010) and light stable isotopes (C, O, S) also new non-traditional stable isotope systems like Ba and Mo may be of particular value for the interpretation of mineral authigenesis (VON ALLMEN et al., 2010; NÄGLER et al., 2011).

- BÖTTCHER, M.E., DIETZEL, M. (2010): EMU Notes in Mineralogy, 10, 139-187
BÖTTCHER, M.E., EFFENBERGER, H.S., GEHLKEN, P.-L., GRATHOFF, G., SCHMIDT, B., GEPRÄGS, P., BAHL-O, R., DELLWIG, O., LEIPE, T., WINDE, V DEUTSCHMANN, A., STARK, A., GALLEGOTORRES, D., MARTINEZ-RUIZ, F (2012): CdE – Geochemistry, 72, 85-89.
NÄGLER, T.F., NEUBERT, N., BÖTTCHER, M.E., DELLWIG, O., SCHNETGER, B. (2011): Chem. Geol., 289, 1-11.
VON ALLMEN, K., BÖTTCHER, M.E., SAMANKASSOU, E. NÄGLER, T.F (2010): Chem. Geol., 277, 70-77

**K-Ar GEOCHRONOLOGY OF IGNEOUS AMPHIBOLE MACROCRYSTALS OF
MIOCENE TO PLIOCENE VOLCANICLASTICS, STYRIAN BASIN, AUSTRIA**

Bojar, H.-P.¹, Bojar, A.-V.^{1,2}, Hałas, S.³ & Wojtowicz, A.³

¹Department of Earth Sciences, Studierzentrum Naturkunde, Universalmuseum Joanneum,
Weinzötlstraße 16, 8045 Graz, Austria

²Department of Geography and Geology, Paris-Lodron University, Hellbrunnerstraße 34, 5020 Salzburg, Austria

³Mass Spectrometry Laboratory, Institute of Physics, Maria Curie-Skłodowska University, 20031 Lublin, Poland

The Styrian Basin basin is situated at the south-eastern margin of the Eastern Alps. Two basement highs separate the Styrian Basin in sub-basins: the Middle Styrian Basement High divides the shallower Western Styrian Basin (with ~800 m thick Neogene sediments) from the Eastern Styrian Basin (with a ~3000 m thick infill). A second, the South Burgenland Basement High, separates the West Pannonian from the Styrian Basin. The north-south trending Auersbach Basement High separates the Eastern Styrian basin in two sub-basins.

The Eastern Styrian Basin hosts distinct volcanic depocentres represented by Miocene (Karpatian to Badenian) shield volcanoes and volcanic tuff intercalations situated within Badenian sediments. A second phase of basaltic volcanism has a Late Miocene to Pliocene age. The Western Styrian Basin hosts only one Middle Miocene volcano. Most of the Middle Miocene volcanics are covered by sediments and are known only from boreholes and geophysical studies.

In this study (BOJAR et al., 2013), we present new K/Ar ages on amphibole phenocrysts of volcaniclastic rocks from the Styrian Basin, Austria, as well as from the adjoining areas. Beside Lower Miocene shield volcanoes and Pliocene effusive alkaline volcanic rocks the eastern Styrian Basin hosts a number of phreatomagmatic tuff occurrences. The tuffs contain the well known mantle xenoliths and frequent amphibole phenocrysts. The new age data indicate that the Late Miocene phreatomagmatic volcanism started at 7.51 Ma (Pontian) and ended at 2.72 Ma (Romanian). The complete interval of the youngest volcanism in the Styrian Basin covers 6 million years, similar to the volcanism of the western part of the Pannonian Basin and the Nógrád/Novohrad area (West Carpathian).

BOJAR H.-P., BOJAR A.-V., HAŁAS S., WÓJTOWICZ A. (2013): Geological Quarterly, 57, 3, doi: 10.7306/gq.1102 (in press).

**SYMPLECTITES IN HIGH PRESSURE GRANULITES FROM THE GFÖHL UNIT
(DUNKELSTEINERWALD, NÖ)**

Bourgin, N.¹, Petrakakis, K.² & Abart, R.¹

¹Department of Lithospheric Research, Althanstraße 14, 1090 Vienna, Austria

²Department of Geodynamics and Sedimentology, Althanstraße 14, 1090 Vienna, Austria

e-mail: a0542762@unet.univie.ac.at

Symplectites in a high pressure granulite from the granulite unit in Dunkelsteinerwald (Gföhl Unit) are investigated. The granulite has an exotic but homogeneous bulk rock composition rich in Mg and Al (14 % normative corundum). It contains garnet (Grt) (app. 50 % pyrope), clinopyroxene ($X_{Mg}=0.95$; Al_2O_3 : 9 wt.%), hornblende (Hbl) ($X_{Mg}=0.88$; Al_2O_3 : 15 wt.%), and plagioclase (Pl) (X_{An} up to 0.83). The primary microstructure is granular, medium- to fine-grained and well equilibrated. Cpx often shows exsolution lamellae and inclusions of Hbl.

Garnets with a size of 2-3 cm are not unusual, but more often they are resorbed and significantly smaller. The large garnets show numerous inclusions, e.g. of kyanite. Along the margins of and along cracks within large garnets, symplectites replace garnet as a breakdown product during decompression at about 700 °C. Different types of symplectite can be discerned comprising Al-Cpx, sapphirine (Spr), spinel (Spl), corundum (Crn), Pl ($X_{An} > 0.95$), orthopyroxene (Opx) and Hbl. Frequently, fine symplectites are enclosed in coarser symplectite phases. Plagioclase forms the symplectite matrix phase and frequently exhibits chemical zoning with decreasing X_{An} towards the symplectite-garnet interface.

Symplectitic growth leads to the formation of chemical zoning within the garnet adjacent to the symplectite replacement front. The composition variation is continuous and takes the form of a diffusion profile. Given that the temperature of symplectite formation can be estimated by Opx-Cpx thermometry, diffusion modelling can provide a clue on the duration of the symplectite forming event.

NEW APPROACHES FOR CHERT SOURCE PROVENANCE STUDIES

Brandl, M.¹, Hauzenberger, C.², Postl, W.³ & Trnka, G.⁴

¹Austrian Academy of Sciences, Inst. OREA, Fleischmarkt 22, 1010 Vienna, Austria

²University of Graz, Department of Earth Sciences, Universitätsplatz 2, 8010 Graz, Austria

³c/o Universalmuseum Joanneum, Department. of Geosciences, Weinzöttlstraße 16, 8045 Graz, Austria

⁴University of Vienna, Institute for Prehistory and Historic Archaeology, Franz-Klein Gasse 1,
1190 Vienna, Austria

e-mail: michael.brandl@oeaw.ac.at

Provenance studies of chert and flint raw materials (silicites) are an important component of archaeological research. The identification of the sources of rocks used for the production of chipped stone tools plays a significant role in the interpretation of lithic assemblages, e.g., revealing routes of migration, intercultural exchange and circulation networks of lithic raw materials (e.g., BARFIELD, 2003; PAWLICKOWSKI, 2008; ZVELEBIL, 2006). A transdisciplinary concept ("Multi Layered Approach" - MLA) presents a clear possibility for successfully sourcing chert and flint. The proposed method consists of a tripartite analytical system: Visual (macroscopical), microscopical and petrological/geochemical. For geochemical analysis, Laser Ablation-Inductively Coupled-Mass Spectrometry (LA-ICP-MS) was applied. LA-ICP-MS allows for the detection of trace element concentrations (0.1 ppm) in rock materials and has been well established in lithic raw material research (SPEAKMAN & NEFF, 2005; BRANDL et al., 2011; BRANDL et al., 2013). For the present undertaking, the MLA was applied to three case studies: 1) the differentiation between two tabular chert sources, (lacustrine – marine); 2) the assignment of radiolarites from the Lower Austrian Krems-Wachtberg site (Upper Palaeolithic) to the Northern Calcareous Alps and to Carpathian sources; 3) the identification of the sources of gunflints dating to the Napoleonic War-period from Schloss Neugebäude (Vienna). Our results demonstrate that it is not sufficient to rely on a single analysis method for chert sourcing. Only a combination of methods with different layers of resolution can lead to a successful determination of the provenance of chert artifacts.

BARFIELD, L.H. (2003): In: TSONEV, T., & MONTAGNARI KOKELJ, E. (eds.): The Humanized Mineral World: Towards social and symbolic evaluation of prehistoric technologies in South Eastern Europe, ERAUL 103, 109-113.

BRANDL, M., HAUZENBERGER, C., POSTL, W., MODL, D., KURTA, C., TRNKA, G. (2011): Quartär 58, 51-65.

BRANDL, M., HAUZENBERGER, C., POSTL, W., MARTINEZ, M.M., TRNKA, G., FILZMOSER, P. (2013): Quaternary International, <http://dx.doi.org/10.1016/j.quaint.2013.01.031>

PAWLICKOWSKI, M. (2008): In: KOSTOV, R.I., GAYDARSKA, B., GUROVA, M.(eds): Geoarchaeology and Archeomineralogy, Proceedings of the International Conference, 29-30 October 2008 Sofia, 18-21.

SPEAKMAN, R. J., NEFF, H. (2005): In: R. J. SPEAKMAN, R.J., NEFF, H.(eds.), Laser Ablation-ICP-MS in Archaeological Research. Albuquerque, 1-15.

ZVELEBIL, M. (2006): Journal of Anthropological Archaeology 25, 178-192.

E ISCHGL METEORITE: FINDING CIRCUMSTANCES, MINERALOGY AND BULK CHEMISTRY

Brandstätter, F.¹, Konzett, J.², Koeberl, C.^{3,4}, Ferrière, L.¹ & Mader, D.⁴

Department of Mineralogy and Petrography, Natural History Museum, Burgring 7, 1010 Wien, Austria

Institute of Mineralogy and Petrography, University of Innsbruck, Innrain 52, 6020 Innsbruck, Austria

³Natural History Museum, Burgring 7, 1010 Wien, Austria

⁴Department of Lithospheric Research, University of Vienna, Althanstrasse 14, 1090 Wien, Austria

e-mail: Franz.Brandstaetter@nhm-wien.ac.at

gl is the seventh meteorite named after an Austrian finding site. It was found in June 1976 mountain road about 2 km NW of the Tyrolean town Ischgl at an altitude of ca. 2000 m e sea level. According to the finder, a single fist-sized black stone had been fallen out of snow of an avalanche. He took the unusual stone to his home and kept it for more than 30 years. In 2007, the finder brought his find to the University of Innsbruck, where its stony nature was confirmed. In 2011, the stone was acquired by the Natural History Museum, Vienna, and subsequently officially classified as a LL6 chondrite (ANDSTÄTTER et al., 2013). The meteorite was investigated by a variety of techniques including optical microscopy, analytical SEM, SEM-CL, EMPA, and INAA. Macroscopically, the meteorite, weighing 710 g, is to a large extent fusion-crusted and exhibits well-developed regmaglypts. Its interior is a uniform light-grey colored rock without any distinct vesicles and shows only minor signs of terrestrial weathering. Microscopically, the meteorite is a monomict breccia consisting predominantly of coarse-grained mm to cm-sized clasts set in a fine-grained breccia matrix. Clasts and matrix are strongly recrystallized and only a few relic chondrules were encountered. Olivine, orthopyroxene and plagioclase are the main silicates. Minor minerals include clinopyroxene, chlorapatite and whitlockite. The opaque phases consist predominately of nickel-iron, troilite, and chromite. In addition, ilmenite and native gold occur as rare constituents. Compositionally, all mineral phases are consistent with the classification of the Ischgl meteorite as LL6 chondrite. Olivines and orthopyroxenes are calibrated with average compositions of Fa_{28.9} and Fs_{23.8} Wo_{2.1} respectively. Plagioclase (Ab₈₅An₁₀Or₅) is oligoclase. The compositions of the Ca-phosphates are in the range expected for equilibrated ordinary chondrites (JOLLIFF et al., 2006). Averaged compositions of the nickel-iron metal phases kamacite (4.42 wt. % Ni, 3.37 wt. % Co) and taenite (38.84 wt. % Ni, 1.10 wt. % Co) agree well with the compositions reported for these phases in LL chondrites (AFIATTALAB & WASSON, 1979). Bulk chemical compositions for 34 major and trace elements were performed for two samples of the Ischgl meteorite. A comparison of the INAA data with the mean bulk concentrations reported by KALLEMEYN et al. (1989) for LL6 chondrites shows an excellent match.

AFIATTALAB, F., WASSON, J.T. (1980): Geochim. Cosmochim. Acta, 44, 431-446.

ANDSTÄTTER, F., KONZETZ, J., KOEBERL, C., FERRIÈRE, L. (2013): Ann. Naturhist. Museum Wien, A, 115, 5-18.

JOLLIFF, B., HUGHES, J.M., FREEMAN, J.J., ZEIGLER, R.A. (2006): Am. Mineral., 91, 1583-1595.

KALLEMEYN, G.W., RUBIN, A.E., WANG, D., WASSON, J.T. (1989): Geochim. Cosmochim. Acta, 53, 2767.

SCANDIUM AND REE-RICH TOURMALINE FROM THE KRACOVICE PEGMATITE (BOHEMIAN MASSIF) AND ITS BREAKDOWN TO ALLANITE

Čopjaková, R.¹, Škoda, R.¹ & Vašinová Galiová, M.^{2,3}

¹Department of Geological Sciences, Masaryk University, Kotlářská 2, 611 37 Brno, Czech Republic
e-mail: copjakova@sci.muni.cz

²Department of Chemistry, Faculty of Science, Masaryk University, Kotlářská 2, 611 37 Brno, Czech Republic
³Central European Institute of Technology, Masaryk University, Kamenice 5, 625 00 Brno, Czech Republic

Kracovice pegmatite dyke (mixed NYF+LCT signature) cuts graphitic gneiss ~300 m W from the edge of the Třebíč Pluton (Moldanubian zone, Czech Republic). From contact inward the pegmatite consists of: a coarse-grained granitic unit (Kfs+Pl+Qtz+Bt+Ms+Tnt), abundant graphic unit (Kfs+Qtz±Bt) evolving to minor blocky K-feldspar and albite complex situated close to a small quartz core. Minor to accessory tourmaline occurs in graphic, blocky K-feldspar and albite units. Other minor to accessory minerals include Y,Sc-enriched spessartine, topaz, Li-micas, beryl, cassiterite, zircon, allanite-(Ce), Nb-rutile, columbite-fergusonite-, samarskite- group minerals, *wolframoxiolite*, F-rich hambergite, monazite-(C) and xenotime-(Y).

Magmatic tourmaline forms typically black columnar crystals (≤ 6 cm long), with composition corresponding to Al-rich schorl (6.92–7.37 apfu Al; 1.96–2.24 apfu Fe; 0.0–0.08 apfu Mg; $Fe_{tot}/(Fe_{tot}+Mg)$ ~0.98; 0.19–0.55 apfu F; X-site vacancy 0.28–0.44 pfu), usually overgrown and/or partly to almost fully replaced by later green magmatic hydrothermal fluor-elbaite (1.4–2.5 wt. % Li_2O ; high Al 6.96–7.32 apfu; variable Fe 0.3–1.45 apfu; high Mn 0.07–0.57 apfu, $Fe_{tot}/(Fe_{tot}+Mg)$ ~0.99; very high Na 0.83–0.99 apfu in X-site; high F 0.87–1.05 apfu). The magmatic Al-rich schorl shows high and variable Sc (42–31 ppm) and Y+REE (17–458 ppm) contents with steep LREE-enriched REE pattern (La_N/Gd_N ratio 10–29). Scandium and Y+REE contents in magmatic Al-rich schorl systematically decrease during tourmaline crystallization reflecting depletion of the melt in Sc,Y,REE I progressive crystallization and coeval crystallization of Y,REE(\pm Sc)-rich phases. Late magmatic-hydrothermal fluor-elbaite is significantly depleted in Sc (18–61 ppm) and Y+REE (4–31 ppm) with flatter REE pattern (La_N/Gd_N ratio 3–12). Both tourmaline generations show deep negative Eu anomaly ($Eu/Eu^* < 0.05$).

Sc,REE-rich central parts of magmatic Al-rich schorl are commonly partly altered and replaced by chlorite and allanite-(Ce). The allanite-(Ce) occurs exclusively in Al-rich schorl in samples where Al-rich schorl is rimmed and partly replaced by fluor-elbaite. The allanite-(Ce) has very steep LREE rich chondrite normalized REE pattern with significant negative Eu anomalies (Eu contents < 1 ppm) and shows unusually high Sc content (≤ 3.3 wt. % Sc_2O_3) as well as Sn enrichment (≤ 1.0 wt. % SnO_2). The replacement is resulted by interaction between Al-rich schorl and the Li- and F-rich pegmatite-derived fluids. REE and Sc required for formation of Sc-rich allanite probably released from dissolved REE and Sc enriched magmatic Al-rich schorl.

This work was supported by the research project GAČR P210/10/0743 and by the European Regional Development Fund project "CEITEC" (CZ.1.05/1.1.00/02.0068).

THE EFFECT OF THE α - β -QUARTZ TRANSITION BOUNDARY IN RE-EQUILIBRATION EXPERIMENTS

Doppler, G., Bakker, R. & Baumgartner, M.

Chair of Resource Mineralogy, Dep Applied Geological Sciences and Geophysics, University of Leoben, Austria
e-mail: gerald.doppler@unileoben.ac.at

Initially synthesized pure H₂O fluid inclusions in quartz are re-equilibrated under hydrothermal experimental conditions. A series of experiments within the α -quartz stability field is compared to a series which is carried out at similar P-T conditions but above the α - β transition boundary. The transition between α - and β -quartz is a major change in crystal properties, and therefore, it may influence the properties of fluids that are trapped in these crystals. Previous experiments (DOPPLER et al., 2013) have evidenced the importance of H₂O diffusion at constant pressures and relative high temperatures. This study illustrates that α - β transition of quartz is another important process of fluid inclusion re-equilibration. A series of re-equilibration experiments has been carried out by using pure D₂O at the experimental temperature of 625°C at 279.3 MPa and 322.2 MPa (α -quartz). A second series of experiments has been re-equilibrated at 675 °C (β -quartz) at the same experimental pressure as it was chosen for the α -quartz experiments. The relative amount of H₂O/D₂O in the fluid inclusions can be easily detected by measuring the melting temperatures T_m (SV \rightarrow LV) due to the linear relationship between T_m (0.0°C H₂O to +3.8 °C D₂O) and concentrations. During re-equilibration initially elongated and irregular shaped fluid inclusions tend to become more ideal and equant shaped. No differences in magnitude of shape changes can be detected regarding eventual differences between re-equilibration in the α -quartz stability field compared to the β -quartz modification. After re-equilibration noticeable changes in composition and density of the initially synthesized pure H₂O fluid inclusions can be recognized. In respect to the magnitude of changes there are considerable differences between α -quartz and β -quartz. The experiments in the β -field show higher T_m (ice) values compared to the experiments that have been carried out at the appropriate pressure conditions in the α -field. Within the α -field changes in density are related to the experimental pressure. At 279.3 MPa fluid inclusions are shifting to lower T_h (LV \rightarrow L) values, whereas at higher pressure they shift to higher homogenisation temperatures. Two experiments have been re-equilibrated with pure H₂O. The changes in density are inverted regarding to the α -field and the β -field. The experiments in the β -field show higher T_m (ice) values compared to the experiments that have been carried out at the appropriate pressure conditions within the α -field. Fluid inclusion changes are more dominant within the β -quartz field than within the α -quartz field at nearly equal P-T conditions. Regarding the T_h (LV \rightarrow L) of two β -quartz experiments it is assumed that the difference in experimental pressure of 43 MPa does not influence the diffusion rate of the fluid species regarding the same shift in homogenization temperatures. The invers changes in density of H₂O re-equilibration experiments are most likely related to the different quartz modifications. We would like to thank the Austrian Research Fund (FWF) for financial support (project no. P 22446-N21).

MINERAL-LIKE ARSENATES: CRYSTAL STRUCTURE OF $\text{Sr}_2\text{Mg}(\text{AsO}_4)_2 \cdot 2\text{H}_2\text{O}$ WITH KRÖHNKITE-TYPE CHAINS

Đorđević, T.

Institut für Mineralogie und Kristallographie, GeoZentrum, Universität Wien, Althanstraße 14, A-1090 Vienna,
Austria
e-mail: tamara.djordjevic@univie.ac.at

In order to understand the role of arsenic in the environment, one has to investigate structural features and stabilities of naturally occurring arsenic compounds. In addition, a study of mineral-related synthetic phases should be very helpful because they can appear as a result of human activities. $\text{Sr}_2\text{Mg}(\text{AsO}_4)_2 \cdot 2\text{H}_2\text{O}$ was synthesised during an on-going research on natural and synthetic arsenates, with a focus on their structural and spectroscopic classification. The crystal structure of the novel, hydrothermally synthesised $\text{Sr}_2\text{Mg}(\text{AsO}_4)_2 \cdot 2\text{H}_2\text{O}$ was refined from single-crystal X-ray diffraction data ($\text{MoK}\alpha$, 298 K, $2\theta_{\max} = 70^\circ$), starting from the atomic coordinates of the isotypic mineral gaitite, $\text{CaZn}_2(\text{AsO}_4)_2 \cdot 2\text{H}_2\text{O}$ (KELLER et al. 2004). The compound is triclinic, space group $P\bar{1}$, with $a = 6.0863(12)$, $b = 7.1542(14)$, $c = 5.6655(11)$ Å, $\alpha = 96.61(3)^\circ$, $\beta = 109.15(3)^\circ$, $\gamma = 108.39(3)^\circ$, $V = 214.46(7)$ Å³, $Z = 1$. The refinement yielded for 1869 ‘observed reflections’ with $F_o^2 \geq 4\sigma(F_o^2)$ $R_1(F)$ of 0.0250. The mean bond distances are $\langle \text{As}-\text{O} \rangle = 1.688$ Å, $\langle \text{Mg}-(\text{O},\text{H}_2\text{O}) \rangle = 2.105$ Å and $\langle \text{Sr}-(\text{O},\text{H}_2\text{O}) \rangle = 2.638$ Å. The positions of all H atoms were found in a difference-Fourier map and isotropically refined.

$\text{Sr}_2\text{Mg}(\text{AsO}_4)_2 \cdot 2\text{H}_2\text{O}$ represents the first Sr compound based on kröhnkite-type chains. This infinite tetrahedral-octahedral chain has a composition of $[\text{M}(\text{XO}_4)_2(\text{H}_2\text{O})_2]$, and is the main structural unit in a large family of compounds with the general formula $A_n\text{M}(\text{XO}_4)_2(\text{H}_2\text{O})_2$ [$A = \text{Na}^+, \text{K}^+, \text{Rb}^+, \text{Cs}^+, \text{Tl}^+, \text{NH}_4^+, \text{H}^+$ or Ca^{2+} ($n = 1, 2$), $\text{M} = \text{Mg}^{2+}, \text{Mn}^{2+}, \text{Fe}^{2+}, \text{Co}^{2+}, \text{Ni}^{2+}, \text{Cu}^{2+}, \text{Zn}^{2+}, \text{Cd}^{2+}, \text{Al}^{3+}, \text{Fe}^{3+}, \text{Sc}^{3+}, \text{In}^{3+}, \text{Tl}^{3-}$, $\text{X} = \text{P}^{5+}, \text{As}^{5+}, \text{S}^{6+}, \text{Se}^{6+}, \text{Cr}^{6+}, \text{Mo}^{6+}, \text{W}^{6+}$]. These compounds are assigned to seven types (triclinic A-C, E, G types and monoclinic D and I types), which differ in their linkage and stacking of the layers (FLECK & KOLITSCH, 2002; KOLITSCH & FLECK, 2006). $\text{Sr}_2\text{Mg}(\text{AsO}_4)_2 \cdot 2\text{H}_2\text{O}$ belongs to structure type A in this classification. Its crystal structure contains $[\text{Mg}(\text{AsO}_4)_2(\text{H}_2\text{O})_2]$ chains oriented along [001] composed of $\text{MgO}_4(\text{H}_2\text{O})_2$ octahedra alternating with each two AsO_4 tetrahedra sharing corners. These chains are connected through Sr-O bonds and one of two hydrogen bonds O5-H1…O4' ($i = -x+1, -y+1, -z+1$) = 2.645(3) Å, into layers parallel to (010), which are further linked by the Sr-O3 = 2.539(2) Å bond and the second hydrogen bond, O5-H1…O4' = 2.649(3) Å, into the three-dimensional structure. The [8]-coordinated Sr atoms occupy interstices between the chains.

Financial support of the Austrian Science Foundation (FWF) (Grant V203-N19) is gratefully acknowledged.

FLECK, M., KOLITSCH, U. (2002): Z. Kristallogr., 217, 453-443.

KOLITSCH, U., FLECK, M. (2006): Eur. J. Mineral., 18, 471-482.

KELLER, P., LISSNER, F., SCHLEID, T. (2004): Eur. J. Mineral., 16, 353-359.

NEW Rb-Sr DATA FROM PERMIAN META-PEGMATITES IN THE AUSTROALPINE MATSCH UNIT

Eberlei, T.¹, Habler, G.¹, Thöni, M.¹ & Schuster, R.²

¹Department of Lithospheric Research, University of Vienna, Althanstraße 14, 1090, Wien, Austria

²Geologische Bundesanstalt, Wien, Neulinggasse 38, 1030, Wien, Austria

e-mail: tobias.eberlei@univie.ac.at

Pegmatites of Permo-Triassic age are widespread in the Austroalpine basement of the Eastern Alps (SCHUSTER et al., 2001). Sm-Nd garnet ages from meta-pegmatites of the Austroalpine Matsch Unit in the range of 263–280 Ma were interpreted to date pegmatite emplacement (HABLER et al., 2009). During the Cretaceous, the meta-pegmatites were deformed at the greenschist–amphibolite facies transition (HABLER et al., 2009), locally producing mylonites with fabric gradients at the cm- to m-scale.

We investigate the relation between Cretaceous deformation and the behaviour of the Rb-Sr system in muscovite clasts in Permian meta-pegmatites. Primary, cm-sized muscovites show a range of deformation-related microstructures, such as kinks, fractures, folds, micro-shearzones and undulous extinction. Rb-Sr muscovite–whole rock ages of coarse-grained fractions range at 240–262 Ma in weakly deformed samples. They are interpreted as minimum ages of Permian cooling below c. 550 °C. In mylonitic meta-pegmatites the Rb-Sr muscovite ages of coarse-grained fractions scatter widely at 249–172 Ma, reflecting an influence of Alpine deformation and/or fluid flow during the Cretaceous.

The new data imply that deformation, supposedly in combination with fluid activity, has affected the Rb-Sr systematics of muscovite clasts in Permian meta-pegmatites, while Permian cooling ages can still be obtained from weakly deformed samples.

HABLER, G., THÖNI, M., GRASEMAN, B. (2009): Miner. Petrol., 97, 149–171.

SCHUSTER, R., SCHARBERT, S., ABART, R., FRANK, W (2001): Mitt. Ges. Geol. Bergb. Stud., 45, 111–141.

ON THE TRUE SPACE-GROUP SYMMETRY OF NORSETHITE, $\text{BaMg}(\text{CO}_3)_2$

Effenberger, H., Miletich, R. & Libowitzky, E.

Institut für Mineralogie und Kristallographie, Universität Wien, Althanstrasse 14, 1090 Wien, Austria
e-mail: herta.silvia.effenberger@univie.ac.at

The crystal structure of norsethite was solved by LIPPMANN (1968) (X-ray powder data, synthetic material) in space group $R\bar{3}2$. EFFENBERGER & ZEMANN (1985) discussed three structure models based on single-crystal two-circle diffractometer data: ordered models in space group (1) $R\bar{3}m$ (most appropriate), and (2) $R\bar{3}2$; (3) split oxygen position model in $R\bar{3}m$.

A re-investigation (NONIUS four-circle diffractometer, CCD detector) was performed at 100, 150, 200, 250 and 273 K. The crystal structure is characterized by layers parallel to (001) of alternating $\text{Ba}^{121}\text{O}_{12}$ and $\text{Mg}^{161}\text{O}_6$ polyhedra with the CO_3 groups in between. With decreasing temperature the cell parameters a and c as well as their ratio c/a decrease. At low temperature the structure refinements according model (1) exhibit minor shortenings of the Ba–O and Ca–O bond lengths (C–O varies insignificantly only) going along with reduced displacements of the Ba, Mg and C atoms; the decrease of the anisotropy is significant for the Ba and Mg atoms only. More complex is the situation for the O atom: at room temperature a strong anisotropic displacement of the O atom with the maximal elongation in the [010] direction occurs. Whereas the equivalent isotropic displacement is proportional to the temperature, its anisotropy is inversely proportional. Successive refinements according to model (2) and (3) were performed.

Images taken with a STOE StadiVari diffractometer (Pilatus 300 K pixel-detector, Mo micro-focus X-ray source) revealed a doubling of the lattice parameter c , however the number of detectable reflections did not allow a structure refinement.

EFFENBERGER, H., ZEMANN, J. (1985): Z. Kristallogr., 171, 275-280.

LIPPMANN, F. (1968): Tschermaks Min. Petr. Mitt., 12, 299-318.

STRUCTURAL AND CHEMICAL INVESTIGATION OF A ZONED SYNTHETIC CU-RICH TOURMALINE

Ertl, A.¹, Vereshchagin, O.S.², Giester, G.¹, Meyer, H.-P.³, Ludwig, T.³,
Rozhdestvenskaya, I.V.² & Frank-Kamenetskaya, O.V.²

¹Institut für Mineralogie und Kristallographie, Universität Wien, Althanstrasse 14, 1090 Wien, Austria

²Department of Mineralogy, Saint Petersburg State University, Universitetskaya nab. 7/9, 199034 St. Petersburg,
Russia

³Institut für Geowissenschaften, Universität Heidelberg, Im Neuenheimer Feld 236, 69120 Heidelberg, Germany
e-mail: andreas.ertl@aln.net

The studied blue Cu-rich tourmaline was synthesized (at 650 °C/1.5 kbar) at the Institute of Mineralogy and Petrography, Novosibirsk (LEBEDEV et al., 1988). It was grown on natural elbaite as seed crystal and it was shown that this overgrowth consists of three different zones. The first tourmaline zone has the formula (EMPA, SIMS) $\sim^X(\text{Na}_{0.8}\square_{0.2})^Y(\text{Al}_{2.0}\text{Cu}_{0.9}\square_{0.1})^Z\text{Al}_6^T(\text{Si}_{5.1}\text{Al}_{0.9})\text{O}_{18}(\text{BO}_3)_3^V(\text{OH})_3^W[\text{O}_{0.7}\text{F}_{0.2}(\text{OH})_{0.1}]$ with lattice parameters $a = 15.835(1)$ Å, $c = 7.093(1)$ Å ($R = 2.4\%$). The enlarged $\langle T\text{-O} \rangle$ distance of 1.625(1) Å is in agreement with the T -site occupancy. The second zone has the formula (EMPA, SIMS) $\sim^X(\text{Na}_{0.8}\square_{0.2})^Y(\text{Al}_{1.8}\text{Cu}_{1.1}\square_{0.1})^Z\text{Al}_6^T(\text{Si}_{5.1}\text{Al}_{0.7}\text{B}_{0.2})\text{O}_{18}(\text{BO}_3)_3^V(\text{OH})_3^W[(\text{OH})_{0.4}\text{F}_{0.3}\text{O}_{0.3}]$ with $a = 15.824(1)$, $c = 7.087(1)$ Å ($R = 2.3\%$). The third zone (highest Cu content with ~14 wt% CuO) has the formula (EMPA, SIMS) $\sim^X(\text{Na}_{0.8}\square_{0.2})^Y(\text{Al}_{1.2}\text{Cu}_{1.8}\square_{0.1})^Z\text{Al}_6^T(\text{Si}_{5.2}\text{Al}_{0.4}\text{B}_{0.4})\text{O}_{18}(\text{BO}_3)_3^V(\text{OH})_3^W[(\text{OH})_{0.6}\text{F}_{0.4}]$. The formula for the third zone, as determined by refinement, is $\sim^X(\text{Na}_{0.8}\square_{0.2})^Y(\text{Al}_{1.6}\text{Cu}_{1.4})^Z\text{Al}_6^T[(\text{Si},\text{Al})_{5.4}\text{B}_{0.6}]\text{O}_{18}(\text{BO}_3)_3^V(\text{OH})_3^W[(\text{OH})_{0.7}\text{F}_{0.3}]$ with $a = 15.849(1)$ Å, $c = 7.087(1)$ Å ($R = 2.5\%$). The reduced $\langle T\text{-O} \rangle$ distance of 1.616(1) Å is in agreement with some B at the T site. Although the $\langle Z\text{-O} \rangle$ distance with 1.906(1) Å is within errors similar to the $\langle Z\text{-O} \rangle$ distances of the other zones, the refinement $\text{Al} \leftrightarrow \text{Cu}$ gives (only for this zone) some evidence for a small amount of Cu (~1%) at the Z site of this very Cu-rich tourmaline. The occurrence of Cu at the Z site was already proposed by VERESHCHAGIN et al. (2013). Although the refined value is higher than the 3σ error, another evidence (e.g., spectroscopic investigation) would be necessary for a final prove of the occurrence of Cu at the Z site. However, the occupancy of significant amounts of B and/or Al at the T site of this synthetic Cu-rich tourmaline seems to be well established.

LEBEDEV, A.S., KARGALCEV, S.V., PAVLYCHENKO, V.S. (1988): In: Proc. Gen. & Exper. Mineral. Growth and properties of crystals. Novosibirsk, Nauka. (in Russian)

VERESHCHAGIN, O.S., ROZHDESTVENSKAYA, I.V., FRANK-KAMENETSKAYA, O.V., ZOLOTAREV, A.A., MASHKOVTEV, R. I. (2013): Am. Mineral.. 98, (in press).

U-PB MICROGEOCHRONOLOGY BY LASER ABLATION ICP-MS: APPLICATIONS, LIMITATIONS AND FUTURE DEVELOPMENTS

Frei, D.

Department of Earth Sciences, Stellenbosch University, Private Bag X1, 7602 Matieland, South Africa
e-mail: dirkfrei@sun.ac.za

Among applications for laser ablation ICP-MS (LA ICP-MS) the microanalytical age dating of U-rich phases employing the U-Th-Pb decay scheme is still one of the most challenging in terms of the required spatial resolution, precision and accuracy. In recent years, the number of laboratories that perform microanalytical U-Pb-Th dating employing LA ICP-MS has increased rapidly. Accordingly, the actual number of the peer-reviewed publications applying this technique is rapidly increasing. However, the absolute number of publications is still low compared to studies using conventional techniques (e.g. ID-TIMS, SHRIMP). Furthermore, a significant number of the papers published over the last decade are dealing with various aspects of improving the technique, showing the need for further developments.

Zircon belongs to the key minerals for unravelling many processes during earth history. The U-Th-Pb systematic in most zircon grains is complex due to alteration processes, such as dissolution, recrystallization and new zircon growth. A spatial resolution of 5 to 40 µm are commonly needed to resolve the different age pattern in complex grains. Up to date, only few studies have shown that they are capable to routinely analyse these subdomains in zircon and to precisely detect low Pb contents, which are relative common, e.g., for young zircons and detrital zircon grains. Therefore, many zircons are currently not amenable to microanalytical U-Pb-Th age dating employing LA ICP-MS.

I present a method for microanalytical U-Th-Pb age dating of zircon and a wide range of other U-rich mineral phases. The method is based on simple off-the-shelf technology (a Resonetics S155 excimer laser ablation system coupled to a Thermo-Finnigan Element II magnetic sectorfield – ICP-MS). The spatial resolution, limited by signal intensity of ^{207}Pb , is usually between 20 µm beam diameter and <20 µm ablation depth. A relative simple approach was used to correct for within-run U-Pb fractionation before normalisation to a repeatedly analysed reference zircon. The internal and external precision (over 4-8 hrs) generally achieved for the $^{206}\text{Pb}/^{238}\text{U}$ (0.5-1 %, 1-2 %, 1s) and the $^{207}\text{Pb}/^{206}\text{Pb}$ (0.5-1.5 % 1s) ratios is comparable to or even better as precision reported by other laboratories, although up to 30 times less material is consumed. The most important factor controlling the error is counting statistics in case of the $^{207}\text{Pb}/^{206}\text{Pb}$ ratio and the reproducibility of the ablation process and sample heterogeneity for the $^{206}\text{Pb}/^{238}\text{U}$ ratio. We will present data from a wide range of different studies currently performed in our laboratories. Analysed grains spanning a wide range of U-bearing minerals (e.g., zircon, baddeleyite, perowskite) demonstrating their natural complexity. The results of these studies will illustrate the abilities but also the outstanding challenges for microanalytical LA ICP-MS dating of complex minerals using the U-Pb-Th decay scheme.

PETROGRAPHIE UND MINERALCHEMIE VON BETAFIT AUS DEM POLLESTAL (ÖTZTAL-STUBAI KRISTALLIN)

Gasteiger, P., Tropper, P., Haefeker, U. & Tessadri, R.

Institut für Mineralogie und Petrographie, Universität Innsbruck, Innrain 52f, A-6020 Innsbruck, Österreich
e-mail: peter.tropper@uibk.ac.at

Im zentralen Bereich des Ötztals (im Pollestal) treten Metakarbonatlinsen umgeben von Metabasiten und granitischen Gesteinen auf. Die Metakarbonate enthalten folgende Paragenese: Klinopyroxen + Tremolit + Phlogopit + Apatit + Pyrit + Geikielit + Zirkonolith + Zirkon + Betafit + Kalzit + Dolomit. Im Rahmen dieser Untersuchungen wurde eine Metakarbonatprobe aus dem Pollestal mittels Elektronenstrahlmikrosonde und Mikro-Raman Spektroskopie genauer untersucht. Diese Probe wird von einer Ader durchzogen die folgende Paragenese enthält: Klinopyroxen + Tremolit + Phlogopit + Apatit + Titanit + REE-, Zirkon-, Nb- und Ti- Phasen. Mikrosondenanalysen lassen auf das Mineral Betafit schliessen das nach der neuen Klassifikation von ATENCIO et al. (2010) als Oxycalcibetafit $\text{Ca}_2(\text{Ti},\text{Nb})_2\text{O}_6\text{O}(\text{U})$ mit einem hohen Urangehalt klassifiziert werden kann. Die Betafite sind mit Zirkon und Geikielit verwachsen und die sie sind chemisch zoniert wobei die TiO_2 Gehalte zwischen 13.2 und 18.9 Gew.% und die Nb_2O_5 Gehalte zwischen 27.3 und 37.3 Gew.% liegen. Nennenswert sind die extrem hohen UO_2 Gehalte von bis zu 21 Gew.%. Die Gesamtsumme variiert zwischen 98 und 100 Gew.% wobei die meisten Summen zwischen 99 und 100 Gew.% liegen, was auf keine oder nur gering Anwesenheit von OH schliessen lässt, oder auf einen Verlust bei der Analyse durch die kleine Korngrösse des Betafits. Mittels Mikro-Raman Spektroskopie wurde festgestellt, dass der Betafit keine bzw nur sehr geringe Mengen an OH in seiner Struktur enthält.

Wie schon KOZLIK (2011) in seiner Arbeit beschrieben hat, kann das Auftreten von Betafit und anderen Ti-Zr-REE-hältigen akzessorischen Minerale ein Hinweis für eine prä-variszische Kontaktmetamorphose sein. Die Entstehung des Betafites kann hier als Mobilisation von HFSE- und REE-reichen Fluids gedeutet werden. Die Fluids zirkulierten wahrscheinlich entlang von Rissen im Gestein und dadurch kam es zur Bildung von den akzessorischen Mineralien. Die nachfolgenden variszische und eo-alpine Metamorphosen hatten auf die Stabilität dieses Minerals wahrscheinlich keinen Einfluss.

ATENCIO, D., ANDRADE, B. M., CHRISTY, G. A., GIERÉ, R., KARTASHOV, M. P (2010): The pyrochlore supergroup of minerals: nomenclature.- doi: 10.3749/canmin.48.3.673.

KOZLIK, M. (2011): Petrologische Untersuchungen zu den Metakarbonaten des zentralen Ötzal-Stubaikristallins (Pollestal)- unveröffentlichte Diplomarbeit. Universität Innsbruck.

ANDROSITE-(Ce) AND FERRIANDROSITE-(Ce) AS INDICATOR FOR LOW-GRADE REE MOBILITY IN THE VEITSCH MN DEPOSIT (STYRIA)

Girtler, D.¹, Troppler, P.¹ & Hauzenberger, C.²

¹ Institute of Mineralogy and Petrography, University of Innsbruck, Innrain 52, A-6020 Innsbruck, Austria

² Institute of Earth Sciences, University of Graz, Universitätsplatz 2, A-8010 Graz, Austria

e-mail: daniela.girtler@student.uibk.ac.at

Several carbonate-hosted Fe and Mn ore deposits occur within the upper Austroalpine Grewywacke Zone. The Mn deposit of Veitsch at the Kaskogel and north of the Friedelkogel consists of lense-shaped carbonate bodies of ca. 1.5 m in length which are thought to have formed as sedimentary or submarine hydrothermal Mn-deposits. The manganese silicates described from this deposit are: tephroite, rhodonite, spessartine, Mn-chlorite, sonolite and friedelite. The Mn-carbonates are rhodochrosite and kutnahorite. Sulfides such as sphalerite, galena, chalcopyrite, Co-pentlandite, linnacite, carrollite, cobaltite and pyrite also occur.

During this investigation in several samples unusual REE-Mn-(V)-bearing minerals of the allanite subgroup were found. The allanite occurs in a veinlet with the mineral assemblage REE-Mn-allanite + tephroite + spessartine + Mn-chlorite + rhodochrosite + kutnahorite + serpentine. The REE-content varies between 0.6 and 1.0 a.p.f.u. in which Ce dominates, and Mn ranges from 1.0 to 1.6 a.p.f.u. In one sample elevated V contents of 0.8-7.3 wt.% V₂O₃ were observed. The BSE images and chemical analysis reveal a complex zoning of the mineral with increasing Fe₂O₃, MnO and decreasing Al₂O₃ and CaO towards the rim, whereas the REE are unzoned except for V-bearing areas. In addition, it is planned to conduct laser-ICP MS analysis of the zoned crystals to obtain the full spectrum of trace elements of these rare minerals. Charge balance considerations and site assignments indicate that the fraction of Mn³⁺ is very low (<0.2 a.p.f.u.). In terms of nomenclature, ARMBRUSTER et al. (2006) suggest that the dominant cations on the A1 and M3 sites are responsible for the correct root name, thus the names ferriandrosite-(Ce) (Mn²⁺ REE Fe³⁺ Al Mn²⁺ (SiO₄)₃ OH) and androsite-(Ce) (Mn²⁺ REE Al Al Mn²⁺ (SiO₄)₃ OH) should be used. For three other occurring compositions (Ca²⁺ REE Fe³⁺ Al Mn²⁺ (SiO₄)₃ OH), (Ca²⁺ REE Al Al Mn²⁺ (SiO₄)₃ OH) and (Ca²⁺ REE V³⁺ Al Mn²⁺ (SiO₄)₃ OH), where Ca occupies the A1 site, an additional root name, which is not specified yet, is required. On the other hand, BONAZZI et al. (2009) observed similar compositions like in this study and named the composition (Ca²⁺ REE Fe³⁺ Al Mn²⁺ (SiO₄)₃ OH) a „relation to ferriallanite-(Ce) along the substitutional vector $\overset{\text{M}^3(\text{Mn}^{2+})}{\rightarrow} \overset{\text{M}^3(\text{Fe}^{2+})}{\rightarrow}$ “

Textural observation indicates that these REE-bearing minerals formed along veins during low-grade (Eo-Alpine greenschist-facies) REE mobility in these Mn-carbonates.

ARMBRUSTER, T., BONAZZI, P., AKASAKA, M., BERMANEK, V., CHOPIN, C., GIERÉ, R., HEUSS-ASSBICHLER, S., LIEBSCHER, A., MENCHETTI, S., PAN, Y., PASERO, M. (2006): Eur. J. Mineral., 18, 551-567.

BONAZZI, P., HOLTSTAM, D., BINDI, L., NYSTEN, P., CAPITANI, G. (2009): American Mineralogist, 94, 121-134.

BACTERIOGENICALLY INDUCED SULFURIC ACID ATTACK ON CONCRETE IN AN AUSTRIAN SEWER SYSTEM

Grengg, C.¹, Mittermayr, F.^{1,2}, Baldermann, A.¹, Böttcher, M. E.³, Leis, A.⁴ & Dietzel, M.²

¹Institute of Applied Geosciences, Graz University of Technology, Rechbauerstraße 12, 8010 Graz, Austria

²Institute of Technology and Testing of Building Materials, Graz University of Technology, Inffeldgasse 24,
8010 Graz, Austria

³ Leibniz Institute for Baltic Sea Research (IOW), Seestraße 15, D-18119 Warnemünde, Germany

⁴RESOURCES – Institute for Water, Energy and Sustainability, Joanneum Research, Elisabethstraße 18/2, 8010
Graz, Austria

e-mail: cyrill.grengg@gmx.at

This study provides insights in the processes that cause severe concrete corrosion and deterioration of an Austrian sewage system, which urgently requires restoration.

Various crucial parameters for detecting alteration features were determined in the field and laboratory, including temperature, alkalinity, pH, and conductivity measurements as well as ion-chromatography, inductively coupled plasma optical emission spectrometry and X-ray diffraction analyses. Furthermore, the concentration of gaseous H₂S, CH₄ and CO₂ within the sewer pipe atmosphere was measured. Dissolved sulfate content of the damaged concrete and the corresponding aqueous solutions were obtained, by precipitation as barium sulfate.

The deterioration of the sewage system is attributed to a couple of complex processes, which are referred to as bacteriogenically induced sulfuric acid attack. Anaerobic bacteria, present within the sewage systems, have consumed the organic matter quantitatively, thereby reducing SO₄²⁻ to H₂S_(g). Changes in the surrounding air pressure or water convection within the sewage chamber subsequently promoted degassing of the H₂S, followed by its oxidation into elemental sulfur or other sulfur containing phases by the aerobic bacteria Acidithiobacilli. This led to the formation of sulfuric acid that reacted with the CH-phases of the concrete to form gypsum (SCRIVER & DE BELIE, 2013), which finally caused the severe damage of the concrete.

Within the most heavily damaged concrete the SO₄ concentrations were calculated to be 14-27 wt. %, which correlate well with abundant gypsum. In contrast, the SO₄ concentration of the aqueous solutions was surprisingly low, ranging between 13 and 41 ppm. The pH of the sewage water fluctuated between 6 and 8 as well as the H₂S_(g) concentrations, which were from below the detection limit up to >100 ppm. The CO_{2(g)} concentration ranged between 400 and 2500 ppm, while the CH₄ concentration remained below the detection limit.

Further investigations, including sulfur isotope measurements, are planned, which may give new insights into the complexity of bacterially controlled reaction paths that finally cause the concrete damage in sewer systems.

SCRIVER, K., DE BELIE, N. (2013): In: BERTON, A., DE BELIE, N., ALEXANDER M. (eds): Performance of Cement-Based Materials in Aggressive Aqueous Environments, 305-318, Springer, Ghent.

ZONATION AND Bi-RICH INCLUSIONS IN ANDRADITE CRYSTALS FROM KOPE SKARN DEPOSIT, SLOVENIA

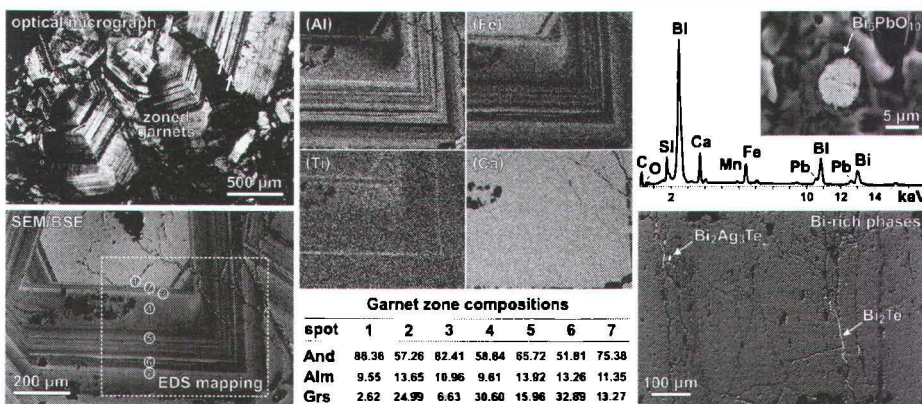
Grom, N.¹, Rečnik, A.², Samardžija, Z.², Vrhovnik, P.¹, Daneu, N.² & Dolenec, T.¹

¹Department of Geology, Faculty of Natural Sciences and Engineering, University of Ljubljana,
Aškerčeva 12, SI-1000 LJUBLJANA, Slovenia

²Department for Nanostructured Materials, Jožef Stefan Institute,
Jamova cesta 39, SI-1000 LJUBLJANA, Slovenia

e-mail: nina.grom@gmail.com

Kope mountains are located in western part of the Pohorje mountain range, which belongs to a south eastern part of the Eastern Alps (NE Slovenia). The Pohorje metamorphic and igneous complex belongs to the eastern continuation of the Periadriatic Lineament shifted northwards. In NW outskirts of Kope mountain intrusions of granodioritic magma into upper Cretaceous carbonate rocks produced an epidote-andradite-hedenbergite skarn with contact metamorphic ore mineralization, dominated by magnetite, which has been mined as iron ore in 18th century (GERMOVŠEK, 1953). We investigated zoned growth and composition of garnets. Electron microscopy study showed that growth zones have a variable composition. They are dominated by andradite with variable fractions of grossular and almandine. In addition to compositional variations of zones, we detected various Bi-rich phase inclusions using energy dispersive X-ray spectroscopy (EDS). These include elementary Bi with traces of tellurium, Bi-tellurides (Bi_3Te and Bi_2Te), unknown Ag-rich Bi-telluride ($\text{Bi}_2\text{Ag}_3\text{Te}$), bismuthinite (Bi_2S_3) as the only sulphide, and oxides bismite (Bi_2O_3) and unknown Pb-rich Bi-oxide ($\text{Bi}_6\text{PbO}_{10}$).



Study of zones and Bi-rich inclusions in andradite garnets from Kope. Backscattered electron (BSE) image shows light and dark bands depending on the ratio of heavy vs. light elements, e.g. the core of the crystal (spot 1) is dominated by andradite (And) while almandine (Alm) and grossular (Grs) fractions are low. Elemental maps for Al, Fe, Ti and Ca are shown above the table. Bi-rich inclusions present in garnets are shown on the right side. EDS spectrum (above), recorded under 30 keV, discloses the presence of Pb in some inclusions.

THE EFFECT OF CLASS 1 H₂O ON A RAMAN ACTIVE T₂ STRETCHING MODE IN Mg-CORDIERITE

Haefeker, U.¹, Kaindl, R.² & Tropper, P¹

¹Institute of Mineralogy and Petrography, University Innsbruck, Innrain 52, A-6020 Innsbruck, Austria

²MATERIALS – Institute for Surface Technologies and Photonics, Functional Surfaces, JOANNEUM RESEARCH Forschungsgesellschaft mbH, Leobner Straße 94, A-8712 Niklasdorf, Austria
e-mail: udo.haefeker@uibk.ac.at

The structure of orthorhombic cordierite consists of six-membered (Al, Si)O₄ rings, which are laterally linked by additional (Al, Si)O₄ tetrahedra. Stacked rings form channels parallel *c* which can incorporate volatiles like H₂O and CO₂ in various amounts. Octahedral sites contain mainly Mg and Fe. Five tetrahedrally coordinated sites and channel sites have to be distinguished in the structure: (M)₂(T₁1)₂(T₂6)₂(T₂3)₂(T₂1)₂(T₁6)O₁₈(Ch0,Ch1/4) (e.g. BERTOLDI et al., 2004). In orthorhombic cordierite Si and Al are fully ordered. The ring tetrahedra T₂1 and T₂3 contain Si and T₂6 contains Al. H₂O is incorporated into the Ch1/4 positions and two classes of H₂O can be distinguished: class 1 H₂O, which is subdivided in three types with different orientations and class 2 H₂O, which interacts with alkali cations and is subdivided in two types with different orientations (KOLESOV & GEIGER, 2000).

Raman spectroscopic investigations of alkali-free synthetic Mg-cordierites with H₂O contents of 0 – 2 wt.% revealed a guest-host interaction between class 1 H₂O and Si-channel tetrahedra. A peak at 1189 cm⁻¹ in anhydrous Mg-cordierite is assigned to T₂1 and T₂3 stretching vibrations (KAINDL et al., 2011). The peak shifts towards lower energies with increasing H₂O contents and occurs at 1186 cm⁻¹ in samples with 2 wt.% H₂O. The channel volatiles (H₂O, CO₂) of natural Mg-rich cordierite (from White Well, Australia) were removed by heating. The comparison of the Raman spectra before and after heating yields a 4 cm⁻¹ peak shift at 1189 cm⁻¹ towards higher energies. An arrestive effect of H₂O and other channel volatiles to the symmetric vibration of adjacent T_{2(Si)} tetrahedra can be described with Raman spectroscopy.

BERTOLDI, C., PROYER, A., GARBE-SCHÖNBERG, D., BEHRENS, H., DACHS, E. (2004): Lithos, 78, 389- 409.

KAINDL, R. , TÖBBENS, D.M., HAEFEKER, U. (2011): American Mineralogist, 96, 1568-1574.

KOLESOV, B.A., GEIGER, C.A. (2000): American Mineralogist, 85, 1265-1274.

RAMAN SPECTROSCOPY OF N₂ IN NATURAL CORDIERITE AND BERYL SINGLE CRYSTALS

Haefeker, U.¹, Kaindl, R.², Tropper, P.¹ & Konzett, J.¹

¹Institute of Mineralogy and Petrography, University Innsbruck, Innrain 52, A-6020 Innsbruck, Austria

²MATERIALS – Institute for Surface Technologies and Photonics, Functional Surfaces, JOANNEUM RESEARCH Forschungsgesellschaft mbH, Leobner Straße 94, A-8712 Niklasdorf, Austria.

e-mail: udo.haefeker@uibk.ac.at

Natural Cordierite with the idealized composition (Mg,Fe)₂[Al₄Si₅O₁₈]*x(H₂O,CO₂) occurs mostly as the orthorhombic polymorph with an ordered Al/Si-distribution on the tetrahedral sites. The structure contains stacked six-membered rings of (Si,Al)O₄ forming channels parallel to the crystallographic *c*-axis. The rings are linked laterally and vertically by additional (Al,Si) tetrahedrons, octahedral sites contain mainly Mg and Fe²⁺. Similarly, the structure of hexagonal beryl with Al₂Bc₃(Si₆O₁₈) contains six-membered rings of SiO₄ stacked along *c* which are laterally linked by BeO₄ tetrahedra, octahedral sites contain Al. Volatiles like H₂O, CO₂ and N₂ can be incorporated into the structural channels of both minerals in various amounts. Natural cordierite single crystals with N₂ contents of 104 and 446 ppm (samples 129875 and H06, LAZZERI, 2012) as well as a beryl single crystal (from Texel complex, Italy) were investigated with micro Raman spectroscopy under ambient conditions. The N₂ stretching vibration occurs at 2325 cm⁻¹ in cordierite and 2328 cm⁻¹ in beryl and is thus shifted towards lower energies in both minerals when compared to N₂ gas. Polarized spectra show that the N₂ molecules in cordierite are incorporated perpendicular to the crystallographic *c* axis and are preferentially aligned parallel to *a*, which is consistent with former optical and X-ray diffraction studies (ARMBRUSTER, 1985). A plot of the N₂ Raman peak intensities vs. N₂ contents in ppm indicates a linear relationship in cordierite. Analogous to cordierite the N₂ molecule in beryl is incorporated perpendicular to *c*.

LAZZERI, K. E. (2012): Lehigh University Thesis, Paper 1327.

ARMBRUSTER, T. (1985): Physics and Chemistry of Minerals, 12, 233-245.

STRUCTURAL AND RAMAN-SPECTROSCOPIC INVESTIGATIONS OF SYNTHETIC HEXAGONAL AND ORTHORHOMBIC Fe-CORDIERITE

Haefeker, U.¹, Kaindl, R.², Tropper, P¹, Krüger, H.¹,
Kahlenberg, V¹ & Orlova, M.¹

Institute of Mineralogy and Petrography, University Innsbruck, Innrain 52, A-6020 Innsbruck, Austria

MATERIALS – Institute for Surface Technologies and Photonics, Functional Surfaces, JOANNEUM

RESEARCH Forschungsgesellschaft mbH, Leobner Straße 94, A-8712 Niklasdorf, Austria.

e-mail: udo.haefeker@uibk.ac.at

Crystal structures of synthetic hexagonal and orthorhombic Fe-cordierite polymorphs with space groups P6/mcc and Cccm were refined from single-crystal X-ray diffraction data to $\chi = 3.14\%$ and $R_{1,\text{ortho}} = 4.48\%$. The substitution of the larger Fe^{2+} for Mg leads to complete structural changes and an increase of the unit cell volumes, with a, c (hex) = 1(16) Å, 9.2852(5) Å and a, b, c (ortho) = 17.2306(2) Å, 9.8239(1) Å, 9.2892(1) Å. Fe poration leads to an increase of the octahedral volumes, although the octahedral diameter reduction of the c-axis decreases in both polymorphs. X-ray powder diffraction analysis indicates a high degree of Al/Si ordering in the orthorhombic polymorph with a distortion of ~0.24 (MIYASHIRO, 1957). Estimations of site occupancies based on the refined tetrahedral volumes result in the following values for hexagonal Fe-cordierite: ~Al for T₁ and ~28% Al for T₂. Raman spectra of the hexagonal polymorph were recorded at ambient conditions and at -190 °C using laser-light with 633 and 532 nm wavelength for excitation.

SHIRO, A. (1957): American Journal of Science, 255, 43-62.

MINERALOGY AND GEOCHEMISTRY OF SOILS OF THE ALNÖ CARBONATITE COMPLEX, SWEDEN

Haslinger, E.¹, Williams, C.T², Fröschl, H.³, Koller, F⁴, Gier, S.⁵ & Ottner, F⁶

¹AIT Austrian Institute of Technology GmbH, Konrad-Lorenz-Straße 24, 3430 Tulln

²Natural History Museum, Dept. Mineralogy, Cromwell Rd., London SW7 5BD, United Kingdom

³Seibersdorf Labor GmbH, 2444 Seibersdorf

⁴Dept. of Lithospheric Research, Universität Wien, Althanstraße 14, 1090 Wien

⁵Dept. of Geodynamics and Sedimentology, Althanstraße 14, 1090 Wien

⁶Institut für Angewandte Geologie, Universität für Bodenkultur, Peter-Jordan-Straße 70, 1190 Wien

e-mail: edith.haslinger@ait.ac.at

The Alnö Carbonatite Complex is located NE of the town Sundsvall, Sweden. The intrusion of carbonatites and alkaline rocks into the host rocks migmatitic gneisses - took place around 560 Ma BP. The differences in soil development as well as the petrology and geochemistry of the soils in this ring-shaped intrusion were studied in soils on gneiss and different types of alkaline rocks. The parent rocks in the soil profiles were unaltered/ slightly fenitized gneisses, fenites, ijolites, sövites and alnöites.

The soils on the alkaline rocks showed anomalous contents of Ba, Cr, F, Nb, Sr, Th, U and REE, which are enriched in the alkaline rocks in minerals such as monazite, perovskite, spinel and sphene and by substitution processes in the crystal structure, e.g. Ti by Nb in perovskite or Ca by Eu in plagioclase. The alkaline dykes in the intrusion strongly influenced the soil mineralogy, geochemistry and pedogenesis in contrast to the soils developed on highly acidic gneiss soil profiles. The differences are also visible in the field by contrasting vegetation which facilitates the detection of alkaline dykes in the densely wooded area of the Alnö Carbonatite Complex.

HASLINGER, E., OTTNER, F., LUNDSTRÖM, U.S. (2007): Geoderma, 142, 127 – 135.

PETROLOGY OF MANTLE XENOLITHS FROM CENTRAL AND SOUTH VIETNAM

Hauenberger, C. A.¹, Konzett, J.², Khoi, N.N.³, Hoang, N.⁴ & Auzinger, T.¹

¹Institute of Earth Sciences, Karl-Franzens-University Graz, Universitätsplatz 2, 8010, Graz, Austria

²Institute of Mineralogy and Petrography, University of Innsbruck, Innrain 52, A-6020 Innsbruck, Austria

³Department of Geology, Hanoi University of Science, 334 Nguyen Trai, Thanh Xuan, Hanoi, Vietnam

⁴Institute of Geological Sciences, Vietnam Academy of Science & Technology, 84 Chua Lang, Dong Da,
Hanoi, Vietnam

e-mail: christoph.hauenberger@uni-graz.at

Neogene volcanism with mainly tholeiitic and alkali basalt affinity is widespread in the southern China and Indochina regions. Mantle xenoliths are commonly found in alkali basalts in south-central Vietnam and consist of refractory spinel lherzolites and subordinate amounts of spinel harzburgites and pyroxenites. Several samples from different localities between the cities of Ban Me Thuot and Saigon were recovered in 2011. The mineral assemblage in most samples consists of the simple lherzolitic mineral assemblage Ol–Opx–Cpx–Sp. In addition to xenoliths, clinopyroxene, zircon and sapphire xenocrysts are commonly observed in the weathered volcanic soil. The Ol, Cpx and Opx crystals are usually equigranular while Sp occurs usually as smaller sized interstitial phase or as partly oriented inclusions in Cpx. Cpx II occurs in some samples as recrystallized “rim” around Cpx I. Cpx I has a very uniform composition between different samples with a typical X_{Mg} ($=Mg/(Mg+Fe^{2+})$) of 0.92 to 0.98, a X_{Na} ($=Na/(Na+Ca)$) of 0.10 to 0.16, a Cr_2O_3 content of 0.6–0.9 wt. % and Al_2O_3 values of c. 6 to 8 wt. %. Cpx II has a lower X_{Na} and Al content as well as higher X_{Mg} and Cr content compared to Cpx I. Orthopyroxene typically has a X_{Mg} of c. 0.90 to 0.93. The X_{Mg} values for Ol differ slightly between different samples but are within 0.84 to 0.94. Spinel grains have a variable composition with X_{Mg} from 0.65 to 0.92 and X_{Cr} ($Cr/Cr+Al+Fe^{2+}$) of 0.08 to 0.25. The use of the Cpx-Opx thermometer (BREY & KOEHLER, 1990), Cpx-Ol thermometer (POWELL & POWELL, 1974) and the Al and Cr in Ol thermometer (DE HOOG et al., 2010) allowed constraining the temperature with 900 to 1100 °C. Pressure was calculated with the Ca in Ol barometer (KOEHLER & BREY, 1990) which gave 1.4 to 2.3 GPa.

Acknowledgement: Financial support from the Austrian Academy of Sciences and ASEA-Uninet is gratefully acknowledged. This is a contribution to IGCP557

BREY, G.P., KOEHLER, T.P. (1990): J. Petrology, 31:1353–1378.

DE HOOG, J.C.M., GALL, L., CORNELL, D.H. (2010): Chem. Geol., 270, 196–215.

KÖHLER, T.P., BREY, G.P. (1990): Geochim. Cosmochim. Acta, 54, 2375–2388.

POWELL, M., POWELL, R. (1974): Contrib. Mineral. Petrol., 48, 249–263.

**GARNET ZONING AND GARNET ISOPOLETH GEOTHERMOBAROMETRY AT
THE TRANSITION BETWEEN THE ÖTZTAL-BUNDSCSUH NAPPE SYSTEM
AND THE KORALPE-WÖLZ HIGH-PRESSURE NAPPE SYSTEM WEST OF THE
TAUERN WINDOW**

Heinisch, M.¹, Micheuz, P¹, Krenn, K.¹, Hoinkes, G.¹ & Tropper, P²

¹Department of Mineralogy and Petrology, Institute of Earth Sciences, Karl-Franzens-University of Graz,
Universitätsplatz 2, 8010 Graz, Austria

²Institute of Mineralogy and Petrography, University of Innsbruck, Innrain 52, 6020 Innsbruck, Austria
e-mail: manuel.heinisch@edu.uni-graz.at

The transition between the Ötztal Complex as part of the Ötztal-Bundschuh Nappe System and the Schneebergzug and Texel Complex, both are parts of the Koralpe-Wölz High Pressure Nappe System, is intensely folded which hampers a clear separation between these units. Based on earlier geological maps rocks of the southern located Texel Complex as part of the Koralpe-Wölz High-Pressure Nappe System appear incorporated into units of the Ötztal-Bundschuh Nappe System. The aim of this study is to clarify this approach by the aid of a NW-SE profile using garnet major element zoning linked with garnet isopleth geothermobarometry. "Jumps" in element distribution of major elements are linked with metamorphic events, like Variscan (MP/MT) in the Ötztal Complex, Permian (LP/HT) in the Texel Complex and eo-Alpine (HP/MT) in both complexes

Two main types of pre-eo-Alpine garnet zoning patterns in the cores, type-1 and type-2 and two main types of eo-Alpine garnet zoning in the rims, type-3 and type-4 have been observed. Type-1 shows typical prograde zoning with decreasing X_{Grs} (Grs_{30} to Grs_8) and bell-shaped X_{Sp}_{S} patterns, as well as increasing X_{Alm} (Alm_{60} to Alm_{70}) and X_{Pyp} (Prp_5 to Prp_{12}) from the inner core close to the rim. Type-2 is characterized by homogeneous contents of X_{Grs} (Grs_{8-10}), X_{Alm} (Alm_{70-75}), X_{Pyp} (Prp_{10-15}) from the inner core to the outer core. The rims of the porphyroblasts show two different garnet zoning types with significantly higher X_{Grs} and can be distinguished into: type-3 with a small jump in X_{Grs} (from Grs_{10} to Grs_{25}), in X_{Alm} (Alm_{75} to Alm_{60}) and in X_{Pyp} (Prp_{15} to Prp_{10}) and type-4 with a higher jump in X_{Grs} (from Grs_{10} to Grs_{30}), in X_{Alm} (from Alm_{75} to Alm_{55}) and in X_{Pyp} (from Prp_{15} to Prp_5). Type-4 comprises a large garnet volume with a continuous decrease in X_{Grs} (Grs_{30} to Grs_{20}) and a continuous increase in X_{Alm} (Alm_{55} to Alm_{65}), and in X_{Pyp} (Prp_5 to Prp_{10}) towards the outermost rims.

To estimate the P-T conditions of pre-eo-Alpine garnet growth, grossular-, almandine- and spessartine isopleths were calculated with the program PERPLEX. The intersections of the isopleths yield 0.7-0.9 GPa and 550-650 °C for the pre-eo-Alpine type-1 core and type-2 core garnets and 0.8-0.9 GPa with 550-600 °C for the eo-Alpine type-3 and type-4 garnet rims. It can be concluded that based on garnet thermobarometry and major element zonation it is more likely that rocks directly exposed north of the Schneebergzug experienced a Variscan than a Permian event, followed by an eo-Alpine metamorphic overprint.

Cr-INCORPORATION INTO KYANITE: A HIGH PRESSURE EXPERIMENTAL AND CRYSTALLOGRAPHIC STUDY

Hejny, C. & Konzett, J.

Institut für Mineralogie und Petrographie, Universität Innsbruck, Inrain 52, A-6020 Innsbruck, Austria
e-mail: Juergen.Konzett@uibk.ac.at

Aluminosilicates are amongst the most important rock-forming minerals of the Earth's crust and their phase relations provide important constraints on the P-T conditions of equilibration of aluminosilicate-bearing assemblages. The high-P polymorph kyanite is not only stable under crustal P-T conditions but its stability may extend in appropriate bulk compositions to transition zone and even lower mantle depths (SCHMIDT et al., 1997). The only significant Al-substituent in natural kyanite is Cr with up to 12.9 wt% Cr₂O₃ reported from mantle rocks (PIVIN et al., 2011). By analogy with garnet, high pressures stabilize Cr in the kyanite structure which is consistent with the fact that Cr-rich (>1 wt% Cr₂O₃) kyanites have only been found so far in high pressure (eclogitic) rocks. High P-T experiments have shown that at 3 GPa/1300 °C up to 25 mol% Cr₂SiO₅ (38.0 wt% Cr₂O₃) can be incorporated into kyanite (LANGER & SEIFERT, 1973).

The present study was initiated (1) to explore the limits of Cr-incorporation in kyanite assuming that P > 3 GPa will stabilize even higher Cr-contents, and (2) to study the site occupancy of Cr and the impact of Cr on the elastic properties of kyanite. Multi-anvil experiments at 7 GPa/1100 °C and 7 GPa/1200 °C in fact yielded Cr-kyanites with 52±1 (n=20) and 67±1 (n=10) mol% Cr₂SiO₅, corresponding to averaged Cr₂O₃ contents of 43.2 and 52.3 wt%, respectively. After run durations of 168–234 hours, Cr-kyanites formed blocky crystals up to 600 x 400 µm in size with a deep emerald-green color. At 7 GPa/1200 °C kyanite coexists with small amounts of eskolaite-corundum solid solution containing 94 wt% Cr₂O₃ and 6 wt% Al₂O₃. The unit cell parameters of Cr-kyanite with X_{Cr₂SiO₅} = 0.67 are as follows a₀ = 7.2305(5) Å, b₀ = 8.0021(8) Å, c₀ = 5.6830(4) Å, α = 90.517(7)°, β = 101.007(8)°, γ = 106.006(6)°; V₀ = 309.59(1) Å³. Due to the larger ionic radius of [V]^{Cr³⁺} (0.615 Å) compared to [V]^{Al³⁺} (0.535 Å) Cr incorporation into kyanite results in a linear increase in the unit-cell parameters with a₀^{Cr-ky}/a₀^{ky} = 1.015, b₀^{Cr-ky}/b₀^{ky} = 1.019, c₀^{Cr-ky}/c₀^{ky} = 1.020 and V₀^{Cr-ky}/V₀^{ky} = 1.054.

SCHMIDT, M. W., POLI, S., COMODI, P., ZANAZZI, P F (1997): Am. Min., 82, 460-466.

PIVIN, M., BERGER, J., DEMAFFE, D. (2011): Eur. J. Mineral., 23, 257-268.

LANGER, K., SEIFERT, F. (1971): Z. Anorg. Allg. Chem., 383, 29-39.

TAILORING OF A HIERARCHICALLY STRUCTURED MATERIAL FROM DIATOMITE

Höllen, D.¹, Klammer, D.², Letofsky-Papst, I.³ & Dietzel, M.²

¹Montanuniversität Leoben, Chair of Waste Processing Technology and Waste Management
Erzherzog-Johann-Str. 18, 8700 Leoben, Austria

²Graz University of Technology, Institute of Applied Geosciences
Rechbauerstraße 12, 8010 Graz, Austria

³Austrian Centre for Electron Microscopy and Nanoanalytics
Steyrergasse 17, 8010 Graz, Austria
e-mail: daniel.hoellen@unileoben.ac.at

Based on a previous study (HÖLLEN et al., 2012), where diatomite was converted into zeolites via the formation of an intermediate phase we adapted the hydrothermal treatment process by decreasing the molarity of the Al-containing KOH solution from 1 M to 0.1 M to slow down the dissolution of diatoms and to prolong the period of metastability of the intermediate phase. This change of experimental parameters yielded after 1 d at 100°C a hierarchically structured material consisting of remaining diatoms with macropores of about 100 nm and newly formed nanoparticles of the intermediate phase. These x-ray amorphous particles consist of a potassium-aluminium-hydroxy-silicate, have a diameter of about 50 nm and are characterized by inner pores with a diameter of only few nm. The intermediate phase can remove heavy metal ions like Cu²⁺, Pb²⁺ and Zn²⁺ very efficiently from aqueous solution. Considering that particulated matter acts as adsorbents for oxyanionic contaminants like AsO₄³⁻, CrO₄²⁻ and MoO₄²⁻ which can be formed during leaching of alkaline wastes (CORNELIS et al., 2008), hierarchically structured materials which can remove dissolved and particulate contaminants simultaneously from aqueous solutions are highly promising.



Figure 1. SEM-SE image of a hierarchically structured material, consisting of a macroporous diatom and nanoporous potassium-aluminium-hydroxosilicates growing in its pores.

CORNELIS, G., JOHNSON, C.A., VAN GERVEN, T VANDESCASTEELE, C. (2008): Applied Geochemistry, 23, 5, 955-976.

HÖLLEN, D., KLAMMER, D.; LETOFSKY-PAPST, I., DIETZEL, M. (2012): Journal of Material Science and Engineering A & B., 2, 10, 523-533.

MINERALOGY AND LEACHABILITY OF IRON AND STEEL WORK SLAGS

Höllen, D.¹, Schubernig, M.¹, Aldrian, A.¹, Czyzykiewicz, P.¹,
Sarc, R.¹, Pomberger, R.¹ & Raith, J.G²

¹ Montanuniversität Leoben, Lehrstuhl für Abfallverwertungstechnik und Abfallwirtschaft, Franz-Josef-Str. 18,
8700 Leoben, Austria

²Montanuniversität Leoben, Lehrstuhl für Rohstoffmineralogie, Peter-Tunner-Straße 5, 8700 Leoben, Austria
e-mail: daniel.hoellen@unileoben.ac.at

Iron and steel work slags are high value secondary resources, which are used in construction works due their beneficial mechanical properties (MOTZ & GEISELER, 2001). However, their application has become highly controversial due to their contents in steel alloy elements like chromium (PILLAY et al., 2003). In this study two different steel work slags (slag I and II) are investigated with respect to their chemistry, mineralogy and leachability. Chemical analyses of main and trace components by X-ray fluorescence spectroscopy (XRF) and ICP-MS, respectively, show that slag I is richer in Al₂O₃ and MnO, but poorer in CaO and MgO than slag II, whereas the Cr₂O₃ content is in the same range.

Mineralogical investigations by X-ray diffraction (XRD) and electron microprobe analyses (EMPA) reveal that one group of phases consisting of wuestite (FeO) and minerals of the mclilite ((Ca,Na)₂(Mg,Al)^{4[1]}[Si₂O₇]I) and spinel ((Mg,Fe²⁺)(Al, Fe³⁺, Cr)₂(F,O)₄) group is present in both slags. However, their particular chemical composition varies a lot due to substitutions of Mg²⁺ for Fe²⁺ in wuestite, between Mg²⁺ and Al³⁺ in melilite and especially between Al³⁺ and Cr³⁺ as well as of F for O²⁻ in the spinel group phases. A second group of phases including kirschsteinite (CaFeSiO₄) and bredigite (Ca₁₇Mg_{0,3}SiO₄) is only present in slag I. The third group of phases is only present in slag II and includes cuspidine (Ca₄Si₂O₇(F,OH)₂), merwinite (Ca₃Mg(SiO₄)₂), monticellite (CaMgSiO₄), calcio-olivine (Ca₂SiO₄), mayenite (Ca₁₂Al₁₄O₃₃), calcite (CaCO₃), magnesite (MgCO₃), fluorite (CaF₂), scheelite (CaWO₄), complex Ca-Nb-Cr-Al-Mg-Ti-F oxides and quartz (SiO₂). However, the most interesting aspect of this study is the first description of Mg-Al-Cr-F-spinels in slag II, in which up to 25 % of oxygen ions are replaced by fluorine!

Leaching experiments performed at distinct pH values show that the leachability of chromium, manganese, iron, barium, arsenic, molybdenum and selenium increases with decreasing pH, whereas the leachability of antimony shows a reverse behaviour. Interestingly, the leachability of chromium increases when F substitutes for O²⁻ in the spinel phases. Thus, attention has to be paid to the crystal chemistry of individual phases in which metal alloy elements are incorporated in slags as well as to the hydrogeochemistry of the aqueous solutions they interact with at the sites where the slags are used for construction purposes. If these aspects are considered, iron and steel work slags maintain environmentally friendly secondary resources for a broad range of applications.

MOTZ, H., GEISELER, J. (2001): Waste Management, 21, 285-293.

PILLAY, K., VON BLOTTNITZ, H., PETERSEN, J. (2003): Chemosphere, 52, 10, 1771-1779.

DRAVITE-SCHORL EVOLUTION IN TOURMALINITE FROM OPARNO CRYSTALLINE COMPLEX, SAXOTHURINGICUM

Houzar, S., Hrazdil, V & Toman, J.

Department of Mineralogy and Petrography, Moravian Museum, Zelný trh 6, 659 37 Brno, Czech Republic
e-mail: shouzar@mzm.cz

Different types of tourmalinites are minor but characteristic rocks in the easternmost part of the Saxothuringicum (Oporno Crystalline complex). They consist of tourmaline (dravite>schorl) and quartz, other minerals (< 1 vol. %) include Fe-rich clinochlore, fluorapatite, K-feldspar, calcite, zircon, monazite-(Ce) and goyazite. Tourmalinites from *Chotiměř* (RADON et al., 2011) and *Oporno* form metamorphic segregations (including vein-like type) hosted in two-mica gneisses. They contain low-vacant dravite (1.53-2.24 apfu Mg), locally Fe-rich (0.57-1.13 apfu Fe in the centre of grains), F-poor (0.04-0.61 apfu) and slightly zoned with higher content of Ca (\leq 0.29 apfu) and Al (\leq 6.35 apfu) in grain rims. Locality *Velké Žernoseky* represents a rare type of tourmalinites ($>$ 90 vol. % Tur, Qtz>>Alm) with dravite-schorl concordantly hosted in garnet mica-schists (Fig. 1a). Tourmaline occurs in three types: (a) the oldest dravite with inclusions of disc-shape calcite and K-feldspar (Fig. 1b), (b) oscillatory and patchy zoned tourmaline on grain rims + quartz and garnet, and (c) zoned tourmaline grains and needle-like aggregates in quartz veinlets. All 3 types of tourmaline have very high contents of Na ($>$ 0.80-0.92 apfu Na) and low F (\leq 0.40 apfu) compared to the most common compositions from alkali tourmaline group (HENRY & DUTROW, 2011). Contents of Al are relatively low (\leq 6.09 apfu). Ca varies from centre to rim (\leq 0.20 apfu) and is not dependent on the calcite inclusions. Younger zones in tourmaline type (a) and the youngest of type (c) correspond to Mg-schorl (1.54-1.85 apfu Fe).

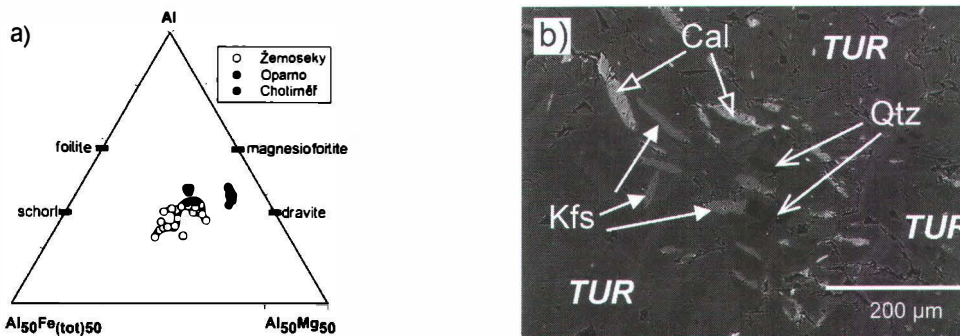


Figure 1. a) Fe-Al-Mg compositional diagram of tourmaline from Oporno Crystalline complex; b) Inclusions of calcite and K-feldspars in zoned dravite (BSE image)

HENRY, F., DUTROW, B. (2011): Canad. Mineralogist, 49, 41-56.

RADOŇ, M., ŽÁČEK, V., RAPPRICH, V., KYCL, P. (2011): Zpr. geol. Výzk. za rok 2010, D-Mineralogie, Petrologie a Geochemie, 177-183.

MANTLE XENOLITHS FROM BONDORÓ VOLCANIC COMPLEX

Janisch, A., Mundl, A. & Ntaflos, T.

Department of Lithospheric Sciences, University of Vienna, Althanstrasse 14, A-1090 Vienna, Austria
e-mail: astrid.janisch@fh-vie.ac.at

The late Miocene Bondoró Volcanic Complex belongs to the Bakony-Balaton-Highland-Volcanic-Field (BBHVF) in the western part of the Pannonian Basin, Hungary

Mantle xenoliths brought to the surface by alkali basalts comprise sp-herzolites, sp-harzburgites and pyroxenites. Two distinct types of textures have been found: fine-grained, equigranular textures that are predominantly foliated and coarse grained, protogranular textures which often exhibit layering of pyroxenes. A striking feature of some harzburgites is a noticeably high modal composition of opx. While phlogopite was only found in one sample, intergranular, percolating melt and melt pockets are common in Bondoró mantle xenoliths.

Whole rock Al_2O_3 and CaO contents range from 1.01 to 1.93 wt% and 0.71 to 3.20 wt%, respectively. Mineral analyzes of primary ol reveal Fo contents of 89.4 to 91.4. Cpx are predominantly Cr-Diopsides with $\text{En}_{48.1-51.9}\text{-Wo}_{43.4-47.7}\text{-Fs}_{3.2-6.1}$ and Mg# of 0.89 to 0.93. Opx compositions are in the range of $\text{En}_{87.8-90.3}\text{-Wo}_{0.8-2.3}\text{-Fs}_{8.1-9.9}$ with Mg# between 90 and 91.8. While Cr# in primary sp range from 12 to 21, secondary sp in melt pockets and melt intrusions reveal higher Cr# of 41 to 55.

Equilibration temperatures calculated using two-pyroxene-thermometer of BREY & KOEHLER (1990) are estimated to be in the range of 950 to 1100 °C at 1.5 GPa pressure. Our study shows that the lithospheric mantle underneath Bondoró is highly heterogeneous.

BREY, G.P., KOEHLER, T. (1990): Journal of Petrology, 31, 1353–1378.

GRAPHENE- AND GRAPHITE-LIKE THIN FILMS FROM AMORPHOUS CARBON COATINGS

Kaindl, R.¹, Pichler, J.², Fischer, R², Jakopic, G¹ & Waldhauser, W¹

¹JOANNEUM RESEARCH, MATERIALS – Institute for Surface Technologies and Photonics, Leobner Straße 94, A-8712 Niklasdorf, Austria

²Graz University of Technology, Institute of Inorganic Chemistry, Stremayrgasse 9/IV, A-8020 Graz, Austria
e-mail: reinhard.kaindl@joanneum.at

Graphene, a flat monolayer of carbon atoms bonded in benzene-type *sechs*er rings with outstanding physical and chemical properties, is subject of intense basic and applied research. This study presents attempts to produce graphene-graphite like thin films by modification of amorphous carbon (a-C) coatings with thermal and plasma treatments (Figure 1), deposited on various substrate materials.

The coatings were deposited by plasma enhanced chemical vapour deposition (PECVD) from C₂H₂ and subsequently etched in Ar plasma and by physical vapour deposition (PVD), using magnetron sputtering from a carbon target. Substrates were Si, Si with a 100 nm thermal SiO₂ layer and Cu and Ni foils. Some coatings were tempered in a nitrogen-filled tubular furnace at 300 ° and 800 °C for 8 hours, 15 minutes, respectively.

Refraction index and absorption coefficient of a PECVD coating deposited at 3 kV accelerating voltage and ion etched at 800 eV are similar to reported data for graphene and graphite. Raman carbon band parameter yielded a G position and full width at half maximum around 1582-1592 and 102-108 cm⁻¹ and I_D/I_G intensity ratios 1-1.6 for etched and tempered PECVD coatings on SiO₂ and sputtered PVD coatings on Cu foils. This suggests a transition from a-C to nanocrystalline graphite with an in-plane correlation lengths <1 nm, almost purely sp²-coordinated network, partly odd membered rings and complete absence of short carbon chains.

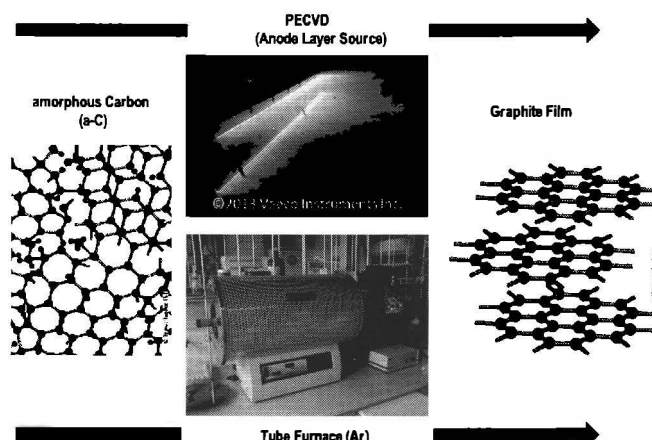


Figure 1. Idea of deposition of PECVD a-C coatings and modification by ion etching and thermal treatment.

**TEXTURAL POSITION AND STRUCTURAL STATE OF ZONED ZIRCONS FROM
MÓRÁGY, HUNGARY AND RASTENBERG, AUSTRIA**

Kis, A., Váczi, T., Weiszburg, T.G. & Buda, Gy.

Department of Mineralogy, Eötvös Loránd University, Pázmány Péter sétány 1/C., H-1117, Budapest, Hungary
e-mail: annamari.kis@gmail.com

Zircons included in and/or encapsulating rock forming minerals of all the three major rock types of the petrologically and geochemically related Variscan plutonic complexes from Mórággy Hills, Hungary and Rastenberg, Austria were characterized for their textural position and for their internal texture.

Zircons of different morphology were hosted by different rock forming minerals at both localities: 1. „normal” calc-alkaline magmatic zircon (S_{24} , S_{25}) in biotite, amphibole and feldspar, 2. flat prismatic zircon (re-determined as AB_5) in biotite and feldspar, 3. elongated, prismatic zircon (P_5) in feldspar and quartz.

Simultaneously these zircons are rich in both single phase and multiphase mineral inclusions. The latter type, consisting Na-free K-feldspar, albite and quartz, found most commonly in elongated zircons, indicates lower temperature crystallization from Si-rich granite melt, confirming that zircon crystallized continuously during the solidification of granitoid magma. Zircons themselves are heavily zoned, showing both primary (growth, normal magmatic with xenocryst core, sector) and secondary (convolute) zoning features.

Cathodoluminescence, backscattered electron imaging and Raman spectroscopy were used for determining the structural state of the zircon zones. Normal and flat zircons show zones of all structural states (well crystallized, intermediate, metamict), while the elongated, zoning free zircons are mainly well crystallized and intermediate.

We believe that these textural and structural state information types are necessary for the reliable age interpretation of the host rock types when using LA-ICP-MS based U-Pb, Th-Pb geochronology of these zircons.

ECLOGITE-FACIES MAFIC OCEANIC AND CONTINENTAL CRUSTAL ROCKS FROM THE AKTYUZ AND MAKBAL COMPLEXES, TIANSHAN MOUNTAINS (KAZAKHSTAN & KYRGYZSTAN): GEODYNAMIC IMPLICATIONS

Klemd, R.¹, Meyer, M.¹, Hegner, E.² & Konopelko, D.³

¹GeoZentrum Nordbayern, Universität Erlangen–Nürnberg, Schlossgarten 5a, D-91054 Erlangen, Germany,

²Department of Earth and Environmental Sciences, LMU München, Theresienstr. 41, D-80333 München,
Germany

³Geological Faculty, St. Petersburg State University, 7/9 University Embankment, 199034 St. Petersburg, Russia
e-mail: Reiner.Klemd@fau.de

The Late Paleozoic Makbal and Aktyuz Complexes in the western Tianshan Mountains of Kazakhstan and Kyrgyzstan consist of HP/UHP metasedimentary host rocks which enclose various high-pressure mafic blocks or boudins. These mafic rocks comprise rare eclogites, garnet amphibolites and newly discovered glaucophanite (glaucophane-garnet-omphacite bearing rock) in the Makbal complex. So far the Aktyuz and Makbal Complexes have been interpreted to predominantly consist of continental lithologies while the mafic rocks were considered as dismembered dikes intruding continental metasediments. This interpretation is mainly based on the geological relationship and bulk rock chemistry of the different rock types. It was further suggested that the Makbal and Aktyuz Complexes formed as tectonic mélanges.

In the present study we combined conventional geothermometry, P-T pseudosection modeling and major and trace element whole rock geochemistry for different mafic samples (eclogites, glaucophanite and garnet amphibolites) in order to shed light on both the metamorphic evolution and the protoliths of the mafic HP rocks in the Makbal and Aktyuz Complexes. Prograde to peak-pressure clockwise P-T paths of both rock types were modeled using garnet isopleth thermobarometry. The results suggest that the eclogite, glaucophanite and the garnet amphibolite samples experienced similar prograde P-T paths and slightly different peak metamorphic conditions between ~520 °C and ~560 °C at ~2.2 GPa to ~2.5 GPa (at Makbal) and ~670 °C at ~2.1 GPa (at Aktyuz) corresponding to burial depths between 70 and 85 km. Whole rock major and trace element analyses and petrological evidence suggest that the different rock types at the Makbal and Aktyuz Complexes most likely originated from various precursor rocks. From the geological relationship and from bulk rock and isotope chemistry of the different rock types the Aktyuz Complex has been interpreted as a continental crustal fragment and the mafic rocks as intrusive and now dismembered dikes. The Makbal garnet amphibolites are believed to represent strongly retrogressed former eclogite-facies rocks that have never been eclogites *sensu stricto* due to an unfavorable alkali-poor bulk composition. The high-pressure mafic samples investigated in this study clearly originated from oceanic crust, which is in contrast with all previous studies suggesting a continental protolith for the mafic HP/UHP rocks.

The mafic high-pressure rocks are believed to represent incoherent segments of exhumed oceanic or continental crust. Juxtaposition of different mafic oceanic and continental crustal rocks is suggested to be due to buoyancy-driven exhumation of the metasedimentary host rock in the subduction channel where dismembered fragments of the subducted oceanic crust were captured in different depth supporting the tectonic mélange formation concept.

PLASTIC DEFORMATION OF ZIRCON: A HIGH-T DEFORMATION DATING TOOL?

Klötzli, U. & Kovaleva, E.

Department of Lithospheric Research, University of Vienna, Althanstrasse 14, A-1090, Vienna, Austria
e-mail: urs.kloetzli@univie.ac.at

Most differential or incremental material motion during tectonic processes is taken up by shear zones. These work at different size scales, temperatures, pressures, fluid compositions and time scales and inevitably involve the deformation of minerals. The unambiguous exact quantification of these parameters is vital for the geologically meaningful reconstruction of tectonic processes. In this respect especially the age and duration of tectonic processes is important.

Traditionally, "ages" of shear zone activity are determined by Rb/Sr and Ar/Ar mica dating. But due to the low closing temperatures in micas temperatures higher than ca. 500 °C cannot be dated by mica chronometry. Thus any shear zone activity above 500 °C is undetectable by these methods. Other possibilities can be Sm/Nd and Lu/Hf dating of garnet or Ar/Ar dating of amphiboles. Garnet dating is problematic because single mineral dating is not possible. Thus internal isochrons or whole rock - mineral isochrons have to be sought. This approach is often hampered by an open system behaviour of rocks undergoing deformation.

The in-situ U/Th/Pb dating of zircon has the potential to overcome the above mentioned drawbacks:

Zircon is plastically deformed by recovery and/or subgrain rotation recrystallisation that indicates formation and migration of dislocations under high-T conditions in a stress field. Plastic deformation in zircon occurs during deformation events due to stresses associated with the collision of zircon crystals with surrounding mineral phases. Different crystals domain showing different amounts of deformation are linked by so called low angle boundaries. These potentially act as a fast diffusion pathways facilitating Pb, Ti, U, Th and trace element mobility in the crystals. Crystal-plastic deformation in zircon can thus cause rapid redistribution (outwards diffusion) of radiogenic Pb which leads to a partial or complete rejuvenation of the U/Th/Pb ages. Due to the high closing temperature of the U/Th/Pb system in zircon (> 800 °C) the detection of such ages potentially allows the dating of the high-T deformation events at $T > 500$ °C. And due to the robustness of zircon low angle boundaries and associated U/Th/Pb age disturbances can be preserved at crustal temperatures for billions of years.

THE CRYSTAL STRUCTURE OF A NEW SECONDARY ZINC MINERAL FROM
LAVRION, GREECE: $Zn_9(SO_4)_2(OH)_{12}Cl_2 \cdot 6H_2O$

Kolitsch, U.^{1,2} & Giester, G.²

¹Mineralogisch-Petrographische Abt., Naturhistorisches Museum, Burgring 7, A-1010 Wien, Austria

²Institut für Mineralogie und Kristallographie, Universität Wien, Geozentrum, Althanstraße 14, A-1090 Wien,
Austria

e-mail: uwe.kolitsch@nhm-wien.ac.at

During a long-term study of new finds, mineral species and slag phases from the famous Pb-Zn-Ag-Fe mining district of Lavrion, Greece (KOLITSCH et al., to be submitted), a new secondary Zn mineral was encountered on material collected underground in the Hilarion mine. The mineral forms tiny, thin hexagonal platelets with a white colour and a slightly pearly lustre. These platy crystals show subparallel intergrowth and form thin crusts associated with a presently unidentified Zn-sulphate hydrate.

The crystal structure was solved from single-crystal X-ray intensity data (CCD area detector; $T = 293$ K) and refined in space group $R\bar{3}$ [$a = 8.275(1)$, $c = 32.000(6)$ Å, $V = 1897.7(5)$ Å³, $Z = 3$] to $R1(F) = 3.87$ % and $wR2_{all} = 9.31$ % for 1694 'observed' reflections with $F_o > 4 \sigma(F_o)$; number of parameters: 77. The derived formula is $Zn_9(SO_4)_2(OH)_{12}Cl_2 \cdot 6H_2O$. The presence of Zn, S, Cl and O was confirmed by semiquantitative SEM-EDS analyses (JEOL JSM-6610LV).

The asymmetric unit contains three unique Zn positions. The first one is (5+1)-coordinated by OH⁻ anions [Zn1-O distances range from 2.025(2) to 2.347(2) Å]. The second one, Zn2, is octahedrally coordinated by H₂O molecules [6x 2.130(3) Å]. The third one, Zn3, is tetrahedrally (3+1) coordinated by three OH⁻ groups and one Cl⁻ anion. The Zn1(OH)₆ polyhedra share edges to form a brucite-like sheet, with 1/7 of the octahedral sites vacant. The Zn3(OH)₃Cl tetrahedra are attached to the brucite-like sheet above and below the vacant site. The SO₄ tetrahedron is linked to the tetrahedral-octahedral sheet by a shared ligand. The Zn2(H₂O)₆ octahedra are located in the interlayer space. Thus, the structural formula may be written as $[^6]Zn2(H_2O)_6[^{5+1}]Zn1_6(OH)_6[^{3+1}]Zn3(OH)_3Cl]_2(SO_4)_2$.

If the simplified formula of the new mineral is halved, giving $Zn_{4.5}(SO_4)(OH)_6Cl \cdot 3H_2O$, the close relation with gordaita, $NaZn_4(SO_4)(OH)_6Cl \cdot 6H_2O$ (ADIWIDJAJA et al., 1997; ZHU et al., 1997), and the secondary slag phase $Ca_{0.5}Zn_4(SO_4)(OH)_6Cl \cdot 4.5H_2O$ (BURNS et al., 1998) becomes obvious. In fact, all three compounds share the same brucite-like octahedral sheet with attached Zn(OH)₃Cl tetrahedra, only the interlayer cation is different (Zn²⁺ vs. Na⁺ and Ca²⁺, respectively). Furthermore, the new mineral contains less interlayer H₂O than the two related compounds.

ADIWIDJAJA, G., FRIESE, K., KLASKA, K.-H., SCHLÜTER, J. (1997): Z. Kristallogr., 212, 704-707.

BURNS, P.C., ROBERTS, A.C., NIKISCHER, A.J. (1998): Eur. J. Mineral., 10, 923-930.

ZHU, L., SEFF, K., WITZKE, T., NASDALA, L. (1997): J. Chem. Crystallogr., 27, 325-329.

PRELIMINARY DATA ON A NEW NATURAL Ca-Ce⁴⁺-ARSENATE AND ITS CRYSTAL STRUCTURE

Kolitsch, U.^{1,2}, Ciriotti, M.E.³ & Blaß, G.⁴

¹Mineralogisch-Petrographische Abt., Naturhistorisches Museum, Burgring 7, A-1010 Wien, Austria

²Institut für Mineralogie und Kristallographie, Geozentrum, Universität Wien, Althanstr. 14, A-1090 Wien, Austria

³Associazione Micromineralogia Italiana, via San Pietro, 55, I-10073 Devesi-Cirié, Italy

⁴Merzbachstr. 6, D-52249 Eschweiler, Germany

e-mail: uwe.kolitsch@nhm-wien.ac.at

At the abandoned Fe-Mn Montaldo mine, Montaldo di Mondovì, Cuneo province, Piedmont, Italy (KOLITSCH et al., 2011), a new Ca-Ce⁴⁺-arsenate mineral was recognised. It forms very small, pale yellow to brown-yellow pseudo-octahedral crystals embedded in matrix. The Montaldo mine is also known for unnamed LaAsO₄ and NdAsO₄ (both occurring as tiny grains) (CABELLA et al., 1999) and an unnamed Ca-Na-Mn³⁺-arsenate (KOLITSCH, 2008).

The crystal structure was solved from single-crystal X-ray intensity data (CCD area detector, $T = 293$ K) and refined in space group $I4_1/a$ [$a = 10.479(2)$, $c = 12.030(2)$ Å, $V = 1390.0(4)$ Å³, $Z = 4$] to $R1(F) = 2.34\%$ and $wR2_{all} = 5.54\%$ for 1275 'observed' reflections with $F_o > 4\sigma(F_o)$. In the asymmetric unit there is one Ca, one Ce, one As and four O sites. Additionally, the structure hosts, in a void, a partially occupied, disordered water(?) site [O occupancy ~ 0.32 ; O-O' = 0.720(14) Å], but this has not been confirmed yet by supplementary methods. A three-dimensional framework is built of AsO₄ tetrahedra (\langle As-O $\rangle = 1.688$ Å), Ca-O polyhedra [(6+3)-coordination with six ligands within 2.51 Å and three additional ligands between 2.775(18) and 3.064(3) Å] and CeO₈ polyhedra (\langle Ce-O $\rangle = 2.368$ Å).

Semiquantitative SEM-EDS analyses and occupancy refinements indicate that Ca is partly replaced by Y, Nd and/or Ce, and that Ce⁴⁺ is partly replaced by Zr, Th, Y, Nd and/or Ca(?). Minor amounts of Si replace As. The derived simplified formula is Ca₄Ce⁴⁺(AsO₄)₄·~1.3H₂O. The Ce valency has been confirmed by bond-valence calculations (ROULHAC & PALENIK, 2003).

The structure of the new Ca-Ce⁴⁺-arsenate is derivable from that of scheelite and isotopic with synthetic Na_{3.68}Dy_{1.44}(SeO₄)₄ and several molybdates and tungstates M_5 REE(Mo/WO₄)₄. The water(?) site of the new mineral is equivalent to one of two alkali sites in these compounds. Additional studies (EPMA, Raman spectroscopy, polarised-light microscopy) are underway

CABELLA, R., LUCCHETTI, G., MARESCOTTI, P. (1999): Can. Mineral., 37, 961-972.

KOLITSCH, U. (2008): Geochim. Cosmochim. Acta 72, Special Supplement 12S, A487.

KOLITSCH, U., CIRIOTTI, M.E., CADONI, M., ARMELLINO, G., PICCOLI, G.C., AMBRINO, P., BLASS, G., ODICINO, G., CIUFFARDI, M. (2011): Micro, 9, 4-21.

ROULHAC, P.L., PALENIK, G.J. (2003): Inorg. Chem., 42, 118-121.

METASOMATISM IN THE LITHOSPHERIC MANTLE BENEATH SOUTHERN
PATAGONIA, ARGENTINA

Kolosova-Satlberger, O.¹, Ntaflos, T.¹ & Bjerg, E.²

¹Department of Lithospheric Research, University of Vienna, Althanstraße 14, 1090 Wien, Austria

²CONICET-Universidad Nacional del Sur, Avenida Colón 80, 8000 Bahía Blanca, Argentina

e-mail: kolosova@gmx.net

Mantle xenoliths from Gobernador Gregores, southern Patagonia are spinel-lherzolites, harzburgites and wherlites. A large number of the studied xenoliths have experienced cryptic and modal metasomatism. The xenoliths are mainly coarse-grained with prevalent protogranular texture but equigranular tabular and mosaic textures are present as well.

Xenoliths that have undergone modal metasomatism bear hydrous phases such as amphibole, phlogopite ± apatite and melt pockets. The latter are of particular interest because of their unusually large size (up to 1 cm in diameter) and freshness. They consist of second generation olivine, clinopyroxene and spinel ± relict amphibole ± sulfides that are surrounded by a yellowish vesicular glass matrix. The melt pockets are found in amphibole- and/or phlogopite-bearing wehrlites and harzburgites as well as anhydrous lherzolites.

There are considerable differences between first and second generation minerals found in melt pockets. While primary olivine has Fo-contents that range from 88.0 to 93.3, second generation olivines in melt pockets vary from Fo_{89.3} to Fo_{94.4}. Both primary and second generation cpx are diopsides with the latter systematically enriched in TiO₂. The glasses that occur in melt pockets or propagate intergranular have compositions varying from trachyandesite to phonolite. The variable composition of the glass could be attributed to host basalt infiltration and decompressional melting of amphiboles.

Textural and mineralogical evidences indicate that amphibole breakdown initiated the melt pocket generation process. It appears that the amphibole breakdown took place rather *en route* and not prior to their transport to the surface.

QUANTITATIVE PHASE ANALYSIS OF LATERITIC BAUXITE WITH NIR-SPECTROSCOPY

Konrad, F. Stalder, R. & Tessadri, R. in cooperation with ABB Suisse

Institute of Mineralogy and Petrography, University of Innsbruck, Innrain 52, A-6020 Innsbruck, Austria
e-mail: florian.konrad@student.uibk.ac.at

The project investigates the applicability of near-infrared spectroscopy for bauxite mining sites, namely the possibility to use this analysis method directly at conveyor belts to guarantee a continuous quantification of bauxite material. The idea is to use modal quantification from XRPD/Rietveld refinement and/or XRF analytics as reference and combine the results with NIR-spectra in a multivariate calibration model.

The material used in this investigation originates from Paragominas, Brazil and consists of the minerals Gibbsite $[Al(OH)_3]$, Kaolinite $[Al_2Si_2O_5(OH)_4]$, Goethite $[FeO(OH)]$, Hematite $[Fe_2O_3]$ and Anatase $[TiO_2]$. To reduce preferred-orientation in XRPD-measurements, samples were ground, sieved and prepared with ethanol on a glass slide. Samples for XRF analytics were prepared with Li-tetraborate fusion technique for major element analysis.

The result of the calibration shows that, for the industrial application of NIR-analytics two crucial points must be considered: (1) it is necessary to crush the bauxite material in order to get unbiased measurements, since bauxite is inhomogeneous with respect to size and modal composition; (2) humidity has a great influence on NIR-spectra in changing band-intensities, which leads to an underestimation of crystalline phase concentrations and needs to be corrected.

In this study, a calibration model is presented using partial-least-squares regression (developed by ABB), dividing samples randomly into a training and test set. The training set generates the model, which is used to predict modal compositions of the test set (Fig. 1). The results show a predictability of the major mineralogical phases within $\pm 5\text{wt\%}$ (2σ). Our results enable a useful application of NIR-spectroscopy at appropriate mining sites.

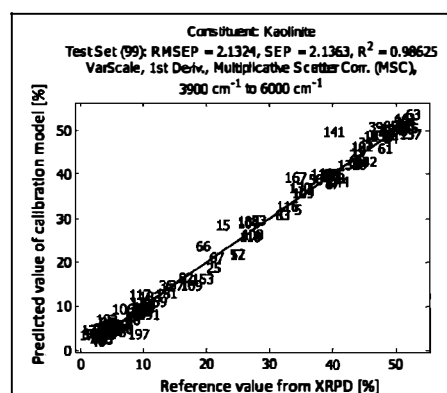


Figure 1

Example of a calibration result for kaolinite in lateritic bauxites: On the x-axis Kaolinite concentrations determined by XRPD/Rietveld (reference values) are shown. The y-axis plots the predicted kaolinite concentrations of a calibration model based on NIR-spectra. Note that RMSEP defines the 1σ -error of reference values vs. NIR-based predictions.

EVIDENCE FOR MANTLE METASOMATISM IN SELECTED SAMPLES FROM THE STYRIAN BASIN

Konrad, L.¹, Hauzenberger, C.A.¹ & Konzett, J.²

¹Institute for Earth Sciences, University of Graz, Universitaetsplatz 2, 8010 Graz, Austria

²Institute of Mineralogy and Petrography, University of Innsbruck, Innrain 52, 6020 Innsbruck, Austria

e-mail: lukas.konrad@yahoo.de

The Pannonian Basin is an extentional back-arc basin surrounded by the Eastern Alps and the Carpathian fold belt. Two main volcanic events can be distinguished within the Pannonian Basin: (i) younger Pliocene to Pleistocene activity, consisting of extension related alkali basalt volcanics, and the (ii) older Eocene subduction related calc alkaline volcanism.

The samples appear as small nodules ranging from 2 to 5 cm in diameter and stuck within the basaltic tuffs. They were collected near the villages of Beistein and Waxenegg and at the prominent locality of Kapfenstein.

They comprise (i) spinel (\pm amphibole) lherzolites (samples KI2, KK1, KI1, Wa2) and (ii) amphibole spinel websterites (samples BS5, WA1). Spinel-amphibole lherzolites are protogranular textured with large olivine, Cr-diopside and orthopyroxene crystals. Pargasites are found in two samples as interstitial grains. Fluid trails in some crystals indicate the presence of fluids as an agent for metasomatic reactions. Ti-pargasites indicate metasomatism in the amphibole spinel websterites. Mantle metasomatism is indicated by an overall enrichment in REE compare to the CI chondrite and a slight enrichment in LREE and MREE compared to the HREE. Amphiboles show a positive anomaly for Sr which is not seen in the coexisting clinopyroxenes.

Clinopyroxenes show a similar chondrite normalized REE pattern as amphiboles with slightly higher values compared to the amphiboles.

P-T calculations show that these samples are derived from the lithospheric mantle at depths of around 50 km corresponding to \sim 930-1070 °C and \sim 10-14 kbar. All samples plot near the Styrian Basin geotherm, but show slightly higher temperatures (or lower pressures) than expected. Temperatures for the Styrian xenoliths were calculated using the aluminium partitioning between olivine and spinel geothermometer (Twcc₂₀₀₈) of WAN et al. (2008). Pressures were estimated using the calcium exchange geobarometer between olivine and clinopyroxene ($P_{\text{KBl}1990}$) of KÖHLER & BREY (1990).

The financial support by the Austrian Acadamy of Science is gratefully acknowledged. This study is a contribution to IGCP 557.

KÖHLER, T.P., BREY, G.P. (1990): *Geochim. Cosmochim. Acta*, 54, 2375-2388.

WAN, Z., COOGAN, L.A., CANIL, D. (2008): *Am. Miner.* 93, 1142-1147.

**MAGMATIC STAUROLITE IN A PEGMATITE FROM THE TEXEL COMPLEX,
SOUTHERN TYROL – EVIDENCE FOR ANATECTIC FORMATION OF BERYL-
COLTAN PEGMATITES IN THE AUSTROALPINE BASEMENT OF THE
EASTERN ALPS**

Konzett, J.¹, Schneider, T.¹, Melcher, F.², Hauzenberger, Ch.³, Mundil, R.⁴ & Fügenschuh, B.⁵

¹Institut für Mineralogie und Petrographie, Universität Innsbruck, Innrain 52, A-6020 Innsbruck, Austria

²Bundesanstalt für Geowissenschaften und Rohstoffe (BGR), Stilleweg 2, D-30655 Hannover, Germany

³Institut für Erdwissenschaften, Universität Graz, Universitätsplatz 2, A-8010 Graz, Austria

⁴Berkeley Geochronology Center, 2455 Ridge Road, Berkeley, CA 94709, USA

⁵Institut für Geologie und Paläontologie, Universität Innsbruck, Innrain 52, A-6020 Innsbruck, Austria

e-mail: Juergen.Konzett@uibk.ac.at

A pegmatite field was studied in the Texel Complex of the Austroalpine Basement, Southern Tyrol, between Val Passiria and Val Racines. It contains pegmatites with Be-Nb-Ta-Sn-U mineralizations with various degrees of differentiation embedded in amphibolite-facies garnet ± staurolite ± kyanite ± paragonite-bearing gneisses or calcite-dolomite marbles. One of the pegmatites contains an unusually diverse assemblage quartz + muscovite + paragonite + albite + accessory garnet + beryl + apatite + zircon + cassiterite + Nb-Ta-rutile + ixiolite-wodginite + columbite-tantalite + tapiolite + U-microlite + cheralite + thorite + uraninite + wyllieite + arrojadite. Tourmaline and K-feldspar are notably absent. HfO₂ contents of up to 13.5 wt% in zircon and Rb and Cs contents of up to 965 ppm and 9700 ppm, respectively, in muscovite indicate a high degree of differentiation. Single grain U-Pb dating of zircon yields 240 Ma consistent with a formation during the Permian metamorphic event (SCHUSTER & STÜWE, 2008). Beryl appears as idiomorphic crystals of up to several cm in length and contains an Al-rich inclusion assemblage with chrysoberyl + staurolite + Zn-spinel + Be-cordierite. Staurolites form perfectly idiomorphic crystals up to 50 x 20 µm which are always intergrown with quartz. They are Fe-rich ($X_{Fe}=0.88-0.98$) and contain variable ZnO contents in the range 0.7-3.7 wt%. Textures of the staurolites and the mode of occurrence as inclusions in beryl indicate a magmatic crystallization from a fluid-saturated melt. To test a possible origin of the staurolite by partial melting of the metapelitic country rocks, experiments at 7 kbar and 700-750 °C were conducted using a garnet-staurolite-paragonite gneiss from the vicinity of the pegmatite as starting material. Preliminary results show that staurolite indeed is stable coexisting with granitic melt at 700 and 750 °C under both water-absent and water present conditions. These results are consistent with those from melting experiments by GARCIA-CASCO et al. (2003) and show that staurolite may be stable as magmatic phase during anatexis of Fe-rich metapelites. In summary both textural and experimental evidence supports an origin of the investigated pegmatites by anatexis of the country rocks during the Permian metamorphic event at $T \geq 700-750$ °C. This mode of pegmatite formation dispenses with the necessity of a genetic association with a granitic intrusive body. The absence of such associated intrusions is a characteristic feature of rare metal-bearing pegmatites of the Eastern Alpine basement (MALI, 2004).

ZIRCON PLASTIC DEFORMATION EXAMPLES FROM THE TAUERN WINDOW

Kovaleva, E. & Klötzli, U.

University of Vienna, Faculty of Earth Sciences, Geography and Astronomy, Department of Lithospheric Research, Althanstrasse 14, UZA 2, A-1090, Vienna, Austria
e-mail: elizaveta.kovaleva@univie.ac.at

Minerals deform during metamorphic events due to stresses associated with collision of the phases. Plastic deformation in zircon occurs due to dynamic recrystallization that indicates formation and migration of dislocations under lower-crustal and upper-mantle conditions.

As far as the low-angle boundaries potentially act as fast diffusion pathways in the crystal lattice, crystal-plastic deformation in zircon can cause rapid out-diffusion of radiogenic Pb and, therefore, influences the results of isotopic dating.

We have made several profiles through the shear zones in the Western Tauern Window, Zillertal Valley, in order to sample gneisses with different deformation degree. We investigated zircons hosted by these rocks with a number of methods, including EBSD mapping. Zircon exhibit different stages of deformation – from undeformed grains through plastically deformed with low-angle boundaries (Fig. 1) and to brittle-deformed individuals. We have identified several mechanisms of plastic deformation in the zircon crystal lattice, depending on the hosting environment, shape and internal inhomogeneity of the grain.

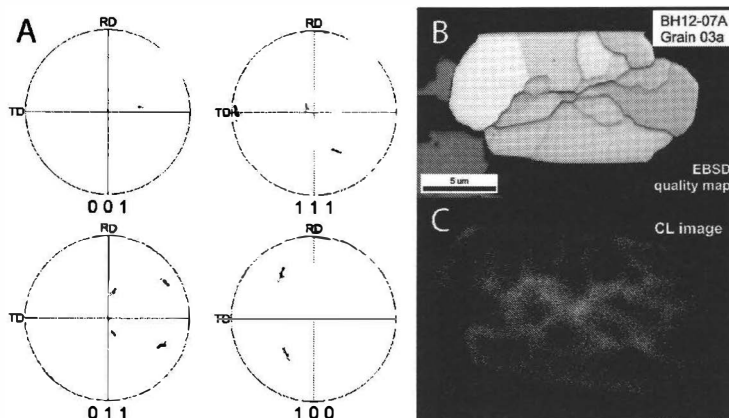


Figure 1. Plastically deformed zircon grain with subgrains (brighter domains on B and dark domains on C), separated by low-angle boundaries (dark lines on B and bright lines on C). A – pole figures with the positions of crystallographic axis of the subgrains; indicates dynamic recrystallization during deformation.

REDDY, S.M., TIMMS, N.E. (2010): Source Abstracts with Programs - Geological Society of America 42 (5), 634.

TIMMS, N.E., KINNY, P., REDDY, S.M., EVANS, K., CLARK, C., HEALY, D. (2011): Chemical Geology 280, 33-46.

GEOCHEMICAL ASPECTS OF THE MINERALISED EARLY CARBONIFEROUS K1-K3 ORTHOGNEISS IN THE FELBERTAL SCHEELITE DEPOSIT (AUSTRIA)

Kozlik, M. & Raith, J.

Montanuniversitaet Leoben, Chair of Resource Mineralogy, Peter Tunner Straße 5, 8700 Leoben, Austria
e-mail: michael.kozlik@unileoben.ac.at

The Felbertal scheelite mine, representing a world-class tungsten deposit, is located in the polymetamorphic units of the Habach Complex (Central Tauern Window) about 8 km south of Mittersill. A mineralised felsic metagranitoid (K1-K3 orthogneiss) of Early Carboniferous age has been suggested as the possible source for the tungsten mineralisation. Petrographic and field-based studies reveal two distinct types of K1-K3 orthogneiss, a leucocratic microcline/muscovite-rich and a more melanocratic biotite-rich variety, respectively. Geochemically they can be classified as metaluminous to weakly peraluminous high-K calc-alkaline monzogranites, which are characterised by a significant enrichment in Nb, Ta, U, W, Mo, Bi, Rb, Cs, Be and lower concentrations of LREE, Zr, and Sr compared to barren Variscan Central gneisses of the Tauern Window. The high SiO₂ content combined with low K/Rb ratios of the K1-K3 orthogneiss ranging from 75 to 115 indicate a highly evolved magmatic system. An increase of Si and Ta with simultaneous decrease in Ba, Sr, P, Cs, Ti, and LREE (e.g. Eu) in the leucocratic variety of the K1-K3 metagranitoid compared with the biotite-rich orthogneiss is interpreted as a result of fractional crystallisation. The segregation of allanite in the melanocratic orthogneiss, being the main carrier of the LREE, causes the higher concentrations of LREE and higher LREE/HREE values in this darker variety. The high Ti contents of the melanocratic type are explained by the high biotite modal abundance in the rocks and the depletion of P in the leucocratic orthogneiss is induced by fractional crystallisation of apatite. Fractionation of feldspar mainly controls the variation of Ba, Sr, and Eu. When comparing the ratios of geochemically similar elements (e.g. Zr/Hf, Nb/Ta) a significant difference between the two K1-K3 orthogneiss varieties is obvious. Zr/Hf decreases from 20-23 in the biotite-rich metagranitoid to 13-14 in the leucocratic variety. In addition Nb/Ta decreases from 8-10 to 5-6, respectively. Hence, the leucocratic K1-K3 orthogneiss represents the more evolved granitoid. There is no positive correlation between Ta and elements that would be typically enriched during metasomatic processes (e.g. Be) but it correlates with HREE, Y and Hf. This supports the idea that the decrease of Nb/Ta is due to fractionation of an accessory phase (samarskite-(Y)?). Magmatic crystallisation of the granite protolith is followed by interaction with mineralising fluids released during the late magmatic-hydrothermal stage of granite crystallisation. This subsequent fluid rock interaction is for example indicated by K/Rb ratios <150 (DOSTAL & CHATTERJEE, 1995) and elevated F contents in biotite and titanite (KOZLIK & RAITH, in press). Geochemical data and field-observations therefore suggest a more complex magmatic evolution of the K1-K3 orthogneiss protolith. At least two injections of granitic melts can be distinguished.

DOSTAL, J., CHATTERJEE, A.K. (1995): Chem. Geol., 123, 67-88.

KOZLIK, M., RAITH, J. (in press): Abstract for the 12th SGA Biennial Meeting.

Fe-Ni-Co-Pb-Zn BEARING COPPER ORES IN THE MAUKEN AREA (RADFELD-BRIXLEGG, NORTH TYROL, AUSTRIA): IMPLICATIONS FOR THE PROVENANCE OF BRONZE AGE “FAHLORE-COPPER” METAL ARTEFACTS IN THE EASTERN ALPS

Krismer, M. & Tropper, P

Institut für Mineralogie und Petrographie, Universität Innsbruck, Innrain 52f, A-6020 Innsbruck (Österreich)
e-mail: Matthias.Krismer@uibk.ac.at

This contribution focuses on copper ores occurring in the Schwazer Trias in the Mauken Area (mining areas: Maukenötz, Silberberg and Geyer) near Radfeld-Brixlegg. The ores are a possible source of fahlore used for Chalcolithic and (Early) Bronze Age copper production. Instead of the galena + sphalerite rich ore occurrences more to the west of the ore belt (Mieminger Kette, Innsbruck Hötting). Ores of the Schwazer Trias are basically dominated by tennantite-rich fahlore group minerals and therefore can be classified as substantial copper ores.

The Mauken Area is located in the eastern most part of the prehistoric and historic silver and copper mining area of Schwaz-Brixlegg. Mining districts in the Mauken Area are characterized by two ore types, which occur in different geological units: 1.) the more common ores consists of more or less monomineralic Fe-Zn-(Hg) tetrahedrite-tennantite and are situated in the Devonian Schwaz Dolomite which is part of the Greywacke Zone. Mining activities of these ores are dated back to the Late Bronze Age. 2.) The second ore type is hosted basically in Anisian carbonates of the Schwazer Trias. The ores show a complex mineralogy with tennantite-rich fahlore-group minerals (in part Ag-rich) as primary copper phase in association with pyrite;bravoite + enargite/luzonite-famatinitite ± chalcopyrite ± thiospinel ± cobaltite-gersdorffite-arsenopyrite ± chalcopyrite ± galena ± sphalerite ± pearceite ± barite which occur as major and minor phases. The mineralogical/chemical composition of these ores is highly variable and changes locally.

The mineralogical and chemical composition of the ores of the Schwazer Trias points to the use for Chalcolithic to Early Bronze Age “fahlore copper” artefacts found at the Kiechlberg hilltop settlement and metallurgical workshop near Thaur (Innsbruck). Few slag, copper and bronze samples contain Sb and/or As and mostly <1 wt.% Ag as minor components with additional impurities of Fe, Co, Ni and Pb.

**COPPER ORE SURVEY IN SOUTH TYROL: POSSIBLE ORE SOURCES FOR THE
LATE BRONZE AGE (LAUGEN CULTURE) SMELTING SITE
FENNHALS/KURTATSCH (SOUTH TYROL, ITALY)**

Krismér, M. & Tropper, P

Institut für Mineralogie und Petrographie, Universität Innsbruck, Innrain 52f, A-6020 Innsbruck (Österreich)
e-mail: Matthias.Krismér@uibk.ac.at

The Late Bronze Age copper smelting site “Fennhals” above Kurtatsch is situated near the border of the Italian provinces South Tyrol and Trentino on the south tyrolean side. The very isolated site is located at 1160 m a.s.l. on the passage to the Nonstal (Trentino) and was discovered in the 70th of the last century. The archaeological record of the smelting site is covered by debris flows and humus layers. The conservation of smelting furnaces, roasting beds and ceramic fragments is therefore good. Beside a still charge filled, clay lined furnace and roasting installations several tuyères, technical ceramics and copper slag fragments complete the record.

The rather isolated geographical position of the smelting site is puzzling since the few larger copper ore occurrences in South Tyrol namely the Pfunderer Berg near Klausen and Prettau in the Ahrntal are 50 km and 110 km air-line distant. In the Nonstal “small copper ores occurrences” are postulated and would be accessible by a five hours march over the Fennberg mountain crest. From the metallogenetic map of BRIGO & OMENETTO (1978) copper ore minerals as major or minor components will be present also in the Ultental which is accessible over the high plateau of the Nonsberg. Other farer distant copper occurrences can be found in the Upper Vinschgau Valley and Ortler region. From the Pb-Zn deposit Schneeberg few chalcopyrite-rich mineralizations are documented. In the Trentino small copper mineralizations are present to the South East of the city of Trento and associated with the magmatism in the Permo-Triassic rocks in the South Alpine (Monzoni intrusion in the Val di Fiemme). Apart from the Nonsberg mineralizations, all known copper ore occurrences are at least 30 km distant (Monzoni, Ulten).

This contribution presents a preliminary survey and mineral-chemical analyses of copper-rich ores from the Pfunderer Berg, Prettau, Schneeberg, Ultental, Monzoni, Upper Vinschgau and Nonsberg and the comparison of the former data with the phase composition of slag samples from the Fennhals smelting site in order to track back the ore to the deposit.

BRIGO, L., OMENETTO, P. (1978): Verh. Geol. B-A., 3, 75-92.

SINGLE-CRYSTAL STRUCTURE AND RAMAN SPECTROSCOPY OF SYNTHETIC CaAlSiO₄F

Krüger, H.¹, Tropper, P¹, Haefeker, U.¹, Kahlenberg, V¹, Többens, D.², Fuchs, M. R.³,
Olieric, V³ & Troitzsch, U.⁴

¹Institute of Mineralogy and Petrography, University of Innsbruck, Innrain 52, 6020 Innsbruck, Austria

²Department of Crystallography, Helmholtz-Zentrum Berlin für Materialien und Energie GmbH, Hahn-Meitner-
Platz 1, 14109 Berlin, Germany

³Swiss Light Source, Paul Scherrer Institute, 5232 Villigen, Switzerland

⁴Research School of Earth Sciences, Australian National University, Canberra

e-mail: hannes.krueger@uibk.ac.at

Titanite is an orthosilicate and its structure consists of chains of TiO₆ octahedra which are linked by isolated Si-tetrahedra. The main coupled substitutions that occur are (Al, Fe³⁺ + F) = (Ti + O) and (Al, Fe³⁺ + OH) = (Ti + O). The extent of the Al + F substitution in natural titanites is high but complete solid solution in the system CaTiSiO₄O-CaAlSiO₄F has only been observed in experimental investigations. TROITZSCH et al. (1999) and TROITZSCH & ELLIS (1999) not only determined the crystal structure of synthetic CaAlSiO₄F but also investigated the structural changes in titanite solid solutions along the join TiO = AlF based on Rietveld analysis. CaAlSiO₄F is monoclinic, belongs to the space group *A2/a* ($a= 6.91$, $b= 8.51$, $c= 6.44$ Å and $\beta= 114.7^\circ$). In this investigation synthetic CaAlSiO₄F, the AlF analog of titanite, has been investigated using single-crystal synchrotron diffraction experiments at Beamline X06DA (Swiss Light Source, Paul Scherrer Institute, Villigen, Switzerland) and for the first time Raman spectroscopy. A single-crystal of 20x15x7 µm³ was selected using a polarising transillumination stereo microscope. The symmetry and reflection conditions are consistent with the model reported by TROITZSCH & ELLIS (1999). Therefore, the known model (*A2/a* setting) was used as a starting point for the structure refinement using Jana2006. Forty parameters were refined including anisotropic displacement parameters, resulting in a final fit of $R_{\text{obs}} = 2.6\%$. The Raman spectrum is characterised by two spectral ranges with a distinct gap in between. The first range (167-593 cm⁻¹) can be subdivided as follows: peaks in the range of 150-361 cm⁻¹ are bending and stretching vibrations involving Ca as well as motions of the tetrahedral and octahedral sites. A second subdivision can be distinguished between 431 and 507 cm⁻¹. The modes at 431 and 470 cm⁻¹ are dominantly caused by tetrahedral torsion and F-displacement perpendicular to *a* with octahedral contribution. Vibrational spectra were calculated in harmonic approximation at G-point from fully relaxed energy optimisations of the crystal structures presented herein, using 3D-periodic density functional theory with Gaussian basis sets and the software CRYSTAL06. The lattice parameters of the fully relaxed structure were in good agreement with the experimental values, with the calculated values 0.8±0.4 % too large; the monoclinic angle was calculated 0.4 ° too large. The agreement of the calculated Raman frequencies with the observed ones was very good, with standard deviation ±7 cm⁻¹ and maximum deviations of ±7 cm⁻¹.

TROITZSCH, U., ELLIS, D.J., THOMPSON, J., FITZ-GERALD, J. (1999): Eur. J. Mineralogy, 11, 955-965.
TROITZSCH, U., ELLIS, D.J. (1999): American Mineralogist, 84, 1162-1169.

Mn₃₃(Si₂O₅)₁₄(OH)₃₈: A NEW MANGANESE PHYLLOSILICATE MINERAL FROM THE TYROL

Krüger, H.¹, Tropper, P.¹, Haefeker, U.¹, Tribus, M.¹, Kahlenberg, V¹,
Wikete, C.², Fuchs, M. R.³ & Olieric, V³

¹Institute of Mineralogy and Petrography, University of Innsbruck, Innrain 52, 6020 Innsbruck, Austria

²Material Technology Innsbruck (MTI), University of Innsbruck, Technikerstraße 13, 6020 Innsbruck, Austria

³Swiss Light Source, Paul Scherrer Institute, 5232 Villigen, Switzerland

e-mail: hannes.krueger@uibk.ac.at

The mineral was discovered in a Mn-rich carbonate layer sandwiched between a serpentinite body and cherts at the locality Staffelsee, Geier in the innermost Wattener Lizum (Tyrol, Austria). Geologically these rocks belong to an Austroalpine nappe called the Tarntal mesozoic. The serpentinite belongs to the Reckner complex and the cherts are part of the Ruhpolding formation. The sample was collected during the diploma thesis of KLIER (2005). Small fragments of crystals have been extracted from a thin-section, and investigated using single-crystal synchrotron diffraction experiments at the X06DA beamline at the Swiss Light Source (Paul Scherrer Institute, Villigen, Switzerland). The crystal structure was solved and refined in space group *Cm* ($a = 17.2760(19)$, $b = 35.957(5)$, $c = 7.2560(8)$ Å, $\beta = 91.359(7)$ ° and $Z = 2$). The structure can be described as a 1:1 single layer silicate (monophyllosilicate), which exhibits a new layer topology. The layers are built from 8-, 6-, 5-, and 4-membered rings in a ratio of 2:9:2:1, respectively (Fig. 1). The unbranched fundamental chain has a periodicity of 7. According to the nomenclature of Liebau, the silicate sheets are *siebener* single layers with the symbol $\{uB,7,1^2\}_{\infty}$ representing the silicate anion. To our best knowledge no other minerals or synthetic structures with *siebener* single layers are known. The free apices of the silicate layer connect to both neighbouring MnO₆ octahedral layers. The hydrogen atoms are bonded to the free oxygen atoms (the ones not bridging between tetrahedra and octahedra) at the surface of the octahedral layers.

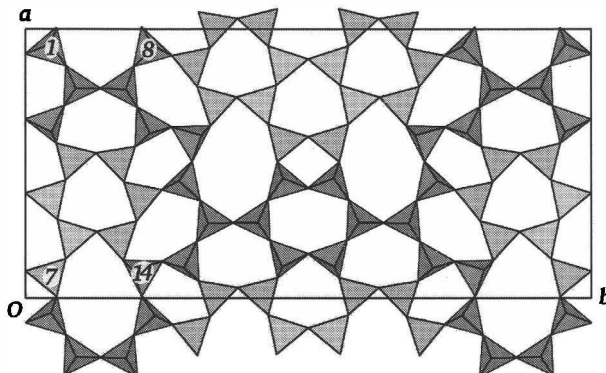


Figure 1: The $\{uB,7,1^2\}_{\infty}$ silicate layer of Mn₃₃(Si₂O₅)₁₄(OH)₃₈. The fundamental *siebener* chain is parallel to *a* (numbered tetrahedra 1-7).

THE HYDRATION OF PERICLASE TO BRUCITE: AN EXPERIMENTAL STUDY

Kuleci, H.¹, Abart, R.¹ & Schmidt, C.²

¹Department of Lithospheric Research, University of Vienna, Althanstraße 14, 1090 Vienna, Austria

²GFZ, Telegrafenberg D 324, 14473 Potsdam, Germany

e-mail: hakan.kuleci@univie.ac.at

The hydration of mantle minerals is an important process in geodynamics as it changes the rock density and thus buoyancy forces of mantle units that are incorporated into orogenic processes. It can be described in terms of the MgO-SiO₂-H₂O model system. For the sake of tractability, we selected the MgO-H₂O subsystem to investigate the hydration of periclase and the formation of brucite, a phenomenon which involves a positive volume change of the solids of about 100 %.

We did dedicated hydration experiments on periclase single crystals, which we machined to cubes with 3x3x3 mm edge length and reacted with water at temperatures ranging from 400 to 530 °C and pressures of 70 to 200 MPa using cold-seal hydrothermal pressure vessels. Run durations were between 30 min. and 2 h. Hydration produced reaction rims of fibrous brucite, which were separated from the reactant periclase by sharp reaction fronts. The end form of brucite is given in Figure 1. The reaction progress was determined from measurement of the remaining periclase and the newly formed brucite volume fractions. Reaction progress was recalculated as average thickness of the brucite layer.

We assumed linear growth kinetics

$$d = k(T) * t,$$

where d is the thickness of the brucite layer in mm, k(T) is the rate constant, and t is time in seconds.

Assuming that the interface reaction is thermally activated we have

$$k(T) = k_0 * \exp(-E_A / R * T),$$

where T is the absolute temperature, E_A is the activation energy for the interface reaction, and k₀ is the pre-exponential factor. From our experiments we estimated 66.35 kJ/mole for E_A and 1.21 mm/s for k₀. Further experiments are in progress.

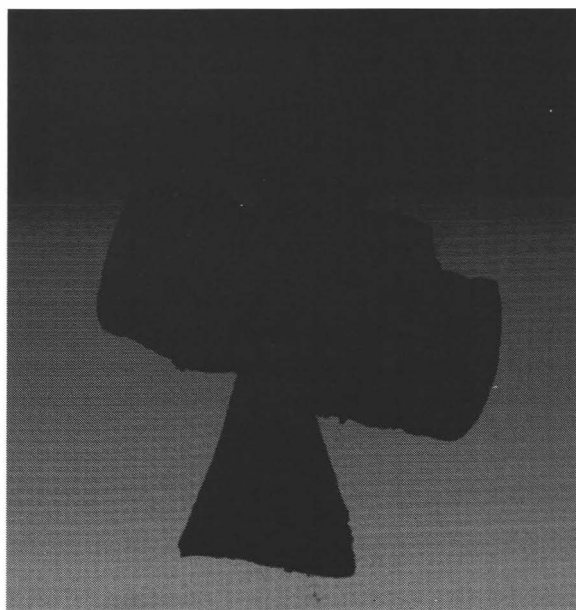


Figure 1, Brucite end form.

GOLD IN THE HISTORIC COPPER DEPOSITS AT FLATSCHACH, STYRIA

Leitner, T¹, Raith, J.G.¹ & Paar, W.H.²

¹Montanuniversitaet Leoben, Chair of Resource Mineralogy, Peter-Tunner-Straße 5, 8700 Leoben, Austria

² Pezoltgasse 46, A-5020 Salzburg

e-mail: johann.raith@unileoben.ac.at

The project area of this Master thesis (LEITNER, 2012) is located NW of Knittelfeld at Flatschach, Schönberg and Tremmelberg. Copper was mined from several vein type deposits (Brunngraben, Weißenbach, Adlitzgraben) in this abandoned mining district. Currently, these historic deposits are re-investigated by Noricum Gold Ltd. for their gold contents.

Copper-gold mineralisation is hosted in a set of NE-SW to NNE-SSW trending and steeply NW dipping vein structures in medium-grade metamorphic rocks of the Austroalpine basement. The immediate host rocks of the mineralisation include a banded metabasite - biotite gneiss sequence containing relicts of metaultramafic rocks, orthogneisses and granite gneiss. The whole sequence is interpreted as part of the Gaaler Schuppenzone, a tectonically fragmented continuation of the Speik Complex (plus others). Tectonically it is assigned to the Silvretta-Seckau nappe system. Formation of the mineralised quartz-carbonate veins postdates the main stage of ductile deformation (main foliation, flat W plunging folds) and amphibolite facies regional metamorphism of Eoalpine age. Sericite-carbonate alteration has been documented around the veins in gneissose rocks.

Based on ore microscopy and EMPA analyses three paragenetic stages can be distinguished. All three are gold bearing. Stage 1 includes the primary hydrothermal ore assemblage characterised by Fe-rich sulfides such as chalcopyrite, pyrite, arsenopyrite with minor associated alloclasite, enargite, bornite, native bismuth, matildite, sphalerite and galena.

Stage 2 includes Cu-rich Fe-poor sulfides like digenite, anilite, covellite etc. and the rare Cu arsenides domeykite and koutekite. Gold of Stages 1 and 2 has similar chemical composition ranging from pure gold (95% Au) to electrum (~70% Au, ~30% Ag). Stage 3 is characterized by a strongly oxidised alteration assemblage (not yet studied in detail) with hematite, cuprite, and various Cu- and Fe-hydroxide and carbonate minerals (goethite, malachite etc.). Gold of Stage 3 is Ag-rich electrum and has higher Hg contents.

The exact age of the Cu-Au mineralisation is not known. However, from geological reasons the timing of mineralization is constrained between the post-peak metamorphic phase of Late Cretaceous regional metamorphism and deposition of the Neogene sediments of the Fohnsdorf-Seckau basin. The Cu-(Au) deposits in the Flatschach area show some similarities with orogenic lode gold deposits, although they document unusual late stage low-temperature hydrothermal (Stage 2) and weathering (Stage 3) processes. During both of these subsequent stages gold was mobilised.

We thank B. Moser and H.P.Bojar from Universalmuseum Joanneum for providing historic material for this study and Noricum Gold Ltd. for permission to publish results of this study.

POTENTIAL ESTIMATION OF RADIATION-INDUCED STRUCTURAL DISORDER WITH REE³⁺ LUMINESCENCE SPECTROSCOPY

Lenz, C. & Nasdala, L.

Universität Wien, Institut für Mineralogie & Kristallographie, Wien, Austria
e-mail: christoph.lenz@univie.ac.at

We present first results of a study addressing whether REE³⁺ luminescence spectroscopy can be used to estimate the degree of structural disorder in natural zircon ($ZrSiO_4$). Our results show that the degree of disorder, as observed from the broadenings and shifts of luminescence bands, generally depends on (1) chemical composition (i.e., structural disorder due to the incorporation of non-formula elements) and (2) structural state (i.e., radiation damage, crystallinity, strain/stress). Effects of radiation-induced disorder were studied on zircon samples from various locations (NASDALA et al., 2006). In that study, single-crystals were cut in two halves. One half each was then subjected to heat treatment in air to anneal the radiation damage, whereas the other half remained in its natural, radiation-damaged state. Comparison of photoluminescence (PL) spectra implies that the full-width-at-half-maximum (FWHM) of certain luminescence bands of trace Dy³⁺ is very sensitive to the accumulation of radiation damage (Figure 1). Interior regions with elevated U and Th content accumulated more radiation-damage over geologic time and hence show the strongest PL band broadening.

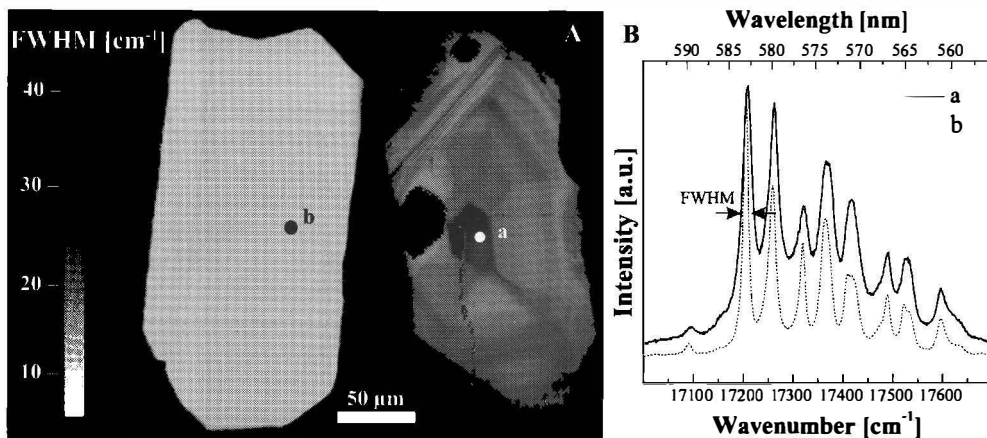


Figure 1. (A) Photoluminescence map (FWHM of the $Dy^{3+} \ ^4F_{9/2} \rightarrow ^6H_{13/2}$ transition) of a cut Archaean gabbro zircon-crystal from the Mulcahy Lake intrusion, Ontario, Canada. The left half was annealed at 1300 °C whereas the right half remained in its natural, radiation-damaged state. (B) Intensity-normalised PL spectra ($\lambda_{exc} = 473$ nm) showing the $^4F_{9/2} \rightarrow ^6H_{13/2}$ transition of trace Dy^{3+} of both crystal halves (analysis points indicated in A).

This research was supported by the Austrian Science Fund (FWF) through grant P24448-N19 to L.N.

NASDALA, L., KRONZ, A., HANCHAR, J.M., TICHOMIROVA, M., DAVIS, D.W. HOFMEISTER, W (2006): Am. Mineral., 91, 1739–1746.

MINERALOGICAL INVESTIGATIONS ON MELTING PRODUCTS FROM INCINERATOR BOTTOM ASHES

Maier, M.¹, Kahlenberg, V¹ & Thome, V²

¹Institute of Mineralogy and Petrography, University of Innsbruck, Innrain 52, A-6020 Innsbruck, Austria
e-mail: csak5686@studentuibk.ac.at

²Fraunhofer-Institut für Bauphysik, Gruppe für Betontechnologie und funktionale Baustoffe,
Fraunhoferstr. 10, D-83626 Valley, Germany

The common process for treating municipal solid waste with the goal of energy production, reduction of volume and combustion of organic components is the incineration. The products of this thermal treatment are so called “incinerator bottom ashes”, whereof 17 million tons accrue in Europe every year. An incinerator bottom ash is a heterogeneous mixture of various components, consisting of ashes, melting products, metal parts and unburned particles. The usage as a secondary construction material is limited to few applications, because of the remaining heavy metals and chlorides in the ashes. Therefore, a major part has to be landfilled.

A promising technique for the selective disintegration of bottom ashes is the electrodynamic fragmentation (BLUHM et al., 2000), where short high voltage pulses are applied to solids embedded in a dielectric fluid such as water. In the course of this study, the extracted melting products have been analysed with respect to their mineralogical and chemical composition by using a combination of different methods of analyses. Special emphasis has been laid on quantitative phase analysis via “Rietveld-Method”. Furthermore, different methods for the determination of amorphous content with X-ray powder diffraction (MADSEN et al., 2011) have been tested on mixtures of known composition and applied to the analysis of melting products. It has been shown that the external standard method, which was first described by O’CONNOR & RAVEN (1988), is appropriate for the phase-quantification of the bottom ashes. The liberated melting products are composed of a vitreous matrix with inclusions of silicates and oxides and contain no more chlorides and sulphates such as Friedel’s salt or ettringite. Regarding a potential re-use of the examined material, its pozzolanic activity has been investigated.

- BLUHM, H., FREY, W., GIESE, H., HOPPÉ, P., SCHULTHEISS, C., STRÄSSNER, R. (2000): IEEE Transactions on Dielectrics and Electrical Insulation, 7, 625 - 635.
MADSEN, I. C., SCARLETT, N. V. Y., KERN, A. (2011): Z. Kristallogr., 226, 944 – 955.
O’CONNOR, B. H., RAVEN, M. D. (1988): Powder Diff., 3, 2-6.

METASOMATIC TITANATES ASSOCIATED WITH CL-RICH AMPHIBOLE AND PHLOGOPITE IN MULTIPLY METASOMATIZED PERIDOTITES FROM LETSENG-LA-TERAЕ, LESOTHO

Mair, P¹, Hauzenberger, C² & Konzett J¹

¹Institute of Mineralogy, University of Innsbruck, Innrain 52, 6020, Innsbruck, Austria
e-mail: P.Mair@studentuibk.ac.at

²Institute of Earth Sciences, University of Graz, Universitaetsplatz 2, 8010, Graz, Austria

The Letseng-La-Terae diamondiferous kimberlite contains a complex suite of upper mantle peridotites, some of these give evidence of multi-stage metasomatism (SIMON et al., 2003). At this point it is described the petrology of two samples, which represent typical coarse, low-temperature garnet and spinel peridotites. The first sample defined as garnet lherzolite, which represents an unusually complex suite of Cr-rich oxides is consisting of spinel + rutile + ilmenite + crichtonite + armalcolite. The second sample characterized as garnet-bearing harzburgite, which has a similar assemblage to the garnet lherzolite, is composed of spinel + rutile + crichtonite. In addition to this assemblage, which has been formed by two different metasomatic events, a rare exotic accessory mineral called djerfisherite was analyzed in the garnet harzburgite that coexists with pentlandite and was formed by metasomatic overprinting (ZACCARINI et al., 2007). Crichtonite is present as tiny inclusion in Cr-rich clinopyroxenes which forms a narrow vein crosscutting the peridotites and is associated with inclusions of Cr-spinel and Cr-Zr-rich rutile, calcic amphibole and phlogopite. The crichtonite-rutile-amphibole-phlogopite association is thought to have been formed by infiltration of a hydrous fluid rich in K-REE-U-Th and Cl. A second metasomatic event apparently involving a hydrous melt caused (1) a partial to complete pseudomorphic replacement of garnet by Al-rich spinel + clinopyroxene + orthopyroxene; (2) replacement of Cl-rich phlogopite-I by F-Ti-Fe-rich and Cl-poor phlogopite-II; (3) modification of the composition of primary clinopyroxene and orthopyroxene along a network of narrow veins to produce Na-Al-poor clinopyroxene and Ca-Al-rich orthopyroxene and (4) formation of Cr-rich armalcolite and ilmenite associated with Na-Al-poor clinopyroxene.

SIMON, N.S.C., IRVINE, G.J., DAVIES, G.R., PEARSON, D.G., CARLSON, R.W. (2003): Lithos, 71, 289-322.

ZACCARINI, F., THALHAMMER O.A.R. (2007): The Canadian Mineralogist, 45, 1201-1211.

CHARACTERISATION OF THE SUBCONTINENTAL LITHOSPHERIC MANTLE BENEATH THE TANZANIA CRATON BASED ON GARNET XENOCRYSTS

Mandl, M.¹, Hauzenberger, C.A.¹, Konzett, J.², Jumanne, R.³, Gobba, J.⁴ & Nguyen, H.⁵

¹Institute of Earth Sciences, University of Graz, Universitätsplatz 2, A-8010 Graz, Austria

²Institute of Mineralogy and Petrology, University of Innsbruck, Innrain 52, A-6020 Innsbruck, Austria

³Williamson Diamond Mine, Petra Diamonds Ltd., Tanzania

⁴Gobbox Ltd., Tanzania

⁵Institute of Geological Sciences, Vietnam Academy of Science and Technology, Vietnam

e-mail: m.mandl@uni-graz.at

Kimberlites from Mwadui, Singida, Nyangwale and Galamba have been emplaced within the northern part of the Tanzania Craton in Archean granitic basement. No mantle xenoliths, but single garnet grains and garnet megacrysts were found in the four visited/sampled kimberlite pipes. These garnets have been studied using major-, trace- and rare earth element compositions in order to obtain information on the underlying upper mantle.

According to the classification scheme of GRÜTTER et al. (2004) the garnets can be distinguished into five different groups (Fig. 1): low-Cr megacrysts (G1), eclogitic garnets (G3), pyroxenitic garnets (G4), lherzolitic garnets (G9) and harzburgitic garnets (G10). Some garnets within group G4 and G10 can be strongly associated with diamonds (G4D and G10D). The different originated garnets reflect a less depleted to depleted mantle (variations in Ti, Zr and Y) that is influenced by metasomatic mantle processes (e.g. melt-type- and phlogopite-type metasomatism). Eclogitic garnets have a low MgO and Cr₂O₃ content and are interpreted to be derived from subducted oceanic crust. These garnets may be related to 2 Ga old eclogites from the Usagaran belt, to the south east of the Tanzania Craton.

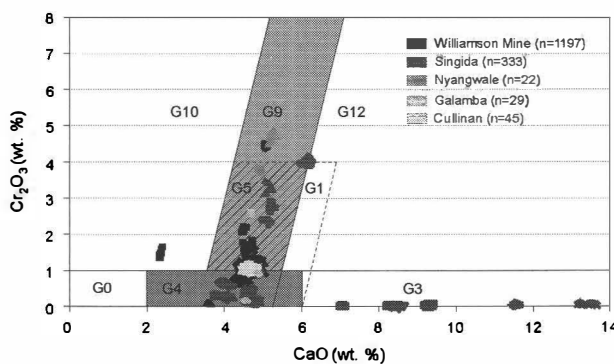


Figure 1. Cr₂O₃ vs. CaO diagram. G-number nomenclature after GRÜTTER et al. (2004): G0= unclassified, G1= low-Cr megacrysts (dashed parallelogram), G3= eclogitic, G4 and G5= pyroxenitic, G9= lherzolitic, G10= harzburgitic, G12= wehrlitic. n= number of analyses.

GRÜTTER, H.S., GURNEY, J.J., MENZIES, A.H., WINTER, F. (2004): Lithos, 77, 841-857.

SYNTHESIS AND CRYSTAL STRUCTURES OF NEW ALKALI-REE-FLUOROSILICATES

Manninger, T. & Kahlenberg, V.

University of Innsbruck, Institute of Mineralogy & Petrography, Inrain 52, A-6020 Innsbruck, Austria
e-mail: volker.kahlenberg@uibk.ac.at

During a systematic study on the crystal chemistry and the synthesis of REE-fluorosilicates by the flux-method using KF and RbF melts as solvents several new compounds were prepared. Therefore, mixtures with a nutrient:flux ratio of 1:1 were homo-genized, loaded in platinum capsules and welded shut. The containers were fired to 1100 °C in a resistance heated furnace, isothermed for 2 h, followed by slow cooling to 800 °C at 5 °C/h and finally quenched to ambient temperature. In all cases transparent crystals of good optical quality (up to several mm in size) could be easily retrieved by dissolving the flux in distilled water. Furthermore, the crystals were characterized by X-ray single-crystal diffraction (performed at 25 °C). The crystal structures of all phases could be solved by direct methods and difference Fourier synthesis. Structure solution was also employed to establish the chemical composition of the following three compounds:

- (1) $K_9Y_3[Si_{12}O_{32}]F_2$, triclinic, space group $P-1$, $a=6.8187(3)$ Å, $b=11.3345(4)$ Å, $c=11.3727(5)$ Å, $\alpha=87.846(3)$ °, $\beta=89.747(3)$ °, $\gamma=80.524(3)$ °, $V=866.36(6)$ Å³, $Z=1$. Salt inclusion compound based on silicate layers with 6-, 8- and 12-membered rings.
- (2) $Rb_2Sc[Si_4O_{10}]F$, tetragonal, space group $I4/m$, $a=11.2619(3)$ Å, $c=8.3053(4)$ Å, $V=1053.37(7)$ Å³, $Z=4$. Tubular chain structure, isotopic with narsarsukite ($Na_2(Ti,Fe^{3+})Si_4O_{10}(O,F)$) (PEACOR & BUERGER (1962)).
- (3) $Rb_2Lu[Si_4O_{10}]F$, monoclinic, space group $P2_1/m$, $a=11.6695(3)$ Å, $b=8.5238(2)$ Å, $c=11.8165(3)$ Å, $\beta=111.753(2)$ °, $V=1091.67(5)$ Å³, $Z=4$. Tubular chain structure.

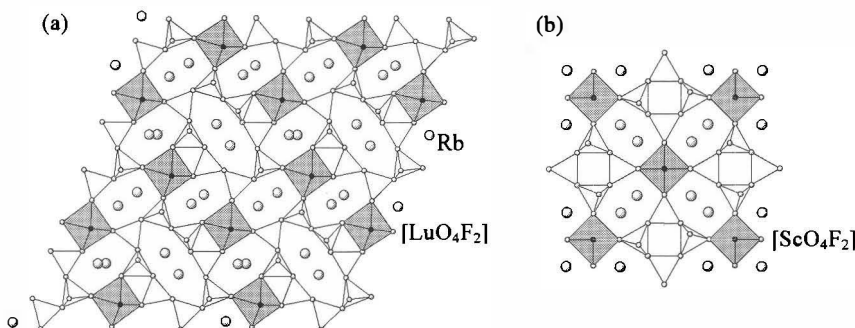


Figure 1. Projections of the crystal structures of (a) $Rb_2Lu[Si_4O_{10}]F$ and (b) $Rb_2Sc[Si_4O_{10}]F$ parallel to the directions of the tubular chains. Linkage between the silicate chains is provided by $(Sc,Lu)O_4F_2$ -octahedra.

PEACOR, D.R., BUERGER, M.J. (1962): Am. Mineral. 47, 539-556.

PETROLOGY OF ECLOGITES AND ASSOCIATED GNEISSES OF THE POLNIK STRUCTURAL COMPLEX (KREUZECK MOUNTAINS, EASTERN ALPS)

Michálek, M.¹, Putiš, M.¹ & Hauzenberger, Ch. A.²

¹Department of Mineralogy and Petrology, Faculty of Natural Sciences, Comenius University, Mlynská dolina, 84515, Bratislava, Slovakia

²Department of Earth Sciences, Karl-Franzens-University Graz, Universitätplatz 2, 8010, Graz, Austria
e-mail: putis@fns.unibask

The region of the Kreuzeck Mountains southeast of the Tauern Window in the Austrian Eastern Alps reveals contrasting early-Cretaceous overprint of the Austro-Alpine (AA) basement complexes from (sub-) greenschist to high-pressure (HP) amphibolite/eclogite facies (HOKE, 1990; PUTIŠ et al., 2002; MICHALEK et al., 2001; KONZETZ et al., 2011). The HP amphibolites to eclogites and the host kyanite-garnet paragneisses and granitic orthogneisses form tectonic lenses of the AA Polnik structural complex along a dextral strike slip shear zone. The eclogites/HP amphibolites and Grt-Ky-St micaschists of the AA Polnik structural complex form tectonic lenses within the MP kyanite-garnet para- and orthogneisses and amphibolites, sporadically containing thin layers of marble and calc-silicate rocks.

The eclogite mineral assemblage is represented by garnet, omphacite, zoisite, amphibole and rutile (M1 stage). Cpx₁(Jd₂₅₋₄₅) – Grt(Alm₅₃₋₅₀Prp₁₉₋₂₃Grs₂₉₋₃₄) pairs were used to obtain temperatures of 600–720 °C at minimum estimated pressures of 1.1–1.7 GPa based on the Jd content found in Omp. Using PERPLE_X (CONNOLLY, 2005), the calculated pseudosection yields peak metamorphic conditions of 630 – 730 °C at 1.4 – 1.7 GPa. Omp (Jd₂₅₋₄₅) is decomposed into symplectite of Cpx₂ (Jd₁₉₋₈) and Pl (An₁₄₋₂₆) during the M2 exhumation stage at a temperature of c. 700 – 650 °C and 1.4 – 1.0 GPa. Subsequent retrogression caused corona textures around garnet consisting of Am (Prg – Al-Fe Prg) and Pl (An₃₄₋₅₂), which indicate the M3 stage of metamorphism. Rt is overgrown by Ilm-Ttn as a result of decompression.

The hosting Grt-Ky-St gneisses are composed of Grt, St, Bt, Ms, Pl, Ky, ±Tur and mostly reflects the retrograde conditions of the M2 stage of metamorphism. A temperature of 650 ± 30 °C at 0.9 ± 0.1 GPa can be calculated by using the Grt-Bt, GRAIL and GASP geothermobarometers. A temperature of 665 ± 15 °C at 0.8 ± 0.08 GPa has been calculated by PT average mode in THERMOCALC 3.31 (HOLLAND & POWELL, 1998) which is comparable to results from Grt-Bt, GASP and GRAIL geothermobarometry.

Acknowledgement: Financial support from APVV-0279-07 is gratefully acknowledged.

CONNOLLY, J.A.D. (2005): Earth Planet Sc. Lett., 236, 524-541.

HOLLAND, T.J.B., POWELL, R. (1998): J Metamorph. Geol., 16, 309-344.

HOKE, L. (1990): Jb. Geol., B.-A., 133, 5-87.

KONZETZ, J., KRENN, K., HAUZENBERGER, CH., WHITEHOUSE, M., HOINKES, G. (2011): J Petrol., 53, 1, 99-125.

MICHALEK, M., PUTIŠ, M., HAUZENBERGER, CH. A. (2011): Cent. Eur. J. Geosci., 3, 197 – 206.

PUTIŠ, M., KORIKOVSKY, S.P., UNZOG, W., OLESEN, N.OE. (2002): Slovak Geol. Mag., 8, 1, 65-87.

**FLUID INCLUSIONS FROM BLUESCHIST-FACIES BOUDIN STRUCTURES
WITHIN THE PHYLLITE-QUARTZITE UNIT OF THE EXTERNAL HELLENIDES,
GREECE**

Micheuz, P., Krenn, K., Fritz, H. & Kurz W

Institute of Earth Sciences, University of Graz, Universitätsplatz 2, A-8010 Graz, Austria
e-mail: peter.micheuz@edu.uni-graz.at

The Phyllite-Quartzite Unit, exposed in the southernmost part of the Mani peninsula, occurs between the medium-grade metamorphosed Plattenkalk Unit and the low-grade metamorphosed Tripolitsa Unit. The unit contains blueschists arranged as boudins which are surrounded by chloritoid-bearing micaschists. HP/LT metamorphism resulted from subduction of the Adriatic plate beneath the Eurasian plate during Eocene time.

On micro-scale, blueschist boudins contain the mineral assemblage glaucophane + chloritoid + phengite + quartz. The surrounding rocks consist of chloritoid + phengite + paragonite + chlorite + quartz. On the basis of Mg/Fe distribution, mineral chemical analysis of chloritoid indicates a prograde growth. Chloritoid porphyroblasts show an internal earlier foliation S1 (D1) and locally pseudomorphic transformations to phengite and chlorite that are accompanied with SSW-directed shearing (D2). D2 is responsible for the penetrative foliation S2.

The post-peak P-T evolution of the Phyllite-Quartzite Unit has been identified by fluid inclusions in boudin structures (sample PM 14) and quartz filled necks (sample PM10). PM 14 consists of recrystallized fine-grained quartz grains (≤ 0.8 mm) and euhedral Mg-dolomite grains (≤ 1.2 mm). PM10 consists of coarse grained quartz (> 3 mm) without Mg-dolomite. Fluid inclusions (FIs) in PM 14 are restricted along intragranular fluid inclusion planes, whereas in PM 10 FIs are arranged as clusters and along intragranular fluid inclusion planes. Both samples are dominated by aqueous saline FIs, predominantly with halite daughter crystals. FIs occur up to 3-phase (S, L, V) at room temperature and indicate on basis of T_e and Raman spectroscopy the chemical system $H_2O-NaCl-CaCl_2$. Last melting of ice (T_m) of about -49°C occurs earlier than last melting of hydrohalite, which coincides well with respective low-temperature Raman spectroscopy. Salinity composition is about 36 mass% NaCl and 17 mass% CaCl₂. Total salinity based on halite solubility lies between 40 and 50 mass%. Different homogenisation temperatures of FIs between samples PM 14 and PM 10 allow a subdivision of their density range into 1.13 to 1.19 and 1.17 to 1.24 g/cm³, respectively.

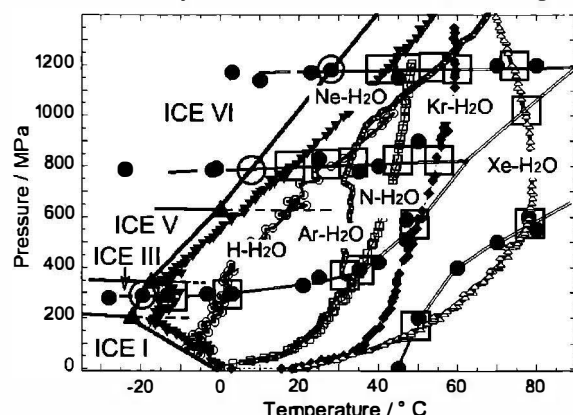
Peak temperatures from blueschists of about 550 °C point to maximum conditions for formation of quartz filled necks (PM 10) between 7 and 9 kbar. Lower densities from the boudin structure (PM 14) between 5.5 and 7.5 kbar indicate conditions for quartz recrystallization accompanied with fluid density re-equilibration during exhumation.

DECOMPOSITION OF CLATHRATE HYDRATES AS INDICATOR OF ANOMALOUS PVT-BEHAVIOUR OF WATER

Mirwald, P W

Inst. für Mineralogie und Petrographie, Univ. Innsbruck, Innrain 52f, A-6020 Innsbruck, Austria
e-mail: peter.mirwald@uibk.ac.at

Clathrate are minerals characterized by an H₂O-cage structure hosting therein various gaseous molecules – mostly of low molecular weight. Because of considerable economical importance, a vast amount of studies is concerned with the complex properties of this mineral group. This study was motivated by a previous work on the compression behaviour of water between 0 ° and 80 °C up to 1.2 GPa (MIRWALD, 2005a) revealing a complex P-T system of anomalies. The PVT anomalies of water may be traced by compression experiments, by detailed determinations of the P-T course of phase transition boundaries (e.g. melting curve of ice), or by decomposition reactions (e.g. dehydration reactions). Dehydration studies on gypsum, portlandite and brucite have shown that the water anomalies actually extent far into the P-T range of petrological relevance (MIRWALD, 2008, 2005b, c). Detailed studies on the P-T relations of clathrate hydrates have been conducted by Dyadin and co-workers (e.g. Dyadin et al., 1999). Out of the great number of investigations those on noble gas hydrates and H- and N-hydrate have been chosen, showing a minimum of interaction between guest molecule and hosting H₂O-cage. The figure gives a view on the previously outlined system of water anomalies (closed circles connected by double lines). At 290, 780 and 1180 MPa the melting curve of ice is characterized by anomalous dP/dT-slope inflections (open circles; MIRWALD, 2010). On the diagram superimposed the decomposition curves of various clathrate hydrates (Ne-, H-, Ar-, N-, Kr- and Xe-H₂O) are given. In all cases the decomposition curves of the clathrate hydrates show at or in



very next vicinity of the water anomalies a discontinuous behaviour of the dP/dT-slope (open squares) that is to be related to the anomalous PVT behaviour of H₂O.

- DYADIN, Y. A., LARIONOV, E. G., MANAKOV, A. Y., ZHURKO, F. V., ALADKO, E. Y., MIKINA T. V, KOMAROV, V. Y. (1999): Mendeleev Commun., 9 (5), 209-210.
 MIRWALD, P. W. (2005a): Journal Chemical Physics 123, 124715, 1-6.
 MIRWALD, P. W. (2005b): Geophys. Res. Abstr. 7, EGU05-A-04554.
 MIRWALD, P. W. (2005c): Eur. J. Mineral., 2005, 17, 537-542.
 MIRWALD, P. W. (2008): Journal Chemical Physics, 128, 074502, 1-7
 MIRWALD, P. W. (2010): Int. Mineral. Ass., 21-27 Aug. 2010; Acta Mineral.-Petrograph. Abstr.-Ser. 6, 813.

ANOMALOUS COMPRESSION BEHAVIOUR OF CORDIERITE

Mirwald, P. W.¹, Miletich, R.² & Loerting, T.³¹Inst. für Mineralogie und Petrographie, Univ. Innsbruck, Innrain 52f, A-6020 Innsbruck, Austria²Inst. für Mineralogie und Kristallographie, Univ. Wien, Althanstrasse 14, A-1090 Wien, Austria³Inst. für Physikalische Chemie, Univ. Innsbruck, Innrain 52a, A-6020 Innsbruck, Austria

e-mail: peter.mirwald@uibk.ac.at.

An increasing number of observations indicate that oxidic compounds, such as water/ice (MIRWALD, 2010), hydrates (DYADIN et al., 1999), quartz and SiO₂-glass (MIRWALD & LOERTING, 2011), may exhibit PVT anomalies. Also dehydration reactions e.g. of NaCl*2H₂O, Mg(OH)₂ (MIRWALD, 2005, 2008) and the compressibility of water (MIRWALD, 2005) indicate anomalous volume behaviour. All these studies base on high precision volumetric experiments ($\Delta V/V \sim 10^{-5}$) performed with a piston cylinder apparatus. A similar volumetric study was performed on cordierite from Soto/Argentina (MIRWALD et al., 1984) up to 1.5 GPa at 25 °C. Parallel, high precision XRD-data (cell volume) were collected with a diamond anvil cell (DAC). Cordierite shows a broad anomaly between 0.35 and 0.75 GPa what is strikingly similar to that one of the SiO₂ materials and also related to the

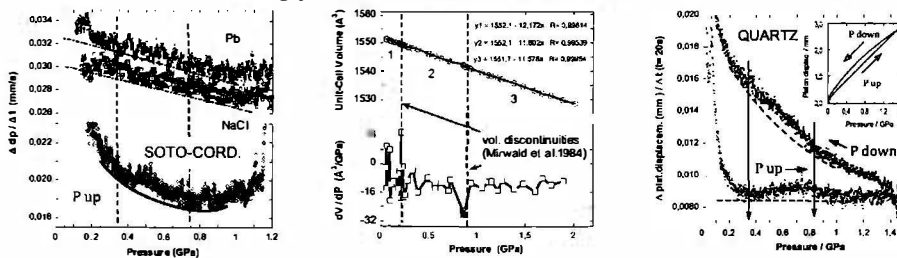


Fig. 1: the left plate displays the compression behaviour of cordierite at increasing pressure, monitored in form of the piston-displacement ($\Delta p d / \Delta t$; $\Delta t = 15$ s) versus pressure with the calibration tracks of Pb and NaCl; the middle plate shows the corresponding cell volume; the right plate gives previous data on quartz.

compressibility of water (MIRWALD, 2005). Furthermore, the ice melting curve (MIRWALD, 2010) and the dehydration reactions of the clathrates of Ne- and H-hydrates (DYADIN et al., 1999) as well as of NaCl*2H₂O show anomalous dP/dT-slope behaviour in that pressure range. All materials studied so far have oxygen as a component in common which insinuates that oxygen is mainly responsible for that anomalous PVT-behaviour.

DYADIN, Y. A., LARIONOV, E. G., MANAKOV, A. Y., ZHURKO, F. V., ALADKO, E. Y., MIKINA T. V., KOMAROV, V. Y. (1999): Mendeleev Commun., 9 (5), 209-210.

MIRWALD, P.W. (2005): J. Chem. Phys., 123, 124715.

MIRWALD, P.W. (2008): J. Chem. Phys., 128, 074502.

MIRWALD, P.W. (2010): IMA2010, 21-27. Aug 2010 Budapest, Acta Miner. Petrographica, Abstr.-Ser. 6, p.813.

MIRWALD, P.W. & LOERTING, T. (2011): Tagung DGK, DMG, ÖMG, Salzburg, 20.- 24.09.2011, Ref. p.91.

MIRWALD, P.W., MALINOWSKI, M., SCHULZ, H. (1984): Phys. Chem. Min., 11, 140.

CONCRETE DETERIORATION - REACTION MECHANISMS REVEALED BY A MULTIPROXY APPROACH

Mittermayr, F.^{1,2}, Baldermann, A.², Klammer, D.², Leis, A.³ & Dietzel, M.²

¹Institute of Technology and Testing of Building Materials, Graz University of Technology, Inffeldgasse 24, 8010, Graz, Austria

²Institute of Applied Geosciences, Graz University of Technology, Rechbauerstraße 12, 8010, Graz, Austria

³RESOURCES – Institute for Water, Energy and Sustainability, Joanneum Research, Elisabethstraße 18/2, 8010, Graz, Austria

e-mail: f.mittermayr@tugraz.at

Deterioration due to aggressive aqueous environments acts as a major threat for the durability of concrete structures. One example is the thaumasite form of sulfate attack (TSA) which preferentially occurs in wet, highly sulfate-loaded and cold (<15 °C) environments such as in underground structures. Despite the fact that the destructive nature of TSA is well known, reaction paths and mechanisms that may even lead to a total destruction of concrete structures are still poorly understood. The aim of this study is to contribute to a deeper understanding by introducing a novel approach based on combined methodologies.

Our multi-proxy approach comprises a range of mineralogical methods such as X-ray diffraction with Rietveld refinement and electron microprobe, hydro-geochemical analyses, e.g. ion chromatography and inductively-coupled plasma-mass spectrometry, and PHREEQC hydrogeochemical modelling. The distribution of stable hydrogen and oxygen isotopes of water were analysed by wavelength scanned cavity ring-down spectroscopy.

The investigations were performed on damaged concrete samples taken from two tunnel sites in Austria, where the locally occurring ground water was classified as slightly aggressive in terms of SO₄ load (DIN EN 206-1. < 600 mg L⁻¹). Severely damaged mushy concrete consisted mainly of thaumasite, secondary calcite, gypsum and aggregate relicts. The expressed interstitial solutions from this altered material were extremely enriched in SO₄ and Cl (> 30000 and 12000 mg L⁻¹, respectively) (Mittermayr et al., 2013). Stable hydrogen and oxygen isotope ratios were feasible for verifying and quantifying the effect of evaporation and distinct degrees of relative humidity. An enormous and linear accumulation of incompatible dissolved ions (e.g. K, Rb and Li) clearly indicates that numerous wetting and drying cycles had occurred. Such a highly dynamic system is considered to have severe destructive effects on concrete structures. With this study we developed a new multi proxy approach to reveal the complexity of alteration processes involving chemical attack on concrete. Thus specific counter measures for structures affected by TSA, designing of advanced concrete admixtures and constructive measures for future projects can be facilitated.

MITTERMAYR, F., BALDERMANN, A., KURTA, C., RINDER, T., KLAMMER, D., LEIS, A., TRITTHART, J., DIETZEL, M., (2013): Cem. Concr. Res., 49, 55-64.

**EXPERIMENTAL DETERMINATION OF Fe-Mg INTERDIFFUSION RATES IN
CLINOPYROXENE AND IMPLICATIONS FOR GEOTHERMOMETRY
INVOLVING FERROMAGNESIAN MINERALS**

Müller, T., Dohmen, R. & Chakraborty, S.

Institut für Geologie, Mineralogie und Geophysik, Ruhr-Universität Bochum, D-44801 Bochum
e-mail: thomas.mueller-1@rub.de

Clinopyroxene (cpx) is a common constituent of many igneous, metamorphic and mantle derived rocks. Spatial variation in the chemical composition of cpx can be interpreted as a record of the magmatic or metamorphic evolution and the partitioning of Fe and Mg between cpx and other ferromagnesian minerals is typically used as a geothermometer. Zoning in such minerals is often the result of diffusive exchange leading to partial disequilibrium profiles. Such profiles can be used to constrain thermal histories if the kinetic parameters are known.

We present experimental data for the chemical interdiffusion of Fe-Mg in natural diopside crystals at ambient pressure, at temperatures ranging from 800 – 1200 °C and oxygen fugacities of 10^{-11} to 10^{-17} bar. Diffusion couples were prepared by ablating an olivine (Fo_{30}) target to deposit a thin film (20 – 100 nm) onto a polished surface of a natural diopside crystal using the pulsed laser deposition (PLD) technique. After diffusion anneals, compositional depth profiles at the near surface region (~ 400 nm) were measured using Rutherford Back-scattering Spectroscopy (RBS).

Experimental results reveal that the data can be described by a single Arrhenius relation without strong dependence of $D^{\text{Fe-Mg}}$ on composition of cpx or oxygen fugacity. $D_\alpha^{\text{Fe-Mg}}$ in a ferromagnesian mineral, α , is arranged in the order spinel > olivine > grt \approx opx > cpx. Diffusion in cpx may thus be the rate limiting process for the freezing of many geothermometers and compositional zoning in clinopyroxene may preserve records of a higher temperature segment of the thermal history of a rock than that recorded in other coexisting mafic minerals. Modelling results suggest that in the absence of pervasive recrystallization, cpx grains will retain compositions from peak temperatures at their cores in most geological settings where peak temperatures did not exceed ~ 1100 °C, but resetting may be expected in slowly cooled mantle rocks, plutonic mafic rocks, or some UHT metamorphic rocks.

LITHOSPHERIC MANTLE HETEROGENEITIES BENEATH SOUTHERN PATAGONIA

Mundl, A.¹, Ntaflos, T.¹, Bjerg, E.A.², Hauzenberger, C.A.³ & Ackerman, L.⁴

¹Department of Lithospheric Research, University of Vienna, Althanstraße 14, 1090 Wien, Austria

²CONICET-Universidad Nacional del Sur, Avenida Colon 80, 8000 Bahia Blanca, Argentina

³Institute for Earth Sciences, University of Graz, Universitätsplatz 2, 8010 Graz, Austria

⁴Academy of Sciences of the Czech Republic, Rozvojova 269, 16500 Prague 6, Czech Republic

e-mail: andrea.mundl@univie.ac.at

Fifty samples were chosen from 6 outcrops in Southern Patagonia. While sample suites from Don Camilo, Gobernador Gregores and Tres Lagos comprise Sp-lherzolites and Sp-harzburgites, samples from Potrok Aike, Salsa and El Ruido, all within Pali Aike Volcanic Field (PAVF), comprise also Sp-Gt-lherzolites and Sp-Gt-harzburgites.

According to Cpx REE patterns, the samples can be divided into 4 groups within Sp-peridotites and 2 within Sp-Gt-peridotites. Group I Sp-peridotites show a depletion in LREE reflecting different degrees of partial melting. Group II shows an enrichment in MREE over LREE and HREE suggesting basaltic melt percolation. Group III REE patterns are flat from HREE to MREE with an enrichment in LREE. Group IV Cpx are in addition enriched in MREE over HREE reflecting stronger metasomatic overprint than Group III. While Group I Sp-Gt-peridotites represents slightly depleted samples with typical REE patterns of Cpx in equilibrium with Gt, Group II Cpx REE patterns show LREE enrichments reflecting metasomatic event(s).

Re-Os analyses of 24 Sp-peridotites reveal highly variable T_{RD} . While T_{RD} at Tres Lagos range from 1 to 1.6 Ga, samples from Don Camilo and Gobernador Gregores yield ages from 0.6 and 0.8 to 1 Ga, respectively. Samples from PAVF yield T_{RD} from 0.3 to 2.3 Ga. A depletion in Pt, Pd and Re in all samples reflect different degrees of partial melting.

REE abundances, different degrees of partial melting and transition reactions from Sp to Gt stability field and vice versa, suggest a very heterogeneous SCLM beneath Southern Patagonia.

CONTACT AUREOLE OF THE SRI SAWAT GRANITE, KANCHANABURI PROVINCE, WESTERN THAILAND

Nantasin, P^{1,2}, Hauzenberger, C.¹, Richoz, S¹, Abu-Alam, T.S.¹ & Wathanakul, P.²

¹Institut für Erdwissenschaften, Universität Graz, Universitätsplatz 2, A-8010 Graz, Austria

²Department of Earth Sciences, Faculty of Science, Kasetsart University, 50 Phahon Yothin Road, Chatuchak, 10900 Bangkok, Thailand
e-mail: prayath@gmail.com

The Sri Sawat granite emplaced to a lower Paleozoic sedimentary succession ranging in the age from Cambrian, Ordovician to Silurian–Devonian ages. Age of emplacement of around 200 Ma and the geochemical characteristics suggest that the Sri Sawat granite is of S-type affinity and belongs to the Central granite belt in Thailand and Southeast Asia. The intrusion developed a contact aureole comprised of hornfels in Cambrian mudstone and metacarbonate in Ordovician argillaceous limestone. The metacarbonate comprises: Tr–Phl calc-silicate (Type I), Cal marble (Type II), Ves–Wo–Di–Grs–Qtz calc-skarn (Type III), and Dol–Cal–Phl±Chl marble (Type IV). *P*–*T* conditions of the contact metamorphism were estimated by pseudosections and mineral isopleths from hornfels samples and yield ~580 – 600 °C and 2 kbar. Based on the pressure of 2 kbar, the isobaric *T*–XCO₂ diagrams of representative samples from Types I, III and IV reveal that the peak equilibrium temperature is ~500 °C, ~660 °C and 420 °C, respectively. Stable C–O isotopes suggest that meteoric infiltration was the source of the fluid in Type I while magmatic infiltration was the source in Type II and IV. Whereas the calc-skarn (Type III) shows a strong influence of magmatic coupled with meteoric fluids.

RETENTION OF RADIATION DAMAGE IN ZIRCON XENOCRYSTS FROM KIMBERLITES, NORTHERN YAKUTIA

Nasdala, L.¹, Kostrovitsky, S.², Kennedy, A.K.³ & Zeug, M.¹

¹Institut für Mineralogie und Kristallographie, Universität Wien, Althanstr. 14, 1090 Wien, Austria

²Vinogradov Institute of Geochemistry, Siberian Branch, Russian Academy of Sciences, Irkutsk, 664033, Russia

³Department of Applied Physics, Curtin University of Technology, Bentley, WA 6102, Australia

e-mail: lutz.nasdala@univie.ac.at

We have studied zircon xenocrysts (that are assumed to originate from lower crustal or upper mantle rocks) from kimberlites from the Kuoika and Ary Mastakh fields in Northern Yakutia. Kimberlite formation has occurred ca. 150–230 Ma ago (compare also GRIFFIN et al., 1999). Our SHRIMP (Sensitive High Resolution Ion MicroProbe) analyses yielded much older, generally concordant U–Pb ages (Fig. 1), which excludes notable U–Pb resetting during kimberlite formation. Also, zircon grains were found to be significantly more radiation-damaged than would correspond to damage accumulation only since the time of kimberlite formation (cf. NASDALA et al., 2001). This observation contradicts the hypothesis that high temperatures during kimberlite events will cause complete structural reconstitution of zircon xenocrysts, by thermal annealing of the accumulated radiation damage.

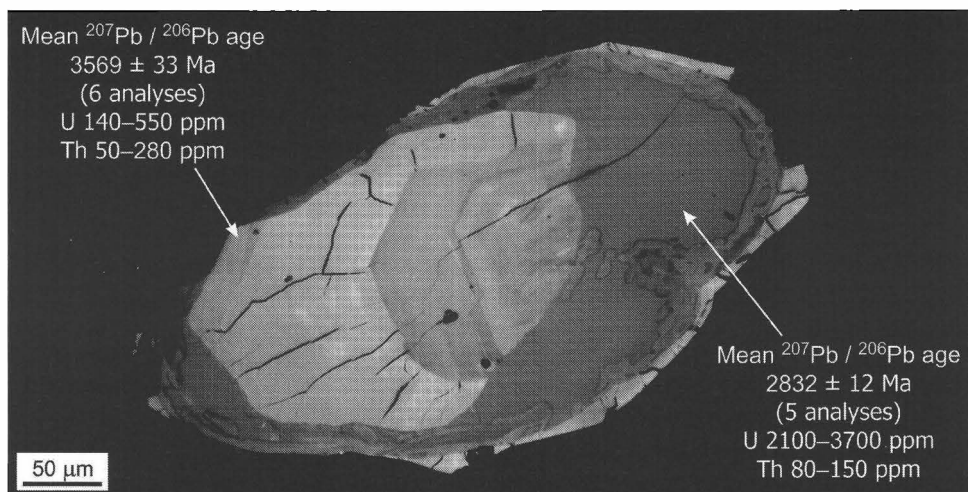


Figure 1. Zircon xenocryst (embedded in epoxy and polished; reflected light image) from the Bargadymalah pipe, Ary Mastakh field, Northern Yakutia, showing a complex internal texture. The zoned core (high reflectance) is partially radiation-damaged whereas the U-rich interior region (dark grey) is fully metamict.

GRIFFIN W.L., RYAN C.G., KAMINSKY, F.V., O'REILLY, S.Y., NATAPOV, L.M., WIN, T.T., KINNY, P.D., ILUPIN, I.P. (1999): Tectonophysics, 310, 1–35.

NASDALA, L., WENZEL, M., VAVRA, G., IRMER, G., WENZEL, T., KOBER, B. (2001): Contrib. Mineral. Petrol., 141, 125–144.

EXPERIMENTAL ALTERATION STUDIES AT THE BENTONITE-CEMENT INTERFACE

Nickel, C.^{1,2} & Warr, L.N.²

¹Institute for Applied Geosciences, Graz University of Technology, Rechbauerstraße 12, 8010 Graz, Austria

²Institute for Geography and Geology, Ernst-Moritz-Arndt University Greifswald,

Friedrich-Ludwig-Jahn-Straße 17a, 17487 Greifswald, Germany

e-mail: claudia.nickel@tugraz.at

The Aspö underground laboratory site (Sweden) is a field study site designed for nuclear waste disposal in a granite-based repository. In order to guarantee the long-term sealing of the repository, a multi-barrier concept is been investigated consisting of a bentonite and cement buffer that surrounds the radioactive containing copper containers. Groundwater interactions with the bentonite buffer are generally well known, but alteration processes directly at the bentonite-cement contact are still poorly constrained. These processes may have a significant impact on the long-term stability and self-sealing capacity of both buffers.

In order to characterize the alteration processes directly at the bentonite-cement contact, two bentonite-cement leaching experiments and one bentonite control experiment were carried out. A water inflow scenario was simulated using a flow-through reaction-cell (WARR & HOFMANN, 2003) with distilled water as the leaching agent. During the hydration period, changes in the mineralogy and chemistry of both air-dried MX-80 bentonite and Portland cement clinker were monitored using X-ray diffraction and transmission electron microscopy analyses over an experimental period of one year.

Within the first 22 h the cement-influenced bentonite hydrated rapidly while the pure bentonite reached its maximum hydration after 963 h. Associated with the rapid water inflow in the cement-bentonite experiments the volume of the bentonite layer strongly increased and subsequently infiltrated the cement layer. Intense cation exchange of Na^+ (0.36 to 0.08 a.p.f.u) for Ca^{2+} (0.08 to 0.12 a.p.f.u.) took place directly at the bentonite-cement contact zone, within the interlayer sites of the montmorillonite. This reaction was associated with the general depletion of the CaO content in the C-S-H phases by a factor of 2.5 compared to the unaltered cement. It was recognized that gypsum, an accessory mineral in the MX-80 bentonite, was completely dissolved during the first hydration period. Ettringite precipitated simultaneously, whereas neither ettringite formation nor gypsum dissolution was observed in the control experiment. It appears that ettringite can weaken the concrete and inhibiting the formation of more cement minerals, i.e. C-S-H phases.

Our results clearly indicate that intense leaching occurs at the bentonite and cement contact in the presence of aqueous solution. The Ca substitution of Na reduces the montmorillonite swelling pressure, and significantly reduces the Ca required for the formation of cement phases. Thus, the cementation process close to the bentonite-cement alteration zone was determined to be incomplete. These alteration processes may have huge impact on destabilizing the clay-cement buffer.

**TOURMALINE (SCHORL-DRAVITE) FROM GRANITIC PEGMATITES
IN VLASTĚJOVICE, CZECH REPUBLIC:
AN INDICATOR OF FRACTIONATION AND IN-SITU CONTAMINATION**

Novák, M., Kadlec, T. & Gadas, P.

Department of Geological Sciences, Masaryk University, Kotlářská 2, 611 37 Brno, Czech Republic
e-mail: mnovak@sci.muni.cz

Tourmaline is a valuable indicator of geochemical processes and it is widely used to monitor degree of fractionation or external contamination of pegmatite melts. Tourmaline-bearing granitic pegmatites cutting various rocks in Vlastějovice exhibit similar size and mostly simple internal structure and mineral assemblages (Tab. 1). The parental granite of the pegmatites cutting Fe-skarn (Footwall granite-pegmatite) is located along the footwall contact of Fe-skarn and underlying orthogneiss body and the relevant pegmatite melts passed several decameters solely through Fe-skarn. Hence, they represent a unique case to study degree of contamination in pegmatites with distinct host rocks and degree of fractionation.

Pegmatite/degree of fractionation	Hostrock/ reaction rim	Fe,Mg,Mn-minerals
Březina/low	migmatized gneiss/none	Tur~Gr>Bt
Nosatá skála/low	pyroxene gneiss/none	Tu>Bt>Grt
Footwall granite-pegmatite/low	orthogneiss/Fe-skarn/thin	Bt>Tu>Amp
Pegmatite No.4/ low	Fe-skarn/moderate	Bt>Tu>Amp
Pegmatite No.12/ low	Fe-skarn/thick	Bt>Tur~Amp
Spessartine pegmatite/moderate	Fe-skarn/none	Bt>Tur>Grt
Elbaite pegmatite/high	Fe-skarn/none	Tur>>Bt

Table 1. Brief review of the pegmatites examined.

Evident Ca,Fe-contamination is seen in tourmaline from all pegmatites cutting Fe-skarn, whereas contamination in the pegmatites from gneisses is negligible. The overall positive correlation Ca-Fe is evident but the individual dikes show rather negative correlation with distinct slopes (Fig. 1). In the pegmatites from gneisses this evolution reflects fractionation of the melt to Ca-poor and Fe-enriched; however, in the contaminated pegmatites this process is more or less overprinted by the Ca, Fe-contamination from host Fe-skarn and fractionation of Mg from Fe is enhanced by contamination. The Footwall granite-pegmatite located between Fe-skarn and orthogneiss exhibits transitional features and corroborate these results. The tourmaline evolution in Vlastějovice also confirms tourmaline as a useful geochemical indicator.

This work was supported by the research project GAP210/10/0743 to MN and PG.

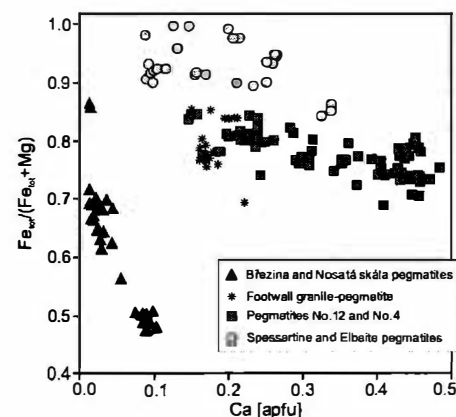


Figure 1. Plot $\text{Fe}_{\text{tot}}/(\text{Fe}_{\text{tot}}+\text{Mg})$ vs. Ca in tourmalines.

**DELAMINATED LITHOSPHERIC MANTLE FROM FAR EAST RUSSIA
AFFECTED BY EXOTIC METASOMATISM**

Ntaflos, Th.¹, Aschchepkov, I.², Koutsovitis, P¹, Hauzenberger, C.³ & Asseva, A.⁴

¹Department of Lithospheric Research, University of Vienna, Althanstraße 14, A-1090 Vienna, Austria

²RAS, Novosibirsk, Russia

³Institute of Earth Sciences, University of Graz, Universitätsplatz 2, A-8010 Graz, Austria

⁴RAS, Vladivostok, Russia

e-mail: theodoros.ntaflos@univie.ac.at

In the back-arc environment of Far East Russia, mantle xenoliths from Sikhote-Alin (KO) and Primorie (SV), Far East Russia are fertile spinel lherzolites with amphibole, phlogopite armalcolite, fassaite and röhnite in some of the studied samples. The KO samples have Mg# varying from 89.1 to 89.9 and are slightly more fertile than the SV samples that have Mg# ranging from 89.8 to 90.4. The cpx REE confirm this trend as the $(La/Yb)_N$ in KO samples range from 0.10 to 1.00 and in SV samples from 0.15 to 1.73.

The clinopyroxene Sr and Nd isotopic ratios range from 0.702599 to 0.703567 and 0.512915 to 513153, repectively, resembling Pacific MORB isotopic ratios.

En route breakdown of disseminated amphibole produces second generation of cpx and olivine and traces of glass as well fassaite and röhnite indicating crystallization at very shallow depths. Melt pockets consisting of Ca-rich glass plagioclase rutile, ilmenite and armalcolite suggest introduction of small amount of an unusual Ti-Ca-rich anhydrous silicate melt at mantle depths.

The studied lithospheric mantle represents the residue after partial melting of up to 5% of a primitive mantle. Despite the fact that the studied area experienced several subducting episodes, the lithospheric mantle appears to be unaffected from the upwelling fluids/melts of the subducted slab(s). Since there is no indication for plume activity, and/or evidence for refertilization, it is likely that the lithospheric mantle has been delaminated as the result of tectonic events (lithospheric attenuation, inverse tectonic) associated with the subduction processes and that the studied spinel lherzolites represent upwelling asthenosphere.

STRUCTURAL CHARACTERIZATION OF LANNONITE FROM THE ANNA MINE, ALSDORF, GERMANY

Oberwandler, L.¹, Pristacz, H.¹, Kolitsch, U.^{2,1} & Lengauer, C.L.¹

¹ Institut für Mineralogie und Kristallographie, Universität Wien – Geozentrum,
Althanstrasse 14, 1090 Wien, Austria

² Mineralogisch-Petrographische Abteilung, Naturhistorisches Museum Wien
Burgring 7, 1010 Wien, Austria.
e-mail: christian.lengauer@univie.ac.at

Lannonite and wilcoxite were first described by WILLIAMS & CESBRON (1983) as two new fluosulfates from the Lone Pine mine, New Mexico, where both occur as weathering products of the primary pyrite-rich ore. The chemical formula was reported to be $\text{HMg}_2\text{Ca}_4\text{Al}_4(\text{SO}_4)_8\text{F}_9 \cdot 32\text{H}_2\text{O}$ and a tetragonal symmetry without centering was derived from X-ray powder data. Due to the quality of the type material, however, no structural information could be obtained for both minerals. Recently PETERSON & JOY (2013) presented a detailed structural description of wilcoxite, $\text{MgAl}(\text{SO}_4)_2\text{F} \cdot 17\text{H}_2\text{O}$.

A second finding of lannonite from the Anna Mine, Alsdorf near Aachen, Germany, was reported by BLASS & STREHLER (1993), where lannonite is formed during the burning and weathering process of a coal dump after spontaneous ignition, i.e. mobilization of volatile components from the coal and formation of acidic solutions, which decompose the surrounding rock. Beside several ammonium and sulfate minerals, e.g. ammoniojarosite, anhydrite, or thermessaite-(NH₄), selenium is also observed in the lannonite-bearing paragenesis. The title compound occurs as clear, colourless, optically uniaxial, tetragonal (square) platelets, which are suitable for single-crystal X-ray investigations at ambient temperature. Even though lannonite has a reported H₂O content of 32 wt.%, it is a stable mineral with Mohs hardness of about 2 and a reported density of 2.22 g/cm³.

The extinction conditions revealed a tetragonal *I*-centered cell ($a = 6.860(1)$, $c = 28.053(5)$ Å, $V = 1320.3(4)$ Å³), and consecutive structure refinements applying the space groups of Laue class *4/m* revealed the correct space group to be *I4/m* ($R_{1\text{all}} = 4.25\%$). The first outcome of the refined structure model is a reduced H₂O and F content leading to $\text{Mg}_2\text{Ca}_4\text{Al}_4(\text{SO}_4)_8\text{F}_8 \cdot 24\text{H}_2\text{O}$ as the corrected chemical formula for lannonite (D_x of 2.100 g/cm³) from this locality. The structure can be described by a columnar sequence along [001] of F-linked CaFO₅-AlF₂(H₂O)₄-MgF₂(H₂O)₄-AlF₂(H₂O)₄-CaFO₅ octahedra terminated by positionally disordered SO₄ tetrahedra. These columns are interlinked by a second type of SO₄ tetrahedra, connecting neighbouring CaFO₅ octahedra.

The crystal-structure determination, together with optical and chemical-analytical data and Raman spectroscopy of the material will be presented and discussed.

We thank Mr. Frank de Wit for kindly providing the samples studied.

BLASS, G., STREHLER, H. (1993): Mineralien-Welt, 4(4), 35-42.

PETERSON, R.C., JOY, B.R. (2013): Canad. Mineral., 51, 107-117.

WILLIAMS, S.A., CESBRON, F.P. (1983): Mineral. Mag., 47, 37-40.

**NEW CONSTRAINTS ON THE TIMING OF THE MAE-PING CORE-COMPLEX
(NW-THAILAND)**

Österle, J., Palzer, M. & Klötzli, U.

Department of Lithospheric Research, University of Vienna, Althanstrasse 14, A-1090, Vienna, Austria
e-mail: juergen.oesterle@email.com

The Mae Ping fault zone (MPFZ) is considered to be one of the major strike-slip shear zones contributing to the lateral extrusion of SE-Asia. Within this fault zone a Core-Complex of ductile deformed amphibolite-facies rocks, the so called Lan Sang Gneisses, occurs. Despite several former investigations some aspects concerning the time, regime and cause of exhumation remain unclear. New detailed structural, petrographical and geochronological investigations of the Lan Sang Gneisses were undertaken to develop for the first time different PT paths for different rock types (an augen-gneiss, a biotit-gneiss and a subvolcanic dyke). Concerning the timing of the MPFZ, an undeformed discordant subvolcanic dyke has been found within the highly deformed Lan Sang Gneisses which is clearly of intrusive nature. LA-ICP-MS U-Th-Pb dating of prismatic and soccerball shaped zircons from this dyke yields an age of 42 ± 2 Ma and suggests a deformation of the MPFZ prior to this time. However, the zircon age of the subvolcanic dyke clearly conflicts with Ar-Ar dating on biotites by LACASSIN et al. (1997) who suggest the timing of the fault zone to be around 30 Ma. Furthermore these results question the MPFZ to be one of the shear zones contributing to the lateral extrusion of SE-Asia during the Himalayan orogenesis. Therefore the deformation could be of Indosinian (Triassic) origin as a result of the collision between Sibumasu and Indochina.

LACASSIN, R., MALUSKI, H., LELOUP, P. H., TAPPONIER, P., HINTHONG, C., SIRIBHAKDI, K., CHUAVIROJ, S., CHAROENRAVAT, A. (1997): Journal of Geophysical Research, Vol. 102, 10,013-10,037.

**FORMATION OF HELECTITE IN THE CAVE DRAGON BELLY
(SARDINIA, ITALY)**

Onuk, P.¹ & Dietzel, M.²

¹Institute of Earth Sciences, University of Graz, Universitätsplatz 2, 8010 Graz, Austria

²Institute of Applied Geosciences, Graz University of Technology, Rechbauerstrasse 12, 8010, Graz, Austria
e-mail: peteronuk@yahoo.com

In the cave Dragon Belly, situated in the Gulf of Orsei (Sardinia, Italy), a special type of irregular speleothem called helectite was found. The apparent helectites solely exist as stalactites. The helectites are grown in all vertical and horizontal directions with a huge variety in size and shape and do not show any affinity to gravity. According to HILL & FORTI (1997) the apparent speleothem is classified as a thread-like variety of helectite, which usually consists of aragonite. In the present case solely calcitic varieties are found.

Thin section analyses indicate that the vertical central canal for solution migration of our calcitic helectites is clogged at the tip. It is suggested that due to this occlusion the water pressure inside the stalactite had been increased and caused the formation of horizontal canals between 30 and 60 µm in diameter which are circularly arranged. These secondary "canalicules" originate in the central canal and radiate in a sinuous shape to the outer surface of the stalactite. Helectites seem to be grown from their canal and if the solution gets into contact with the atmosphere, precipitation of CaCO₃ occurs due to CO₂ degassing.

Optical mineral orientation analyses show that the stalactite consists of concentric arranged single crystallites with pronounced spacing between individual crystals and the helectite consists of calcite crystals with identical structural orientation. SEM imaging indicates rather uniform crystallite size and shape on straight parts of the helectites which may lead to an equally distributed water film with rather constant precipitation conditions. Interestingly at the bended parts the crystallites on the inside of a bend are significantly smaller than on the outside. Thus inside the bend the specific surface area is much higher vs. the outside. We assume that significantly differences in precipitation rates - e.g. induced by a change in wettability, water film thickness and/or CO₂ degassing kinetics - result in distinct crystal sizes for inside vs. outside areas of a bend. The elevated need in volume by CaCO₃ formation at the outside of a bend (big crystals) finally leads to a helix shaped form which gives the helectite its name.

HILL, C., FORTI, P. (1997): Cave Minerals of the World. National Speleological Society, 463pp.

MINERALIZATION OF THE MAFIC-ULTRAMAFIC ROCKS OF THE LAS AGUILAS – LAS HIGUERAS AREAS, SAN LUIS PROVINCE, ARGENTINA

Onuk, P.¹, Mogessie, A.¹, Bjerg, E.² & Krenn, K.¹

¹Institute of Earth Sciences, University of Graz, Universitaetsplatz 2, 8010 Graz, Austria

²INGEOSUR and Departamento de Geología, Universidad Nacional del Sur, San Juan 670,
8000 Bahía Blanca, Argentina

e-mail: peteronuk@yahoo.com

Within the Sierras de San Luis, a part of the Sierras Pampeanas (central Argentina), mafic – ultramafic rocks consisting of norites, gabbros, anorthosites, orthopyroxenites and dunites are exposed as lenses and strike about 120 km NNE-SSW with a width of ca. 30 km. The geotectonic setting of the mafic-ultramafic intrusions is thought to be an extensional back-arc basin which developed during the last stages of the Famatinian orogeny. A detailed investigation of a drill core (LAS5/3) profile from the Las Aguilas area has been made in order to document the petrography of the mafic-ultramafic rocks as well as the intercalated basement with depth. The study is focused on sulphides, Platinum-group mineral concentrations as well as fluid inclusions. It is shown that these rocks are characterized by a moderate to high-grade base metal sulfide (BMS) mineralization. Sulfides include chalcopyrite, pentlandite and pyrrhotite showing primary magmatic and secondary mineralization textures. The platinum group minerals (PGM) such as merenskyite-melonite group minerals and cobaltite group minerals are related to the BMS and to the Cr-spinel-rich ultramafic part of the intrusion and occur as primary and secondary mineral phases. Primary PGM's occur as inclusions in sulfides and the secondary occur in veins or between BMS and silicates as a result of remobilization and precipitation processes. The secondary PGM's seem to have crystallized at about 500 °C based on the Pd-Bi-Te plot of HOFFMAN & MACLEAN (1976). Textually and geochemically three different types of chromium spinel were distinguished. Type 1) iron-rich spinel with magnetite rim and mainly homogeneous cores. Type 2) show alumina-rich and chromium-poor rims as well as an increasing trend in chromium and iron. Cores point to a decrease in alumina content. Type 3) is a homogenous chromium spinel. These findings are similar to those reported by FERRACUTTI et al. (2006). Three different groups of primary CO₂-N₂-CH₄ inclusions were identified in plagioclase and quartz by last melting temperatures T_m of the carbonic phase and Raman Spectroscopy. Fluid densities are derived from homogenization temperatures T_h of the vapor bubble, which ranges from 16.3 °C to -25.5 °C. Fluid inclusions reflect a decrease in densities with increasing depth within the drill core. It is important to note that the fluid inclusions in the hanging-wall basement at a depth of 40 meters represent the formation conditions of the Famatinian orogenic event of ~6 kbar at 600 °C. Fluid inclusions in samples at 60 meters and 120 meters depth can be related to the pressure and temperature conditions of the mafic-ultramafic intrusion with an estimated pressure of ~4 kbar at 600 °C in the footwall.

FERRACUTTI, G., MOGESSIE, A., BJERG, E. (2006): N. Jahrbuch Mineral. Abhandlungen, 183-1, 63-77
HOFFMAN, E. L., MACLEAN, W. H., (1976): Economic Geology, 71, 1461-1468.

SYNTHESIS AND STRUCTURAL EXAMINATIONS ON LTA-TYPE ZEOLITE

Ormándi, S. & Dódony, I.

Department of Mineralogy, Eötvös Loránd University, Pázmány Péter sny. 1/C, 1117 Budapest, Hungary
e-mail:ormszil2@gmail.com

Zeolites were just curiosity for a long time, but nowadays the usage of their names is increasing, and zeolites become very important materials in environmental issues and industry. Why did that change? As usual, the main progress in the knowledge on zeolites was the successful structure determination.

Zeolites have a complex aluminosilicate framework structures. These frameworks are opened with large channels and interconnected cages. We can use zeolites in gas and petroleum industry, water softening, sewage treatment, agriculture, paper production, radioactive waste treatment as well as construction materials too. The structural channels and voids are occupied by loosely bound cations and water molecules that we can remove and replace without disrupting the tetrahedral framework. This means that a zeolite structure is among the best candidate to perform cation exchange, adsorption molecular sieving (passing a gas or liquid through a zeolite), dehydration and rehydration processes, in addition it can be resistant to high energy radiation too (TSCHERNICH, 1992).

The present work focuses on preparation and structure determination of sodalite-related zeolites using X-ray and electron diffraction techniques. I synthetized LTA-type zeolite crystals from metakaolinite starting material with alkaline (NaOH) method. Then I replaced Na^+ with Cs^+ , and measured the resulted structural changes, using X-ray powder diffraction. The LTA crystals revealed cube and sphere shapes under scanning electron microscope. X-ray powder diffraction measurements on Na-LTA, acid treated LTA and Cs-LTA were performed. The hkl and intensity data sets were the inputs for structure determination using the SIR (Semi Invariant Reconstruction) and SHELLX program packages. Due to overlapping reflections, some sample resulted in high R factor values. However, the resulted LTA-type framework proved to be evident.

TSCHERNICH, R. W. (1992): Zeolite of the world. Geoscience Press Inc., USA.

**NEW CONSTRAINTS ON THE MAE PING CORE-COMPLEX,
NW-THAILAND: IS IT AN INDOSINIAN RELICT?**

Palzer, M., Österle, J. & Klötzli U.

Department of Lithospheric Research, University of Vienna, Althanstraße 14 (UZA II), 1090 Vienna, Austria
e-mail: a0821104@unet.univie.ac.at

The Mae Ping fault zone is seen as one of the major strike-slip shear zones in SE-Asia trending NW-SE over 500 km across Thailand. Within this fault zone, a 150 km long and 5 km wide core-complex with ductile deformation of amphibolite-facies rocks containing lenses of an older high-grade px-amph-pl paragenesis occurs. These so called Lan Sang Gneisses are named after the outcrops situated in the Lan Sang National Park. Despite several former investigations (LACASSIN et al., 1997) some aspects concerning the time, regime and cause of exhumation remain unclear. Further on, the old granulite-facies paragenesis has never been studied in detail. Older models constitute a restraining bend within a left-lateral regime as the origin of the exhumation. New detailed structural, petrographical and geochronological investigations were undertaken to develop different PTt-paths for different rock types with special emphasis on the lenses of old high grade rocks. We use detailed field investigations on a profile in Lan Sang National Park, thin sections, electron microprobe analyses, geothermobarometry as well as zircon and monazite ages of three different rock types. On the basis of our observations and measurements, we try to reconstruct the different PTt paths.

First results now question the model of a restraining bend and lead us to the conclusion that the origin of the amphibolite-facies deformation may lie in the late Triassic Indosinian Orogeny.

LACASSIN, R., MALUSKI, H., LELOUP, H., TAPPONNIER, P., HINTHONG, C., SIRIBHAKDI, K., CHUAVIROJ, S., CHAROENRAVAT, A. (1997): Journal of Geophysical Research, 102 B5, 10013-10037.

PETROLOGICAL AND GEOCHEMICAL STUDIES OF MANTLE XENOLITHS
FROM RIO NEGRO PROVINCE, ARGENTINA

Papadopoulou, M.¹, Ntaflos, T.¹, Bjerg, E.² & Gregoire, M.³

¹Department of Lithospheric Research, University of Vienna, Althanstrasse 14, A-1090 Vienna, Austria

²Universidad Nacional del Sur, San Juan 670, B 8000, Bahia Blanca, Argentina

³Observatoire Midi Pyrénées, University of Toulouse III, France

e-mail: a0904343@unet.univie.ac.at

The Comallo, N. Patagonia, are depleted sp-lherzolites, sp-harzburgites, wehrlites and clinopyroxenites. The studied samples are fine-grained with a dominant well-equilibrated equigranular texture whereas protogranular and porphyroclastic textures are rare. The rock forming minerals are olivine, ortho- and clinopyroxene and spinel. Relictic amphibole and phlogopite are present as well. The amphibole, where present, has been destabilized and shows breakdown reaction at the margin, forming second generation of ol, cpx and sp.

The Fo content in the lherzolites and harzburgites range from 90.8 to 92.0, and in the wherlites from 89.0 to 90.0. Clinopyroxene is diopside with 3.0 wt% Al₂O₃ in the rim and up to 4 wt% in the core. Spinel is Cr₂O₃-rich with Cr#=0.426.

LA-ICP-MS analyses on clinopyroxene show that the studied mantle xenoliths are strongly depleted in HREE [(Dy/Lu)_N= 0.4-0.7] and LREE [(La/Sm)_N= 0.3-0.8] but enriched in MREE [(Sm/Nd)_N= 1.3-1.7]. The HFSE compared to their neighbour elements exhibit strong negative anomalies suggesting that the studied peridotites are the residues of high degree of partial meltings. Using the model of fractional melting the calculated extraction of basaltic components is high and ranges between 30 and 33%.

The presence of disseminated amphibole and phlogopite, indicates that the lithospheric mantle underneath Comallo in N. Patagonia, has experienced limited modal metasomatism, whereas the trace elements in clinopyroxene show they have barely been affected by this metasomatism.

KRISTALLOGRAPHISCHE KURIOSITÄTEN

Pertlik, F & Zirbs, W.

Institut für Mineralogie und Kristallographie der Universität Wien, Geozentrum
Althanstraße 14, A-1090 Wien, Österreich.
e-mail: franz.pertlik@univie.ac.at

Die Kristallographie als eigenständige Wissenschaft wurde Ende des 18. Jahrhunderts noch eher geringschätzig betrachtet. Erst im Laufe des 19. Jahrhunderts erfuhr sie eine allmähliche Aufwertung im Kanon der Wissenschaften. Nach BEKKERHINN & KRAMP (1793): „*Vorrede. Was nützt die Kristallographie? Gar nichts. Die Abänderungen der Kristallformen gehen schon beim nämlichen Mineral ins unendliche; groß ist die Zahl der bestimmten, noch größer die der unbestimmten Kristallformen; viele tragen keine Merkmale irgend einer Kristallisation an sich; viele andere sind überhaupt keiner Kristallisation fähig. Diese hängt ausserdem von so vielen, auf verschiedene Art und jeden Augenblick anders wirkenden Ursachen ab; sogar die Temperatur der äusseren Luft und das Sonnenlicht spielen ihre Rolle dabei; so dass es am Ende gar keine den Bestandtheilen der Körper eigne Kräfte, sondern ein ungefähres Werk des Zufalls, ein gewisser Fortuitus concursus atomorum war, der den Kristallen ihre Bildung gab. Und überhaupt, alle die Dreikke, Vierekke, so klein, dass man sie oft kaum sieht, gehören in die Mathematik, und sind ganz unter der Würde der Mineralogie. Der ächte Naturforscher bleibt nicht auf der Oberfläche stehen; er dringt ins Innre der Natur hinein, von der Fakkel der Chemie beleuchtet erforscht er die jedem Körper eignen Verhältnisse seiner Bestandtheile; und auf diese, nicht auf die vergängliche Form, gründet er seine Klassifikation der natürlichen Erzeugnisse“*

VOLGER (1854) führte an Stelle der zu dieser Zeit bereits gebräuchlichen und auch heute benutzten Nomenklatur eine neuartige Synonymik für einige Kristallsysteme und für alle in diesen auftretenden Flächenformen ein: Vollflächner... Gänzling, Halbflächner..Hälbling, Viertelflächner... Viertling. Als Beispiele für das kubische System wurden angeführt (Hälbling...Gänzling; in Klammern die Anzahl der jeweiligen Flächen):

Timpling... Eckling (4...8)
Höckertimpling...Buckling (12...24)
Buckeltimpling...Höckerling (12...24)

Kommentar aus dem Werk KENNGOTTs (1855) mit nicht zu übersehender Ironie: „*Durch diese Bereicherung der Nomenklatur glaubte Volger die Symbolik entbehrlich gemacht zu haben, welche nach seiner Ansicht bei Weitem nicht das leistet, was durch seine Benennung erreicht wird, da diese eine bequeme Ausdrucksweise für Schrift und Rede ergibt. Nach seinen eigenen Worten ist seine Benennung der Combinationsgestalten stets die genaueste und die bei dieser äussersten Genauigkeit sich ergebende Länge und Unbequemlichkeit derselben dürfte doch noch immer übertroffen werden von allen hergebrachten Bezeichnungsweisen, auch wenn dieselben sich weit von einer ähnlichen Genauigkeit entfernt halten*“

- BEKKERHINN, K. & KRAMP, C. (1793): Kristallographie des Mineralreichs. Joseph Stahel, Wien.
KENNGOTT, A. G. (1855): Synonymik der Krystallographie. Carl Gerold und Sohn, Wien.
VOLGER, G. H. O. (1854): Die Krystallographie oder Formenlehre der stoffeinigen Naturkörper. Stuttgart.

**ANISOTROPIC DIFFUSION IN ALKALI FELDSPAR: RECONSTRUCTION OF
THE COMPOSITION-DEPENDENT DIFFUSION COEFFICIENTS**

Petrishcheva, E., Abart, R. & Schaeffer, A.-K.

University of Vienna, Department of Lithospheric Research, Althanstrasse 14, A-1090, Vienna, Austria
e-mail: elena.petrichcheva@univie.ac.at

Reconstruction of intrinsic system parameters such as particle mobilities or diffusivities from experimentally observable data is a complicated and practically-relevant inverse mathematical problem. An important example is given by nonlinear diffusive transport in one spatial dimension where the diffusion coefficient is an unknown function of concentration. Here reconstruction of the diffusivity versus concentration is performed using a known semi-scale solution of the diffusion equation.

The above technique can be generalized for the case of the anisotropic nonlinear diffusion. To this end we prepared many plane-parallel samples with different orientations with respect to the crystal structure. The effective diffusivity along a specific direction is reconstructed from the measured concentration profile. The full diffusion tensor is derived from the set of effective diffusivities.

We use this approach to obtain the diffusivity tensor for Na-K interdiffusion in alkali feldspar and reveal its dependence on concentration. The results are tested by solving the nonlinear diffusion equation and comparing the numerical solutions with the experimentally observed concentration profiles.

**EVOLUTION OF THE SECKAU CRYSTALLINE BASEMENT
(SECKAU MOUNTAINS, EASTERN ALPS): IMPLICATIONS FOR PRE-ALPINE
MAGMATISM AND ALPINE METAMORPHISM**

Pfingstl, S.¹, Hauzenberger, C.¹, Kurz, W¹ & Schuster, R.²

¹Institute of Earth Sciences, University of Graz, Heinrichstrasse 26, A-8010 Graz, Austria

²Geologische Bundesanstalt, Neulinggasse 38, A- 1030 Wien, Austria

e-mail: walter.kurz@uni-graz.at

The massif of the Seckau mountains (Seckauer Tauern) is mainly built up of granitoids, overprinted by Eoalpine (Cretaceous) deformation during nappe stacking and subsequent extension, and greenschist facies metamorphism. Whole rock Rb-Sr age data of ca. 432 Ma and 350 Ma were assumed to indicate the protolith ages (SCHARBERT, 1981).

In this study, a suite of granitoids was geochemically analysed by X-ray fluorescence (Bruker Pioneer S4) in order to derive the processes of magmatic evolution and differentiation. In general, three types of magmatites can be distinguished: granites, granodiorites and quartz-monzonodiorites. The first two form the majority, whereas the intermediate quartz-monzonodiorites are only locally exposed.

Following the A/CNK discrimination diagram a clear distinction between S- and I- Type granitoids can be established. The S- type granites are mainly part of the structurally uppermost sections and are covered by Permian to Lower Triassic metasedimentary sequences of the Rannach Formation.

Within the AFM diagram all granitoids are characterized by a calcalkaline trend. This suggests formation of the melts during a subduction process. Within the R1-R2 diagram, the granitoids are related to both pre-plate collision, syn-collision and post-collision uplift settings.

We therefore suggest that the granitoids of the eastern Seckau massif are part of an intrusion sequence during distinct stages of a plate tectonic cycle, i.e. from pre- to post collision, and that the related magmas differentiated from intermediate (quartz-monzonodiorites) I-type to acidic (granites, granodiorites) S-type.

Biotites separated from the granitoids yield Rb-Sr age data between 83 and 87 Ma, and 80 to 76 Ma. These ages are assumed to represent cooling ages related to the exhumation of the Seckau massif subsequent to Eo-Alpine greenschist facies metamorphism.

SCHARBERT, S. (1981): Mitt. Ges. Geol. Bergbaustud. Österr., 27, 173-188.

MINERALOGICAL, GEOCHEMICAL AND ISOTOPIC CHARACTERISATION OF EVAPORITES FROM THE "HALLSTÄTTER SALZBERG"

Praschl, S.¹, Leis, A.², Benischke, R.², Schramm, M.³,
Böttcher, M.E.⁴, Daxner, G.⁵ & Dietzel, M.¹

¹University of Technology (Rechbauerstraße 12, 8010 Graz, Austria

²Joanneum Research (Leonhardstraße 59, 8010 Graz, Austria

³Federal Institute for Geosciences and Natural Resources, Stilleweg 2, 30655 Hannover, Germany

⁴Leibniz-Institute for Baltic Sea Research, IOW, Seestrasse 15, 18119 Warnemünde, Germany

⁵Salinen Austria AG, Steinkoglstrasse 30, 4802 Ebensee, Austria

e-mail: Stefan.Praschl@student.tugraz.at

The evaporites of the deposit "Hallstätter Salzberg" had been the subject of numerous studies, but significant gaps of knowledge still remained with respect to their formation, transformation conditions and characteristic features of individual facial units. In order to provide new insights of the latter aspects two drill cores through the deposit with a total length of 619 m were investigated using a combined mineralogical-petrological and (isotope) geochemical methodology.

The Br content of halite (NaCl) varies between 64 and 223 µg (Br) / g (NaCl) (average: 124 ± 25 ; n = 67) which indicates no significant secondary solution metamorphism on halite. The Br content of halite increases along the profile towards the hanging layer and reflects changes in the degree of evaporation in distinct horizons.

$\delta^{34}\text{S}/\delta^{32}\text{S}$ -isotope values of sulfate minerals exhibit two significant trends: (i) $\delta^{34}\text{S}$ values varying between 10.6 and 12.8 ‰ (average 11.5 ± 0.7 ‰; n = 16), which are typical for marine sulfates of Upper Permian age. Notably, $\delta^{34}\text{S}$ values of Mg-sulfates ($\delta^{34}\text{S} = 10.9 \pm 0.4$ ‰; n = 6) such as polyhalite ($\text{K}_2\text{Ca}_2\text{Mg}[\text{SO}_4]_4 \cdot 2\text{H}_2\text{O}$) are isotopically lighter compared to anhydrite (CaSO_4) dominated horizons ($\delta^{34}\text{S} = 11.8 \pm 0.6$; n = 10). (ii) $\delta^{34}\text{S}$ values from 28.5 to 30.8 ‰ (average 29.5 ± 1 ‰; n = 4) of anhydrite, associated with dolomite ($\text{CaMg}[\text{CO}_3]_2$) and organic rich layers, indicate marine sulfates from the Triassic "Röt event", but values are up to ≈ 2 ‰ isotopically heavier than previously reported isotope signatures for the "Hallstätter Salzberg".

In the Upper Permian, the onset of evaporation led to halite precipitation. An increasing degree of evaporation yield finally in polyhalite formation (Alpine Haselgebirge Fm.). In the Triassic, halite precipitation at lower evaporation degree resulted in lower Br content of halite (Reichenhall Fm.) compared to the Permian salts. Mineral transformation processes are discovered by relicts of anhydrite in polyhalite, polyhalite in anhydrite, anhydrite in görgeyite ($\text{K}_2\text{Ca}_5[\text{SO}_4]_6 \cdot \text{H}_2\text{O}$), glauberite ($\text{Na}_2\text{Ca}[\text{SO}_4]_2$) in anhydrite, and by glauberite rims around polyhalite minerals. A notable feature is the occurrence of kalistrontite ($\text{K}_2\text{Sr}[\text{SO}_4]_2$), which was observed in the Eastern Alps for the first time. Accordingly, an enhanced (age) classification of the investigated layers and stratigraphic units are presented and depicted secondary impacts on the composition of the deposit due to solution metamorphism are discussed.

**THERMAL BEHAVIOUR OF THE NEW MINERAL CAIRNCROSSITE,
 $\text{Sr}_2\text{Ca}_7(\text{Si}_4\text{O}_{10})_4(\text{OH})_2 \cdot 15\text{H}_2\text{O}$.**

Pristacz, H., Giester, G., Rieck, B. & Lengauer, C.L.

Institut für Mineralogie und Kristallographie, Universität Wien – Geozentrum,
Althanstrasse 14, 1090 Wien, Austria
e-mail: christian.lengauer@univie.ac.at

The name Cairncrossite is given to a new mineral characterized with the formula $\text{Sr}_2\text{Ca}_7(\text{Si}_4\text{O}_{10})_4(\text{OH})_2 \cdot 15\text{H}_2\text{O}$. It occurs as white, micaceous crystals lining vughs in manganese ore from the Wessels Mine, Kalahari Manganese Field, South Africa, well known for the occurrence of new and rare minerals (e.g. GIESTER & RIECK, 1996). It is associated with richterite, manganoan sugilite, pectolite and represents the last formed mineral due to metasomatic alteration of the primary, carbonate-rich manganese minerals within the calc-silicate skarn assembly.

The atomic arrangement of the triclinically distorted, pseudohexagonal crystal structure – $P\bar{1}$, $a = 9.624(2)$, $b = 9.634(2)$, $c = 15.657(3)$ Å, $\alpha = 100.80(1)$, $\beta = 91.22(1)$, $\gamma = 119.80(1)$ °, $V = 1226.2(4)$ Å³, $Z = 1$ – can be classified as a phyllosilicate with layers parallel to (001). This main structural motif can be described as a brucite-like sheet of edgesharing $\text{CaO}_4(\text{OH})_2$ octahedra sandwiched by single layers of SiO_4 tetrahedra, i.e. unbranched vierer single layer (LIEBAU, 1985), which exhibit two conformations of six-membered rings. Between these layers dimers of $\text{SrO}_2(\text{O}_w)_6$ polyhedra are intercalated together with hydrogen bonded water molecules. Minerals with a similar structural motif are found in the gyrolite and reyerite groups, which inevitably lead to the class of calcium silicate hydrates (CSH) playing an essential role in the strong exothermic hydration of Portland cement (TAYLOR, 1964).

During the routine thermal analysis of cairncrossite the mineral exhibit a two-phase endothermic loss of the 15 water molecules in the range 25 – 400 °C, followed by a small endothermic event with endset around 570 °C and a significant endothermic weight loss at 700 °C, which coincides to a dehydroxylation of the material. Due to the bonding scheme of the intercalated Sr-polyhedra a complete structural disintegration on dehydration would be anticipated, however, the mineral exhibits a full rehydration capability up to 400 °C. The further heating revealed the formation of a Sr-substituted CSH phase comparable to $\text{Ca}_7\text{Si}_{16}\text{O}_{38}(\text{OH})_2$, also known as K-phase (GARD et al., 1981). After dehydroxylation the K-phase decomposes to wollastonite-2M and an up to now unknown compound.

These thermogravimetric studies (TGA, DSC) and in situ high-temperature X-ray powder diffractometry of the new mineral cairncrossite will be presented and discussed.

GIESTER, G., RIECK, B. (1996): Mineral. Magazine, 60, 795-798.

LIEBAU, F. (1985): Structural Chemistry of Silicates. Springer, Heidelberg.

TAYLOR, H.F.W. (1964): The Chemistry of Cements. Academic Press, London.

GARD, J.A., LUKE, K., TAYLOR, H.F.W. (1981): Cem. Concr. Research, 11, 659-664.

MINERALOGY AND GENESIS OF PEGMATITE-LIKE VEINS IN SERPENTINITE ELUVIUM AT NOVÁ VES NEAR OSLAVANY (CZECH REPUBLIC)

Prokop, J.¹, Losos, Z.¹, Karásek, J.² & Čopjaková, R.¹

¹Department of Geological Sciences, Masaryk University, Kotlářská 2, 611 37 Brno, Czech Republic

²Lieberzeitova 12, 614 00 Brno - Husovice, Czech Republic

e-mail: 175358@mail.muni.cz, losos@sci.muni.cz

The studied locality belongs to the Gföhl unit (Moldanubian zone) at the eastern margin of the Bohemian Massif. Remnants of veins with pegmatite character were found in eluvium of a small serpentinite body situated at Nová Ves near Oslavany. Three groups of vein material (NV1, NV2, NV3) differing in their internal structure, mineral assemblages and chemical composition of minerals were distinguished.

Mineral assemblage NV1 (Kfs + Qtz + Plg ± Tur ± Chl) consists of medium- and coarse-grained, brown-grey K-feldspar, grey albite (An_{2-9}), quartz and minor greenish-brown columnar tourmaline. Tourmaline is replaced by K-feldspar and smectite-like minerals. Accessory titanite is typically associated with altered tourmaline, xenotime and monazite are rare. About 70 vol. % of the bulk composition in the assemblage NV2 (Plg ± Amp ± Preh ± Chl) consists of coarse-grained pale-brown andesine (An_{38-42}). Subordinate green amphibole is developed at the rims of the vein samples and may represent the contact between the pegmatite and the host rock. Quartz and primary K-feldspar are absent but late secondary K-feldspar occurs in fissures within the andesine. Andesine is often pseudomorphosed by prehnite but its replacement by chlorite, clinozoisite, sericite and albite was also observed. Zircon and tourmaline are rare. The group of NV3 vein samples has rather similar mineral assemblage (Plg + Tur ± Preh ± Chl) as NV2 group. Blocky pale-brown labradorite-bytownite (An_{69-85}) and dark-green tourmaline are dominant. Tourmaline occurs in form of clusters and aggregates. Plagioclase is often pseudomorphosed by prehnite and also by chlorite and thompsonite. Tourmaline is partly replaced by pumpellyite-(Al) and/or chlorite. Apatite, celsiane-hyalophane and zircon are accessory minerals. These three assemblages can be clearly distinguished by the basicity of plagioclase. The chemistry and compositional trends of tourmalines from 3 distinct parageneses described above are also different. Dravite-uvite from NV2 (NV3) samples exhibits rimward increase in Ca, Mg, Fe and decrease in Na, Al. Dravite of the NV1 assemblage, enriched in Al, exhibits predominance of Mg over Fe and increase of Na, Mg and Fe combined with decrease of Al and X-site vacancy.

The crystallization of tourmaline and plagioclases was probably controlled by the activities of mobile elements during the mixing of parent melt (rich in Na, Al, Si, B) with the elements derived from the host serpentinite (rich in Mg and Ca). The features of pegmatite-like vein fragments from Nová Ves are unique in several aspects: (a) extremely variable anorthite content in plagioclases (An_{02-85}); (b) abundance of younger Ca-rich minerals (prehnite, pumpellyite, clinozoisite, thompsonite); (c) activity of some volatiles in forming melt (particularly B); (d) only local presence of quartz and K-feldspar and finally; (e) predominant coarse-grained character of primary minerals. These features are similar to those observed at other contaminated pegmatites hosted by serpentinite such as Drahonín, Věžná, Smrček, Věchnov etc.

This work was supported by the research project GAČR P210/010/0743 to Z.L.

METAMORPHIC EVOLUTION OF THE KORALPE-WÖLZ HIGH-P/T NAPPE
PILE EAST OF THE TAUERN WINDOW (EASTERN ALPS): RECORD FROM
SILICEOUS DOLOMitic MARBLES AND SCAPOLITE-BEARING
CALCSILICATE ROCKS

Puhr, B.¹, Hoinkes, G.¹, Schuster, R.² & Poyer, A.¹

¹University of Graz, Institute of Earth Sciences, Universitätsplatz 2, 8010 Graz, Austria

²Geological Survey of Austria, Neulinggasse 38, 1030 Vienna, Austria

e-mail: barbara.puhr@uni-graz.at

Siliceous dolomitic marbles and calcsilicate rocks of the Koralpe-Wölz nappe pile east of the Tauern Window were investigated regarding their petrological and mineralchemical characteristics in order to reconstruct the metamorphic evolution of this rock type during pre-Alpine and eo-Alpine events. An increasing metamorphic gradient along a cross-section from north to south is reflected within the siliceous dolomitic system CM(A)SCH by a change of the eo-Alpine diagnostic mineral assemblages:

(I) Dol+Qz+Cal, (IIa) Tr+Dol+Cal+Qz, (IIb) Tr+Qz+Cal, (IIIa) Tr+Cal+Di+Dol, (IIIb) Di+Dol+Cal and (IV) Di+Fo+Dol+Cal±Chu±Chl. Cal-Dol-solvus-temperatures yield 437 - 480 °C corresponding to X_{MgCO_3} -values between 0.03 and 0.039 in the northernmost part of the nappe pile (Wölz Complex). To the south the first occurrence of Tr within the Greim Complex is characterized by 540 - 562 °C (X_{MgCO_3} of around 0.05). Di was formed further south in the Rappold (660 - 691 °C), Koralpe-Saualpe (680 - 740 °C), Millstatt and Pohorje Complexes. These temperatures reflect X_{MgCO_3} -values scattering from 0.09 to 0.13. Fo of type (IV) as well as rare Di-coronas around Tr are explained by high $X_{\text{H}_2\text{O}}$ -contents.

Type (V) assemblage Fo+Spl+Dol+Cal can be found in the Sieggraben area. There, Fo may be produced at high temperatures (Permian?) of up to 850 °C (X_{MgCO_3} around 0.2), which result from reintegration of thick Dol-lamellae in Cal. Di-Dol-coronas around Fo were formed at about 750 °C (corresponding X_{MgCO_3} -values of 0.15). These temperatures are yielded from the reintegration of smaller bleb-like or patchy Dol-exsolutions, which represent exsolution at a later stage.

The different generations of Dol-exsolutions, Fo of type (V) and Di-relics in eo-Alpine Tr indicate a pre-Alpine (Permian?) evolution.

In calcsilicate rocks of the CASCH-system from the Koralpe mountain range meionitic Scp is a rare constituent and is accompanied by Cpx, Czo, Cal, Qz, Amp, Pl and Afs. Activity-corrected T-X_{CO₂}-calculations ($a_{\text{Mei}}=0.06-0.08$, $a_{\text{Grs}}=0.08-0.13$, $a_{\text{An}}=0.44-0.69$, $a_{\text{Czo}} \approx 0.86$) point to high minimum temperatures for the formation of the Scp-bearing assemblage between about 670 °C in the north and 800 °C in the south of the Koralpe. As these temperatures do not fit to the eo-Alpine metamorphic gradient, they may indicate Scp-formation during the Permian metamorphic event.

The formation of complex An-Czo-Grs-coronas around Scp needs significantly higher $X_{\text{H}_2\text{O}}$ -contents at lower temperatures of about 650 °C at maximum and is ascribed to the eo-Alpine overprint.

CARBONATE FORMATION AT ALKALINE CONDITIONS

Purgstaller, B.¹, Niedermayr, A.² & Dietzel, M.¹

¹University of Technology, Institute of Applied Geosciences, Rechbauerstraße 12, 8010 Graz, Austria

²Ruhr University Bochum, Institute of Geology, Mineralogy and Geophysics, Universitätsstraße 150,
44801 Bochum, Germany

e-mail: purgstaller@student.TUGraz.at

Calcium Carbonate (CaCO_3) can be induced by CO_2 uptake in Ca^{2+} ion bearing alkaline solutions as it is valid for many natural and man-made environments, e.g. formation of travertine and scaling (CLARK et al., 1992 and DIETZEL et al., 1992). However, significant gaps of knowledge exist with respect to reaction kinetics (CO_2 uptake and CaCO_3 precipitation) in alkaline solutions as well as in respect to distinct CaCO_3 polymorph formation.

In the present study CO_2 uptake and CaCO_3 precipitation were experimentally studied by diffusion of CO_2 through a polyethylene membrane from an inner into an outer solution containing 10 mM of CaCl_2 (25 °C). The pH was kept constant during two analogous sets of experiments at 8.30, 9.00, 10.00 11.00 or 11.50 by titration using diluted NaOH solution.

By exceeding an IAP (Ion Activity Product) threshold CaCO_3 is formed in the outer solution. (Micro)Raman and XRD pattern indicate the CaCO_3 polymorphs calcite, vaterite and aragonite. Calcite and vaterite were precipitated at all pH values, whereas aragonite was only present at $\text{pH} \geq 11.00$. The evolution of the NaOH titration curve and Ca^{2+} concentration reflects parameters like the CO_2 uptake rate (\propto ACAR: aqueous CO_3^{2-} accumulation rate; NIEDERMAYR et al., 2013) and the overall precipitation rate of CaCO_3 (R_{CaCO_3}). At elevated pH of the outer solution the ACAR is significantly higher and less time for nucleation of CaCO_3 , t_{fc} , is required compared to lower pH conditions (e.g. pH 8.30 and 10.00 result in $\text{ACAR} = 9.2 \pm 0.1$ and $121 \pm 0.6 \mu\text{M h}^{-1}\text{l}^{-1}$ and $t_{fc} = 8.3 \pm 0.3$ and 1.6 ± 0.5 h, respectively). At $\text{pH} \geq 11.00$ the CaCO_3 nucleation and precipitation begins instantaneously after starting the experiment. Interestingly, at the given total experimental time of 20 h the relative Ca^{2+} concentration decrease (equivalent to the amount of precipitated CaCO_3) was similar (22 ± 4 mol% in respect to initial Ca^{2+} concentrations) for all experiments. This can be explained by the significantly higher R_{CaCO_3} values subsequent to nucleation at low versus high pH (e.g. pH 8.30 and 10.00 with $R_{\text{CaCO}_3} = 645 \pm 64$ and $178 \pm 15 \mu\text{M h}^{-1}\text{l}^{-1}$, respectively) which correlates with a general decrease of the surface concentration of $>\text{CaHCO}_3^0$ at the CaCO_3 surfaces (e.g. RUIZ-AGUDO et al., 2011 for calcite). Thus, the combined effect of the aqueous carbonate accumulation rate and the precipitation rate of CaCO_3 controls the quantity of CaCO_3 precipitation in alkaline environments.

CLARK, I.D., FONTES, J.-C., FRITZ, P. (1992): *Geochim. Cosmochim. Acta*, 56, 2041-2050.

DIETZEL, M., USDOWSKI, E., HOEFS, J. (1992): *Applied Geochemistry*, 7, 177-184.

NIEDERMAYR, A., KÖHLER, S.J., DIETZEL, M. (2013): *Chemical Geology*, 340, 105-120.

RUIZ-AGUDO, E., PUTNIS, C.V., RODRIGUEZ-NAVARRO, C., PUTNIS, A. (2011): *Geochim. Cosmochim. Acta*, 75, 284-296.

ARSENIC-ENRICHED Cu-Ni-PGE MINERALIZATION IN WETLEGS, DULUTH COMPLEX, ST. LOUIS COUNTY, MINNESOTA, USA

Raič, S.¹, Mogessie, A.¹, Benkó, Z.¹, Molnár, F.², Hauck, S.³ & Severson, M.³

¹University of Graz, Universitätsplatz 2, 8010 Graz, Austria

²Geological Survey of Finland, Helsinki, Finland

³NRRI, University of Minnesota, 5013 Miller Trunk Highway, Duluth MN 55811, U.S.A.

e-mail: sara.raic@edu.uni.graz.at

As one of the biggest layered mafic intrusions worldwide, the Duluth Complex (1.1 Ga) in NE Minnesota, USA, is known for its Cu-Ni-PGE (platinum group elements) mineralization in magmatic sulphide ore deposits along its western margin. The investigation area in deposit Wetlegs, located in the Partridge River intrusion is of great interest, due to the highly mineralized zones up to the top units of the drill cores. Three drill cores were sampled for a detailed stratigraphic and petrographic study, chemical analyses of silicate phases and ores in mineralized horizons. The drill core lithology consists of troctolites (Pl, Ol, Px rich rocks) with alternating layers of anorthositic, gabbroic and ultramafic rocks. Mineralization occurs in the basal troctolites. Sulphide mineralogy is characterized by pyrrhotite, chalcopyrite, pentlandite, as well as cubanite-chalcopyrite segregations ± bornite, covellite, sphalerite and molybdenite. Oxides are primarily ilmenite and magnetite. Mineralization hosted by hydrothermal alteration phases mainly contains chalcopyrite associated with fibrous to fine grained chlorite and amphibole. Additional ore minerals related to this type of mineralization are Ni-arsenides, Ni-Co-sulpharsenides and Ni-antimonides including nickeline [(Ni, Co, Fe)As], maucherite (Ni₁₁As₈), safflorite [(Co, Fe, Ni)As₂], cobaltite [(Co, Fe, Ni)AsS], gersdorffite [(Ni, Co, Fe) AsS], allocasite [(Ni, Co, Fe)AsS] and ullmannite [(Ni, Co, Fe)SbS]. All these phases show large variations in their Ni-Co-Fe distribution. Ni-arsenides (maucherite, safflorite and nickeline) mainly occur as inclusions in Ni-Co sulpharsenides (cobaltite) in hydrothermally altered ultramafic rocks where they are associated with hydrous silicates such as chlorite and amphibole. This may indicate an earlier formation of Ni-arsenides followed by Ni-Co sulpharsenides. Sulpharsenides and arsenides containing significant concentrations of Pd and Rh are documented. These Pd-Rh-enriched phases occur as inclusions in Ni-Co sulpharsenides, Ni-arsenides, chalcopyrite and pyrrhotite. Pt-arsenides are associated with hydrous silicates. The presence of Ni-Sb-arsenides in footwall rocks may suggest the metasedimentary Virginia formation as a potential source of arsenic and antimony. These elements were mobilized by hydrothermal fluids and introduced in the crystallizing magma to form arsenic-enriched Cu-Ni-PGE mineralization within the basal ultramafic rocks. δ³⁴S-data of sulphides from representative samples of the Wetlegs drill cores vary between 2.04 and 22.80 %. This suggests the involvement of crustal materials in addition to the magmatic source of sulphur in the Cu-Ni-PGE mineralization as has also been documented in previous studies (MOGESSIE et al., 1991, MOGESSIE & STUMPFL, 1992). *FWF (P23157-N21) financial support to A. Mogessie and from the Dean of Students, University of Graz to S. Raič is acknowledged.*

MOGESSIE, A., STUMPFL, E., WEIBLEN, P. (1991): Econ. Geol., 86, 140-152.

MOGESSIE, A., STUMPFL, E. (1992): Australian Journal of Earth Sciences, 39, 315-325.

CALCIUM CARBONATE FORMATION IN FLUIDIZED BED PELLET REACTORS TO REDUCE Ca, U AND DOC IN DRINKING WATER (UPPSALA, SWEDEN)

Rauschenbach, J.¹, Köhler, S. J.², McCleaf, P.³, Höllen, D.⁴ & Dietzel, M¹

¹Institute of Applied Geosciences, Graz University of Technology, Rechbauerstrasse 12, 8010 Graz, Austria

²Department of Aquatic and Environmental Sciences, Swedish University of Agricultural Sciences (SLU),
Box 7050, 75007 Uppsala, Sweden

³Uppsala Water and Waste Company, Gränby Water Treat Plant, Edith Södergransgatan 11, Box 1444,
75144 Uppsala, Sweden

⁴Institute for Sustainable Waste Management and Technology, Montan University of Leoben,
Franz-Josef-Straße 18/l, 8700 Leoben, Austria
e-mail: 03rausch@stud.uni-graz.at

Pellet softening technique by using fluidized bed pellet reactors is applied to reduce the hardness of drinking water about up to 50 % (e. g. HOFMAN et al., 2007). Uranium and dissolved organic carbon (DOC) concentrations are also significantly lowered due to the above treatment, but until now quotations and mechanisms for U and DOC reduction are not revealed.

Pellet softening is based on the addition of slaked lime into a reactor containing water and quartz pellets. Accordingly, dissolved calcium and carbonate ions precipitate mostly on the quartz grains. The pellets covered with CaCO_3 and additional suspended solids are separated from the water within a continuous process. This overall treatment results in

- (i) Ca reduction up to 64 % (from 92 down to 34 mg L⁻¹ of Ca),
- (ii) Slcalcite decrease from 0.7 to 0.2,
- (iii) Decrease of U content up to 23 % (from 0.022 down to 0.017 mg L⁻¹), and
- (iv) DOC reduction of up to 14 % (from 3.6 down to 3.1 mg L⁻¹).

XRD, IR and Raman pattern indicate calcite as precipitate. In some cases low-magnesium calcite was observed, but no aragonite occurs. The U concentration of the bulk carbonate scaling ranges from 1 to 12 mg kg⁻¹ in the CaCO_3 covering, but can even reach 90 mg kg⁻¹ in the CaCO_3 sludge, which is rich in TOC (up to 13 %). Elemental zoning of U, Mg etc. throughout calcite horizons could not be identified by both LA-ICP-MS and Micro-Raman spectroscopy.

It is well known that U is incorporated in CaCO_3 (REEDER et al., 2001), but it can also form complexes with DOC, such as humic acids (e.g. RANVILLE et al., 2007). In the present study ultrafiltration was used to investigate aquo complex formation of U with DOC to quantify the amount of DOC-bounded U. In an experimental approach a correlation between U and DOC content was observed in the filtrated solutions, where at 30 kDa the U and DOC concentrations are reduced up to 40 and 15 %, respectively.

HOFMAN, J., VAN DER HOEK, J. P., NEDERLOF, M., GROENENDIJK, M. (2007): Water, 21, 21-24.

RANVILLE, J. F., HEBDRY, M. J., RESZAT, T. N., XIE, Q., HONEYMAN, B. D. (2007): Journal of Contaminant Hydrology, 91, 233-246.

REEDER, R. J., NUGENT, M., TAIT, C. D., MORRIS, D. E., HEALD, S. M., BECK, K. M., HESS, W. P., LANZIOTTI, A. (2001): Geochimica et Cosmochimica Acta, 65 (20), 3491-3503.

THE $C2/c$ - $P2_1/c$ PHASE TRANSITION WITHIN THE SYNTHETIC
CLINOPYROXENE-SERIES $\text{NaFeGe}_2\text{O}_6$ - $\text{LiFeGe}_2\text{O}_6$

Redhammer, G.J. & Tippelt, G.

Abteilung Mineralogie, Fachbereich Materialforschung & Physik, Universität Salzburg, Hellbrunnerstr. 34,
5020 Salzburg, Österreich
e-mail: guenther.redhammer@sbg.ac.at

The mineral group of the pyroxenes is known to exhibit several phase transitions as a function of temperature and pressure. At ambient conditions, the most frequent occurring structure is the high temperature $HT-C2/c$ structure, which transforms to $P2_1/c$ at low temperatures or at high pressures. This was described e.g. by REDHAMMER & ROTH (2004) for $\text{LiM}^{3+}\text{Si}_2\text{O}_6$ clinopyroxenes, showing transition temperatures between 210 and 340 K. The analogue $\text{LiM}^{3+}\text{Ge}_2\text{O}_6$ compounds display $P2_1/c$ symmetry at room temperature and transform to $C2/c$ symmetry at much higher temperatures. $\text{LiFeGe}_2\text{O}_6$ shows a $P2_1/c$ to $HT\ C2/c$ transition at 789 K, thus shifted by more than 500 K (REDHAMMER et al., 2010). The germanium analogue to aegirine, $\text{NaFeGe}_2\text{O}_6$, exhibit $C2/c$ symmetry at room temperature (REDHAMMER et al., 2011), thus a transition from $C2/c$ to $P2_1/c$ symmetry within the $(\text{Na}_{1-x}\text{Li}_x)\text{FeGe}_2\text{O}_6$ solid solution series is to be expected.

The synthetic samples show $C2/c$ symmetry up to a composition of $\text{Na}_{0.5}\text{Li}_{0.5}\text{FeGe}_2\text{O}_6$, for higher Li-contents, the $P2_1/c$ symmetry is observed. Using single crystal X-ray diffraction and thermal analysis a T - X phase diagram of the stability of the corresponding symmetries was established (see Figure). The unit cell volume decreases with increasing Li - content, at the phase transition composition a discontinuity and a change in slope is observed. Such discontinuities are valid for all lattice parameters a , b , c and the monoclinic angle; additionally average as well as individual bond lengths for Li-O, Fe-O and Ge-O are subject of smooth variations with Li-content, with more or less pronounced discontinuities at the phase transition. Evident e.g. is the variation of the O3-O3-O3 bridging angle of tetrahedral chains: it decreases from 185 ° to 174 ° with increasing Li-content, at the phase transition two independent chains arise in the $P2_1/c$ phase with kinking angles of 199 ° and 155 °. For the composition of $\text{Na}_{0.6}\text{Li}_{0.4}\text{Ge}_2\text{O}_6$ and $\text{Na}_{0.7}\text{Li}_{0.3}\text{Ge}_2\text{O}_6$ low temperature in situ X-ray diffraction experiments were done to follow the $C2/c$ - $P2_1/c$ phase transition also as a function of temperature.

REDHAMMER, G.J., ROTH, G. (2004): Z. Krist., 219, 585-605.

REDHAMMER, G.J., CÁMARA, F., ALVARO, M., NESTOLA, F., TIPPELT, G., PRINZ, S., SIMONS, J., ROTH, G., AMTHAUER, G. (2010): Phys. Chem. Minerals, 37, 685-704.

REDHAMMER, G.J., SENYSHYN, A., MEVEN, M., ROTH, G., PRINZ, S., PACHLER, A., TIPPELT, G., PIETZONKA, C., TREUTMANN, W., HOELZEL, M., PEDERSEN, B., AMTHAUER, G. (2011): Phys. Chem. Minerals, 38, 139-157.

CRYSTAL AND MAGNETIC SPIN STRUCTURE OF GERMANIUM-HEDENBERGITE, CaFeGe₂O₆

Redhammer, G.J.¹, Senyshyn, A.², Roth, G.³ & Tippelt, G.¹

¹Abteilung Mineralogie, Fachbereich Materialforschung & Physik, Universität Salzburg, Hellbrunnerstraße 34, A-5020 Salzburg, Österreich

²Forschungsneutronenquelle Heinz Maier-Leibnitz (FRM II), Lichtenbergstraße 1, D-85747 Garching bei München, Deutschland

³Institut für Kristallographie, RWTH Aachen, Jägerstraße 17/19, D-52066 Aachen, Deutschland

e-mail: guenther.redhammer@sbg.ac.at

Structure-property relations in pyroxenes have been studied for many decades. The interest was then mainly triggered by the important role of pyroxenes as rock forming minerals in the lower crust and upper mantle, especially with respect of phase transitions at non ambient conditions. In the last years it was established that the transition metal bearing pyroxenes also have a rich magneto-chemistry (e.g. REDHAMMER et al. 2011, 2012). As part of our ongoing studies on magnetic properties of minerals / pyroxenes we here present results of the magnetic and nuclear structure of CaFeGe₂O₆, the germanium-analogue to the mineral Hedenbergite.

The title compound has been synthesized at 1273 K in evacuated SiO₂-glass - tubes. Powder neutron diffraction data collected between 4 K and 300 K were used to evaluate the magnetic spin as well as the nuclear crystal structure and its *T* - evolution. CaFeGe₂O₆ is monoclinic, *C*2/*c*, *a* = 10.1778(5) Å, *b* = 9.0545(4) Å, *c* = 5.4319(3) Å, β = 104.263(3) °, *Z* = 4 at room temperature. No change of symmetry was observed down to 4 K. Below 43 K, additional magnetic Bragg reflections appear, which can be indexed on the basis of a commensurate magnetic propagation vector *k* [1,0,0]. The successful description of the magnetic spin structure reveals a ferromagnetic spin coupling within the Fe²⁺O₆ M1 chains, while the coupling between the chains is antiferromagnetic. Spins are oriented collinearly within the *a*-*c* plane and form an angle of ~60 ° with the crystallographic *a*-axis. The magnetic moment at 4 K amounts to about 4.4 μ B. The observed magnetic structure is similar to that of other Ca-clinopyroxenes. The present data is put into context with the structural and magnetic properties of other pyroxenes – among them magnetoelectric and multiferroic pyroxene-type compounds.

REDHAMMER, G.J., SENYSHYN, A., MEVEN, M., ROTH, G., PRINZ, S., PACHLER, A., TIPPELT, G., PIETZONKA, C., TREUTMANN, W., HOELZEL, M., PEDERSEN, B., AMTHAUER, G. (2011): Phys. Chem. Minerals, 38, 139-157.

REDHAMMER, G.J., SENYSHYN, A., TIPPELT, G., PIETZONKA, C., TREUTMANN, W., ROTH, G., AMTHAUER, G. (2012): Am. Min., 97, 694 – 706.

MIXING OF AQUEOUS SOLUTIONS – IMPACT ON DISSOLUTION AND
PRECIPITATION OF CALCIUM CARBONATE

Rinder, T^{1,2} & Dietzel, M.²

¹GET/CNRS , 14 Avenue Édouard Belin, 31400 Toulouse, France

²Institute of Applied Geosciences, Graz University of Technology Rechbauerstraße 12, 8010 Graz, Austria
e-mail: rinder.thomas@gmx.net

The potential to dissolve calcite in a fluid created by mixing of two aqueous solutions, which are both saturated with respect to calcite ($SI_{Calcite} = 0$), has been demonstrated by BOEGLI (1964). In contrast, little attention has been paid to the potential for the mixing of two calcite saturated aqueous fluids to provoke calcite precipitation. This possibility is likely in a number of alkaline systems including limestone dissolution at closed system conditions, carbonate sinter formation in terrestrial lakes, carbonate scaling, and throughout the dissolution of mafic silicates. In such systems fluid mixing is a crucial factor for evaluating solution compositions and mechanisms of carbonate precipitation (e.g. RINDER et al., 2013).

Here we present aqueous solution mixing models within the $\text{CaCO}_3\text{-CO}_2\text{-H}_2\text{O}$ system at alkaline conditions. Our results display a complex behaviour with respect to the potential dissolution and precipitation of calcite. Mixing of aqueous solutions with different chemistry, but both at $SI_{Calcite} = 0$, may yield in solutions super- or undersaturated with respect to calcite. This is even true for groundwater, which originated from limestone dissolution. The redistribution of carbonate species as a function of pH leads to supersaturation with respect to calcite in the mixed solution, as a critical pH for redistribution of HCO_3^- into CO_3^{2-} is reached.

BOEGLI, A. (1964): Erdkunde, 18, 83–92.

RINDER, T., DIETZEL, M., LEIS, A. (2013): Appl. Geochem., (in press).

Na-K INTERDIFFUSION IN ALKALI FELDSPAR – COMPOSITION DEPENDENCE, ANISOTROPY AND CHEMICALLY INDUCED STRESS

Schaeffer, A.-K.¹, Petrishcheva, E.¹, Habler, G.¹, Abart, R.¹, Rhede, D.² & Zaefferer, S.³

¹ University of Vienna, Althanstraße 14, 1090 Vienna, Austria

² GFZ German Research Centre for Geosciences, Telegrafenberg, 14473 Potsdam, Germany

³ Max-Planck-Institute for Iron Research, Max-Planck-Straße 1, 40237 Düsseldorf, Germany

e-mail: anne-kathrin.schaeffer@univie.ac.at

Cation exchange experiments have been conducted using crystallographically oriented plates of gem quality sanidine.

The geometry of the observed diffusion fronts can be explained by a composition dependent interdiffusion coefficient $D(X_{Or})$. Using the Boltzmann transformation we extracted the composition dependence of D from our measured data in the composition range $0.5 < X_{Or} < 1$ in the directions normal to (001) and (010). At 850 °C the interdiffusion coefficient is nearly constant for the composition range $0.50 < X_{Or} < 0.96$ for both directions before rising steeply at higher X_{Or} . Interdiffusion normal to (001) is faster by a factor of about ten than normal to (010).

Comparison of our data with theoretically calculated interdiffusion coefficients derived from literature data (FOLAND, 1974; KASPER, 1975) using the Manning relation showed that while interdiffusion normal to (001) shows a rough fit the slower interdiffusion normal to (010) deviates significantly from what would be expected.

The strong direction dependence of the diffusion profiles indicates that interdiffusion might be influenced by chemically induced coherency stress across the diffusion front. A new method cross correlating shifts in EBSD Kikuchi patterns has been employed to estimate stress and lattice distortion.

CHRISTOFFERSEN, R., YUND, R.A., TULLIS, J. (1983): American Mineralogist, 68, 1126 -1133.

FOLAND, K.A. (1974): Geochemical Transport and Kinetics, 77-98.

KASPER, R.B. (1975): Ph.D. thesis, Brown University, Providence, Rhode Island.

CHEMICAL AND ISOTOPIC COMPOSITION OF SOIL SOLUTIONS FROM CAMBISOLS (AUSTRIA) – FIELD STUDY AND EXPERIMENTS

Schön, W.¹, Dietzel, M.¹ & Leis, A.²

¹Institute of Applied Geosciences, Graz University of Technology, Rechbauerstraße 12, 8010 Graz, Austria

²Institute of Water, Energy and Sustainability, Joanneum Research, Elisabethstraße 18, 8010 Graz, Austria

w.schoen@student.tugraz.at

In most natural surroundings soil solutions are primarily gained from the uptake of meteoric water. Subsequently infiltration, capillary exchange, bioresponse, evaporation etc. result in complex and individual gas-water-solid systems. Knowledge on the chemical and isotopic composition of soil solution and its evolution is highly relevant for environmental and forensic studies, but respective systematic and combined field and experiment studies are rare.

The composition of solids and interstitial solutions of individual horizons has been investigated for three cambisols in Styria (Austria). The solutions were separated from the soils by compaction method at hydraulic pressures of 27 and 55 MPa, corresponding to respective matric potentials (mp).

The soils consist mainly of quartz, chlorite, muscovite and plagioclase with associated silicates like kaolinite, vermiculite and smectite due to weathering processes. No significant vertical variability was visible. The pH of the soil solution typically increases with depth and elevated mp. Concentrations of dissolved ions such as Ca^{2+} and Mg^{2+} increase at high mp, which correspond to higher δD and $\delta^{18}\text{O}$ values. Lab experiments for wetting and evaporation indicate higher concentrations of dissolved components of the soil solutions at higher δD and $\delta^{18}\text{O}$ values. Field-related and experimental results are discussed in respect to the impact of seasonality, evaporation, wetting and mp-related interstitial distribution of the (isotope) geochemical compositions of the separated soil solutions.

TORSIONAL DEFORMATION OF CALCITE

Schuster, R.¹, Abart, R.¹ & Schafler, E.²

¹Department of Lithospheric Research, University of Vienna, Althanstrasse 14, 1090, Vienna, Austria

²Faculty of Physics, University of Vienna, Boltzmanngasse 5, 1090, Vienna, Austria

e-mail: roman.schuster@univie.ac.at

Torsional deformation is one of the most important methods of experimental rock deformation. The Paterson type apparatus is the most commonly used torsional deformation machine in the earth sciences. It allows for torsional deformation of cylindrical samples at temperatures up to 1600 K and at pressures up to 500 MPa (PATERSON & OLGAARD, 2000). A different torsional deformation method that is currently hardly used in geosciences is High Pressure Torsion (HPT). It was developed in materials science to synthesize and investigate bulk nanostructured materials. It permits deformation experiments under substantially higher pressures than the Paterson apparatus of up to 10 GPa and at temperatures up to 800 K. A schematic of this method is shown in Fig. 1. The disk shaped sample is placed in a cavity between two anvils. After pressure of several GPa is applied on the sample, one of the anvils is then rotated. The friction between sample and anvils leads to shear deformation of the sample. HPT is known from various studies in particular on metals to lead to pronounced grain refinement and to very high defect densities (ZHILYAEV & LANGDON, 2008). This deformation method is applied on calcite to study the microstructural evolution during deformation. Calcite is particularly suitable for HPT deformation, since it can be plastically deformed at relatively low temperatures and undergoes two phase transformations in the pressure range that can now be reached with HPT

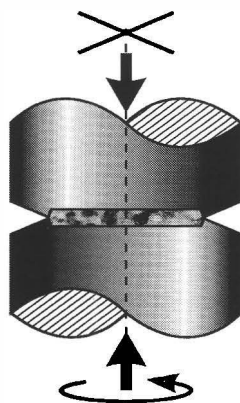


Figure 1. Schematic drawing of HPT-deformation

INFLUENCE OF NON-ANALYZED LIGHT ELEMENTS ON RESULTS OF ELECTRON MICROPROBE

Škoda, R., Čopjaková, R. & Novák, M.

Institute of Geological Sciences, Masaryk University, Kotlarska 2, 611 37 Brno, Czech Republic
e-mail: rskoda@sci.muni.cz

The electron microprobe (EMP) has become a common analytical technique in geosciences over last three decades. The EMP analysis is based on measuring of characteristic X-rays generated during interactions of accelerated electrons with a sample. The measured characteristic X-ray has to be corrected by a function including various factors such as atomic number of the sample, absorption and fluorescence effects. For accurate matrix correction calculations is crucial to set the exact composition of analyzed phase. The modern EMP machines automatically process the measured intensities of characteristic X-rays by a matrix correction procedure taking into account chemical composition of the sample, e.g. PAP (POUCHOU & PICHOIR, 1984) and φ - (ϱz) (MERLET 1994). During a "common" EMP analysis, fluorine and heavier elements are usually measured and O content (in oxide phases) is calculated by a valence and all these elements are automatically involved into the matrix corrections. A higher content of B, C, Be, Li and H in minerals should be involved in to the matrix corrections as well, because the incomplete input dataset for the matrix correction calculations leads to an incorrect final analytical results. To optimize the matrix corrections and consequently analytical output, it is important to: 1) include the non-analyzed oxides of light elements (H_2O , CO_2 , B_2O_3 , BeO , Li_2O) into matrix corrections of analyzed minerals, 2) set the right O content in minerals with high halogen content (e.g. topaz $Al_2SiO_4F_2$). An electron microprobe analysis of tourmaline and topaz proceeded by φ - (ϱz) matrix correction routine (MERLET, 1994) excluding and including of non-analyzed elements are shown in Table 1.

	SiO_2	Al_2O_3	MgO	FeO	Na_2O	F	B_2O_3	H_2O	Total	Si	Al	Mg	Fe	Na	F		
1a*	37.43	33.60	6.67	6.54	2.24	1.24	n.i.	n.i.	87.72	6.000	6.350	1.595	0.879	0.696	0.626		
1b*	36.74	33.69	6.78	6.61	2.29	1.31	10.63	2.68	100.73	6.000	6.484	1.653	0.903	0.723	0.675		
	SiO_2	Al_2O_3	F	Total	Si	Al	F	* contains also 0.10 CaO and 0.24 TiO_2									
2a	32.78	56.85	20.5		110.13	1.000	2.043	1.978		n.i. -not involved in to matrix corrections							
	Si	Al	F	O	Total	Si	Al	F	used conditions: 15kV, 10 nA, 8 μm dia.								
2b	17.29	26.64	10.81	n.i.	54.74	1.000	1.604	0.925		standards: Si, Al-sandidine, Mg-olivine,							
2c	15.51	29.83	19.32	35.34	100.00	1.000	2.001	1.842		Fe-almandine, Na-albite, F-topaz							

Table 1. Influence of non-analyzed elements on the on results of the EMP analysis. 1a*-analysis of tourmaline (in wt.% ox.), 1b*-the same analysis of tourmaline including 3.3 wt.% B and 0.3 wt.% H involved in matrix corrections. 2a- analysis of topaz (in wt.% ox.), 2b-the same analysis of topaz (in wt.% elm.), O not determined, 2c- the same analysis of topaz (in wt.% elm.), O (up to 100 wt.%) involved in matrix corrections. Tourmaline and topaz formula was calculated on the basis of Si = 6 and 1, respectively.

Financial support of grant GACR P210/10/0743 of the Grant Agency of Czech Republic is acknowledged.

MERLET, C. (1994): Microchim. Acta., 114-115, 363-376.

POUCHOU, J. L., PICHOIR, F. (1984): Rech. Aerosp., 1984, 3, 167-192.

OH-DEFECTS IN DETRITAL QUARTZ GRAINS

Stalder, R.¹ & Neuser, R.D.²¹ Universität Innsbruck, Innrain 52f, A-6020 Innsbruck, Austria² Ruhr-Universität Bochum, Universitätsstraße 150, D-44780 Bochum

e-mail: roland.stalder@uibk.ac.at

OH-defects of 95 detrital quartz grains from 4 localities in North-west Germany were studied by Infrared (IR) microscopy. By applying novel analytical strategies, the water contribution of fluid and mineral inclusions was minimised and the amount of water incorporated as OH-point defects was quantified. The defect water concentration in all studied quartz grains ranges between 0 and 50 wt ppm H₂O with a mean value around 10 wt ppm. Grains from the investigated sandstones (a Carboniferous sandstone from Essen and Triassic "Buntsandstein") exhibit in average nearly three times higher defect water concentrations (18 wt ppm) than grains from North Sea beach sands (6.5 wt ppm). This difference (Figure 1) may reflect the different source regions of the respective quartz grains, namely predominant provenance from Central Europe and predominant provenance from the Baltic Shield, respectively.

IR spectra of the detrital quartz grains were compared to reference spectra from samples of known localities and rock types in order to identify potential sources from which the quartz grains were sampled. Most detrital quartz grains exhibit IR signatures typical for granites (showing an Al-specific band at 3378 cm⁻¹) and regional metamorphic rocks, but also absorption bands typical for pegmatites and hydrothermal quartz (showing a Li-specific band at 3480 cm⁻¹) are observed. In contrast, IR signatures typical for high-pressure origin (i.e., hydrogarnet substitution with an absorption band at 3585 cm⁻¹) and for tourmaline-bearing rocks (showing a B-specific band at 3595 cm⁻¹) are subordinate to insignificant. From some grains also cathodoluminescence (CL) spectra were recorded and compared to the results from IR spectroscopy. No correlation between water content and CL colour was revealed, especially when a change in CL colour during excitation is not strong, underlining the potential of IR spectroscopy to add new aspects for the characterisation of quartz grains of unknown origin.

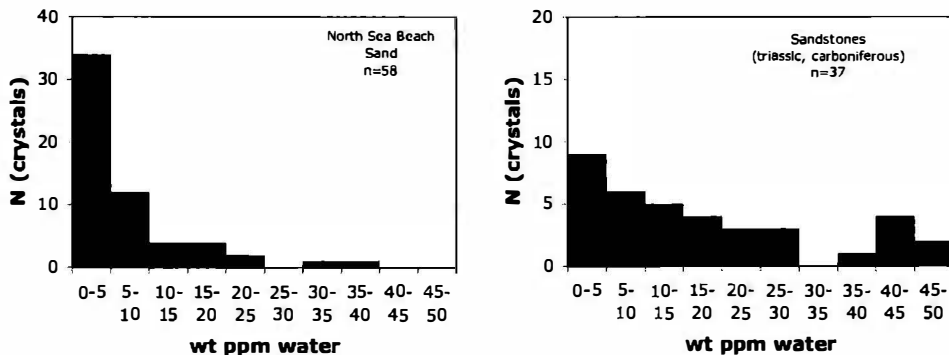


Figure 1. Histogram showing the defect water content of detrital quartz grains, reflecting different source regions (North Sea: predominantly from the Baltic Shield; Sandstones: mostly from Central Europe)

GEOCHEMISTRY AND STRUCTURE OF DOLOMITE AND CALCITE AT OKER (GERMANY)

Stickler, C.P.¹, Deditius, A.P.¹, Baldermann, A.¹, Leis, A.² & Dietzel, M.¹

¹Institute of Applied Geosciences, Graz University of Technology, Rechbauerstrasse 12, 8010 Graz, Austria

²Institute of Water, Energy and Sustainability, Joanneum Research, Elisabethstrasse 18, 8010 Graz, Austria

e-mail: christian.stickler@student.tugraz.at

Precipitation of dolomite under low-temperature conditions in modern aquatic environments is limited due to the inhibitory effect of Mg²⁺ ions. This effect seems to be less effective in anoxic, organic-rich sediments with abundant bacterial sulfate reduction.

To shed a light on the process of dolomite formation under (Mg, S)-rich environments we investigated a partly dolomitized limestone of Upper Jurassic age (~153 Ma) that was formed at shallow marine, sabkha conditions at Oker (Langenberg, Germany). X-ray diffraction (XRD), electron microprobe (EMP) analysis, and δ¹⁸O and δ¹³C isotope measurements were conducted to decipher the geochemical and structural relationship between dolomite, low-Mg calcite (LMC), and high-Mg calcite (HMC) at bulk and micro-scale. The investigated lithological profile starts with layers of massive limestone that gradually transform into fine-grained dolomite followed by a thick limestone horizon at the upper part of the section.

The lower unit consists of micritic limestone of marine origin and is characterized by an isotopic composition of -1.7 to -2.9 ‰ of δ¹⁸O, and 1.3 to -0.7 ‰ of δ¹³C, VPDB. The upper limestone unit has isotopic characteristics of -1.8 to -3.4 ‰ of δ¹⁸O and -1.6 to -4.0 ‰ of δ¹³C, VPDB, indicative of deposition under marine to sabkha conditions. The lower limestone consists of LMC with the chemical composition: (Ca_{0.93-0.996}Mg_{0.003-0.03}Mn_{0-0.054}Sr_{0-0.001}Na_{0-0.001}Fe_{0-0.001})_{0.99-1.0}[(C_{0.94-1}S_{0-0.004})O₃]₂. The transitional contact zone between the lower limestone and the dolomite consists of fine-grained, < 50 μm in size, dolomite, LMC, and HMC (listed from core to rim) deposited in single grains in the alternate mode. EMP analyses of the dolomite cores, ~10-15 μm in diameter, revealed excess of Ca and significant amounts of S (2500 ppm of SO₃); (Ca_{0.97-1.14}Na_{0-0.01})_{0.97-1.14}(Mg_{0.75-0.97}Fe_{0-0.02}Mn_{0-0.01})_{0.76-0.99}[(C_{0.998-1.0}S_{0-0.002})O₃]₂. Sulfur was not detected in the subsequently deposited LMC, (Ca_{0.86-0.99}Mg_{0.006-0.05}Fe_{0-0.004}Na_{0-0.002}Mn_{0-0.001})_{0.96-0.97}CO₃, and HMC, (Ca_{0.64-0.78}Mg_{0.19-0.32}Fe_{0-0.004}Na_{0-0.003}Mn_{0-0.002})_{0.91-0.99}CO₃. The “pure” dolomite (2.2 to 1.7 ‰ of δ¹⁸O and 1.7 to -0.1 ‰ of δ¹³C, VPDB) has a composition of (Ca_{1.03-1.24}Na_{0.001-0.006}Sr_{0-0.001})_{1.03-1.25}(Mg_{0.76-0.95}Fe_{0-0.02}Mn_{0-0.002})_{0.76-0.95}[(C_{0.98-0.998}S_{0.001-0.02})O₃]₂, consists of euhedral crystals with a diameter of 2-50 μm, and shows few microns thick, alternating growth zones of S and Fe. XRD analyses confirmed the dolomite to be non-stoichiometric, with 51-54 mol% of CaCO₃. The degree of order in dolomite, with respect to ideal dolomite super structure, decreases from 83 % to 42 % with increasing S content from 0.02 to 0.06 S atoms per formula unit, respectively.

The variation in the isotopic composition (δ¹⁸O and δ¹³C), distribution, and concentration of Mg, Sr, Fe, and S in calcite and/or dolomite indicates cyclic and abrupt changes of the chemistry of interstitial solution during carbonates formation. The plausible scenario of carbonate evolution involves decrease in sea level coupled with high evaporation degrees which led to increasing Mg/Ca ratios and thus alteration of primary LMC to HMC, subsequently transformed to dolomite.

CHEMISTRY OF XENOTIME-(Y) FROM BERYL-COLUMBITE PEGMATITES OF THE PÍSEK REGION (CZECH REPUBLIC)

Švecová, E.^{1,2}, Čopjaková, R.¹, Losos, Z.^{1,2} & Cícha, J.³

¹Dept. of Geological Sciences, Masaryk University, Kotlářská 2, 611 37 Brno, Czech Republic

²CEITEC, Masaryk University, Kotlářská 2, 611 37 Brno, Czech Republic

³Prácheň Museum, Velké nám. 114, 397 24 Písek, Czech Republic

e-mail: 211679@sci.muni.cz, losos@sci.muni.cz

Xenotime-(Y) from the albite unit with abundant tourmaline of the beryl-columbite Písek granitic pegmatites have been studied with focus on monitoring of the mineral assemblages, successional position, chemical variability of xenotime, the input of U, Th and REE elements in the structure of the xenotime and to determine their substitution mechanisms.

Primary magmatic xenotime-(Y) forms large euhedral grains (up 2 mm) usually in association with zircon, monazite-(Ce) and U-rich Y,REE,Ti,Nb-oxides. Sometimes it forms hypoparallel intergrowths with zircon. Primary xenotime in association with metamict zircon shows magmatic zonal structure with strongly metamict domains. Later xenotime commonly forms along cracks in monazite, or occurs as small inclusions in monazite, moreover, tiny cherlite inclusions are common in later xenotime as well as in surrounding monazite. Furthermore, small later xenotime inclusions occur in highly altered domains of U-rich Y,REE,Ti,Nb-oxides. Rarely, later xenotime together with K-feldspar and Fe-oxides fill cracks in the primary magmatic xenotime. Formation of later xenotime is the result of dissolution-reprecipitation processes during interaction between early magmatic monazite/Y,REE,Ti,Nb-oxides and pegmatite derived fluids.

Primary unaltered xenotime has low to medium concentration of REE (0.17-0.31 apfu) with the highest contents of Dy (0.04-0.08 apfu), Yb (0.02-0.05 apfu), Er (0.02-0.04 apfu), Gd (0.02-0.04 apfu) and Sm (0.01-0.02 apfu). It is characterized by variable U contents (0.5-6.4 wt.% UO₂) and low to medium amount of Th (0.2-4.1 wt.% ThO₂) with high U/Th ratio (commonly 1.3-5.7). Minor Zr (up 2.0 wt.% ZrO₂) and Si (0.1-2.8 wt.% SiO₂) are common in xenotime. The metamict domains in magmatic xenotime lost variable amounts of P, Y, HREE (mainly Yb, Er and Lu), and they are significantly enriched in Ca (up 6.2 wt.% CaO), Th (up 9.4 wt.% ThO₂) and F (up 3.2 wt.% F). Moreover, Zr (up 4.9 wt.% ZrO₂), Fe (up 2.5 wt.% FeO), Sc (up 0.3 wt.% Sc₂O₃) and Ce enrichment was observed in some metamict domains. The U/Th ratio (0.2-1.3) decreases significantly in metamict domains due to the Th enrichment. Later xenotime has lower U and Th contents (0.2-4.5 wt.% UO₂; 0.1-2.4 wt.% ThO₂) compared with primary magmatic xenotime. Moreover, later xenotime along cracks in monazite shows lower contents of the heaviest REE (Er, Yb, Lu). The significant negative Eu anomalies (Eu b.d.l. of EMP) are typical for all types of xenotime. Uranium and thorium enter non-metamict xenotime via (U,Th)SiREE₁P₁ substitution vector, mainly coffinite component (USiO₄) is important. The Ca contents in non-metamict xenotime are very low and exchange vector CaThREE₂ is negligible.

This work was supported by the EU-projects „Research group for radioactive waste repository and nuclear safety“ (CZ.1.07/2.3.00/20.0052), “CEITEC-Central European Institute of Technology” (CZ.1.05/1.1.00/02.0068) and GACR P207/11/0555 of the Grant Academy of the Czech Republic.

ON THE PRESENCE OF HYDROUS DEFECTS IN DIFFERENTLY COLOURED WULFENITES (PbMoO_4): AN INFRARED AND OPTICAL SPECTROSCOPIC STUDY

Talla, D.^{1,2}, Wildner, M.¹, Beran, A.¹, Škoda, R.² & Losos, Z.^{2,3}

¹Institut für Mineralogie und Kristallographie, Universität Wien, Althanstraße 14, 1090 Wien,
Austria

²Department of Geological Sciences, Masaryk University, Kotlářská 2, 611 37 Brno, Czech Republic

³CEITEC, Masaryk University, Kotlářská 2, 611 37 Brno, Czech Republic

e-mail: sutra@volny.cz

Several samples of wulfenite, PbMoO_4 , varying in colour from colourless to yellow, orange and red, have been characterised by means of IR and optical absorption spectroscopy and by microprobe analyses. A distinct pleochroic band group with absorption maxima centred at 3380 and 3150 cm^{-1} can be seen in the IR spectra of wulfenite single-crystals, indicating the presence of hydroxyl groups. The pleochroic and thermal behaviour of the OH stretching bands along with deuteration experiments, as well as results obtained from synthetic flux-grown samples, exclude the presence of submicroscopic hydrous mineral inclusions (mainly considered were phases belonging to the alunite-crandallite mineral group) as their primary origin. Whereas jarosite and plumbogummite, in which the OH absorption bands coincide in shape and position with the IR absorption phenomena visible in wulfenite, decompose already at 250 °C, the OH bands of wulfenite persist up to 500 °C. A significant CO_2 absorption pattern which evolves upon heating the samples to 500 °C is attributed to the decomposition of included carbonates (siderite and smithsonite), which were found by means of a scanning electron microscope and EDX analyses.

The pleochroic scheme and the band positions were used to postulate a model for the OH incorporation mode, based on the assumption of vacancies on Mo and Pb sites in the structure of this ‘nominally anhydrous mineral’, where the latter case presumes an interstitial OH group occupying the vacant Pb position.

Optical absorption spectra of coloured natural samples show a broad and polarised band around 23000-24000 cm^{-1} , preceding the fundamental UV absorption edge, which has been identified as the reason for the colour of the mineral. The comparison with synthetic PbMoO_4 single-crystals, doped with variable amounts of Cr^{4+} , yielded conclusive evidence that trace amounts of the CrO_4^{2-} anion group, substituting for MoO_4^{2-} , determine the variable colour. Besides, in one sample, trace amounts of Nd^{3+} have been spectroscopically identified.

To confirm the assignment of the observed absorption patterns to Nd, a PbMoO_4 sample doped with Nd^{3+} has been synthesised using the coupled substitution $\text{Nd}^{3+}\text{As}^{5+} \rightarrow \text{Pb}^{2+}\text{Mo}^{6+}$. In natural samples, V^{5+} is believed to provide the necessary charge balance, as samples with observable REE bands have enhanced contents of V_2O_5 .

MINERAL CHEMISTRY AND PETROLOGY OF CHROMIUM-BEARING KYANITES FROM THE POHORJE MOUNTAINS, SLOVENIA

Taferner, H.¹, Hauzenberger, C. A.¹ & Konzett, J.²

¹Institute of Earth Sciences, Karl-Franzens-University Graz, Universitätplatz 2, 8010, Graz, Austria

²Institute of Mineralogy and Petrography, University of Innsbruck, Innrain 52, A-6020 Innsbruck, Austria

e-mail: christoph.hauzenberger@uni-graz.at

Eo-Alpine eclogites are commonly found in the southern parts of the Pohorje Mountains, Slovenia. Geochemical characteristics suggest an olivine, pyroxene, plagioclase and spinel bearing gabbroic cummulate as precursor rock. Turquoise coloured chromium-bearing kyanites in eclogites from the Pohorje Mountains, Slovenia, attracted attention in two samples, PM22 and PM26. Two different textures can be observed: (1) A first type characterised by tiny Cr-spinel inclusions within larger turquoise coloured kyanite (Fig. 1a) and (2) a second type formed around larger chromite crystals together with Cr-rich corundum (up to 9.1 wt% Cr₂O₃) and pargasitic amphibole (Fig. 1b). Cr₂O₃ values in kyanite reach up to 14.4 wt%. Net transfer reactions, between garnet, clinopyroxene, phengite, kyanite and quartz/coesite, were used for *PT* estimates. The calibration of KROGH RAVNA & TERRY (2004) resulted in highest pressures and temperatures close to the Qz-Coe transition with T = ~810 °C and P = ~2.9 GPa, while the dataset of HOLLAND & POWELL (1998) resulted in the lowest peak metamorphic conditions of ~2.2 GPa and 720 °C for the same reaction set. The calibration of BRANDELIK & MASSONNE (2004) is between both values with *PT* conditions of c. 2.5 GPa and temperatures around 710–760 °C. Zr in rutile thermometry was applied for independent temperature determination giving a mean of 748 °C.

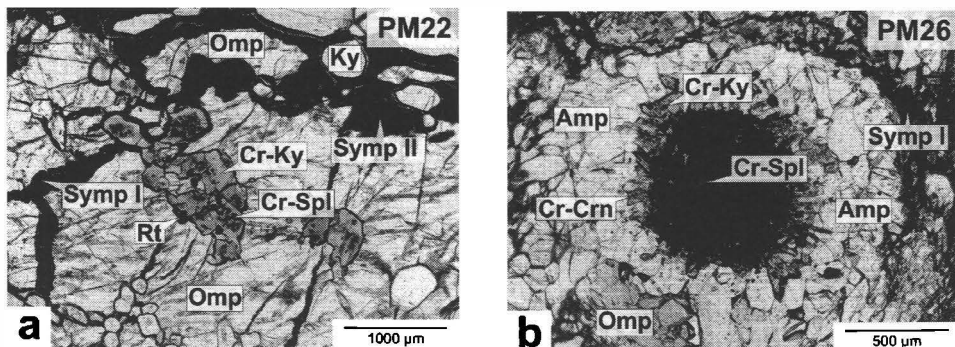


Figure 1. (a) Cr-kyanite with abundant chromite inclusions. (b) Cr-kyanite and Cr-corundum crystallized around a large Cr-Sp grain. Symp I = symplectite around Omph; Symp II = symplectite around kyanite.

BRANDELIK, A., MASSONNE, H.-J. (2004): Computers and Geosciences, 30, 909-923.

HOLLAND, T.J.B., POWELL, R. (1998): Journal of Metamorphic Geology, 16, 309-344

KROGH RAVNA, E.J., TERRY, M.P. (2004): Journal of Metamorphic Geology, 22, 579-592.

Ca₂Mg(NO₃)₆*12H₂O – FIRST RESULTS ON A NEW COMPOUND RETRIEVED FROM CHIMNEY DEPOSITS OF A COMBINED HEAT AND POWER PLANT

Tessadri, R., Kahlenberg, V., Schmidmair, D. & Haefeker, U.

University of Innsbruck, Institute of Mineralogy & Petrography, Innrain 52, A-6020 Innsbruck, Austria
e-mail: richard.tessadri@uibk.ac.at

Nitrate minerals containing alkaline earth cations are rather rare. So far only two hydrous natural species have been reported in the literature: nitrocalcite (Ca(NO₃)₂*4H₂O, RIBAR et al., 1973) and nitromagnesite (Mg(NO₃)₂*6H₂O, SCHEFER & GRUBE, 1995). In the field of technical mineralogy, on the other hand, both phases have attracted much more interest. For example, both compounds are among the most common deterioration agents responsible for salt attack of buildings and monuments. Furthermore, nitromagnesite has been studied intensively as a potential thermal energy storage material (ZALBA et al., 2002). To the best of our knowledge no synthetic or natural hydrous Ca-Mg-nitrate has been reported so far. The results of the present investigation will fill this gap.

Starting point for this study was a routine X-ray powder diffraction phase analysis of a series of samples which were obtained from incrustations of an exhaust gas chimney of a combined heat and power plant located in Malchow/Germany. Phase analysis using the current version of the PDF-4 database showed the existence of a small amount of anhydrite as well as bassanite. However, the majority of the peaks could not be attributed to any phase or phase mixture contained in the powder diffraction file. A re-examination of the residual under a petrographic microscope revealed that the sample contained a large number of colourless transparent crystals. A single-crystal of good optical quality was further studied by X-ray single-crystal diffraction (performed at 25 °C). The crystal structure could be solved by direct methods and difference Fourier synthesis. Structure solution was also used to establish the chemical composition: Ca₂Mg(NO₃)₆*12H₂O. The presence of water as well as nitrate moieties in the structure was confirmed by micro-Raman spectroscopy. Basic crystallographic data of the previously unknown material are as follows: trigonal symmetry, space group *R* -3, *a*=10.5583(5) Å, *c*=19.5351(10) Å, *V*=1885.98(16)Å³, *Z*=3, *R*(|*F*|)=0.0248 for 744 reflections with *I*>2σ(*I*). Principal structural building units are columns containing an alternating sequence of Mg(H₂O)₆-octahedra and CaX₉ tricapped trigonal prisms. (X:H₂O molecules, O atoms from the nitrate groups). Linkage between the polyhedra of a single column as well as between neighbouring columns is provided by hydrogen bonding. Using the result of the structural investigation a quantitative phase analysis of the incrustations based on the Rietveld method could be accomplished.

RIBAR, B., DIVJAKOVIC, V., HERAK, R., PRELESNIK, B. (1973): Acta Cryst., B29, 1546-1548.

SCHEFER, J. , GRUBE, M. (1995): Mat. Res. Bull., 30, 1235-1241.

ZALBA, B., MARIN, J.M., CABEZA, L.F., MEHLING, H. (2003): Appl. Therm. Eng., 23, 251-283.

CONCRETE DETERIORATION – FORMATION CONDITIONS TRACED BY CRYSTAL WATER OF SULFATE MINERALS

Thaller, D.¹, Mittermayr, F^{1,2}, Baldermann, A.¹, Fischer, R.³, Leis, A.⁴ & Dietzel, M.²

¹Institute of Applied Geosciences, Graz University of Technology, Rechbauerstraße 12, 8010 Graz, Austria

²Institute of Technology and Testing of Building Materials, Graz University of Technology, Inffeldgasse 24, 8010 Graz, Austria

³ Institute of Inorganic Chemistry, University of Technology, Stremayrgasse 9/IV, 8010 Graz, Austria

⁴RESOURCES – Institute for Water, Energy and Sustainability, Joanneum Research, Elisabethstraße 18/2, 8010 Graz, Austria

e-mail: daniel.thaller@student.tugraz.at

Concrete damage caused by secondary formation of hydrous sulfate minerals (e.g. thaumasite, ettringite and gypsum) may cause serious problems concerning the durability of concrete structures. Cracking due to volume dilatation and disintegration of CSH-phases significantly reduces the overall lifespan of affected structures, whereby high costs for servicing and renovation are incurring. Despite numerous reports, detailed knowledge of the reaction mechanisms and conditions for the formation of hydrous sulfate minerals in concretes is still lacking (NEVILLE, 2004).

In a recently performed study in Austrian tunnels damaged concrete was identified as a consequence of the thaumasite form of sulfate attack (TSA) (MITTERMAYR et al., 2013). The severe concrete damage was shown to be caused by a highly dynamic system of drying and wetting cycles by applying a multiproxy approach. Evaporation of interstitial solutions loaded by ground water has led to a massive increase of SO₄ concentration which triggered the formation of sulfate hydrate minerals.

For the present study the above described damaged concrete material containing thaumasite Ca₃Si(OH)₆(CO₃)(SO₄)•12H₂O and gypsum CaSO₄•2H₂O was used. A novel approach by extracting the crystal water and analysing its isotopic signature is used to discover their formation conditions. The crystal water was extracted via a cold trap attached to a Schlenk line setup. δ²H and δ¹⁸O were measured by wavelength scanned cavity ring-down spectroscopy. As internal standards lab-synthesized gypsum and ettringite (Ca₆Al₂(SO₄)₃(OH)₁₂•26H₂O) were used.

The crystal water from 5 damaged concrete samples was successfully and quantitatively recovered. The δ²H and δ¹⁸O values yielded in -57.1 ±4.0 and -3.4 ±1.0 ‰, respectively. Compared to the average value of the local ground water (δ²H = -83.0 ‰; δ¹⁸O = -12.0 ‰) a significant discrimination of the light vs. heavy isotopes was found in the crystal water (MITTERMAYR et al., 2013). Ultimately evaporation degrees of highly concentrated SO₄ interstitial solutions (5000 up to 50000 mg L⁻¹) can be validated from isotopic composition of crystal water tracing the individual formation conditions of damaging sulfate minerals.

MITTERMAYR, F., BALDERMANN, A., KURTA, C., RINDER, T., KLAMMER, D., LEIS, A., TRITTHART, J., DIETZEL, M. (2013): Cem. Concr. Res., 49, 55-64.

NEVILLE, A. (2004): Cem. Concr. Res., 34, 1275-1296.

COMPOSITIONAL VARIATION OF Ba-RICH WHITE MICAS FROM TWO DIFFERENT GEOLOGICAL SETTINGS

Tribus, M.¹, Pomella, H.², Tropper, P¹ & Linner, M.³

¹Institute of Mineralogy and Petrography, Faculty of Geo- and Atmospheric Sciences, University of Innsbruck,
Innrain 52, 6020 Innsbruck, Austria

²Institute of Geology and Paleontology, Faculty of Geo- and Atmospheric Sciences, University of Innsbruck,
Innrain 52, 6020 Innsbruck, Austria

³Geological Survey of Austria, Neulinggasse 38, 1030 Wien, Austria

e-mail: martina.tribus@uibk.ac.at

Ba-micas can occur in a variety of geological environments. The formation of Ba-rich micas is strongly influenced by the presence of hydrothermal fluids and thus can be classified as a product of metasomatic processes. Ba-rich muscovite/paragonite, so called ganterite, is a dioctahedral white mica represented by a 1:1 mixture between the true micas muscovite/paragonite and the hypothetical Ba brittle mica with an ideal composition of $[Ba_{0.5}(Na+K)_{0.5}]Al_2[Si_{2.5}Al_{1.5}]O_{10}(OH)_2$ (GRAESER et al., 2003; JAMBOR & ROBERTS, 2004). As the interlayer position is filled up to 50% by monovalent cations ganterite is a member of the true micas.

(1) The Ba-rich white micas of the first study occur in the Lienz contact aureole adjacent to the Oligocene Lienz/Edenwald tonalite in the surrounding fine-grained mica schists of the Austroalpine basement. Thermometric calculations for the innermost part of the aureole yielded temperatures of 640 ± 24 °C. The Ba content in the white mica reaches up to 13.38 wt.% BaO, even though Ba is not the dominant interlayer cation. The formula of a typical Ba-rich white mica is $[Ba_{0.37}K_{0.41}Na_{0.22}]_{1.00}[Al_{1.93}Mg_{0.02}Fe_{0.03}Ti_{0.02}]_{2.00}[Si_{2.66}Al_{1.34}]O_{10}(OH)_2$. Based on the chemical composition of the mica endmembers paragonite and muscovite, the Ba-rich mica in this study can be formed by a combination of the coupled substitution $[Ba][Al^{IV}] = [K]_{.1}[Si]_{.1}$ and the simple $[Na] = [K]_{.1}$ exchange vector. Complete solid solutions between muscovite and Ba-rich white micas were observed since Ba contents range from 0.07 wt.% up to 13.38 wt.% BaO.

(2) The Ba-rich white mica of the second study was found in the highly deformed marble belt close to the Meran-Mauls fault, which is part of the Giudicarie fault system. The marble layer occurs within the paragneisses of the Meran-Mauls Basement and has been overprinted under Variscan amphibolite-facies and eo-Alpine/Alpine greenschist-facies condition. The Ba-rich white mica is associated with celsian + barite + calcite + dolomite. The variation in the BaO content of the micas ranges from 0.49 wt.% up to 8.78 wt.%. As most of the white micas in this study are “phengitic”, the incorporation of Ba can be described by the coupled substitution $[Ba][Al^{VI}][Al^{IV}]_2 = [K]_{.1}[Mg]_{.1}[Si]_{.2}$. The formula of a low Ba-mica (0.96 wt.% BaO) is $\square_{0.10}[Ba_{0.02}K_{0.86}Na_{0.01}Ca_{0.01}]_{0.90}[Al_{1.56}Mg_{0.42}Fe_{0.01}Ti_{0.01}]_{2.00}[Si_{3.48}Al_{0.52}]_{4.00}O_{10}(OH)_2$. This indicates a 50:50 composition along the muscovite – aluminoceladonite solid solution.

GRAESER, S., HETHERINGTON, C., GIERÉ, R. (2003): Canadian Mineralogist, 41, 1271-1280.

JAMBOR, J.L., ROBERTS, C. (2004): American Mineralogist, 89, 1826-1834.

**THERMODYNAMIC MODELLING OF IN-SITU ECLOGITIZATION OF
METAPELITES FROM VAL SAVENCA (SESIÀ ZONE, WESTERN ALPS)**

Tropper, P.

Institute of Mineralogy and Petrography, University of Innsbruck, Innrain 52f, A-6020 Innsbruck, Austria
e-mail: peter.tropper@uibk.ac.at

A common feature of HP and UHP terranes is the subduction of lower crustal rocks to great depths. Previous investigations have shown that this process is triggered by fluids present during an eclogite-facies metamorphic overprint. Key examples of these processes are exposed in the metapelites at Val Savenca and the metagranites of Monte Mucrone, both in the Sesia-Lanzo Zone, Italy, where Alpine eclogite-facies metamorphism and fluid flow led to partial transformation of Variscan amphibolite-eclogite facies metapelites (garnet + biotite + sillimanite + K-feldspar + plagioclase + quartz) and metagranites (garnet + biotite + K-feldspar + plagioclase + quartz) to zoisite ± jadeite + kyanite + phengite + quartz with associated jadeite veins. This transformation took place under *P-T* conditions of 1.7 – 2.1 GPa at 600 °C and low *a(H₂O)* of 0.3-0.6. The textures in the Val Savenca metapelites show relict igneous biotite which is rimmed by a thin rind of garnet. The replacement of plagioclase by jadeite + zoisite + kyanite + quartz takes place also along former fractures. Within the jadeite + zoisite + kyanite + K-feldspar pseudomorphs after plagioclase, jadeite and quartz coexist with K-feldspar. Jadeite also shows some late stage replacement by omphacite at the rims, which was also observed in jadeite-rich veins in adjacent samples. Biotite is replaced by the assemblage phengite + omphacite ± kyanite if it is adjacent to former plagioclase, otherwise by phengite + rutile/titanite, or only by phengite. These omphacitic areas contain no zoisite. Former metamorphic K-feldspar seems to recrystallize during Alpine metamorphism, as suggested by development of a homogeneous host with included needles of zoisite and jadeite. The extreme development of microdomains can best be studied by investigating garnet and clinopyroxene zoning. Garnet grows in two generations, namely garnet from the primary assemblage and garnet growing around biotite is pyrope-rich. The grossular content increases during the Alpine metamorphic overprint and garnets growing adjacent to plagioclase domains are very grossular-rich. Clinopyroxenes also show strong compositional variations depending on the microdomain in which they grew. The compositions range from jadeite (>90% Jd) to omphacite (ca. 40% Jd). Thermodynamic modelling of individual microdomains was done by calculating pseudosections of stoichiometric mixtures of protolith minerals using the program DOMINO (DE CAPITANI & PETRAKAKIS, 2010). Protolith plagioclase composition was calculated using image analysis and yielded a plagioclase composition ranging between 30% and 50% anorthite component. The aim of the pseudosection calculations was two-fold: 1.) to reproduce the observed mineral assemblage and 2.) to provide constraints on the amount of fluid present in the transformation. The results so far indicate that the amount of fluid was low, otherwise paragonite would have formed instead of jadeite in the plagioclase domains. Reproduction of the observed mineral assemblage has only been partly successful so far since biotite is still stable in the calculations.

**DER ZUSAMMENBRUCH VON STAUROLITH UND KYANIT IM WESTLICHEN
AUSTROALPIN ALS MONITOR FÜR DEN GRAD DER EO-ALPINE
METAMORPHOSE**

Tropper, P

Institut für Mineralogie und Petrographie, Universität Innsbruck, Innrain 52f, A-6020 Innsbruck, Österreich
e-mail: peter.tropper@uibk.ac.at

Es handelt sich hier um die petrographische und petrologische Bearbeitung von Proben aus austroalpinen Basementkomplexen, westlich des Tauern Fensters, nämlich Ötztal-Stubai Kristallin, Matscher Decke, Patscherkofelkristallin, Silvretta Kristallin, Meran Mauls Kristallin und Ortler-Campo Kristallin. In diesen polymetamorphen Kristallinkomplexen treten makroskopisch sichtbare Staurolithpseudomorphosen auf. Die variszische Metamorphose gilt eindeutig als das dominierende Ereignis in allen Kristallinkomplexen, welche die wesentlichen Mineralparagenesen und die Gefüge bildete. Die Druck- und Temperaturbedingungen der Metapelite können aufgrund der Mineralparagenesen im Bereich um 550-670 °C und 3-8 kbar festgelegt werden. Die dominante Mineralparagenese umfasst Staurolith, Granat, und manchmal alle drei Aluminiumsilikate, wobei Kyanit die dominante Modifikation ist. Die eo-alpidische Metamorphose ist im Ötztal-Stubai Kristallin variabel und reicht von ca. 300 °C im NW zu ca. 600 °C im SE. Im Patscherkofel Kristallin und im Ortler Campo Kristallin erreichte die eo-alpidische Metamorphose 420 °C bis 500 °C. Im Silvrettakristallin hingegen erreicht die eo-alpine Metamorphose nur ca. 350 °C. Petrographische Untersuchungen haben ergeben, dass Staurolith immer Teil der prä-alpidischen Paragenese ist und er im Zuge der eo-alpidischen Metamorphose umgewandelt wird. Der Grund für diese Umwandlung liegt in den niedrigeren Temperaturen (300-520 °C), die bei der eo-alpidischen Metamorphose herrschten. Staurolith zerfällt zu 1.) Chlorit + Muskovit, 2.) Chlorit + Muskovit + Chloritoid, 3.) Chlorit + Paragonit + Granat, 3.) Chloritoid + Margarit + Korund. Kyanit wiederum zerfällt zu 1.) Muskovit oder 2.) Margarit + Chlorit. Ziel dieser Arbeit ist es die Mineralreaktion zu eruieren und die *P-T* Bedingungen einzuzgrenzen, die zum Zerfall von Staurolith bzw. Kyanit führen. Staurolith zerfällt immer unter Zufuhr von H₂O in der Anwesenheit von Plagioklas bzw. Biotit. Gleicher gilt für den Zusammenbruch von Kyanit. Die berechnete Lage der Mineralreaktionen mittels des Programms THERMOCALC, ergab, dass der Zerfall dieser beiden Phasen eigentlich nur temperaturabhängig ist, da die Reaktionen in einem *P-T* Diagramm steil stehen. Die Untersuchung ergab auch, dass der beobachtete Chloritoid-Isograd im westlichen Austroalpin immer an den Zerfall von Staurolith gebunden ist und dass der Zerfall von Kyanit zu Margarit im Meran Mauls Kristallin wahrscheinlich eo-alpidische grünschieferfazielle Bedingungen anzeigt.

**HOW DO EXPERIMENTS AND CALCULATIONS COMPARE? EXPERIMENTS
VERSUS PSEUDOSECTIONS: A TEST FROM HIGH-P/HIGH-T GRANULITES AND
THE ROLE OF Ti AND F IN BIOTITE**

Tropper, P.¹ & Hauzenberger, Ch.²

¹Institute of Mineralogy and Petrography, University of Innsbruck, Innrain 52, A-6020 Innsbruck, Austria

²Institute of Earth Sciences, University of Graz, Universitätsplatz 2, A-8010 Graz, Austria

e-mail: peter.tropper@uibk.ac.at

Large bodies of Variscan felsic high-*P*/high-*T* granulites with the assemblage quartz + ternary feldspar (mesoperthite) + garnet + rutile ± kyanite occur in the Southern Bohemian Massif. They are thought to have formed at 950–1050 °C and 1.5–1.9 GPa, from granitic protoliths. In order to assess the processes of high-*P*/high-*T* granulite formation, fluid-absent piston cylinder experiments were conducted with granitic gneiss as starting material (K-feldspar + plagioclase + quartz + biotite + muscovite), whose chemical composition almost perfectly matches the main granulite type of the Southern Bohemian Massif. The experimental conditions were chosen to simulate the metamorphic P-T path determined for the granulites, with runs at 750 – 1000 °C / 1.6 GPa, (prograde path), at 950 °C / 1.4 GPa and 800 – 900 °C / 1.2 GPa (retrograde path). The experiments in the temperature range of 850 – 1000 °C all yielded the typical granulite assemblage garnet + ternary feldspar + quartz ± kyanite ± rutile. The melt-forming reaction observed in the experiments is: biotite + plagioclase + quartz = garnet + ternary feldspar + melt. At pressures of 1.6 GPa, this reaction commences at temperatures >750 °C and goes to completion between 800 °C and 850 °C. In the isobaric section at 1.6 GPa, both biotite and muscovite are present at 750 °C and 800 °C. Up to 850 °C, two feldspars are present in the experiments, albeit with a strong decrease in the modal amount of plagioclase from 18 vol.% at 750 °C to <1 vol.% at 850 °C. In runs at 900 °C and 1000 °C, Na-rich alkali feldspar is no longer stable and a K-rich alkali feldspar appears instead as the only feldspar phase. Experiments at 1.2 GPa show assemblages and textures similar to runs at 1.6 GPa with biotite being stable at 800 °C and plagioclase consumed by partial melting between 800 °C and 900 °C.

In order to compare the experimental results with theoretical predictions, pseudosections with the programs PERPLEX (CONNOLLY & PETRINI, 2002) and DOMINO (De CAPITANI & PETRAKAKIS, 2010) and the updated database of HOLLAND & POWELL (1998) were calculated. The calculated phase relations and modes are in good agreement with the experimental results. The only major discrepancy lies in the stability of biotite, which is grossly underestimated in the calculations using both programs (prediction is 100 °C lower at 1.6 and 1.2 GPa). Electron microprobe analyses showed that biotite contains up to 5 wt.% TiO₂ and 2 wt.% F. Although Ti contents can be considered empirically in Ti-biotite activity models, no biotite activity model involving F yet exists.

CONNOLLY, J.A.D., PETRINI, K. (2002): Journal of Metamorphic Geology, 20, 697–708.

DE CAPITANI, C., PETRAKAKIS, K. (2010): American Mineralogist, 95, 1006–1016.

HOLLAND, T.J.B., POWELL, R. (1998): Journal of Metamorphic Geology, 16, 309–344.

EXPERIMENTELLE UNTERSUCHUNGEN ZUR KNOCHEN- GESTEINSWECHSELWIRKUNG IN BRANDOPFERPLÄTZEN

Tropper, P & Spielmann, M.

Institut für Mineralogie und Petrographie, Universität Innsbruck, Innrain 52f, A-6020 Innsbruck, Österreich
e-mail: peter.tropper@uibk.ac.at

In den Alpen gibt es eine Vielzahl von prähistorischen Brandopferplätzen, die Menschen der Vorzeit aus religiösen aber auch praktischen Gründen angelegt haben. Diese Brandstätten erkannten die Archäologen aufgrund von Schlackenfunden, Keramikbruchstücken, sowie Knochen oder Schmuckstücken, (GLEIRSCHER et al., 2002), mineralogisch wurden die Schlacken von zwei Brandopferplätzen von TROPPER et al. (2004) und SCHNEIDER et al. (2012) untersucht. In dieser Arbeit wurden experimentelle Untersuchungen bei hohen Temperaturbedingungen (1200°C), die denen der prähistorischen Brandstätten gleichen, zwischen verschiedenen charakteristischen Gesteinen der Ostalpen und Knochenbruchstücken simuliert um herauszufinden ob diagnostische Mineralphasen entstehen und ob die Brandbedingungen bei Brandopferplätzen im Labor reproduzierbar sind. Die mineralogischen Beobachtungen aus den Schlacken der Brandopferplätze und die experimentellen Untersuchungen von Tropper et al. (2006) konnten dabei zum Großteil reproduziert werden. Es wurden diagnostische Minerale wie Whitlockit und P-hältiger Olivin in den Experimenten reproduziert. Des Weiteren wurden im Paragneis- sowie im Amphibolitexperiment P-hältige Klinopyroxene erkannt welche P_2O_5 Gehalte bis zu 3 Gew.% aufweisen. Die Olivine enthalten Phosphorgehalte zwischen 0-4.6 Gew.%, wobei die P-reichen Konzentrationen nur in den Experimenten mit Quarzphyllit gefunden wurden. P-hältiger Olivin in Kombination mit Whitlockit kann daher in Quarzphylliten auf jeden Fall als diagnostisch anerkannt werden, da TROPPER et al. (2006) ebenfalls P-reiche Olivine in Metapeliten gefunden hatten. Die P-hältigen Klinopyroxene könnten in Kombination mit Whitlockit ebenfalls Indikatoren für Knochen-Gesteinswechselwirkung in Gneisen und Granatamphiboliten darstellen. Das Auftreten von metallischem Eisen weist auf extrem niedrige fO_2 Bedingungen im Experiment hin die in den bereits untersuchten Brandopferschlacken allerdings nicht nachgewiesen werden konnten. Die Anwesenheit von Whitlockit + P-hältigem Olivin lässt daher auf die Verbrennung von Knochenmaterial schließen, was experimentell reproduziert werden konnte. P-hältiger Olivin alleine, muss jedoch nicht auf den Zusammenbruch von Knochenmaterial zurückzuführen sein, auch Holz kann als Phosphorquelle dienen, da es 1-2 Gew.% P_2O_5 enthält. Die Anwesenheit von P-hältigem Klinopyroxen wurde in bisher untersuchten Schlacken noch nicht beschrieben, jedoch ist anhand der Ergebnisse dieser Untersuchungen durchaus damit zu rechnen.

- GLEIRSCHER, P., NOTHDURFTER, H., SCHUBERT, E. (2002): Das Rungger Egg. Philipp von Zabern.
SCHNEIDER, P., TROPPER, P., KAINDL, R. (2012): Mineralogy and Petrology, 107, 327-340.
TROPPER, P., KONZETT, J., RECHEIS, A. (2006): Mitteilungen der Österreichischen Mineralogischen Gesellschaft, 152, 47-56.
TROPPER, P., RECHEIS, A., KONZETT, J. (2004): European Journal of Mineralogy, 16, 631-640.

RAMAN-SPECTROSCOPY OF CORDIERITES FROM Na-IN-CORDIERITE EXPERIMENTS: CHEMICAL VS. STRUCTURAL EQUILIBRIUM

Tropper, P.¹, Haefeker, U.¹ & Wyhlidal, S.²

¹Institute of Mineralogy and Petrography, University of Innsbruck, Innrain 52f, A-6020 Innsbruck, Austria

²AIT, Austrian Institute of Technology, A-2444 Seibersdorf, Austria

e-mail: peter.tropper@uibk.ac.at

WYHLIDAL et al. (2008) investigated the Na-incorporation in cordierite in natural samples using two different quartzphyllites (SP: Na, Si-rich; W: Na, Si-poor). The experiments were performed in a hydrothermal apparatus as well as a piston-cylinder apparatus. In order to provide estimates on the degree of equilibration in the experiments, structural investigations such as Raman-spectroscopy and chemical constraints from compositional reversals and pseudosection calculations were performed on samples from both experimental series.

Structural constraints: In order to provide structural constraints on the degree of structural equilibration in the experiments Raman spectroscopic investigations of newly grown cordierites as a function of temperature were done. Synthetic Mg-cordierite has two structural transitions and transforms from the hexagonal over a modulated state to the orthorhombic structure mainly as a result of Al-Si ordering. The cordierites of the experimental series SP and W show a clear temperature-dependent ordering as indicated by the extent of peak splitting in the 530-600 cm⁻¹ region. For instance in SP sample 18 at 550°C peak splitting is the least developed indicating the lowest Al-Si ordering state. The distance between the peaks at 555.5 cm⁻¹ and 575 cm⁻¹ is 19.5 cm⁻¹ and almost no peak splitting is visible. Experiment 17 was synthesized at 730 °C and the sample shows the highest degree of ordering as indicated by the distance between the peaks at 554 cm⁻¹ and 576 cm⁻¹ of 22 cm⁻¹ and the shape of the clearly visible peak splitting. The data show that hydrothermally synthesized cordierites grow initially as the disordered polymorph and thus show temperature-dependent Al-Si ordering.

Compositional constraints: Compositional reversals were run in a first step at 0.3 GPa at 680 °C for 720 h and then in a second step at 580 °C for another 720 h. The results of both starting materials show that the Na contents of cordierite started to re-equilibrate which is shown by the overlap of the Na values which were obtained at 580 °C. Pseudosection calculations were undertaken for both whole-rock compositions in the system KNCFMTiASH using the program THERIAK-DOMINO. The amount of the coexisting fluid phase H₂O taken was assumed to be the LOI. The agreement between the calculated and the observed mineral assemblages in both experimental series is only satisfactory but the onset temperature of melt formation is the same at 680 °C. It is also noteworthy that muscovite is more stable in both sets of experiments than in the calculations. Although this discrepancy is large and varies between 30 °C and 110 °C it could be due to minor F and/or Cl contents in the micas which we did not analyse.

The results of this study indicate that even if theoretical, geothermometric and experimental constraints points towards attainment of chemical equilibrium in the experiments, structural disequilibrium features despite the long run times (>300 h) can still occur.

WYHLIDAL, S., THÖNI, W.F., TROPPER, P., MIRWALD, P. (2008): EMPG XII, Innsbruck Univ. Press, 118.

HOT, HOTTER, HOTTEST: EXTREME CASES OF ANTHROPOGENIC PYROMETAMORPHISM

Tropper, P., Haefeker, U., Schneider, P., Braunhofer, D. & Pupp, M.

Institute of Mineralogy and Petrography, University of Innsbruck, Inrain 52f, A-6020 Innsbruck, Austria
e-mail: peter.tropper@uibk.ac.at

This contribution summarizes the results of petrological investigations concerning extremely high- T pyrometamorphism of anthropogenic nature. Three cases will be described: 1.) slags from sacrificial burning sites, 2.) formation of pseudofulgurites and 3.) petrography of slags from the first atomic blasts, the so-called trinitites.

In the first study the occurrence of P-rich olivine and the tri-calcium phosphate (TCP) stanfieldite in partially molten quartzphyllites from the ritual immolation site at the Goldbichl, near Innsbruck in the Tyrol, Austria is reported. The pyrometamorphic rocks contain mostly the mineral assemblage olivine + orthopyroxene + plagioclase + spinel + glass. During the investigation of slag samples from this prehistoric ritual immolation site, extremely P-rich, apatite-bearing micro-domains were found. In these domains phosphorane olivine was found coexisting with plagioclase and a tri-calcium phosphate phase showing stanfieldite $\text{Ca}_4(\text{Mg}, \text{Fe}^{2+}, \text{Mn}^{2+})_5(\text{PO}_4)_6$ composition. Schematical Schreinemakers analysis in the system $\text{CaO}-\text{Al}_2\text{O}_3-\text{FeO}-\text{SiO}_2-\text{P}_2\text{O}_5-\text{H}_2\text{O}$ shows that P-rich olivine (fayalite-sarcopside solid solution) can form from mineral reactions involving chlorite, apatite and quartz and show that the occurrence of P-rich Fe-olivines spans a large T -range but is restricted to domains with high $\alpha(\text{SiO}_2)$. The estimated temperatures are in the range of 1000-1200 °C.

In the course of the second investigation an exceptionally well-preserved fulgurite-like aggregate from Kaltenbach, district Vitis, Lower Austria, Austria was analysed. The pseudofulgurite is mainly composed of glass and contains partially- and fully fused and deformed relict fragments as well as newly formed minerals. The presence of mullite, baddeleyite instead of zircon, osumilite and Fe-P, Fe-Si-P, Fe-Si-Ni globuli enable to constrain a lower T of formation of 1500-1800 °C. Currently experimental investigations concerning pseudofulgurite formation are being conducted and investigated.

The third investigation deals with the so-called trinitites, glasses that formed in the course of the first nuclear blast at the Trinity site in New Mexico. These glasses contain only relict quartz and zircon fragments. In contrast to the pseudofulgurites abundant baddeleyite was found stemming from the breakdown of zircon indicating temperatures overstepping 1680-1770 °C greatly. Raman-spectroscopic investigations are currently being undertaken to investigate the nature of the baddeleyite modification.

The latter two examples clearly illustrate that the obtained temperatures have to be regarded only as lower temperature estimates since the duration of these processes is extremely short and hence the overstepping of the zircon breakdown temperature must be quite significant.

DER ZUSAMMENBRUCH VON ZIRKON IN TRINITITEN

Tropper, P., Pupp, M. & Tessadri, R.

Institut für Mineralogie und Petrographie, Universität Innsbruck, Innrain 52f, A-6020 Innsbruck, Österreich
e-mail: peter.tropper@uibk.ac.at

30 Meilen östlich von Socorro liegt „Trinity Site“, der Ort in der Wüste New Mexikos an dem am 6. Juli 1945 die erste Atombombe gezündet wurde. Während des Zweiten Weltkrieges arbeiteten amerikanische Wissenschaftler unter der Leitung von J. Robert Oppenheimer am Manhattan Project an der Entwicklung der Atombombe zum Zwecke des Kriegseinsatzes. Doch bevor sie effektiv in Kampfhandlungen eingesetzt werden konnte, musste die Plutoniumbombe einem Testlauf unterzogen werden. Damit begann der Bau des bis dahin größten Labors unter freiem Himmel am „Alamogoro Bombing Range“ jenem Teil der Wüste der schon dem Militär gehörte. Straßen, Bunker, Forschungsgebäude und ein 30 m hoher Turm aus Stahl wurden am Detonationsort errichtet. Am 6. Juli 1945 um 5:29:45 Uhr morgens explodierte die erste Atombombe der Welt. Über 12.000 m erhob sich die pilzförmige Wolke in den Himmel. Drei Bundesstaaten weiter war das Licht der Explosion immer noch zu sehen. Der Stahlturm verdampfte vollständig, rund um den Detonationsort bildete sich ein grünliches Glas, das man später Trinitit taufte. Die Wucht der Explosion entsprach in etwa jener, die beim Einsatz von 19 Kilotonnen TNT entstehen würde. Ein Krater von 2.9 m Tiefe und 335 m Breite entstand. Das Glas der Trinitite ist meist SiO_2 -reich mit über 70 Gew.%, jedoch in Bereichen mit hohen ZrO_2 Konzentrationen bis zu 15 Gew.% sind die Gläser auch SiO_2 ärmer (ca. 56 Gew.% SiO_2). Zr-reiche Schlieren sind im Glas recht häufig anzutreffen. Die CaO Gehalte sind auch variabel zwischen 4 und 14 Gew.%. Die Zusammensetzung variiert stark je nach Art der Domäne in der das Glas gebildet wurde. Viele Quarze sind nicht vollständig aufgeschmolzen und bleiben reliktisch zurück. Häufig ist jedoch das Zirkinoxid Baddeleyit (ZrO_2) zu finden, dass als Ansammlung weißer Kugelchen in Zr-reichen Schlieren auftritt. Ab einer Temperatur von 1680 °C ist Zirkon nicht mehr stabil und er zerfällt in seine Oxide ZrO_2 und SiO_2 , wobei es sich hier um ein SiO_2 -Glas handelt. In einem Bereich findet sich sogar noch ein vollständiger Zirkon, der am Rand von einem massigen Baddeleyit-Saum umgeben ist. Dieser Bereich wurde auch Raman-spektroskopisch untersucht um mögliche Aussagen über verschiedene ZrO_2 Modifikationen (monoklin vs. tetragonal) zu treffen. Vorläufige Mikrosondenanalysen aus diesem Bereich lassen auch auf mehrere Zr-Si-O Verbindungen in diesem Saum schliessen. Die Anwesenheit von weit mehr Baddeleyit als Zirkon lässt darauf schließen, dass die Temperatur weit über 1680-1770 °C gestiegen sein musste, wobei in der Literatur ca. 5000 °C angegeben werden (HERMES & STRICKFADEN, 2005).

HERMES, R.E., STRICKFADEN, W.B. (2005): Nuclear Weapons Journal, 2 (LALP-5-067).

PETROGRAPHISCHE UNTERSUCHUNGEN PRÄHISTORISCHER (END-NEOLITHIKUM-SPÄTBRONZEZEIT) KERAMIK VOM KIECHLBERG

Tropper, P¹, Trauner, S.¹ & Töchterle, U.²

¹Institut für Mineralogie und Petrographie, Universität Innsbruck, Innrain 52, A-6020 Innsbruck, Österreich

²Institut für Archäologien, Universität Innsbruck, Langer Weg 11, A-6020 Innsbruck, Österreich

e-mail: peter.tropper@uibk.ac.at

Die Untersuchungen an keramischem Material, das lange Zeit die Bodenlagerung unbeschadet übersteht und meist in großen Mengen gefunden wird, nehmen einen bedeutenden Anteil der archäologischen Forschungstätigkeit ein. Bei entsprechender Materialeignung und ausreichender Probenmenge gibt es eine Fülle von Fragen im Umfeld archäologischer Forschung die sich mit der mineralogischen Analyse von Keramik-Dünnenschliffen klären lassen:

- Technologie der Keramikherstellung, Aussagen über Brenntemperatur.
- Geographische Herkunft des keramischen Rohmaterials.
- Vergleich räumlich getrennt aufgefunder, aber formenkundlich vergleichbarer Objekte.
- Trennung lokaler Ware von Importen.
- Werkstättenzuweisung nach qualitativen und quantitativen Keramikmerkmalen.
- Nachweis technologischer Kontinuität oder Diskontinuität über kulturelle Grenzen

Der Kiechlberg bei Thaur (Tirol) ist seit 2007 im Rahmen des Spezialforschungsprogramms HiMAT (History of Mining Activities in the Tyrol and Adjacent Areas) Gegenstand umfassender archäologischer Untersuchungen. Die vorliegende Untersuchung befasst sich mit der petrographischen Untersuchung von 23 dort gefundenen Keramikfragmenten. Laut der stilistischen Gliederung konnten die Proben in drei typologische Hauptgruppen unterschieden werden: bayrisch, südalpin (trientinisch) und lokal. Ziel dieser Arbeit war es, herauszuarbeiten, welche petrographischen Charakteristika die Keramiken aufweisen und ob diese mit lokalen Magerungsmaterialien hergestellt, oder importiert wurden. Es konnte festgestellt werden, dass 1.) sich die südbayrischen sowie die trientinischen Keramikscherben deutlich von den lokalen unterscheiden und 2.) dass in allen drei Gruppen Keramikfragmente wieder-verwertet wurden. Laut 1.) ist ein Import somit wahrscheinlich. Ohne weitreichendere chemische Untersuchungen, sowie vergleichende Untersuchungen von lokalen, trientinischen und südbayrischen Keramikfragmenten können diese Aussagen jedoch noch nicht mit Sicherheit getätigert werden. In einer Keramikprobe, die als Schmelztiegel diente, wurden Schlackenreste gefunden, welche mittels Elektronenstrahlmikrosonde untersucht wurden. Die Schlacken bestehen aus Olivinen, Klinopyroxenen sowie Fe-reichem Glas. Auffallend ist, dass die einzelnen Minerale größere Mengen von Zn einbauen. Eine Verhüttung von Zn-hältigen Erzen (Kupferkies + Zinkblende?) ist wahrscheinlich. Weiters wurde eine weiße Inkrustierungsmasse aus einer Dekoration in einer Keramikprobe untersucht. Die Analyse mittels Raman-Spektroskopie ergab, dass es sich um Hydroxyl-Apatit handelt. Es wurde hier also Knochenmaterial zermahlen und als Paste in die Ritzungen eingepresst.

MINERALOGIE UND PETROLOGIE EXPERIMENTELL ERZEUGTER PSEUDOFULGURITE

Tropper, P.¹, Volgger, A.¹, Pasker, J.² & Fickert, L.²

¹Institut für Mineralogie und Petrographie, Universität Innsbruck, Innrain 52f, A-6020 Innsbruck, Österreich

² Institut für elektrische Anlagen, Technische Universität Graz, Inffeldgasse 18/1, A-8010 Graz, Österreich

e-mail: peter.tropper@uibk.ac.at

Fulgarite sind sehr seltene, röhrenförmige und glasige Naturphänomene, die durch die extreme Hitze eines Blitzschlages entstehen können. Ein Gestein, das durch einen Erdschluss einer Hochspannungsleitung und der damit verbundenen Aufheizung des Bodens entstanden ist, nennt man einen Pseudofulgurit. Dessen Entstehung setzt eine entsprechend lange Einwirkungsdauer des Erdenschlusses und eine entsprechend große Wärmeentwicklung voraus: Ein Erdenschluss stellt in einem kompensiert betriebenen Netz, dessen Erdfehlerstrom kleiner als die Löschgrenze ist, einen erlaubten Betriebszustand dar. Da darüber hinaus im Erdenschlussfall die Versorgung der Stromabnehmer mit elektrischer Energie erhalten bleibt, kann man in einem ländlichen Netz hinsichtlich der Erdenschluss-Einwirkungsdauer von einer Zeitspanne in der Größenordnung von einer halben Stunde bis zu zwei Stunden ausgehen. Da hierbei durch die Wirkungsweise der Parallelschaltung von Leiter-Erde-Kapazität des Netzes und Petersenspulen-Induktivität der Erdenschlussstrom begrenzt ist und das Netz somit eine Stromquellen-Charakteristik aufweist, ist die Freisetzung von thermischer Energie an der Fehlerstelle, also die elektrische Leistung, i. W. nur vom Übergangswiderstand zwischen Leiter(-seil) und Erde abhängig. Messungen dieses Widerstandes haben typische Werte im Bereich von 100 Ohm ergeben, womit sich durch einen mit 50 A angenommenen Erdenschlussstrom eine thermische Leistung im Bereich von 250 kW ergibt. Bedingt durch die schlechte Wärmeleitfähigkeit des Erdbodens ergeben sich unter Einbeziehung der spezifischen Wärmekapazität in der Umgebung der Fehlerstelle beträchtliche Endtemperaturen des Erdbodens.

Am 16. 10. 2012 wurden gemeinsam vom Institut für elektrische Anlagen der TU Graz und der KELAG in Obervellach (Kärnten) experimentelle Untersuchungen über Erdschlüsse durchgeführt. Die Versuche wurden mittels am Boden liegendem Leiterseil bei 5-15 A und ca. 11500 V durchgeführt. Im Fehlerfall bricht diese Spannung auf 1000 V ein und der Strom geht auf 5 A zurück. Im Zuge des Erdenschlusses kam es zur Bildung von glasigen Aggregaten, den Pseudofulguriten.

Im Rahmen dieser Untersuchungen sollen Limits für die petrologischen Entstehungsbedingungen (Temperatur, T , Sauerstoffpartialdruck, fO_2) dieser Pseudofulgurite abgeschätzt werden. Dazu wird eine petrographische und mineralchemische Beschreibung des Pseudofulgurits mittels Polarisationsmikroskopie, der Elektronenstrahlmikrosonde und dem Raman-Spektrometer durchgeführt. Der Mineralbestand des Bodens ist Granat + Plagioklas + K-Feldspat + Muskovit + Quarz + Rutil + Apatit + Zirkon + Pyrit. Durch die starke Pyrometamorphose entstanden Glas + Baddeleyit + Fe/Fe-Si-S Tröpfchen + Spinell. Speziell die Umwandlung von Zirkon zu Baddeleyit + Glas lässt auf extrem hohe Temperaturen von >1600 °C schliessen.

CONTENT OF CHALCOPHILE ELEMENTS IN LAKE KALIMANCI SURFACE SEDIMENTS (REPUBLIC OF MACEDONIA)

Vrhovnik, P¹, Rogan Šmuc, N.¹, Dolenec, T.¹, Serafimovski, T², Tasev, G.² & Dolenec, M.¹

¹Faculty of Natural Sciences and Engineering, University of Ljubljana, Department of Geology,
Aškerčeva cesta 12, 1000 Ljubljana, Slovenia

² Faculty of Mining, Geology and Polytechnics, University "Goce Delčev-Štip", Goce Delčev 89,
2000 Štip, Macedonia
e-mail: petra.vrhovnik@gmail.com

In present study we examine the chalcophile element contents in Kalimanci Lake surface sediments (eastern Macedonia). The mineral composition of surficial lake sediments is dominated by quartz, plagioclases (albite, anorthite), phengite, clinochlore, K-feldspars, illite and muscovite. Lake Kalimanci occasionally also contains calcite, sphalerite, epidote, gypsum, clinopyroxenes, olivine and pyrite which in some cases contain As. Geochemical investigation revealed high concentrations of chalcophile elements in surficial lake sediments with average values [mg kg⁻¹]: Ga 21.13, Cu 415.1, Pb 6059, Zn 8420, As 67.7, Cd 56.6, Sb 1.77, Bi 10.1 and Ag 5.58. Furthermore correlation analysis was applied among studied chalcophile elements and major elements. The results show high positive correlations ($0.45 < r > 0.89$, $0.01 < p > 0.00$) of Ca and Mg with all chalcophile elements. Meanwhile other major elements have lower negative correlations with chalcophile elements. Furthermore, enrichment factor (EF) was also calculated to explain the origin of studied chalcophile elements and their pollution intensity. EF mean values follows as listed: Ga 1.26, Cu 17.02, Pb 312.86, Zn 121.08, As 46.92, Cd 0.59, Sb 9.27, Bi 0.08 and Ag 0.12. Regarding to calculated EF it can be concluded that Cu, Pb, Zn and As have anthropogenic origin (from nearby active Pb-Zn mine), meanwhile others originate from the background rocks.

JOANNEUMITE, Cu(C₃N₃O₃H₂)₂(NH₃)₂, A NEW MINERAL SPECIES WITH AMMINE AND ISOCYANURATE GROUPS

Walter, F¹ & Bojar, H.-P²

¹Institute of Earth Sciences, University of Graz, Universitätsplatz 2, 8010 Graz, Austria

²Department of Geosciences, Universalmuseum Joanneum, Weinzötlstraße 16, 8045 Graz, Austria

e-mail: franz.walter@uni-graz.at

The new mineral joanneumite was found at Calleta Pabellon de Pica, Tarapaca region, Chile. Joanneumite occurs as spherical aggregates of hypidiomorphic, mm-sized violet crystals associated with salammoniac, dittmarite, aphthitalite and brushite. The mineral (IMA 2012-001) is named for the 200th anniversary of the foundation of the Universalmuseum Joanneum. Joanneumite is triclinic, space group $P\bar{1}$, $a = 4.982(1)$, $b = 6.896(1)$, $c = 9.115(2)$ Å, $\alpha = 90.53(3)$, $\beta = 97.85(3)$, $\gamma = 110.08(3)$ °, $V = 290.8(1)$ Å³, $Z = 1$ (at 100 K).

The chemical composition, X-ray powder- and FTIR-data of joanneumite and the synthetic bis(isocyanurato)diammine-copper(II) are identic. Due to the lack of suitable natural crystals, single crystal structure refinement was done with synthetic joanneumite, which crystallized from the melt of Cu(II) chloride dihydrate and urea. The crystal structure was solved with direct methods (program SHELXS). Least-squares refinement using anisotropic displacement parameters for all non-hydrogen atoms was carried out with the program SHELXL97 (SHELDRICK, 2008) and yielded $R1 = 0.024$ for 1153 unique reflections with $F_o > 4\sigma(F_o)$.

The basic structural unit in the joanneumite structure is similar to that of ammineite, CuCl₂(NH₃)₂, (BOJAR et al., 2010). The two chlorine atoms of ammineite are replaced by two isocyanurate groups in the joanneumite structure (Fig. 1a-c). The copper centre has distorted square-planar coordination and the Cu(C₃N₃O₃H₂)₂(NH₃)₂ molecules are cross-linked by hydrogen bonds from 1.92 to 2.31 Å, forming a three dimensional network (Fig. 1d) with good cleavage parallel (010).

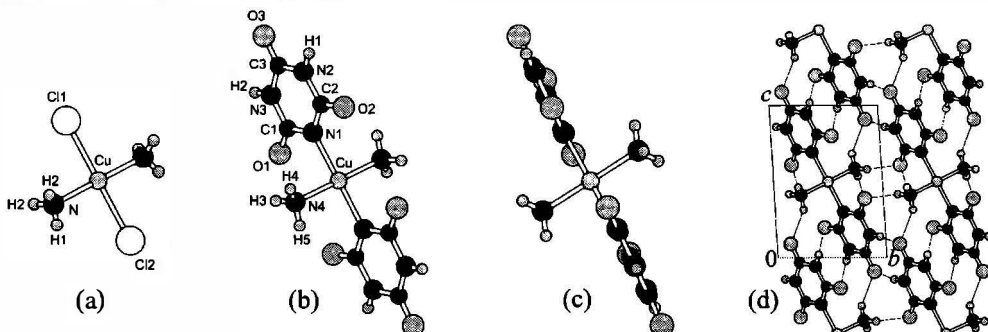


Figure 1. The basic structural units of ammineite (a), joanneumite (b, c) and the crystal structure of joanneumite with outlined hydrogen bonds (single lines), view along [100] (d).

COLOUR ENHANCEMENT OF RATANAKIRI (CAMBODIA) GEM ZIRCON

Wittwer, A.¹, Nasdala, L.¹, Wildner, M.¹, Wanthanachaisaeng, B.²,
Bunnag, N.² & Giester, G.¹

¹Institut für Mineralogie und Kristallographie, Universität Wien, Althanstraße 14, 1090 Wien, Austria

²Faculty of Gems, Burapha University, Chanthaburi 22170, Thailand

e-mail: a.wittwer@gmx.at

Gem zircon from the Ratanakiri province, Northeastern Cambodia, is famous for its particularly rich blue colouration (BALMER et al., 2011). The blue colour is however not natural but produced only by dry heating of initially brown to reddish brown stones at ca. 1000 °C under reducing conditions for several hours. We present first results of a study of the Ratanakiri zircon that focuses on its mineralogical characterisation and possible causes of the colour change. Gem-quality zircon specimens (6–19 mm in size) were oriented using a single-crystal X-ray diffractometer, and pairs of doubly polished slabs were produced. One slab each was subjected to heat treatment. Raman, luminescence and X-ray analyses on natural and heated slabs did not yield significant differences, indicating that the Ratanakiri zircon has accumulated negligible amounts of radiation damage. The brown colour of the natural material is due to a combination of broad absorption bands near 20500 and 12000 cm⁻¹ and an intense absorption edge extending into the blue region. After heating, the absorption is less intense and dominated by a newly formed, pleochroic colour centre near 15500 cm⁻¹.

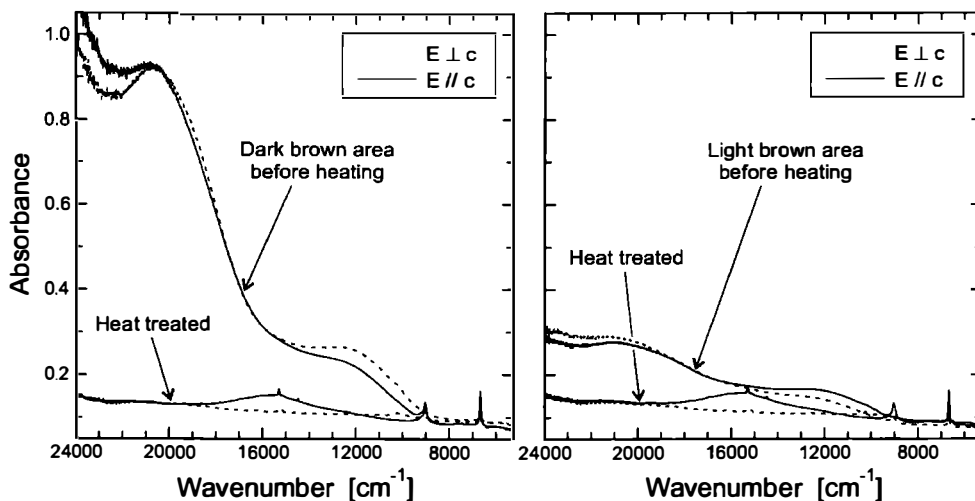


Figure 1. Optical absorption spectra for two zones in one oriented zircon slab (left, intensely coloured area; right, light area), obtained before and after heat treatment.

BALMER, W.A., SMITH, M.H., SRIPRASERT, B., WAN THANACHAISAENG, B. (2011): Ratanakiri, the legendary zircon province of Cambodia. Abstracts of GIA's 46th Gemstone Gathering, Bangkok, Thailand, May 25, 2011.

**EXPERIMENTAL CONSTRAINTS ON THE PERMIAN CONTACT
METAMORPHIC EVENT IN METAPELITES FROM THE SOUTHERN RIM OF
THE BRIXEN GRANODIORITE (SOUTH TYROL, ITALY)**

Wyhildal, S.¹ & Tropper, P²

¹AIT, Austrian Institute of Technology, Konrad Lorenz Straße 24, 3430 Tulln/Donau, Austria

²Institut für Mineralogie und Petrographie, Universität Innsbruck, Innrain 52f, A-6020 Innsbruck, Österreich

e-mail: peter.tropper@uibk.ac.at

e-mail: stefan.wyhildal@ait.ac.at

The Permian Brixen Granodiorite is located south of the Periadriatic Lineament in the eastern part of the Southalpine basement complex and comprises a series of tonalitic, granitic and granodioritic intrusions which were emplaced during the Permian into the country rocks of the Variscan Brixen Quarzphyllites. The depth of the intrusion was less than 10 km ($P \leq 0.3$ GPa) and only a small, about 200 meters wide, contact aureole formed at the southern rim of the Brixen Granodiorite near the village Franzensfeste and yielded an increase in temperatures from 540 °C in the outermost aureole to > 700 °C in the innermost aureole. Within the contact aureole four different zones can be distinguished based upon mineralogical, mineral chemical and textural features. Approximately 200 m from the granite contact zone I occurs. The rocks from this zone are macroscopically still quartzphyllites and are characterized by two texturally and chemically different generations of micas and the appearance of cordierite. Zone II is characterized by quartzphyllites containing pseudomorphs of cordierite + biotite after garnet. The inner contact aureole starts approximately 50 m from the granite contact and shows already typical hornfels textures. This zone is characterized by the first occurrence of andalusite. In the innermost area, ca. 10 m from the granite contact, spinel and corundum occur. Geothermometry (two-feldspar, Ti-in-biotite) yielded an increase in temperature from 540 °C in the outermost aureole to < 740 °C in the innermost aureole.

In order to put additional constraints on the metamorphic overprint besides geothermobarometric investigations, the aim of this investigation was to compare natural mineral assemblages and mineral compositions from the highest grade zones of the hornfelses at the southern rim of the Brixen granodiorite with mineral assemblages which are produced experimentally at approximately the same P - T conditions, using the same starting materials. Experiments were performed in a hydrothermal apparatus at 0.3 GPa and temperatures of 580 °C and 650 °C using two natural quartzphyllite samples from the area as starting materials. At a temperature of 650 °C the amount of H₂O present varied from 0 µl to 5 µl H₂O and newly formed cordierite and biotite were observed in all run products. At H₂O = 5 µl, wide-spread melting occurs and K-feldspar, plagioclase, aluminosilicate and melt occur in addition. The agreement between the observed textures and mineral compositions therefore allows putting additional constraints on the T conditions of this contact metamorphic event.

WYHLIDAL, S., W. F. THÖNY, W. F., TROPPER, P., KAINDL, R., HAUZENBERGER, C., MAIR, V. (2012): Mineralogy and Petrology, 106, 173-191.

**REE-KARBONATE IN DER DIORITISCHEN INTRUSIONSBREKZIE BEI
SCHRAMMBACH (SÜDTIROL/ITALIEN): INDIKATOR FÜR TIEFTEMPERIERTE
REE MOBILISATION**

Zöll, K., Tropper, P & Haefeker, U.

Institut für Mineralogie und Petrographie, Universität Innsbruck, Innrain 52f, A-6020 Innsbruck, Österreich
e-mail: peter.tropper@uibk.ac.at

Ziel dieser Untersuchung ist die petrologische Bearbeitung der Kontaktaureole zwischen der permischen Dioritinvasion (Lokalename Klausenit) und dem grünschieferfaziellen Brixner Quarzphyllit, bei Schrammbach im Südtiroler Eisacktal (I). Eine lateral stark ausgeprägte Aureole ist nach ersten Felduntersuchungen nicht auszumachen. Trotzdem ist der Kontaktbereich deutlich ersichtlich. Der Randbereich ist durch das Auftreten einer Intrusionsbrekzie gekennzeichnet. In dieser Brekzie sind sowohl Komponenten des Quarzphyllites und von Quarziten als auch dioritische Gesteinsbruchstücke aufgearbeitet. Die Bruchstücke sind höchst variabel in ihrer Größe, sie reichen von wenigen hundert µm bis zu mehreren dm. Im Dünnschliff ersichtlich kam es teilweise zum postdeformativen Überwachsen der Komponenten mit Chlorit-Turmalinsäumen. Die Matrix besteht hauptsächlich aus graugrünem, feinkörnigem stark zersetzen Diorit, der vorwiegend aus Plagioklas und reliktischem Klinopyroxen besteht. Quarz tritt untergeordnet überwiegend als Zwickelfüllungen auf. Nach der kontaktmetamorphen Überprägung kam es zu einer alpidischen (?) Alteration der Gesteine durch die Villnößer Störung. Die gesamten Aufschlüsse liegen nämlich in den westlichen Ausläufern des Störungssystems. Es kam in Verbindung mit dieser Störung zu einer späten Mobilisierung von Fluidphasen, welche zur Alterierung des primären Mineralbestandes führte. Dabei wurde vor allem der Plagioklas weitgehend zersetzt. Das ursprüngliche magmatische Gefüge blieb jedoch, gut sichtbar, erhalten. Gleichzeitig kam es zu einer ausgeprägten Remobilisierung von seltenen Erden, die zur Bildung von REE-hältigem Karbonat führte. Dieses konnte mittels Ramanspektroskopie eindeutig als Synchisit identifiziert werden.

Beim pseudohexagonalen Synchisit handelt es sich um ein REE-Karbonat mit der Formel $\text{Ca}(\text{REE})(\text{CO}_3)_2\text{F}$ das in sein Kristallgitter vorwiegend Ce, La und Nd einbaut. Weiters konnten mittels Elektronenstrahlmikroskopie erhöhte Gehalte von Y, Pr, Sm, Eu und Gd nachgewiesen werden. Synchisite treten hauptsächlich als tieftemperierte, spät-hydrothermale Bildungen in Graniten und Syeniten auf und daher wurden die REE wahrscheinlich durch Interaktion eines $\text{F}-\text{CO}_2-\text{Ca}$ -reichen Fluides möglicherweise spätalpidisch mobilisiert.

ALPHABETICAL LISTING OF CONTRIBUTORS

Abart R.	31, 45, 86, 113, 125, 127
Abu-Alam T.S.	32, 100
Ackerman L.	99
Aldrian A.	67
Arehart G.	39
Artac A.	33
Ashchepkov I.	42, 104
Aßbichler D.	34
Asseva A.	104
Auzinger T.	63
Azimzadeh A.M.	35
Baldermann A.	36, 57, 97, 130, 135
Bakker R.	49
Bauer C.	37
Baumgartner M.	49
Bechtold A.	38
Benischke R.	115
Benkó Zs.	39, 120
Beran A.	132
Berninger U.-N.	40
Beukes J.J.	41
Bjerg E.A.	76, 99, 108, 111
Blaß G.	75
Blümel A.	42
Böttcher M.E.	43, 57, 115
Bojar H.-P.	44, 147
Bojar A.-V.	44
Bourgin N.	45
Brandl M.	46
Brandstätter F.	47
Braunhofer D.	142
Buda Gy.	71
Bunnag N.	148
Cesare B.	15
Chakraborty S.	98
Cícha J.	131
Ciriotti M.E.	75
Čopjaková R.	48, 117, 128, 131
Czyzykiewicz P.	67
Daneu N.	58
Daxner G.	115
Deditius A.P.	130

Dietzel M.	36, 57, 66, 97, 107, 115, 119, 121, 124, 126, 130, 135
Dódony I.	109
Dohmen R.	98
Dolenec M.	146
Dolenec T.	58, 146
Doppler G.	49
Đorđević T.	50
Eberlei T.	51
Effenberger H.	52
Ertl A.	53
Ferrière L.	47
Fickert L.	145
Fischer R.	70, 135
Frank-Kamenetskaya O.V.	53
Frei D.	54
Fritz H.	94
Fröschl H.	62
Fuchs M.R.	84, 85
Fügenschuh B.	79
Gadas P.	103
Gasteiger P.	55
Gauert C.D.K.	41
Ghorbani M.	35
Gier S.	62
Giester G.	53, 74, 116, 148
Girtler D.	56
Gobba J.	91
Grathoff G.H.	36
Gregoire M.	42, 111
Grengg C.	57
Grießhaber E.	28
Grom N.	58
Hejny C.	65
Habler G.	51, 125
Haefeker U.	55, 59, 60, 61, 84, 85, 134, 141, 142, 150
Hałas S.	44
Haslinger E.	62
Hassan M.	32
Hauck S.	39, 120
Hauenberger C.A.	46, 56, 63, 78, 79, 90, 91, 93, 99, 100, 104, 114, 133, 139
Hegner E.	72
Heinisch M.	64
Hejny C.	65
Hoad O.	37
Hoang N.	63

Höllen D.	66, 67, 121
Hoinkes G.	64, 118
Houzar S.	68
Hosseinzadeh G.	35
Hrazdil V.	68
Jakopic G.	70
Janisch A.	69
Jerabek P.	31
Jordan G.	28, 40
Jurnanne R.	91
Kadi K.	32
Kadlec T.	103
Kahlenberg V.	61, 84, 85, , 89, 92, 134
Kaindl R.	59, 60, 61, 70
Karásek J.	117
Kelm K.	28
Kennedy A.K.	101
Khoi N.N.	63
Kis A.	71
Klanuner D.	66, 97
Kleindl R.	72
Klötzli U.	73, 80, 106, 110
Koeberl C.	47
Köhler S.J.	121
Kolitsch U.	74, 75, 105
Koller F.	62
Konopelko D.	72
Konrad F.	77
Konrad L.	78
Konzett J.	47, 60, 63, 65, 78, 79, 90, 91, 133
Kolosova-Satlberger O.	76
Kostrovitsky S.	101
Koutsovitis P.	104
Kovaleva E.	73, 80
Kozlik M.	81
Krenn K.	37, 64, 94, 108
Krismar M.	82, 83
Krüger H.	19, 61, 84, 85
Krumpel G.	37
Kuleci H.	86
Kurz W.	94, 114
Lenz C.	88
Leis A.	57, 97, 115, 126, 130, 135
Leitner T.	87
Lengauer C.L.	105, 116

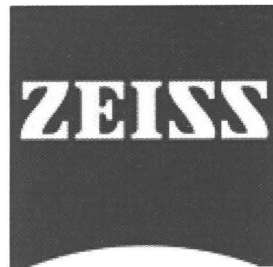
Letofsky-Papst I.	66
Libowitzky E.	52
Linner M.	136
Loerting T.	96
Losos Z.	117, 131, 132
Ludwig T.	53
Mader D.	47
Maier B.	28
Maier M.	89
Mair P.	90
Mandl M.	91
Manninger T.	92
McCleaf P.	121
Melcher F.	79
Meyer M.	72
Meyer H.-P.	53
Micheuz P.	64, 94
Michálek M.	93
Miletich R.	21, 33, 52, 96
Mirwald P.W.	95, 96
Mittermayr F.	57, 97, 135
Moayyed M.	35
Mogessie A.	39, 108, 120
Molnár F.	22, 39, 120
Müller T.	98
Mundil R.	79
Mundl A.	69, 99
Nasdala L.	88, 101, 148
Nantasin P.	100
Nestola F.	33
Neuser R.D.	129
Nickel C.	102
Niedermayr A.	119
Novák M.	103, 128
Nguyen H.	91
Ntaflos T.	42, 69, 76, 99, 104, 111
Oberwandler L.	105
Oelkers E.H.	40
Österle J.	106, 110
Onuk P.	107, 108
Olieric V.	84, 85
Orlova M.	61
Ormándi S.	109
Ottner F.	62
Paar W.H.	87

Palzer M.	106, 110
Papadopoulou M.	111
Pascual J.	37
Pasker J.	145
Pertlik F.	112
Petrakakis C.	45
Petrishcheva E.	113, 125
Pfingstl S.	114
Pichler J.	70
Pippinger T.	33
Pomberger R.	67
Pomella H.	136
Postl W.	27, 46
Poulson S.	39
Praschl S.	115
Prikhodko V.S.	42
Pristacz. H.	105, 116
Prokop J.	117
Proyer A.	34, 118
Puhr B.	118
Pupp M.	142, 143
Purgstaller B.	119
Putiš	93
Raič S.	39, 120
Raith J.G.	67, 81, 87
Rauschenbach J.	121
Rečnik A.	58
Redhammer G.J.	33, 122, 123
Rhede D.	125
Richoz S.	100
Rieck B.	116
Rinder T.	124
Rogan Šmuc N.	146
Rogers N.	37
Rollinger B.	37
Roth G.	123
Rozhdestvenskaya I.V.	53
Samardžija Z.	58
Sarc R.	67
Schaeffer A.-K.	113, 125
Schafer E.	127
Schnahl W.W.	28
Schmidmair D.	134
Schmidt C.	86
Schneider P.	142

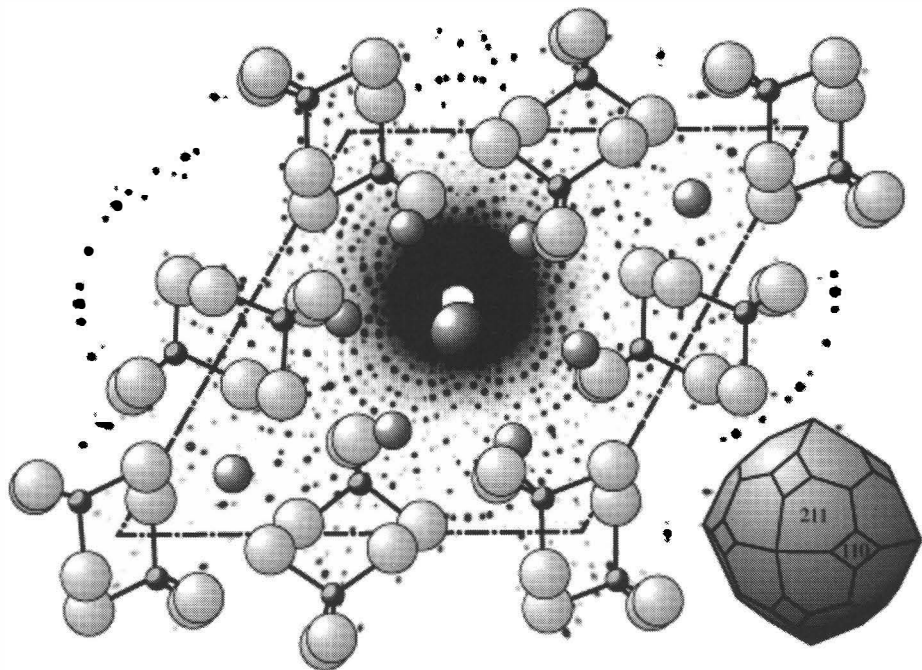
Schneider T.	79
Schön W.	126
Schott J.	40
Schramm M.	115
Schubernig M.	67
Schuster R.	51, 114, 118, 127
Senyshyn A.	123
Serafimovski T.	146
Severson M.	39, 120
Škoda R.	48, 128, 132
Spielmann M.	140
Švecová E.	131
Stalder R.	77, 129
Stickler C.P.	130
Stüwe K.	32
Taferner H.	133
Talla D.	132
Tasev G.	146
Tessadri R.	55, 77, 134, 143
Thaller D.	135
Thome V.	89
Thöni M.	51
Tippelt G.	122, 123
Többens D.	84
Töchterle U.	144
Toman J.	68
Trauner S.	144
Tribus M.	85, 136
Trnka G.	46
Troitzsch U.	84
Tropper P.	55, 56, 59, 60, 61, 64, 82, 83, 84, 85
Tropper P.	136, 137, 138, 139, 140, 141, 142, 143, 144, 145, 149, 150
Váczi T.	71
Vašinová Galiová M.	48
Vereshchagin O.S.	53
Vrhovnik P.	58, 146
Volgger A.	145
Waldhauser W.	70
Walter F.	147
Wanthanachaisaeng B.	148
Warr L.N.	36, 102
Wathanakul P.	100
Weiszburg T.G.	71
Wildner M.	38, 132, 148
Williams C.T.	62

Wikete C.	85
Wittwer A.	148
Wojtowicz A.	44
Wyhlidal S.	141, 149
Zaefferer S.	125
Zeug M.	101
Ziegler A.	28
Zirbs W.	112
Zöll K.	150

MINPET 2013 SPONSORS



ORIGINALARBEITEN
ORIGINAL PAPERS



**ANWENDUNG DES Zr-IN-RUTIL GEOTHERMOMETERS IN PYROPQUARZITEN
DES UHP DORA MAIRA MASSIVES (PIEMONTE, ITALIEN)**

von

Daniel Dutzler & Peter Tropper

Institut für Mineralogie und Petrographie
Universität Innsbruck, Innrain 52f, A-6020 Innsbruck, Österreich

Abstract

In this investigation, the Zr-in-rutile geothermometer was applied to the pyropquartzites from the Dora Maira Massif in the Western Alps (Piemont, Italy). These rocks contain the following mineral assemblage: kyanite + pyrope + talc + chlorite + quartz/coesite ± jadeite ± phengite which was metamorphosed under P-T conditions of $>750^{\circ}\text{C}$ and $>3\text{ GPa}$. Optimized electron microprobe measurements yielded Zr contents in rutile inclusions in pyrope ranging from 121 to 173 ppm. Application of the calibrations of ZACK et al. (2004), FERRY & WATSON (2007) and WATSON et al. (2006) yielded temperatures between $620\text{--}669^{\circ}\text{C}$. These results are approximately 100°C lower than the temperatures obtained from conventional geothermobarometry (SCHERTL et al., 1991). Application of the calibration of DEGELING (2002), which contains a pressure correction yields temperatures between 760 and 780°C which are in very good agreement with the data from conventional geothermometry. Application of the calibration of TOMKINS et al. (2007) which was specifically designed for coesite-bearing assemblages results interestingly in lower temperatures of $670\text{--}690^{\circ}\text{C}$. Although this discrepancy is not resolved yet, it shows that application of this geothermometer to UHP rocks only yields consistent results if a pressure correction is applied.

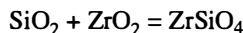
Zusammenfassung

Im Zuge dieser Untersuchung wurde das Zr-in-Rutil Geothermometer an den Pyropquartziten des Dora Maira Massives in den Westalpen (Piemont, Italien) angewendet. Bei diesen Gesteinen handelt es um Metaquarzite mit der Mineralparagenese Kyanit + Phengit + Pyrop + Talk + Chlorit + Quarz/Coesit ± Jadeit, die eine Metamorphose mit Temperaturen von $>750^{\circ}\text{C}$ und Drucken von $>3\text{ GPa}$ durchlaufen haben. Optimierte Messbedingungen an der Mikrosonde ergaben Zr Gehalte in den Rutileinschlüssen in Pyropen zwischen 121 und 173 ppm. Die erhaltenen Temperaturen mittels der Kalibrationen von ZACK et al. (2004), FERRY & WATSON (2007) und WATSON et al. (2006) schwanken zwischen $620\text{--}669^{\circ}\text{C}$, was jedoch um ca. 100°C niedriger als die Metamorphosetemperatur ist (SCHERTL et al., 1991).

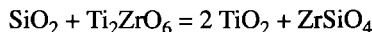
Verwendet man jedoch die Kalibration nach DEGELING (2002), die eine Druckkorrektur ermittelte, so ergeben sich Temperaturen zwischen 760 und 780°C, welche mit den Literaturangaben sehr gut übereinstimmen. Die Anwendung der Druckkorrektur von TOMKINS et al. (2007) für Rutile im Coesit-Stabilitätsfeld ergab interessanterweise niedrigere Temperaturen von 670-690°C. Obwohl die Diskrepanz zwischen den beiden Kalibrationen noch unklar ist, zeigt dieses Beispiel deutlich, dass dieses Geothermometer stark druckabhängig ist.

Einführung

In der Geothermobarometrie ist mit dem vermehrten Aufkommen der Spurenelementanalyse ein großes Interesse an der Spurenelementsystematik von metamorphen Mineralen wie Monazit und Xenotim entstanden (HEINRICH et al., 1997; PYLE et al., 2001). In diesem Zusammenhang wurde auch die Spurenelementzusammensetzung des Minerale Rutil genauer untersucht. Rutil (TiO_2) baut neben den Elementen Ti und O auch noch Zr, Nb, Mo, Sn, Sb, Hf, Ta, W ein. ZACK et al. (2004) untersuchten dabei die Systematik des Zr-Einbaus in Rutil. Dabei wurde festgestellt, dass der Zr-Gehalt stark temperaturabhängig ist. Die Bufferung des Zr-Gehaltes des Rutils, der mit Quarz und Zirkon koexistiert, kann durch folgende Modellreaktion beschrieben werden:



Jedoch sind Quarz und Baddeleyit (ZrO_2) inkompatibel und daher ist noch eine andere Zr-Phase in dem System SiO_2 - ZrO_2 - TiO_2 stabil, nämlich Srilankit (Ti_2ZrO_6 , WILLGALLIS et al., 1983) und es kann daher eine weitere Modellreaktion aufgestellt werden:



Diese Reaktion ist nun für den Zr Einbau im Rutil welcher mit Quarz und Zirkon koexistiert verantwortlich. Mittlerweile gibt es auch mehrere experimentelle Kalibrationen dieses Geothermometers (z.B. DEGELING, 2002; WATSON et al., 2006; FERRY & WATSON, 2007; TOMKINS et al., 2007). Es ist das Ziel dieser Arbeit diese unterschiedlichen Kalibrationen an Rutilen aus den UHP Gesteinen des Dora Maira Massivs anzuwenden und zu vergleichen, wie es bereits in UHP Gesteinen aus W-China durchgeführt wurde (ZHANG et al., 2010).

Geologischer Überblick

Das Dora Maira Massiv befindet sich an der inneren Seite des westlichen Alpenbogens und erstreckt sich über max. 70 km vom Val Susa im Norden, bis ins Val Maira im Süden. Das Dora Maira Massiv ist zusammen mit der Monte Rosa und der Gran Paradiso Einheit, Teil der inneren penninischen Zone und bildet den südöstlichen Rand der europäischen Kontinentalplatte, bzw. auch kontinentale Bruchstücke innerhalb des penninischen Ozeans (DAL PIAZ & LOMBARDO, 1986).

Das Dora Maira Massiv weist einen internen Aufbau aus drei Haupteinheiten auf; der Pinerolo, der Venasca und der Dronero Einheit welche unterschiedliche starke Metamorphosen durchlaufen haben. Die Venasca Einheit ist in zwei Untereinheiten geteilt, welche die „heisse“ Coesit-Eklogiteinheit und die „kalte“ Eklogiteinheit genannt werden (CHOPIN et al., 1991).

Diese „heisse“ Coesit- Eklogiteinheit beinhaltet die UHP (ultra-high pressure) Gesteine und ist im Wesentlichen aus zwei Gesteinstypen aufgebaut 1.) Massive Quarz-Kyanit-Granat-Phengit-schiefer mit einer Mächtigkeit von bis zu 300 m und 2.) massive Paragneise mit einer Mächtigkeit von bis zu 500 m welche die Quarz-Kyanit-Granat-Phengit Schiefer sowohl unter- als auch überlagern. Untergeordnet können auch noch Eklogite und Marmore mit den Schiefern assoziiert sein. Innerhalb der Paragneise kommen über und unterhalb der Quarz-Kyanit-Granat-Phengit-schiefer, die sog. Pyropquarze als Boudins vor. Diese Gesteine zeigen eine sehr ungewöhnliche und extrem Mg-reiche Mineralparagenese. Der Höhepunkt der Metamorphose wird bei einem Druck von >3 GPa und einer Temperatur von ca. 700-750°C angenommen. (CHOPIN, 1984; SCHERTL et al., 1991; CHOPIN et al., 1991; CHOPIN, 2003). Die Umwandlung von Quarz zu Coesit findet nämlich erst bei einem Druck \geq 2.5-2.8 GPa und bei Temperaturen von 700-800°C statt. Auch der hohe Si-Gehalt der Phengite in dieser Mineralparagenese ist ein Indikator für eine extrem druckbetonte Metamorphose von 3-3.5 GPa (SCHERTL et al., 1991). Die maximal herrschenden Temperaturen können durch das Stabilitätsfeld von Talk + Phengit begrenzt werden, welches in etwa bei 750-800°C liegt (SCHERTL et al. 1991). Die maximalen P-T Bedingungen sind demnach 3.3 ± 0.3 GPa und 750 ± 30 °C.

Analytische Messmethode

Die Konzentration von Zr im Rutil wird mittels der Elektronenstrahlmikrosonde nach der Methode von ZACK et al. (2004) gemessen. Die Analysen wurden mit einer JEOL 8100 SUPERPROBE am Institut für Mineralogie und Petrographie an der Universität Innsbruck gemessen. Jedoch wurden die Einstellungen der Mikrosonde im Vergleich zu ZACK et al. (2004) für die Messung von Zr optimiert, wodurch die Detektionslimits um den Faktor 4 von 80 ppm auf 20 ppm verbessert werden konnten. Die Beschleunigungsspannung betrug 20 kV und die gewählte Spannung betrug 120 nA bei einem Strahldurchmesser von $5\text{ }\mu\text{m}$. Ein Problem bei den Messungen, kann das eventuelle Vorhandensein von submikroskopischen Zirkoneinschlüssen sein, da diese die Zirkongehalte in die Höhe schnellen lassen, jedoch kann diese Fehlerquelle vermieden werden, indem man die gemessenen Si-Konzentrationen als Qualitätskontrolle heranzieht. Denn bei der Analyse von reinem Rutil liegt der Si-Gehalt meist unter dem Detektionslimit (< 45 ppm). Messungen bis ca. 200 ppm können toleriert werden, entweder als mögliche „wahre“ Komponenten von Rutil, oder in Folge von nahe gelegenen Silikaten. Erst Proben mit einem Si-Gehalt von mehr als 200 ppm wurden von weiteren Untersuchungen ausgeschlossen, falls der Zr-Gehalt merklich höher war, als in anderen Rutilproben.

Petrographie der Pyropquarze

Die grobkörnigen Pyropquarze haben eine Zusammensetzung der Matrix aus: Kyanit + Phengit + Quarz + Pyrop und untergeordnet Talk ± Jadeit. Als Akzessorien sind Rutil, Zirkon und Ellenbergerit sowohl in der Matrix, als auch in Form von Einschlüssen im Kyanit oder im Pyrop zu finden. Die Granat Megakristalle beinhalten neben Coesit (Abb. 1) auch die Paragenese Rutil + Zirkon + Chlorit + Talk (Abb. 2, 3) und die Paragenese Rutil + Zirkon + Chlorit + Talk + Kyanit + Ellenbergerit (Abb. 4). Die gemessenen Rutile stammen alle aus einem Pyropkristall.

Abbildung 1:

Dünnschlifffoto von Coesiteinschlüssen (*Coe*) im Pyrop (*Py*, II Nicols). Die Bildbreite beträgt 2 mm.

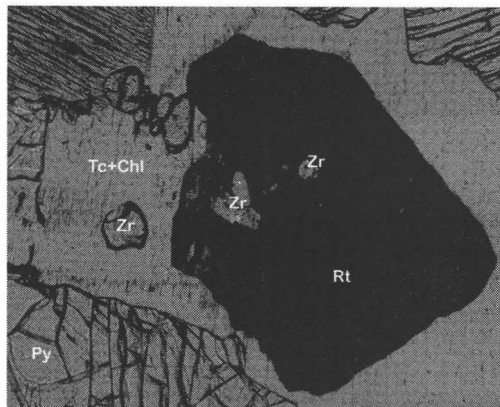
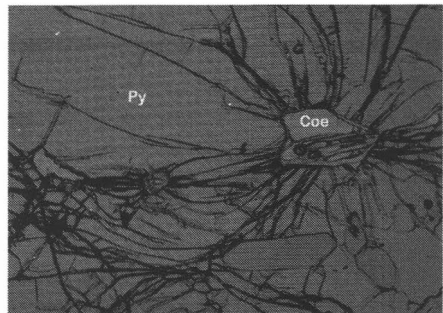


Abbildung 2:

Dünnschlifffoto von Rutil- (*Rt*), Chlorit (*Chl*), Talk (*Tc*) und Zirkon (*Zr*)-Einschlüssen im Pyrop (*Py*, II Nicols). Die Bildbreite beträgt 1 mm.

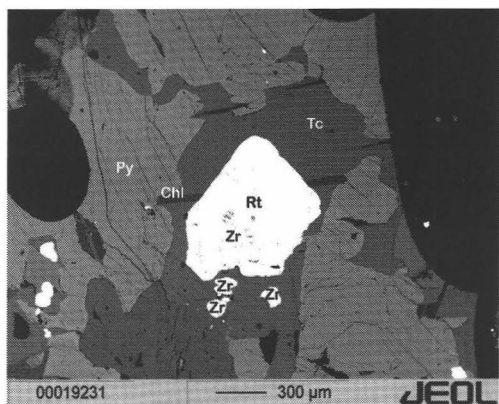
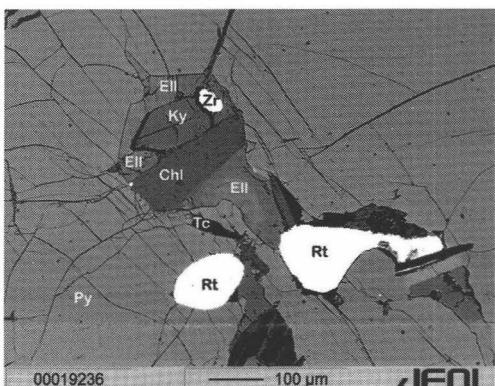


Abbildung 3:

BSE Bild von Rutil (*Rt*) und Zirkon (*Zr*)-Einschlüssen im Pyrop (*Py*), zusammen mit Talk (*Tc*) und Chlorit (*Chl*).



Überblick über die Kalibrationen des Zr-in-Rutil Geothermometers

ZACK et al. (2004) stellten einen empirischen Zusammenhang zwischen dem Zr Gehalt im Rutil und der Metamorphosetemperatur her. Um eine genaue Kalibration des Zr-in-Rutil Geothermometers durchzuführen kompilierten ZACK et al. (2004) die chemischen Daten von 31 Proben aus insgesamt 15 Lokalitäten. Diese Proben decken den gesamten Temperaturbereich des Zr-in-Rutil Geothermometers von 430-1100°C ab. Die bereits existierenden Untersuchungen zu den geothermometrischen Daten dieser Proben zeigen allerdings einen recht großen Unsicherheitsbereich von bis zu $\pm 50^\circ\text{C}$. ZACK et al. (2004) legten ein spezielles Augenmerk bei der Probenauswahl darauf, dass Rutil als Einschlüsse im Granat vorkommt da diese am besten erhalten sind und von retrograder Überprägung weitgehend geschützt sind. Die gemessenen Zr-Konzentrationen der Rutilkörner (303 Analysen bei 234 einzelnen Körnern aus 31 Proben) in der Untersuchung von ZACK et al. (2004) variieren zwischen 30-8400 ppm. Es wurde auch keine systematische Zonierung erkannt. Das Ausmaß der Schwankung der Zr Gehalte in den verschiedenen Rutilkörnern einer Probe hängt von der maximal erreichten Temperatur ab. Unterhalb von 700°C sind die Zr Gehalte relativ gleichbleibend und zeigen keine Korrelation mit der textuellen Position des Rutil in der Probe. Hingegen zeigt sich bei Rutilen aus Proben mit $T > 700^\circ\text{C}$, dass die Zr-Gehalte in denjenigen Kristallen am größten waren die als Einschlüsse in Granat oder Orthopyroxen vorkamen. Die Rutil in der Matrix zeigten meist geringere Zr Gehalte. Die Korrelation der Zr-Gehalte mit den Temperaturen der zugehörigen Proben lässt erkennen, dass es hier einen Zusammenhang gibt, der mit folgender Arheniusgleichung beschrieben werden kann (ZACK & LUVIZOTTOW, 2006):

$$T(\text{°C}) = 134.7 * \ln(\text{Zr in ppm}) - 25$$

Aufgrund der Kalibrierung dieses Thermometers mittels natürlicher Proben, deren P-T Bedingungen mittels konventioneller Geothermobarometrie ermittelt wurden, besteht eine gewisse Ungenauigkeit von $\pm 50^\circ\text{C}$.

WATSON et al. (2006): Im Unterschied zu ZACK et al. (2004), verwendeten WATSON et al. (2006) bei der Kalibration ihres Geothermometers nicht natürliche Proben, sondern sie verwendeten experimentelle Daten von Rutilen, welche in der Anwesenheit von Zirkon und Quarz bei Drücken von 1 bis 1.4 GPa und Temperaturen von 675 bis 1450°C gezüchtet wurden. Zusätzlich wurden diese noch mit Proben aus 6 natürlichen Gesteinen, die Drücken von 0.35-3 GPa und Temperaturen von 470-1070°C ausgesetzt waren, verglichen. Bei den 17 synthetischen Proben ergaben sich je nach Temperatur Zr Gehalte von 504-89525 ppm. In den natürlichen Proben machten WATSON et al. (2006) in insgesamt ca. 120 Rutilen, pro Korn meist mehrere Messungen, für welche Zr Gehalte von 25 ppm (in den Sifnos Blauschiefern) bis hin zu 13300 ppm (in den Labait Harzburgiten) gemessen wurden. Durch Korrelation aller Daten zeigte sich, dass eine sehr deutliche $\log(\text{Zr})$ Gehalte zu $1/T$ Beziehung besteht. Daraus ließ sich folgende Gleichung ableiten:

$$T(\text{°C}) = (-4470 / (7.36 + \log(\text{Zr in ppm}))) - 273$$

FERRY & WATSON (2007): Bei dieser Kalibration wurde das Augenmerk vor allem darauf gerichtet, wie sehr sich eine Veränderung der α_{SiO_2} (der Aktivität von Quarz) auf die Zr-Gehalte in Rutil und somit auch auf die daraus resultierenden Temperaturen, auswirkt. Dadurch ergab sich eine neue Art der Temperaturberechnung, durch die es nun möglich ist, auch in quarz-untersättigten Gesteinen (mit $\alpha_{\text{SiO}_2} < 1$) den Zr Gehalt in Rutil als Geothermometer anzuwenden. Verwendete Proben zur Kalibrierung waren auch in diesem Fall die Proben von WATSON et al. (2006). Neben der Temperatur hat auch die Aktivität (α_{SiO_2}) eine entscheidende Auswirkung auf die Zr Gehalte in Rutil. So zeigte sich in eigens für diese Untersuchungen angestellten Experimenten, dass in mit Zirkon koexistierenden Rutilen bei 800°C und 2 GPa und der höchst möglichen α_{SiO_2} (gepuffert durch Quarz) die Zr-Gehalte bei 1697 ± 56 ppm liegen. Während bei Rutilen in quarzuntersättigten Milieus und bei gleichen P-T Bedingungen deutlich höhere Zr-Gehalte von 2411 ± 176 ppm vorliegen. Eine Probe von Rutil bei 1350°C, 1 GPa und der kleinst möglichen α_{SiO_2} wies sogar extrem hohe Zr Gehalte von 101100 ± 1600 ppm auf. Aufgrund dieser Ergebnisse wurde die folgende Gleichung abgeleitet:

$$T(\text{°C}) = (-4530/(-7.42) + \log(\text{Zr in ppm}) + \log \alpha_{\text{SiO}_2}) - 273$$

Es wurden in den vorhergehenden Studien Temperaturen aus Rutilen aus Hochdruckgesteinen abgeleitet, aber der explizite Einfluss des Druckes auf die Zr Gehalte in Rutil wurde nicht systematisch untersucht. Ein signifikanter Einfluss des Druckes auf diese Geothermometer muss es aber geben, da die Substitution des größeren Zr^{4+} durch das kleinere Ti^{4+} Kation eine Abnahme der Zr-Substitution in Rutil mit steigendem Druck zur Folge hat.

DEGELING (2002) führte Experimente > 1000°C bei unterschiedlichen Drucken (0.001-2 GPa) durch und zeigte durch den Vergleich von verschiedenen Proben, die gleichen Temperaturen aber unterschiedlichen Drucken von 1 und 2 GPa ausgesetzt waren, dass es je nach Temperatur zu Abweichungen von ~26°C bei 500°C bis zu ~90°C bei 1100°C kommen kann. Die folgende Gleichung (aus SPEAR et al., 2006) wurde aufgestellt:

$$T(\text{°C}) = (89297.49 + 0.63*(P-1)/(8.3411*\ln(8.76*107/(\text{Zr in ppm}))) + 33.46) - 273$$

TOMKINS et al. (2007) führten weitere Experimente, basierend auf den Experimenten von DEGELING (2002) durch und weiteten den Druckbereich von 1 bar bis 3 GPa bei 1100-1300°C auf. Aus den Daten ermittelten sie Kalibrationen für die Paragenesen; Rutil + Zirkon + α -Quarz, Rutil + Zirkon + β -Quarz und Rutil + Zirkon + Coesit auf. Die Gleichung für das Zr-in-Rutilthermometer im Coesitstabilitätsfeld ist:

$$T(\text{°C}) = (88.1 \cdot 0.206 * P / (0.1412 - 0.0083144 * \ln(\text{Zr in ppm})) - 273$$

Diskussion

Würde der Druck in der Berechnung nicht berücksichtigt, muss man mit grossen Unsicherheiten (ca. ~70°C(GPa) in der Anwendung rechnen, worauf FERRY & WATSON (2007) hingewiesen haben. Daraus folgt für die Proben, des Dora Maira Massives, dessen Druck bei >3 GPa liegt, das der druckabhängige Fehler (oberhalb von 1 GPa pro GPa ca. ~70°C) bei ca. 140°C liegen würde!

Auf eine weitere Fehlerquelle weisen FERRY & WATSON (2007) hin, da sie bewiesen, dass der Zr-Gehalt in Rutil sehr stark von α_{SiO_2} abhängig ist, diese aber nicht immer exakt bestimmbar ist. Bei $\alpha_{\text{SiO}_2} < 0$ zeigte sich sogar, dass das Zr-in-Rutil Geothermometer nach der Gleichung von FERRY & WATSON (2007) sogar unbrauchbar wird. Auch durch retrograde Überprägung kann es zu einer Veränderung der Zr-Gehalte kommen (CHERNIAK et al., 2007). Dies gilt nur für relativ langsame Abkühlraten, bei sehr rascher Abkühlung kommt es zu keiner Neueinstellung der Zr-Gehalte. Rutileinschlüsse in Granat ergeben die höchsten Temperaturen, während Matrixrutile eher retrograde Temperaturen anzeigen (ZHANG et al., 2010). Am häufigsten kommt es zu Änderungen des Zr-Gehaltes in Matrixrutilen da sie häufig in Kontakt mit retrograden Fluiden kommen. Unter diesen Bedingungen wäre eine nachträgliche Modifizierung der Zr Gehalte möglich.

Zur Untersuchung der maximalen Temperaturen während des Höhepunktes der Metamorphose mittels Zr-in-Rutil Geothermometrie wurden in 2 Dünnschliffen von Pyrop-Megakristallen insgesamt 13 Messungen an 11 verschiedenen Rutileinschlüssen vorgenommen (Tabelle 1). Das Ergebnis waren Zr Gehalte die zwischen 121 ppm und 173 ppm.

Tabelle 1:
Gemessene Zr-Gehalte in den Rutileinschlüssen.

	Zr[ppm]
Rt_kern-1	151
Rt_rand-1	132
Rt_kern-2	121
Rt_rand-2	126
Rt_kern-3	149
Rt_kern-4	148
Rt_kern-5	149
Rt_kern-6	145
Rt_kern-7	164
Rt_kern-8	173
Rt_kern-9	160
Rt_kern-10	128
Rt_kern-11	149

	ZACK et al. (2004)	WATSON et al. (2006)	FERRY & WATSON (2007)	DEGELING (2002)	TOMKINS et al. (2007)
Rt_kern-1	651	590	591	772	685
Rt_rand-1	633	580	582	766	674
Rt_kern-2	621	574	576	763	668
Rt_rand-2	626	577	579	764	671
Rt_kern-3	649	589	590	772	684
Rt_kern-4	648	588	590	772	683
Rt_kern-5	649	589	590	772	684
Rt_kern-6	645	587	588	771	682
Rt_kern-7	662	596	597	776	692
Rt_kern-8	669	600	601	779	696
Rt_kern-9	659	594	596	775	690
Rt_kern-10	629	578	580	765	672
Rt_kern-11	649	589	590	772	684

Tabelle 2:
Ergebnisse der Zr-in-Rutil-Geothermometrie.
Die Berechnungen mit DEGELING (2002) und TOMKINS et al. (2007) wurden bei 3.5 GPa durchgeführt.
Die Berechnung mit der Kalibration von FERRY & WATSON (2007) wurde bei $\alpha_{\text{SiO}_2} = 1$ durchgeführt.

Die aus diesen Gehalten abgeleiteten Temperaturen schwanken also je nach P-unabhängiger Kalibration (ZACK et al., 2004; WATSON et al., 2006; FERRY & WATSON, 2007) zwischen 574-669°C (Tabelle 2), was im Vergleich zu den bereits ermittelten Höhepunkttemperaturen (SCHERTL et al., 1999) viel zu niedrige Temperaturen darstellt. Korrigiert man diese Ergebnisse jedoch mittels der Druckkorrektur von DEGELING (2002) bei Drucken von 3.5 GPa so ergeben sich korrigierte Temperaturen zwischen 760 und 780°C, welche wiederum mit den Höhepunkttemperaturen sehr gut übereinstimmen, was aber interessant ist, da DEGELING (2002) nur Experimente bis 2 GPa, also im Quarzstabilitätsfeld, durchführte. Interessanterweise aber ergeben die Temperaturen nach TOMKINS et al. (2007), die bei ähnlichen Drucken von 3 GPa durchgeführt wurden, für die Rutileinschlüsse im Coesitstabilitätsfeld leicht zu niedrige Temperaturen von 670-690°C bei 3.5 GPa! Der Trend dieser Ergebnisse stimmen mit den Ergebnissen von ZHANG et al. (2010) aus W-China gut überein, obwohl in deren UHP Gesteinen, die Kalibration von TOMKINS et al. (2007) die plausibelsten Werte ergab. Leider wurde in deren Gesteinen die Korrektur von DEGELING (2002) nicht angewendet.

Mögliche Unsicherheiten bezüglich der Temperaturen stellen folgende Faktoren dar: 1.) Da bei keinem einzigen gemessenen Rutil in unmittelbarer Nähe freier Quarz bzw. Coesit anzufinden war ist es fraglich ist ob für α_{SiO_2} der Wert 1 angenommen werden kann. Die Abhängigkeit von α_{SiO_2} wurde auch in keiner der beiden Kalibrationen mit Druckkorrektur experimentell berücksichtigt. Tabelle 3 zeigt die Variation der Temperatur nach FERRY & WATSON (2007) als Funktion von α_{SiO_2} wobei die Temperaturen bei hohen α_{SiO_2} am höchsten sind und drastisch mit sinkender α_{SiO_2} abfallen. 2.) Retrograde Überprägung durch spätere Diffusion (CHERNIAK et al., 2007) kann jedoch als Fehlerquelle eher ausgeschlossen werden, da zum einen nur Rutileinschlüsse im Pyrop untersucht wurden, und zum anderen die Abkühlraten wahrscheinlich zu rasch waren um eine Diffusion des Zr zu gewährleisten. 3.) Möglicherweise sind die Zr-Gehalte in den Rutilen mittels Elektronenstrahlmikrosonde zu niedrig und daher ist es geplant weitere Messungen mittels Laser-ICP-MS als Vergleich durchzuführen. 4.) Es ist auch möglich dass diese Rutileinschlüsse im Granat ein Wachstumsstadium vor dem Temperaturhöhepunkt darstellen und daher die Temperaturen aus der Kalibration von TOMKINS et al. (2007) richtig sind.

Zr[ppm]	α_{SiO_2}	T(°C)
151.00	1.00	591
	0.90	584
	0.80	576
	0.70	567
	0.60	556
	0.50	544
	0.40	530
	0.30	513
	0.20	490
	0.10	453

Tabelle 3:
*Abhängigkeit der Temperaturen nach
FERRY & WATSON (2007) von α_{SiO_2}*

Danksagung

Martina Tribus wird für Ihre Hilfe an der Mikrosonde, Fritz Koller für seine Kommentare und Richard Tessadri für das Editorial Handling gedankt.

Literatur

- CHERIAK, D.J., MANCHESTER, J. & WATSON, E.B. (2000): Zr and Hf diffusion in rutile. - *Earth and Planetary Science Letters*, 261, 267-279.
- CHOPIN, C., HENRY, C. & MICHARD, A. (1991): Geology and Petrology of the coesite-bearing terrain, Dora Maira Massif, Western Alps. - *European Journal of Mineralogy*, 3, 263-291.
- CHOPIN, C. (2003): Ultrahigh-pressure metamorphism: tracing continental crust into the mantle. - *Earth and Planetary Science*, 212, 1-14.
- CHOPIN, C. (1984): Coesite and pure pyrop in high-grade blueschists of the western Alps: A first record and some consequences. - *Contributions to Mineralogy and Petrology*, 86, 107-118.
- DAL PIAZ, G.V. & LOMBARDO, B. (1986): Early Alpine eclogite metamorphism in Penninic Monte Rosa-Gran Paradiso basement nappes of the NW Alps. - *Geological Society of America Memoir*, 164, 249-265.
- DEGELING, H. (2002): Zr equilibria in metamorphic rocks. Unveröffentlichte Doktorarbeit, Australian National University, 231 S.
- FERRY, J.M. & WATSON, E.B. (2007): New thermodynamic models and revised calibrations for the Ti-in-zircon and Ti-in-rutile thermometers. - *Contributions to Mineralogy and Petrology*, 154, 429-437.
- HEINRICH, W., ANDREHS, G. & FRANZ, G. (1997): Monazite-xenotime miscibility gap thermometry. I. An empirical calibration. - *Journal of Metamorphic Geology*, 15, 3-16.
- PYLE, J.M., SPEAR, F.S., RUDNICK, R.L. & MCDONOUGH, W.F. (2001): Monazite-Xenotime-Garnet Equilibrium in Metapelites and a New Monazite-Garnet Thermometer - *Journal of Petrology*, 42, 2083-2107.
- SCHERTL, H.P., SCHREYER, W. & CHOPIN, C. (1991): The pyrope-coesite rocks and their country rocks at Parigi, Dora Maira Massif, western Alps: detailed petrography, mineral chemistry and PT-path. - *Contributions to Mineralogy and Petrology*, 108, 1-21.
- TOMKINS, H.S., POWELL, R. & ELLIS, D.J. (2007): The pressure dependence of the zirconium-in-rutile-thermometer. - *Journal of Metamorphic Geology*, 25, 703-713.
- WATSON, E.B., WARK, D.A. & THOMAS, J.B. (2006): Crystallization thermometers for zircon and rutile. - *Contributions to Mineralogy and Petrology*, 151, 413-433.
- WILLGALLIS, A., SIGMANN, E. & HETTIARATCHI, T. (1983): Srilankite, a new Zr-Ti-oxide mineral assemblages. - *Journal of Metamorphic Geology*, 1, 151-157.
- ZACK, T., MORAES, B. & KRONZ, A. (2004): Temperature dependence of Zr in Rutile: empirical calibration of a rutile thermometer. - *Contributions to Mineralogy and Petrology*, 148, 471-488.
- ZACK, T. & LUVIZOTTOW, G.L. (2006): Application of rutile thermometry to eclogites. - *Mineralogy and Petrology*, 88, 69-85.
- ZHANG, G., ELLIS, D.J.; CHRISTY, A.G., ZHANG, L. & SONG, S. (2010): Zr-in-rutile thermometry in HP/UHP eclogites from Western China. - *Contributions to Mineralogy and Petrology*, 160, 427-439.

received: 12.06.2013.

accepted: 20.06.2013.

JOHANN FIBIG (*~1720 †1792)
EDITION SEINER MINERALOGISCH ORIENTIERTEN DRUCKSCHRIFT
„STUDIUM DER NATURGESCHICHTE“ UND KOMMENTARE ZU SEINEM
„HANDBUCH DER MINERALOGIE“

von

Franz Pertlik

Institut für Mineralogie und Kristallographie
Universität Wien, Geozentrum, Althanstraße 14, A-1090 Wien, Österreich

Abstract

The presented article is a homage to Johann Fibig (*~1720 † 21.10.1792, Mainz), professor of natural sciences at the University in Mainz. His scientific work comprises more than one dozen articles about teaching and study of the topics mineralogy and biology. Further topics were respectful articles dedicated to the archbishop of Mainz. J. Fibig was honoured by a lot of memberships to scientific societies in Mainz, Berlin, and in Paris.

In the booklet “Studium der Naturgeschichte” the change from a descriptive to an experimental mineralogy was a theme, discussed for the first time in a scientific paper. Especially the influence of chemical analyses in systematic mineralogy, contrary to morphological descriptions, was mentioned to be a helpful tool.

Vorbemerkungen

In der Wissenschaftsdisziplin Mineralogie vollzog sich in der zweiten Hälfte des 18. Jahrhunderts sowohl in der Forschung als auch in der Lehre ein Paradigmenwechsel in der Klassifikation des Objekts Mineral, der von einer reinen Beschreibung an Hand der Morphologie zu einer Systematik auf Grund der chemischen Zusammensetzung führte. Wegbereiter dieses Wechsels waren unter anderem J. H. Pott (1746), Professor der Chemie und Pharmazie in Berlin, und J. G. Wallerius (1747), Professor der Chemie in Uppsala. Auf diese Änderung in der Betrachtung der Mineralogie wurde von J. G. Lehmann bereits 1751 in seinem Werk „Kurze Einleitung in einige Theile der Bergwerks=Wissenschaft“ hingewiesen (Wiedergabe der Seiten 62-63):

Eintheilung des Mineralreichs.

Ich theile demnach alle unterirdischen Schätze 1) in blosse Erden, 2) in Salze, 3) in verbrennliche Mineralien, 4) in Metalle, 5) in Steine. Wäre ich willens die Sache chymisch durchzugehen, so würde ich in meiner Eintheilung derer Erden und Steine

billig auch nach ihrer Verhältniß in chymischen Versuchen mich richten müssen, und da würde ich mich keiner bessern, als des berühmten Hrn. Prof. Potts, bedienen können; da ich aber in dieser meiner ganzen Einleitung mit niemanden als mit Anfängern zu thun habe, welche wenig oder keinen Begriff von der Chymie haben, und ich denselben zum Anfange die Dinge nur dem äusserlichen Ansehen nach will kennen lernen, so werde ich mich auch in deren Claßificierung größtentheils nach dem äusserlichen Ansehen, Gehalt rc. [Glyphe für et cetera] richten.

In der von J. Fibig 1784 verfassten Schrift „Uiber das Studium der Naturgeschichte - Ein Programm“, welche eine kurze Zusammenfassung (Originaltext 16 Druckseiten) des Studiums der Naturgeschichte als eines Zweiges der Naturwissenschaften darstellt, hat der Autor diesem Paradigmenwechsel bereits Rechnung getragen. Diese Schrift stellt somit einen der ersten allgemein gehaltenen Studienführer dar, in welchem vor allem die Mineralogie behandelt wurde.

Neben diesem Studienführer hat J. Fibig lediglich ein weiteres bedeutendes mineralogisch orientiertes Werk, ein Lehrbuch/Handbuch, herausgegeben: das „Handbuch der Mineralogie“ (1787). Dieses basiert bereits in allen Teilen auf einer Systematik der Minerale, die auf der chemischen Zusammensetzung aufbaut, und Fehlinterpretationen durch rein morphologische Beschreibungen wurden aufgezeigt.

Im Zusammenhang mit der akademischen Lehre des Faches Naturgeschichte ist zu erwähnen, dass die Fächer Mineralogie, Zoologie und Botanik an den Universitäten des deutschen Sprachraumes bis Ende des 18. Jahrhunderts überwiegend an den medizinischen Fakultäten gelehrt wurden (PERTLIK & ULRYCH, 2001). Dies erklärt auch, dass J. Fibig, ein promovierter Mediziner, als Professor diese Fächer an der Universität Mainz vortrug. Ebenso war sein Nachfolger auf dem Lehrstuhl für Naturgeschichte (Botanik) an der Universität Mainz, Jakob Fidelis Ackermann (*1765 †1815), promovierter Mediziner.

Biographisches zu Johann Fibig

J. Fibig wurde etwa 1720 geboren. Sowohl in dem lexikalischen Werk von Meusel (1796) als auch bei Poggendorff (1863) wird kein Geburtsdatum, sondern nur Sterbedatum und Sterbeort, 21. Oktober 1792 und Mainz, angegeben. In diesen beiden Werken ist als akademischer Grad Doktor der „Arzneygelehrtheit“ angeführt. Die in dem Werk “The Library. Curtis Schuh’s Bibliography of Mineralogy” (2011) als Beruf genannte Bezeichnung “German lawyer” entbehrt jeglicher historischer Grundlage (vgl. Abbildungen 1 und 2).

Die wenigen bekannten persönlichen Daten, Mitgliedschaften und Ehrungen sind den folgenden Absätzen zu entnehmen, wobei auf die exakte Wiedergabe Wert gelegt wurde.

Allgemeines zum wissenschaftlichen Werk von Johann Fibig

Das Werkverzeichnis von J. Fibig (Anhang 1) zeigt, dass der Schwerpunkt seiner wissenschaftlichen Arbeit auf der Mineralogie und Chemie lag, die weiteren Fachdisziplinen der Naturgeschichte, Botanik und Zoologie in seinem Werk jedoch etwas in den Hintergrund traten.

ALFRED HIMMELBAUER
STETTER

Studium der Naturgeschichte.

Ein Programm

des

Johann Fibig,

der Universität Docto^r, der Naturgeschichte öffentl.
icher Lehrer, der Gesellschaft naturforschender
Freunde in Berlin, und des Museums
zu Paris Mitglied.



L. Stessner

Mainz,

ausdruckt in der Ausführung bei eisernen Buchdruckerey
bei Johann Benjamin Gallus.

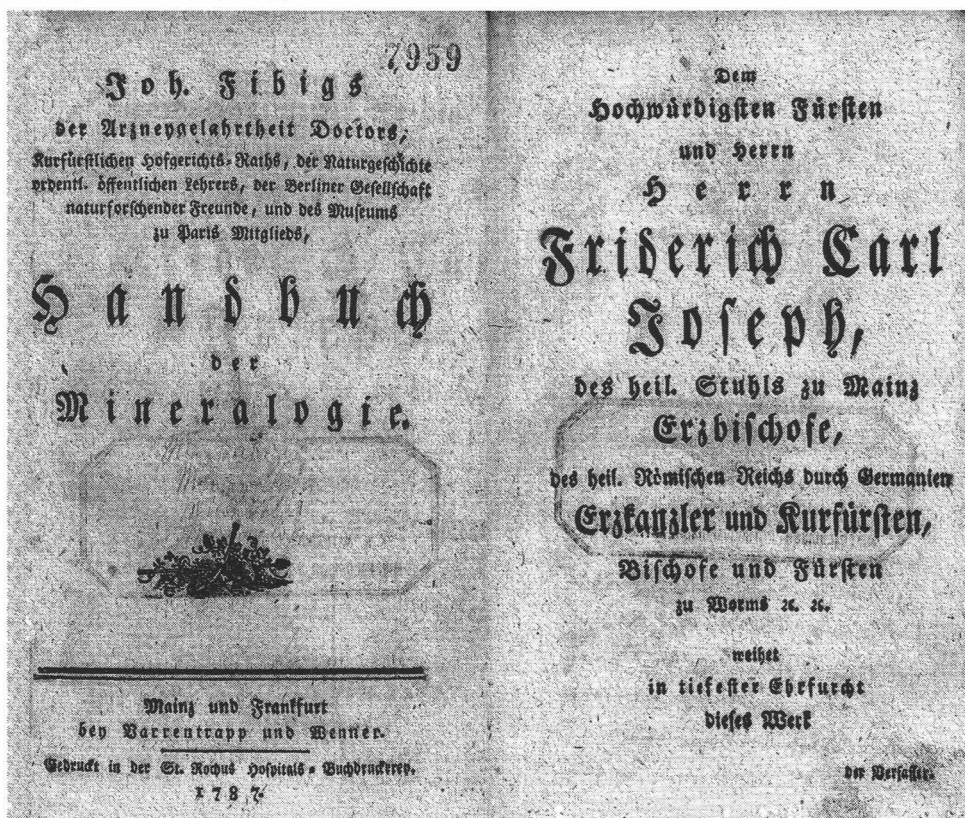
1784

Abbildung 1

Das Studium der Naturgeschichte, Titelseite (Original im Besitz von F. Pertlik).

Abbildung 2

Handbuch der Mineralogie, Titelseiten (Original im Naturhistorischen Museum in Wien aufliegend).



Die beiden ersten erhaltenen Schriften aus den Jahren 1778 und 1779, die als anlassgebundene „Gelegenheitsschriften“ bezeichnet wurden, enthalten Aufzeichnungen von Laudationes anlässlich einer Verleihung der Doktorwürde beziehungsweise eine Sammlung von Dankreden. Die Drucklegung einer Doktorarbeit gemeinsam mit K. Strack erfolgte 1781.

In den Jahren 1784 und 1787 verfasste J. Fibig seine beiden Werke über die Naturgeschichte und die Mineralogie (im nächsten Kapitel kommentiert).

Im Jahre 1790 arbeitete J. Fibig bei der Übersetzung einer Schrift von L. C. H. Macquart aus dem Französischen unter dem Titel „Beschreibung einer auf Befehl der Regierung nach dem Norden gemachten Reise“ mit. Die mit B. S. Nau herausgegebene Sammlung wissenschaftlicher Artikel „Bibliothek der gesamten Naturgeschichte“ (1789 bis 1790) und die „Naturgeschichte des Pflanzenreiches“ (1791), stellen weitere Standardwerke - in Teilen lexikalisch aufgebaut - zur Lehre der Naturgeschichte dar.

Zu bemerken ist, dass zwei Werke aus den Jahren 1784 und 1785, welche sich auf die Insektenkunde beziehen und in einigen Biographien Erwähnung fanden, eindeutig nicht J. Fibig zugeordnet werden können.

Inhaltliche Darstellung und Kommentar zu „Studium der Naturgeschichte“

Von den im 18. Jahrhundert gelehrt drei Zweigen der Naturgeschichte wurde in der Schrift „Studium der Naturgeschichte“ (im Original 16 Seiten, als Anhang 2 in voller Länge transkribiert) eingangs die Mineralogie behandelt, ab Seite 8 wird auf den Stand der Forschung und der Lehre des Faches Botanik eingegangen und ab Seite 13 findet die Zoologie Erwähnung. Die Titelseite ist in Abbildung 1 wiedergegeben.

Kommentar zum Inhalt:

Zu Beginn erwähnt J. Fibig die ersten Versuche, die Minerale in ihrer Gesamtheit in ein Schema einzurichten. Diese waren von C. Linné und G. Buffon (persönliche Daten siehe Anhang 2) unternommen worden, wobei weitestgehend die äußeren Kennzeichen, also die Gestalt dieser „Fossilien“, zu deren Charakterisierung herangezogen wurden. Als eine weitere wichtige Bestimmungsmethode wurde von D. Pott die analytische Chemie herangezogen, wobei dieser jedoch lediglich das Verhalten der Minerale beim Erhitzen, die Lötrohrmethode, in seinen Schriften ausführlich beschrieb. Erweiterungen der Analysenmethoden gehen auf die Chemiker J. Wallerius und A. Cronstedt zurück, die die Nass-Chemie zur Bestimmung von Mineralen ausbauten und kritisch gegen die von C. Linné vertretene Methode auftraten.

J. Fibig weist des Weiteren auf die Chemiker J. Henkel, A. Marggraf, C. Scheele und T. Bergmann als Vertreter der chemischen Schule in der Mineralogie hin. Auf A. Werner, als einer der Mitbegründer einer mineralogischen Terminologie, und seine Betrachtungen zu Entstehung, Wachstum und Veränderung von Fossilien wurde auf den Seiten 6 und 7 ausführlich eingegangen. Kurze Absätze sind in dem der Mineralogie gewidmeten Teil abschließend noch über den Bergbau und die Bergwerke zu finden.

In dem der Zoologie und Botanik gewidmeten Teil wurde auf keinen Wissenschaftler näher eingegangen, welcher sich zu Lebzeiten J. Fibigs mit diesen Wissenschaften beschäftigte. Der Autor zitiert lediglich Gelehrte des Altertums, wie Plinius oder Aristoteles. Ganz allgemein kann dieser Teil als Hinweis auf die Problematik in der systematischen Erfassung der Objekte dieser Wissenschaften angesehen werden, sein didaktischer Wert jedoch als gering erachtet werden.

Johann Fibigs Handbuch der Mineralogie

Vorrede

Gerne hätte ich mich des im vorigen Jahre erschienen vortrefflichen Grundrisses des Mineralsystems von Hrn. geheimen Bergrath Gerhard, meinem unvergeßlichen Lehrer zu meinen Vorlesungen über die Mineralogie bedient, wenn mir derselbe nicht für viele meiner Zuhörer, welche durch chemische Kenntnisse zur Mineralogie noch nicht vorbereitet sind, zu kurz geschienen hätte: daher fange ich in der Einleitung der Mineralien mit den Salzen an, um meinen noch unvorbereiteten Zuhörern, soviel als möglich, zuvor chemische Kenntnisse beyzubringen, bey welcher Gelegenheit ich die nöthigsten chemischen Versuche mache.

Dieß ist auch die Ursache, warum ich verschiedene Salze z. B. vegetabilisches Laugensalz, vitriolisirten Weinstein s. s. w. Körper welche eigentlich ins Mineralreich nicht gehören, sondern nur zufälliger Weise dahineingekommen sind, mit anfühere, um die Lehre von den Salzen desto vollständiger vortragen zu können.

Uebrigens halte ich mich für belohnt genug, wenn ich durch dieses Lehrbuch meinen Zuhörern, wie ich bey dem Vortrage über die ersten abgedruckten Bogen bemerkte zu haben glaube, das Studium einer so schweren, und abschreckenden Wissenschaft erleichtere, und dieselbe in meinen Kollegien so vorbereite, daß sie nachher durch eigenen Fleiß größere Fortschritte in der Mineralogie machen können.

Mainz den 16. April 1787.

In dieser Vorrede zum Handbuch der Mineralogie legt der Verfasser die Grundzüge seines Werkes dar und begründet die für seine Zeit doch etwas unübliche Erweiterung eines Lehrbuches der Mineralogie durch Beispiele aus der Chemie. Das Werk selbst stellt, wie im 18. Jahrhundert üblich, eine Hommage an den Landesherrn, den Kurfürsten von Mainz, dar, wie aus den Titelseiten in Abbildung 2 ersichtlich. Eine weitere Huldigung an den Kurfürsten Friedrich Karl Joseph von Erthal aus dem Handbuch der Mineralogie ist als Anhang 3 wiedergegeben.

Dem Stand der Wissenschaft entsprechend, konnte eine deutliche Abgrenzung der Mineralogie von der Petrographie, wie heute üblich, nicht mit letzter Konsequenz vorgenommen werden. Als Grund ist der Stand der Wissenschaften Chemie und Physik anzusehen, welche als helfende Wissenschaften selbst noch in einem Entwicklungsstadium waren. Dessen ungeachtet ist die von J. Fibig aufgestellte Systematik der Minerale der heute gebräuchlichen Einteilung in modernen Lehrbüchern absolut ebenbürtig. Er weist bereits darauf hin, dass neben den äußerer „sinnlichen Kennzeichen“ auch die inneren, chemischen und physikalischen Kennzeichen zur Charakterisierung heranzuziehen wären. Weiters sollten die von ihm als „empirische Kennzeichen“ angeführten Parameter in der Systematik Beachtung finden. Unter diesen Parametern wurden von ihm die Genese und Paragenese der Mineralien verstanden.

Die im Handbuch beschriebenen Minerale teilt J. Fibig in vier Klassen und einen Anhang ein: I.) Salze; II.) Erden und Steine; III.) Brennbare Mineralien; IV.) Metalle; Anhang: Vulkanische Produkte. Diese Klassen wurden weiters in Ordnungen und Abschnitte unterteilt. Im Anhang 3 ist eine Transkription der „Eintheilung der Mineralien“ zu finden.

Im Gegensatz zu dem von J. Fibig in seiner Vorrede zitierten Werk von Bergrath Gerhard (GERHARD, 1781; 1782) stellt sein Handbuch der Mineralogie ein durchaus modern anmutendes Lehrbuch dar, in welchem erstmals, und das war signifikant neu, eine strikte Trennung der Wissenschaften Mineralogie und Kristallographie erfolgte.

Während sich bei GERHARD (1782) zum Beispiel unter dem Begriff „Wasserstein“ noch kristallographische und morphologische Bezeichnungen wie „stumpfer, prismatischer, zwölfseitiger, sechseitiger Wasserstein“, neben solchen aus der Mineralogie, wie Kalkrahm und Tropfstein, finden, sind derartige kristallographische Benennungen, wie aus Anhang 4 ersichtlich, bei J. Fibig bereits eliminiert. Zu dem Begriff Wasserstein (SCHRÖTER, 1788):

Wassersteine, Porus, Petra alcalina calcaria lamellis conflata heißen bei Herrn Gerhard die alkalischen kalkartigen Steine, welche aus Blättern zusammengesetzt sind.

Obwohl ein Pionier in der Erstellung eines Systems in der Mineralogie, fand J. Fibig für diese Leistung in der Fachwelt nur wenig Anerkennung. Selbst noch Friedrich Mohs (1836) stand der Chemie als Hilfswissenschaft der Mineralogie skeptisch gegenüber, wobei er behauptete, dass die Naturgeschichte des Mineralreichs der Chemie nicht bedürfte (PERTLIK & SEIDL, 2008). Erst Mitte des 19. Jahrhunderts war es Franz Xaver Zippe (1859), der der modernen, chemisch orientierten Systematik in der Mineralogie zum Durchbruch verhalf.

Ehrungen und Mitgliedschaften

Kurfürstlich mainzischer Hofgerichtsrath.

Professor der Naturgeschichte und Botanik an der Universität Mainz.

Mitglied der physikalisch=ökonomischen Gesellschaft zu Mainz.

Mitglied der Akademie nützlicher Wissenschaften zu Erfurt.

Mitglied der Berliner Gesellschaft naturforschender Freunde.

Mitglied des Pariser Museums.

Biographische Erwähnungen

Deutsches biographisches Archiv (DBA) I 317, 68-70; II 364, 257.

<http://db.saur.de/WBIS/basicTextDocument.jsf>.

Angeführt werden neben einigen persönlichen Daten drei weitere Nekrologie, J. Fibig betreffend.

Meusel, Johann Georg (1796): Fibig (Johann). - Lexikon der von 1750 bis 1800 verstorbenen deutschen Schriftsteller, Band 3, Seite 328 (Kurzbiographie mit der Anführung folgender Veröffentlichungen [4-9]):

D. der Arzneygel. Kurfürstl. Mainzischer Hofgerichtsrath, ordentlicher Professor der Naturgeschichte und Beysitzer der Kameralfakultät auf der Universität zu Mainz: geb. zu ... gest. am 21 Oktober 1792.

Poggendorff, J. C. (1863): Fibig Johann. - Biographisch-Literarisches Handwörterbuch zur Geschichte der exacten Wissenschaften. Erster Band, A-L, Seiten 742-743. Verlag von Johann Ambrosius Barth. Leipzig. (Kurzbiographie mit der Anführung folgender Veröffentlichungen [7-9]):

Dr. Med., Kurfürstl. Mainzischer Hofgerichtsrath und Prof. d. Naturgeschichte a. d. Universität Mainz; geb. - , gest. 21. Okt. 1792.

Rötger, Gotthilf Sebastian: Nekrolog für Freunde deutscher Literatur 1791-1794. Band II, Seiten 48-49. Helmstädt; C. G. Fleckeisen.

The Library. Curtis Schuh's Bibliography of Mineralogy (2011).

<http://www.minrec.org/libdetail.asp?id=377>.

Angeführt werden neben einigen persönlichen Daten drei Nekrologie J. Fibig betreffend, sowie die Veröffentlichungen [7,9].

Dank

Für Anregungen, weiterführende Diskussionen und technische Hilfe dankt der Autor Frau HR Dr. Vera M. F. Hammer und Herrn Wolfgang Brunnbauer, Naturhistorisches Museum Wien, Herrn Univ. Doz. Mag. Dr. Johannes Seidl, Archiv der Universität Wien, sowie Herrn Ing. Wolfgang Zirbs, Institut für Mineralogie und Kristallographie der Universität Wien.

Literatur

- Gerhard, Carl Abraham (1781 / 1782): Versuch einer Geschichte des Mineralreiches. Erster Theil - Zweyter Theil.
– Bey Christian Friedrich Himpurg, Berlin.
- Lehmann, Johann Gottlob (1751): Kurze Einleitung in einige Theile der Bergwerks=Wissenschaft. – Berlin bey Christoph Gottlieb Nicolai (192 Seiten).
- Mohs, Friedrich (1836): Leichtfassliche Anfangsgründe der Naturgeschichte des Mineralreiches. Erster Theil.
Terminologie, Systematik, Nomenklatur, Charakteristik. – Wien. Gedruckt und im Verlage bei Carl Gerold.
- Pertlik, Franz; Ulrych, Jaromir (2001): Lehre der Geowissenschaften im Rahmen des Faches Naturgeschichte an der Universität Wien im Zeitraum von 1787 bis 1848. - Berichte der Geologischen Bundesanstalt, Band 53, 55-60.
- Pertlik, Franz; Seidl, Johannes (2008): Lehrveranstaltungen an der Universität Wien mit Bezug zur Mineralogie von 1786 bis 1848. – Mitteilungen der Österreichischen Mineralogischen Gesellschaft 154, 69-82.
- Pott, Johannes Henricus (1746): Chymische Untersuchungen, welche fürnehmlich von der Lithogeognosia oder Erkäntniß und Bearbeitung der gemeinen einfacheren Steine und Erden ingleichen von Feuer und Licht handeln. – Verlag Christian Friedrich Voß, Berlin.
- Schröter, Johann Samuel (1788): Lithologisches Real= und Verballexikon, in welchem nicht nur die Synonymen der deutschen, lateinischen, französischen und holländischen Sprachen angeführt und erläutert, sondern auch alle Steine und Versteinerungen ausführlich beschrieben werden. – 8. Band. Frankfurt Mayn bei Barrentrapp und Wenner. Seite 342.
- Wallerius, Johann Gottschalk (1747): Mineralogia eller Mineral Ricket indelt och beskrivet. – Stockholm (Ins Deutsche übersetzt von Johann Daniel Denso).
- Zippe, Franz Xaver Maximilian (1859): Lehrbuch der Mineralogie mit Naturhistorischer Grundlage. – Wien. Wilhelm Braumüller.

received: 14.12.2012.

accepted: 07.01.2013.

Anhang 1: Werkverzeichnis von Johann Fibig.

Dieses Verzeichnis wurde an Hand der angeführten biographischen Erwähnungen und eigenen Recherchen in den nationalen und internationalen Bibliotheken zusammengestellt. Die Zitate [4] und [6], verschiedentlich J. Fibig zugeschrieben, wurden unzweifelhaft nicht von ihm verfasst. Er war Mitglied der Berlinischen Gesellschaft Naturforschender Freunde, hat jedoch zu keiner ihrer Jahresschriften einen Beitrag geliefert.

1778 - [1] Oden, als der wohlgebohrne hochgelehrte Herr Karl Kaspar Siebold dem Herrn Georg Kast den 7 Februarius 1778 die Doctorwürde in der Arzneygelehrtheit ertheilte. – Verlag Franz Ernst Nitribitt, Würzburg (Gelegenheitsschrift).

1779 - [2] Pfeil, Matthes; Fibig Johann: Kurze Dankreden als der hochwürdigste Herr Herr Friderich Karl Joseph, Erzbischof zu Mainz von dem hochwürdigsten Herrn Herrn Franz Ludwig, Bischofe zu Bamberg und Wirzburg den 1. October 1779 Abschied nahmen. - Verlag Franz Ernst Nitribitt, Würzburg (Gelegenheitsschrift).

1781 - [3] Fibig, Johann; Strack, Karl: De febre pituitosa. – Dissertation.

1784 - [4] Beschreibung des Sattelträgers (Gryllus Ephippiger). – Schriften der Berlinischen Gesellschaft Naturforschender Freunde 5, 260-263.

Im Originaltext wird als Autor(in) angegeben: D. Fiebig [sic].

1784 - [5] Uüber das Studium der Naturgeschichte. Ein Programm. - Gedruckt in der Kurfürstlich privilegierten Buchdruckerey, bey Johann Benjamin Wailandt. 1784. 16 Seiten.

1785 - [6] Ueber eine neue Art von Insekten. - Schriften der Berlinischen Gesellschaft Naturforschender Freunde 6. In diesem Jahrgang der Schrift wurde unter anderem gedruckt: „Beiträge zur Insektengeschichte“ von Siegmund von Hohenwarth; Seiten 334-360. Jeglicher Hinweis auf Fi(e)big fehlt.

1787 - [7] Handbuch der Mineralogie. - Barrentapp und Wenner, Frankfurt und Mainz. Gedruckt in der St Rochus Hospitals=Buchdruckerey. 392 Seiten.

1790 - [8] Macquart, Louis-Charles-Henri; Fibig, Johann; von Nau, Bernhard Sebastian: Beschreibung einer auf Befehl der Regierung nach dem Norden gemachten Reise: enthaltend Abhandlungen über mehrere Gegenstände der Mineralogie: Beschreibung der in die königl. Sammlung abgegebenen merkwürdigsten Stücke: eine Ortsbeschreibung von Moskau mit vielen interessanten statistischen Bemerkungen; 628 Seiten. – In der Hermannischen Buchhandlung, Frankfurt am Main (Aus dem Französischen übersetzt. Mit Anmerkungen begleitet von Fibig und Nau). 628 Seiten.

1789 – 1790 - [9] Fibig, Johann; von Nau, Bernhard Sebastian: Bibliothek der gesammten Naturgeschichte. – Barrentapp und Wenner, Frankfurt und Mainz. 784 Seiten.

1791 - [10] Einleitung in die Naturgeschichte des Pflanzenreichs nach den neuesten Entdeckungen. – Mainz; Kurfürstlich-Privilegierte Universitäts-Buchhandlung. 446 Seiten.

**Anhang 2: Transkription der Druckschrift das „Studium der Naturgeschichte“
(Original im Besitz von F. Pertlik).**

Seite 1 und 2:

Über das
Studium der Naturgeschichte.
Ein Programm
von
Johann Fibig,
der Arzneygelehrtheit Doktor, der Naturgeschichte öffent=
licher Lehrer, der Gesellschaft naturforschender
Freunde in Berlin, und des Museums
zu Paris Mitglied.
Mainz,
gedruckt in der Kurfürstl. privilegirten Buchdruckerey,
bey Johann Benjamin Wailandt.
1784.

Seite 3:

Die Natur in ihren unzähligen, unendlich mannigfaltigen Produkten zu betrachten, scheint über die Kräften des menschlichen Verstandes zu seyn. Der Schauplatz, auf welchem die ungeheure Menge von vierfüßigen Thieren, von Vögeln, Fischen, Insekten, Pflanzen, Mineralien u. s. w. sich seiner Neugierde darstellen, ist unübersehbar, die Geschichte dieser natürlichen Körper unermesslich. Ein einziger Theil dieser Geschichte konnte die geschicktesten Beobachter ihr ganzes Leben lang beschäftigen, und doch hatten sie am Ende nur noch unvollkommene Bruchstücke in diesen Theilen

Seite 4:

*geliefert, viele waren nur mühsame Sammler, beschrieben ängstlich jede Kleinigkeit von den äußersten Gestalten der natürlichen Körper, betrachteten die Natur in ihren Studierstuben und Kabinetten, und verfertigten trockene Namen=Verzeichnisse. Nur sehr wenige hatten Stärke des Geistes und Muth genug mit Riesenschritten auf der Bahne des unendlichen fortzuwandeln, und einen philosophischen Blick auf das Ganze zu werfen. Um Genien hervorzuzeigen mussten Jahrhunderte gebähren. Unsers zeugte **Linne** und **Buffon**. Der Naturkündiger muß zwei Eigenschaften besitzen, die einander entgegengesetzt zu seyn scheinen; den scharfen Blick eines feurigen Kopfes, der mit einmal ein großes Ganze übersehen kann, und die Gedult des kalten Beobachters, der mühsam jeden Gegenstand zergliedert. Seltene äusserst seltene Verbindung! Wenn man die beschwerliche Bahne nur mit einem flüchtigen Blicke durchläuft, die der Mineralog wandeln muß, um in seinem Fache sich über die Mittelmäßigkeit zu erheben, und eine Stufe der Vollkommenheit zu erreichen, wenn man all die glücklichen Umstände erwagt, die sich vereinigen müssen, einen Mineralogen vom ersten Range zu bilden; so muß man erkennen, wie viel dazu gehöre, nur in einem Theile der Naturgeschichte es weit zu bringen.*

Seite 5:

Der Mangel der Organisation, die unbestimmte veränderliche äußere Gestalt der Fossilien haben es nothwendig gemacht, ihre Bestandtheile zu untersuchen, um sie gründlich kennen zu lernen. Die äußern Kennzeichen derselben sind unzulänglich, und täuschen oft die besten Beobachter. Jene Mineralogen, die sich zu viel auf äußere Kennzeichen verließen, irrten weit mehr, als jene, die es mit der chemischen Untersuchung derselben zuweit trieben. Die Verbindung beider Mittel ist nothwendig, zur gründlichen Kenntniß der Fossilien zu gelangen.

Die Zergliederung der Fossilien ist die schwerste verwickelste Arbeit für den Chemisten. Vor **Pott** kannte man die Erden und Steine noch sehr wenig. Er war der erste, der die mühsamen Versuche mit denselben angestellt. Man hatte die Untersuchung derselben vernachläsigt, und sie entweder für unnütz gehalten, oder man wusste nicht, wie man mit den harten Körper des Steinreichs zu Werke gehen sollte, ihre Bestandtheile kennen zu lernen. Nach **Pott** bis auf **Waller und Kronstädt** untersuchte man die Fossilien bloß durch das Feuer. Die Mineralogie gewann dadurch auf einer Seite, auf der andern waren eine Menge Irrthümer eingeschlichen, wie es nicht anderst seyn konnte, da man sich eines so gewaltsamen Mittels, wie das Feuer ist, bedien=

Seite 6:

te, die Bestandtheile der Mineralien kennen zu lernen. **Waller und Kronstädt** machten eine neue Bahne, bedienten sich des nassen Wegs bei der Untersuchung der Mineralien, und da diese beiden Männer zugleich Bergleute und Gelehrte waren, so stieg die Mineralogie auf einen unerwarteten Grad der Vollkommenheit. **Kronstädt's** Werk bleibt daher immer ein für Mineralogen und Bergleute unentbehrliches Buch.

Man kann nicht begreifen, wie **Linne** noch nach ihm eine Mineralogie schrieb, die so wenig der Erwartung entsprach, die man von den Schriften eines so großen Naturkündigers haben muste. **Henkel, Margraf, Scheele und Bergmann** der Schwede, Chemisten vom ersten Range, lehrten uns durch ihre vortrefflichen Versuche eine Menge Mineralien besser zu kennen. Zu der Zeit, wo die Chemisten Licht in der Mineralogie verbreiteten, vernachläsigte man auf der andern Seite ein eben so wichtiges Hilfsmittel, die äußern Kennzeichen.

Werner einer der feinsten Beobachter unter den Mineralogen bearbeitete diesen Theil der Mineralogie besonders, setzte die äußern Kennzeichen besser, als all seine Vorgänger auseinander, setzte die Begriffe fest die man mit gewissen in der Mineralogie

Seite 7:

gebräuchlichen Ausdrücken zu verbinden hat, und verbannte alles zweideutige und unbestimmte. Man ließ diesem Manne nicht durchaus Gerechtigkeit widerfahren, und viele verließen aus Gemächlichkeit, oder aus Unvermögen ihren Schlendrian nicht.

Nebst der Kenntniß der Bestandtheile, und der äußern Gestalt der Fossilien sind die Geburtsstätte derselben, die Art ihrer Entstehung, die mannigfaltigen Veränderungen, die im Schooße der Erde mit ihnen vergehn, ihre Lage u. s. w. die wichtigsten und angenehmsten Gegenstände für den Mineralogen. Nur in den neuern Zeiten, wo sich Männer von Einsichten und Beobachtungsgeist auf die Bergwerkskunde gelegt, rastlos, und jeder Gefahr trotzend die Höhlen der Gebirge durchgekrochen sind, hat man deutlichere Begriffe von den Lagerstätten der Mineralien. Nur seitdem einige eben dieser Bergwerkskundigen Philosophen und Chemisten zugleich waren, weiß man etwas weniges, von ihrer Entstehung, von ihrem Wachsthume, und

*von den Veränderungen, die sie in ihrem natürlichen Zustande erlitten haben.
Pott, Waller, Kronstt, Henkel, Lehmann, Skopoli, von Born, von Saussure,
Ferber, Charpentier, Gerhard, Werner,*

Seite 8:

Scheele und Bergmann der Schwede stehn unter den Mineralogen oben an. Nur die vereinigten Krften dieser Mnner konnten die Geschichte des Mineralreichs zu jenem Grade der Vollkommenheit bringen, zu welchem sie in unsren Zeiten gediehen ist; und doch mu man erstaunen, wenn man den rastlosen Fleiß, den Beobachtungsgeist, die philosophische und chemische Kenntnisse, den Enthusiasmus dieser Mnner fr ihr Fach erwegt, dass eben diese Geschichte noch nicht vollstndiger ist.

Das erste Hinderni, welches in dem Studium der Naturgeschichte aufsttzt, ist die Menge der natrlichen Gegenstnde. Wirft man einen Blick auf ein zahlreiches Kabinet von gesammelten Naturprodukten, in einem botanischen Garten auf die Menge von Pflanzen, so ist die erste Empfindung Erstaunen, der erste Gedanke ein demuthigendes Misstrauen auf uns selbst. Man kann sich nicht vorstellen, wie es mglich sey, so viel Gegenstnde nur der auern Gestalt nach kennen zu lernen. Ein anders Hinderni, welches sich dem Fortgange unserer Kenntnisse entgegensemmt ist die Beschwerni die unzhligen Produkten so vieler Gegenden zusammenzubringen. Es fodert viel Zeit, Aufwand, Sorgen eine ansehnliche Mineralien= oder Thiersammlung zu machen, eine betrchtliche Menge Pflanzen in einem Garten

Seite 9:

zu erziehen. Mit was fr Beschwernissen ist es verbunden die Mineralien und Pflanzen an ihren Geburtsorten kennen zu lernen, die Thiere im Stande ihrer Wildheit, ihre Lebensart, ihre Instinkte, ihre Sitten zu beobachten. Viele bewohnen die hohen Gebirge, andere die Tiefe der Flsse und des Meers, andere die verborgensten unbewohntesten Gegenden des Erdbodens, andere bleiben nur eine Zeitlang bei uns, wandern aus einem Klima ins andere, andere entziehen sich durch ihre Kleinheit dem freien Auge des Forschers, sie fliehen fast alle die Gegenwart des Menschen ihres Tyrannen. Es ist ein seltenes glckliches Ungefr, wenn der Naturkndiger sie in ihrem natrlichen Zustande belauschen kann. Hat der Zoolog noch das seltene Glück lebendige Thiere, die man erzieht, beobachten zu knnen, so sieht er doch nur das was die Gefangenschaft, Erziehung, Nahrungsmittel verndertes Klima an ihnen verdorben haben.

Diese Beschwernisse schrecken jene nicht ab, die den Nutzen der Naturkunde erwegen, die einsehen, dass der Philosoph, der Arzt, der Oekonom, und der Knstler durch dieselbe jenen Grad der Vollkommenheit in ihren Wissenschaften erreichen, der sie fr die menschliche Gesellschaft ntzlich macht, und ber den Pbel erhebt, mssen Anfnger nicht ab-

Seite 10:

schrecken. Da es nun so viele Hilfsmittel giebt die Naturgeschichte zu studieren, da die unermdeten Bemhungen so vieler Naturkndiger, vorziglich der neuern, das Studium der Naturgeschichte so sehr erleichtert haben.

Es entsteht nur hier die Frage welcher Weg nher sey zur Kenntni der natrlichen Dinge zu gelangen. Ob es besser sey viel oft, und ohne Absicht ohne Ordnung zu sehen, oder ob die Methode den Weg zur grndlichen Kenntni der natrlichen Krper verkrzt?

Jene rohen Begriffe, die wir uns von sinnlichen Gegenständen ohne Fleiß, ohne Anweisung und Absicht machen, sind, wenn es nicht einfache Körper sind, jedem eigen, und bei mehreren verschieden. Diese Ungleichheit der Begriffe von den nämlichen Gegenständen verursacht weiter keine Unordnung im gemeinen Leben, wenn von gemeinen Sachen die Rede ist. Man kennt die Sache sogleich wenn man ihren Namen hört. Ganz anderst verhält es sich, wenn die Gegenstände nicht gemein sind, wenn sie in Menge vorkommen, und viele unter sich ähnlich sind. Das Gedächtniß behält von selbigen nur jene Merkmale; die sehr auffallen, und bei Betrachtung einer Menge löscht der stärkere Eindruck

Seite 11:

den schwächern aus. Wenn von dergleichen Gegenständen die Rede ist, so wird jener, der entweder die Namen, oder die Sachen selbst, die dadurch angezeigt werden vergessen hat, kein Hilfsmittel haben sich dieselbe wieder vorzustellen. Wenn ein solcher einen Gegenstand beschreiben sollte, so würden jene Merkmale die Beschreibung ausmachen, die ihm am meisten aufgefallen sind, und diese Beschreibung würde der Ausdruck der ihm eignen Idee des Gegenstands seyn.

Nun ist von den wenigsten Naturprodukten die Kenntniß ausgebreitet und gemein; wenn man sie auf die angeführte Art wollte kennen lernen, könnte man sich wohl versprechen, dass dieser Weg zur gründlichen Kenntniß der Natur führe. Ein Mensch mit den besten Sinnen, mit der lebhaftesten Einbildungskraft, mit dem besten Gedächtniß, der in die vortheilhafteste Lage versetzt wär eine Menge Naturprodukte zu sehn, würde Jahre lang sie ansehn, ohne zu wissen, aufwas er besonders in Betrachtung dieser Gegenstände seine Aufmerksamkeit zu richten habe, ohne sie voneinander unterscheiden zu lernen, ohne sich die Menge wieder vorstellen zu können, er würde vielleicht endlich durch Hilfe seines guten Kopfes den Weg der Erfinder wandeln sich eine eigne Methode in seinem Kopfe machen, wodurch er sich die Kennt=

Seite 12:

niß derselben erleichterte, und sein Gedächtniß unterstützte, endlich nach langer Zeit erst dahin kommen, wo man schon war, als die Naturgeschichte noch in ihrer Kindheit gewesen.

*Die ersten Kräuterkundigen haben viel von den Heilkräften, und vom ökonomischen Nutzen der Pflanzen geschrieben, ohne sie selbst deutlich zu beschreiben, sie setzten unglücklicher Weise die historische Kenntniß derselben als bekannt voraus, oder zeichten sie wenn sie Lehrer waren, ihren Schülern. Jene, von welchen noch kein Nutzen bekannt war, führten sie kaum an. Die neuern Botaniker konnten nur aller angewandter Mühe ohngeachtet nicht errathen, mit was für Pflanzen sie Versuche gemacht haben, und kennen die meisten Pflanzen nicht, welche sie anführen. Traurig genug, dass die Erfahrung so vieler Jahrhunderte für uns von keinem Nutzen ist. **Theophrast** soll über fünf hundert Gattungen von Pflanzen gekannt haben, und **Plinius** führt über tausend an. Er handelt aber nur von ihrer Kultur von ihrem medizinischen und ökonomischen Nutzen, und in wie weit sie zur Zierde der Gärten dienten, er beschreibt sie sehr wenig, besonders jene wo er noch keinen Nutzen kannte. Es ist wahrscheinlich, dass die ersten und ältern Kräuterkundiger nicht viel besser die Pflanzen kannten als unsere empirische Gärtner*

Seite 13:

und Apotheker. Die Botanik stand auch zu ihren Zeiten in keiner großen Achtung, die Griechen und Römer betrachteten sie nicht als eine besondere Wissenschaft, sondern nur in Bezug auf die

Gärtnerey den Ackerbau, die Heilkunst u. s. w.

Wenn **Aristoteles** und **Plinius** uns viel wichtiges und nützliches von den Eigenschaften der Thiere in ihren Schriften hinterlassen haben, so ist es kein Wunder, sie waren Philosophen und Genien vom ersten Range. Auch ließ **Alexander** mit großen Unkosten aus allen Theilen der Welt Thiere sammeln und setzte den **Aristoteles** in den Stand, sie beobachten zu können. Er kannte daher ihre Lebensart, ihre Instinkte, ihre innere Struktur sehr genau, und besser als viele neuere Naturkündiger. Er kannte eine Menge Thiere und ohne Zweifel die Unterscheidungs-kennzeichen von vielen, ohne sich weitläufig in Beschreibungen einzulassen. Er hielt unglück-licher Weise diese Beschreibungen nicht für so nothwendig. Er hat in seinen Schriften über die Natur der Thiere der Nachwelt einen Schatz von Beobachtungen hinterlassen, und gewiß mehr dadurch genützt, als durch seinen Dialektik.

Plinius arbeitete nach einem sehr weitläufigen und vielleicht zu ausgedehnten Plane. Sein weit=

Seite 14:

sehender Geist wollte alles umfassen, und fand die Natur noch für ihn zu klein. Er handelt in seiner Naturgeschichte von Mineralien, Pflanzen und Thieren, von Himmel und Erde, von der Arzneykunst, von Schiffart, von freien und mechanischen Künsten, von allen natürlichen Wissenschaften und menschlichen Künsten. Er wusste nicht allein, was er zu seiner Zeit wissen konnte, sondern hatte noch jene Leichtigkeit im Großen zu denken, wodurch die Wissenschaften ihren Zuwachs erhalten, jene Feinheit im Nachdenken, von welcher der gute Geschmack abhängt, er theilt seinen Lesern eine gewisse Freiheit zu Denken und Künheit des Geistes mit, der Philosophen bildet. Sein Werk ist, wenn man will, eine Kompilation von allem dem, was von ihm geschrieben war, eine Kopie von allem was wichtig und nützlich zu wissen war, aber diese Kopie hat so viel herrliche Züge, diese Kompilation ist so wohlgerathen, dass sie viel Originalwerken, die von dem nämlichen Stoffe handeln, vorzuziehen ist.

Die Geschichte und genaue Beschreibung der natürlichen Körper sind zween Hauptvorwürfe, auf die man im Studium der Naturgeschichte sein Augenmerk richten muß. Die alten sind in Ansehung der Geschichte vieler natürlicher Körper zum Beispiele der Thiere so weit vielleicht über die neueren Natür=

Seite 15:

kündiger, als diese in der Beschreibung der äußern Gestalt über die alten sind.

Man muß die Methoden in der Naturgeschichte nicht für Hauptgrundsätze der Wissenschaft selbst ansehen, sondern als Zeichen, die man erfunden hat, um sich besser zu verstehen, als verschiedene Gesichtspunkte, unter welchen die Naturkündiger die Natur betrachtet haben. Eine Methode ist ein wohlgerathnes Wörterbuch, wo man die verschiedenen Namen der Gegenstände nach der von dem Verfasser festgesetzten Idee geordnet findet. Die Versuche natürlicher Methoden waren bisher alle fruchtloß, und nur sehe [sic!] unvollständige Fragmente. Die Natur geht in ihren Produkten stufenweiß, sie verlaufen sich ineinander wie die Farben, und ihre Nuancen sind oft nur zu fein als dass es immer möglich sey, die feine Linie anzugeben, wo eine aufhört und die andere anfängt. Dem ungeachtet haben die künstlichen Methoden ihre großen Vortheile, sie zeichen dem Anfänger die Übersicht des Unermesslichen in einem kleinen Raume, unterstützen das Gedächtniß, lehren ihn auf was er in Betrachtung der natürlichen Gegenstände zu sehn hat, helfen ihm nach einer gewissen zweckmässigen Ordnung, und durch angemessene Benennungen die gesehnen Gegenstände sich leichter wieder vorzustellen. Man muß aber endlich alle

Methoden studieren, sich die mancherley Gesichtspunkte bekannt machen, unter welchen die Naturkündiger die Natur betrachtet haben.

Nach der gründlichen historischen Kenntniß der natürlichen Körper geht der gute Kopf weiter, vergleicht seine einzelnen Beobachtungen, zieht allgemeine Grundsätze daraus wodurch für die Naturlehre neue Aussichten geöffnet werden. Sein Hauptzweck ist der Nutzen der natürlichen Körper. Er bildet sich alsdenn durch gründliche Kenntnisse in der Naturgeschichte vorbereitet leicht zum Oekonomen, zum Arzten, zum Philosophen oder zum Künstler.

Im „**Studium der Naturgeschichte**“ erwähnte Wissenschaftler

- Alexander; * 356 v. Chr., Pella, † 323, v. Chr., Babylon.
Aristoteles; * 384 v. Chr., Stageira (Chalkidike), † 322 v. Chr., Chalkis (Euböa).
Bergman(n), Torbern Olaf; * 1735, Katrineberg (Schweden), † 1784, Medevi (Schweden).
Born, Ignaz Edler von; * 1742, Alba Julia (Rumänien), † 1791, Wien.
Buffon, Georges Louis Leclerc; * 1707, Montbard (Frankreich), † 1788 Paris.
Charpentier, Johann Friedrich Wilhelm Toussaint von; * 1738, Dresden, † 1805, Freiberg.
Cronstedt (Kronstädt), Axel Frederik von; * 1722, Tübingen (Schweden), † 1765, Säter (Schweden).
Ferber, Johann Jacob; * 1743, Carlskrona (Schweden), † 1790, Bern.
Gerhard, Carl Abraham; * 1738, Lerchenborn bei Liegnitz (Schlesien), † 1821 Berlin.
Hen(c)kel, Johann Friedrich; * 1678, Merseburg, † 1744, Freiberg.
Lehmann, Johann Gottlob; * 1719, Langenhennersdorf (Sachsen), † 1767, St. Petersburg.
Linné, Carl von; * 1707, Södra Råshult (Småland), † 1778, Uppsala.
Marg(g)raf, Andreas Sigismund; * 1709, Berlin, † 1782, Berlin.
Plinius, Gaius Secundus (der Ältere); * 23, Como, † 79, Stabiae.
Pott, D. Johannis Henrici; * 1692, Halberstadt (Deutschland), † 1777, Berlin.
Saussure, Horace-Bénédict de; * 1740, Conches (Genf), † 1799, Genf.
Scheele, Carl Wilhelm; * 1742, Stralsund (Deutschland), † 1786, Köping (Schweden).
Skopoli, Giovanni Antonio; * 1723, Cavalese (Italien), † 1788, Pavia.
Theophrast(us); * 371 v. Chr., Eresus (Lebos), † 287 v. Chr., Athen.
Waller(ius), Johan Gottschalk; * 1709, Stora Mellösa (Schweden), † 1785, Uppsala.
Werner, Abraham Gottlob; * 1749, Wehrau (Polen), † 1817, Dresden.

Anhang 3: Huldigung an den Kurfürsten Friedrich Karl Joseph von Erthal.

(* 3. Jänner 1719, Mainz; † 25. Juli 1802, Aschaffenburg).

*Hochwürdigster Erzbischof,
Gnädigster Kurfürst, und Herr
Herr!*

Ew. kurfürstlichen Gnaden errichteten den Lehrstuhl der Naturgeschichte auf hiesiger Universität, damit die Kandidaten der Arzney, der Kameralwissenschaft und Philosophie dadurch desto gründlicher den übrigen Theilen ihrer Wissenschaften studieren können.

Höchstdieselbe unterstützten mich großmüthigst auf meinen Reisen, damit ich mich in meinem so weitläufigen Fache vervollkommnen konnte, stifteten auf hiesiger Universität eine ansehnliche Sammlung von Mineralien, und anderen Naturalien, und ließen einen botanischen Garten anlegen.

Unvergeßlich wird jedem Patrioten all das Große seyn, was unter der Regierung Ew. Kurfürstlichen Gnaden geschehen ist, unauslöschlich bey mir das Dankgefühl für die große, vielfältige Gnaden, welche Höchstdieselbe mir zufließen ließen, gränzenlos meine Freude, wenn Höchstdieselbe auf diese meine Schrift, welche ich Ew. Kurfürstl. Gnaden unterthänigst widme und zu Füßen lege, mit gnädigsten Blicke herabsehen, und ich hoffen darf, daß ich die erhabensten Absichten meines gnädigsten Landesvaters einst zu erfüllen im Stande und der höchsten Gnaden nicht ganz unwürdig sey.

*Ew. kurfürstl. Gnaden
u. gn. Herrn
Herrn
untertänigster
Joh. Fibig.*

Anhang 4: Die Einteilung der Mineralien im Handbuch der Mineralogie verfasst von J. Fibig.

Erste Klasse. Salze

- Erste Ordnung. Saurer Salze.
- Erste Abtheilung. Gemeine Säuren.
- I. Vitriolsäure.
- II. Salpetersäure.
- III. Kochsalzsäure.
- Zweite Abtheilung. Abweichende Säuren.
- IV. Flüsäure.
- V. Arseniksäure.
- VI. Wasserbleisäure.
- VII. Tungsteinsäure.
- VIII. Phosphorsäure.
- IX. Boraxsäure.
- X. Bersteinsäure.
- XI. Luftsäure.

Zwote Ordnung. Laugensalze.

- I. Mineralisches Laugensalz.
- II. Vegetabilisches Laugensalz.
- III. Flüchtiges Laugensalz.
- Dritte Ordnung. Zusammengesetzte Salze.
- I. Vitriolisierter Weinstein.
- II. Glaubersalz.
- III. Bittersalz.
- IV. Aluan.
- V. Vitriol.
- VI. Salpeter.
- VII. Kochsalz.
- VIII. Salmiak.
- IX. Borax.

Zwote Klasse. Erden und Steine.

- Erste Hauptabtheilung.
- Gleichartige Erd- und Steinarten.
- A. Einfache nur aus einer Grunderde bestehende.
- Erste Ordnung. Alkalische Erden und Steine.
- Erster Abschnitt. Alkalisch=kalchartige Erden und Steine.
- I. Kalcherde.
- II. Kalchstein.
- III. Kalchspath.
- IV. Stinkstein.
- Zweyter Abschnitt. Alkalisch=bittersalzige Erden.
- Gerhards Salzstein.
- Dritter Abschnitt. Alkalisch=alaunische Erden.
- Alaunerde.
- Vierter Abschnitt. Alkalisch=schwererdige Erd- und Steinarten. Schwerstein.
- Zwote Ordnung. Gypsige Erd- und Steinarten.
- I. Gyps.
- II. Gypsspat.
- Dritte Ordnung. Schwerspathartige Erden und Steine.
- I. Schwerspatherde.
- II. Schwerspath.
- Vierte Ordnung. Flüsse.
- Fluß.
- B. Gemischtere Erden und Steinarten.
- Erste Ordnung. Glasartige Steine.
- I. Quarz.
- II. Hornstein.
- III. Praser.
- IV. Kiesel.
- V. Jaspis.
- Zwote Ordnung. Thonige Erden und Steine.

I. Thon.

- II. Trippel.
- III. Glimmer.
- IV. Feldspath.
- Dritte Ordnung. Thonige=kalchartige Erden und Steine.
- I. Mergel.
- II. Schiefer.
- III. Edelgestein.
- IV. Granat.
- V. Schörl.
- VI. Turmalin.
- VII. Zeolith.
- VIII. Pechstein.
- Vierte Ordnung. Kießlich=bittersalzige Erden und Steine.
- I. Speckstein.
- II. Talk.
- III. Amyanth.
- Fünfte Ordnung. Bittersalzig=kalcherdige Steine.
- Gerhards Blätterstein.
- Sechste Ordnung. Steine, welche aus Kießelerde, Schwererde, Alaunerde und Kalcherde bestehen.
- Leberstein.
- Zwote Hauptabtheilung.
- Ungleicherliche Steine.
- Erster Abschnitt. Krystallinische.
- I. Granit.
- II. Gneuß.
- Zweiter Abschnitt. Ungeformter Schnitt.
- I. Porphy.
- II. Ophit.
- Dritter Abschnitt. Zusammengeküttere.
- I. Breccia.
- II. Sandstein.

Dritte Klasse. Brennbare Mineralien.

- Erste Abtheilung. Gemeine.
- Erster Abschnitt. Einheimische.
- Schwefel.
- Zweyter Abschnitt. Fremde.
- I. Torf.

II. Steinkohle.

- III. Bergöl.
- IV. Erdharz.
- Zwote Abtheilung. Abweichende.
- I. Diamant.
- II. Reißblei.

Vierte Klasse Metalle.

- I. Gold
- II. Platin.
- III. Silber.
- IV. Quecksilber.
- V. Bley.
- VI. Kupfer.
- VII. Eisen.
- VIII. Zinn.
- IX. Zink.
- X. Wismuth.
- XI. Spiegelglas.
- XII. Arsenik.
- XIII. Kobolt.
- XIV. Nickel.
- XV. Braunstein.
- XVI. Schwermetall.

Anhang. Von vulkanischen Produkten.

DER EINFLUSS DES TITANIT-AKTIVITÄTSMODELLS AUF DIE LAGE VON
TITANIT-INVOLVIERENDEN MINERALREAKTIONEN AUS DEN METABASITEN
DES SPRONsertales (SÜDTIROL, ITALIEN)

von

Martina Tribus & Peter Tropper

Institut für Mineralogie und Petrographie
Universität Innsbruck, Innrain 52f, A-6020 Innsbruck, Österreich

Zusammenfassung

Die Lage von berechneten Mineralreaktionen ist stark von der Wahl der Aktivitätsmodelle der beteiligten Phasen abhängig. In dieser Untersuchung von Metabasiten aus dem Spronsertal wurden ausgewählte titanit-involverende Reaktionen auf ihre Abhängigkeit von der Wahl des Aktivitätsmodells für Titanite hin untersucht. In den Untersuchungen wurde deutlich, dass je nach verwendetem Titanit-Aktivitätsmodells diese titanit-involverenden Reaktionskurven im *P-T* Raum versetzt werden. Dabei markieren jene Berechnungen, welche mit dem molekularen Aktivitätsmodell durchgeführt worden sind, die *P* Untergrenze und die Reaktionskurven, welche auf dem gekoppelten Mischungsmodell basieren, die *P* Obergrenze. So beträgt der Versatz der Reaktionskurven bei einem X_{Ti} Unterschied von ca. 0.02 bereits zwischen 10°C und 50°C und 0.4 bis 1.5 kbar, je nach Reaktion und stöchiometrischen Koeffizienten von Titanit.

Einführung

Grundlage für die Berechnung von Mineralreaktionen bildet die Aktivität der in die Reaktion involvierten Minerale. Diese ist von dem verwendeten Aktivitätsmodell abhängig. Wichtigste Größe für die Berechnung von Aktivitätsmodellen ist das chemische Potential einer Phase (μ_i), das sich aus dem Standardpotential (μ_i^0) und aus der Abweichung von diesem idealen Verhalten, die von der Aktivität der Komponente i der Phase (a_i) abhängig ist, zusammensetzt. Daher gilt: $\mu_i = \mu_i^0 + RT \ln a_i$. Das chemische Standardpotential kann in thermodynamischen Tabellen nachgeschlagen werden, während sich die Aktivität (a_i) aus den mineralchemischen Messungen (zum Beispiel an der Mikrosonde) der Phasen in den Proben ergibt. Die Aktivität bildet somit die Brücke zwischen der idealisierten Annahme vom Mischungsverhalten der Phasenkomponenten (z.B. Almandin etc.) und der reellen Zusammensetzung eines Minerals. Man unterscheidet zwischen idealen und nicht-idealnen Aktivitätsmodellen (SPEAR, 1995).

Ideale Mischungsmodelle: Diese idealen Modelle zeichnen sich durch eine ideale Mischbarkeit zwischen den Phasenkomponenten aus. Dabei nehmen die Mischungsenthalpie (ΔH_{mixing}) und das Mischungsvolumen (ΔV_{mixing}) jeweils einen Wert von 0 an. Die Mischungsentropie (ΔS_{mixing}) ist allerdings niemals 0. Daher gilt: $\mu_i = \mu_i^0 + RT \ln X_i$. Je nach Mischungsverhalten unterscheidet man zwischen einem molekularen und einem ionischen Mischungsmodell (SPEAR, 1995).

Molekulares Mischungsmodell: Das einfachste, in Mineralen aber nie tatsächlich verwirklichte Modell, ist das molekulare Mischungsmodell. Dieses Modell geht von der Annahme aus, dass die Komponenten als ganze Formeinheiten, also als Moleküle, unabhängig von ihren kristallographischen Positionen im Gitter mischen. Beispiel am Granat: $X_{\text{Py}} = X_{\text{Mg}} = a_{\text{Py}}$. Dieses Modell gibt daher die Obergrenze für die numerischen Werte der Aktivitäten dar.

Ionisches Modell (mixing on sites): Dieses Modell basiert auf der Annahme, dass die Mischung der Kationen auf bestimmten kristallographischen Plätzen im Gitter auftritt. Dabei kann zwischen einfachen und komplexen Mischungen unterschieden werden. Die einfache ionische Mischung impliziert eine Mischung auf einem bestimmten Gitterplatz. Beispiel am Granat: $(\text{Fe}, \text{Mg})_3\text{Al}_2\text{Si}_3\text{O}_{12}$; $a_{\text{Alm}} = X_{\text{Fe}}^3$ oder $a_{\text{Py}} = X_{\text{Mg}}^3$. Das komplexe ionische Modell erlaubt Mischungen auf mehreren kristallographischen Plätzen. Es gilt die Annahme einer statistischen Verteilung der Komponenten. Beispiel am Granat: $(\text{Fe}^{2+}, \text{Ca})_3(\text{Al}, \text{Fe}^{3+})_2\text{Si}_3\text{O}_{12}$; $a_{\text{Alm}} = X_{\text{Fe}^{2+}}^3 \cdot X_{\text{Al}}^2; a_{\text{Andr}} = X_{\text{Ca}}^3 \cdot X_{\text{Fe}^{3+}}^2$. Dieses Modell gibt die Untergrenze für die numerischen Werte der Aktivität an, da hier mehrere Molenbrüche miteinander multipliziert werden. Diese zwei ionischen Modelle erlauben eine zufällige Mischung auf den jeweiligen Gitterplätzen (random mixing on all sites). In einigen Mineralen kommt es aber zu einem gekoppelten Kationenaustausch auf bestimmten kristallographischen Positionen. Gute Beispiele dafür sind die Tschermak-Substitution ($\text{MgSi} \leftrightarrow \text{AlAl}$) oder die Plagioklas-Substitution ($\text{NaSi} \leftrightarrow \text{CaAl}$). Man spricht dann vom ideal gekoppelten Mischungsmodell. Beispiel am CATS: $\text{Ca}^{\text{M}2}\text{Al}^{\text{M}1}(\text{Al}, \text{Si})^{\text{T}}\text{O}_6$; $a_{\text{CATS}} = 4 \cdot X_{\text{Ca}}^{\text{M}2} \cdot X_{\text{Al}}^{\text{M}1} \cdot X_{\text{Si}}^{\text{T}} \cdot X_{\text{Al}}^{\text{T}}$. Bei diesem Modell muß allerdings ein zusätzlicher Korrekturfaktor (beim Beispiel CATS „4“) angewandt werden damit die Aktivität des reinen Endgliedes wieder einen Wert von 1 annimmt.

Nicht-ideale Mischungsmodelle: In den nicht-idealnen Aktivitätsmodellen gilt $\Delta V_{\text{mixing}} \neq 0$ und $\Delta H_{\text{mixing}} \neq 0$. Diese Abweichungen vom idealen System werden mittels eines Korrekturfaktors welcher als Aktivitätskoeffizient (γ) bezeichnet wird, beschrieben. Solche nicht-idealnen Mischungsmodelle beinhalten also neben der mineralchemischen Zusammensetzung (X_i) zusätzlich einen Aktivitätskoeffizienten (γ). Daher gilt wieder: $\mu_i = \mu_i^0 + RT \ln a_i$. Die Aktivität a_i einer Komponente i in der Mischphase ist das Produkt aus dem Molenbruch X_i und dem Aktivitätskoeffizienten der Komponente i einer Mischphase und kann angeschrieben werden als $a_i = X_i \cdot \gamma_i$. Beispiel am Granat (Almandin-Komponente im Granatmischkristall): $\text{Fe}^{2+}3\text{Al}_2\text{Si}_3\text{O}_{12}$; $a_{\text{Alm}} = (X_{\text{Fe}} \cdot \gamma_{\text{Fe}})^3 \cdot (X_{\text{Al}} \cdot \gamma_{\text{Al}})^2$. Der Aktivitätskoeffizient ist eine Funktion von mineralchemischer Zusammensetzung (X_i), P und T . Mit zunehmender Temperatur nähert sich dieser Koeffizient dem Wert 1 an. Die Mischungsenthalpie, die Mischungsentropie und die Gibbsche freie Energie dieser Mischung sind daher nicht-ideal. Diese Energie setzt sich aus einem idealen und einem nicht-idealnen („excess“) Anteil zusammen. Die Polynome, welche diese Exzessfunktion beschreiben, beinhalten Koeffizienten, die sog. Margules Parameter (W_G).

Natürliche nicht-ideale Mischkristalle zeichnen sich entweder durch eine symmetrische (reguläre) oder eine asymmetrische (subreguläre) Exzessfunktion aus. Je nachdem unterscheidet man zwischen symmetrischen (mit einem Margules Parameter) und asymmetrischen (mit zwei Margules Parametern) Mischungsmodellen (SPEAR, 1995).

Geologischer Überblick und Petrographie der Metabasite

Im SE des Ötztal-Stubai Komplexes liegt der HP-betonte Texel Komplex. Dieser wird zum sog. eo-Alpinen Hochdruckgürtel (eo-Alpine High Pressure Belt = EHB) gezählt. Im N und NW wird dieser Texel Komplex vom Ötztal-Stubai Komplex überlagert. Im S überlagert der Texel Komplex die Austroalpinen Einheiten des Ortler-Campo Complexes und im SE grenzt er an die Südalpinen Einheiten. Lithologisch setzt sich der Texel Komplex im Bereich des Spronsertals und des Saltausertals hauptsächlich aus Metasedimenten zusammen. Untergeordnet treten Orthogneise, Amphibolite, Eklogit-Amphibolite, Eklogite und Metakarbonate auf. Bei den untersuchten Proben aus dem Spronsertal handelt es sich um Amphibolite mit folgender Hauptparagenese:



Als Ti-führende Phasen kommen in den Amphiboliten aus dem Spronsertal die Minerale Titanit, Ilmenit und Rutil vor, wobei Titanit am häufigsten vertreten ist. Die Akzessorien Ilmenit und Rutil treten nie als eigenständige Körner auf, sondern bilden immer Einschlüsse im Titanit (Abb. 01). Rutil und Ilmenit sind häufig miteinander verwachsen, sodaß sich keine exakte Aussage bezüglich der Kristallisationsfolge machen lässt. Während die Ilmenite und Rutile ausschließlich in xenomorpher Form vorliegen, zeigen einige Titanite den typischen briefkuvertförmigen Habitus senkrecht zur kristallographischen c-Achse. Der Gehalt an Al in den Titaniten liegt zwischen 0.03 und 0.05 apfu, an (F+OH) zwischen 0.04 und 0.07 apfu und die Werte für Fe³⁺ streuen zwischen 0.006 und 0.012 apfu (TRIBUS, 2009).

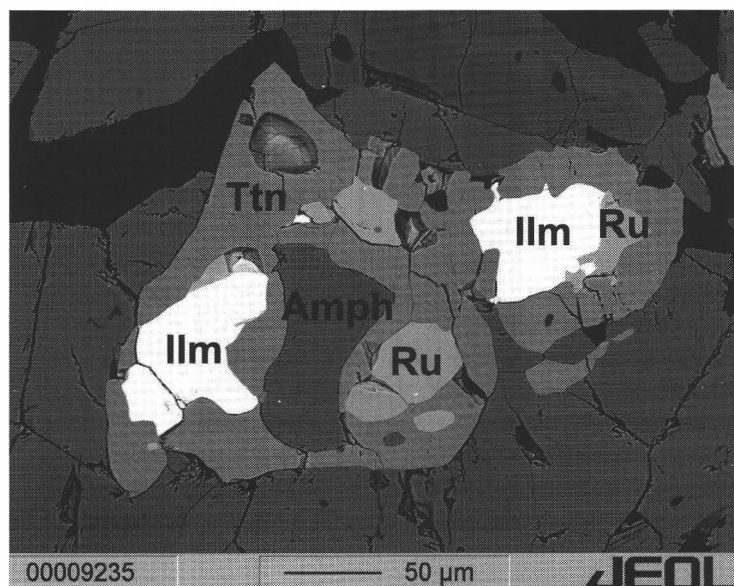


Abb.01.:
BSE-Bild von Titanit-
Ilmenit-Rutil-Aggregaten
mit Amphibol-Einschluss..

Titanit-Aktivitätsmodelle

In den letzten Jahren wurden in mehreren Arbeiten diverser Autoren die thermodynamischen Eigenschaften und Stabilitäten von Titanit-Mischkristallen diskutiert (TROPPER et al. 2002, 2008; HARLOV et al., 2005 ; TROITZSCH & ELLIS, 2002). Abweichungen von der idealen Titanit-Zusammensetzung ($\text{CaTiSiO}_4\text{O}$) ergeben sich durch Kationen- und Anionen-Substitutionen [$\text{Ca}(\text{Ti}, \text{Al}, \text{Fe}^{3+})\text{SiO}_4(\text{O}, \text{F}, \text{OH})$]. Die dominierenden strukturellen Einheiten im Titanit sind Ketten von TiO_6 -Oktaedern, welche über eine Ecke miteinander verknüpft sind. Diese Ketten sind über SiO_4 -Tetraeder verbunden. Das führt zur Bildung eines $[\text{TiOSiO}_4]^{2-}$ -Gitters mit großen Hohlräumen in denen Ca-Atome in irregulären, siebenfach koordinierten Polyedern angeordnet sind. Ein SiO_4 -Tetraeder ist über eine seiner Kanten mit einem solchen CaO_7 -Polyeder verknüpft. Ein TiO_6 -Oktaeder teilt sich vier seiner Kanten mit dem CaO_7 -Polyeder. Es gibt pro Formeleinheit ein O-Atom, O1, das nicht an ein SiO_4 -Tetraeder gebunden ist, und welches durch OH und F ersetzt werden kann. Diese O1-Position stellt jenes O-Atom dar, welches zwei TiO_6 -Oktaeder in der Kette miteinander verbindet (DEER, HOWIE & ZUSSMAN, 1992) (Abb. 02).

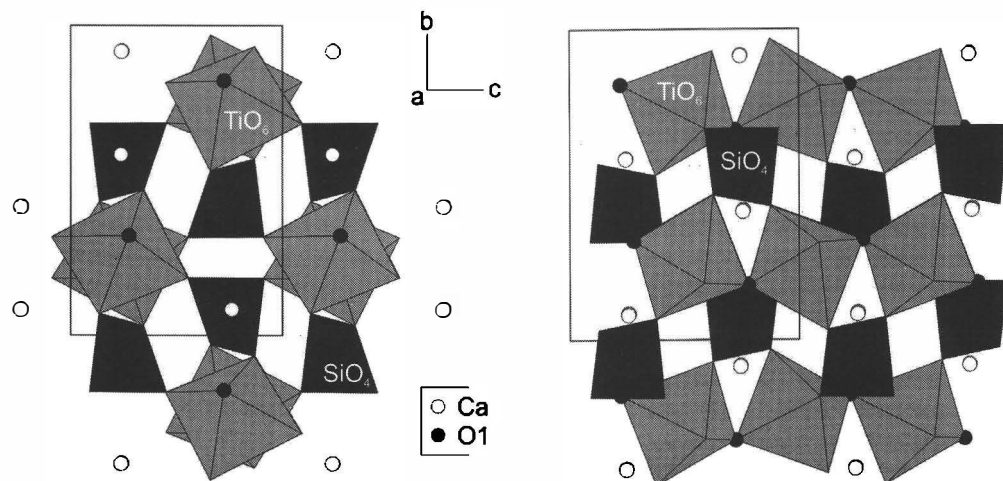


Abb.02.:

Titanit-Struktur mit eingetragener O1-Position (schwarze Punkte); senkrecht zur kristallographischen a-Achse (rechts), und senkrecht zur kristallographischen c-Achse (links).

Die Substitution von Kationen kann auf jeder der drei Kationen-Positionen (Ti, Ca, Si) stattfinden. In natürlichen, krustalen Gesteinen spielt die Substitution auf der Si-Position allerdings eine untergeordnete Rolle. In den Aktivitätsmodellen wird ausschließlich die Kationen-Substitution auf der oktaedrischen Ti-Position berücksichtigt. Neben Ti und Al kann auf dieser Position zudem Fe^{3+} eingebaut werden. Um den Ladungsverlust durch den Einbau der trivalenten Kationen Fe^{3+} und Al auszugleichen, wird das Sauerstoffatom auf der O1-Position durch F oder OH ersetzt. Durch die Substitution von $\text{Al}+\text{F} \leftrightarrow \text{Ti}+\text{O}$ wird die Struktur des Minerals nicht verändert. Diese $\text{Al}+\text{F}$ Substitution kann in natürlichen Titaniten sehr ausgeprägt auftreten, trotzdem gibt es keine vollständige Mischbarkeit im System $\text{CaTiSiO}_4\text{O} - \text{CaAlSiO}_4\text{F}$.

Diese kann nur experimentell erreicht werden (TROITZSCH & ELLIS, 2002; TROPFER et al., 2002). Die Al+OH \leftrightarrow Ti+O Substitution in Richtung Al-OH Endglied, Vuagnatit, hingegen verläuft nicht isostrukturell. Der zunehmende Einbau von Al führt zu einer Kontraktion der Oktaeder und dadurch zu einer Verkleinerung der Titanit-Einheitszelle. Diese Tatsache zeichnet Al-reiche Titanite als Indikatoren für erhöhte Druckbedingungen aus. Während Al-F Titanite über einen weiten *P* Bereich vorkommen ist das Auftreten der Al-OH Substitution typisch für niedrig temperierte Bedingungen (ENAMI, et al., 1993).

Ideale Titanit-Aktivitätsmodelle: Das einfachste, molekulare Modell, geht davon aus, dass die Kationen-Substitution ausschließlich auf der Ti-Position auftritt und somit der Anteil an Ti auf dieser Position (X_{Ti}) der Aktivität $a_{CaTiSiO_4O} = X_{Ti}$ entspricht. MANNING & BOHLEN (1991) untersuchten das random mixing Modell, welches zufällige Mischungen auf allen Kationen-Positionen und den fünf Anionen-Positionen erlaubt. Dadurch ergibt sich eine Titanit-Aktivität von $a_{CaTiSiO_4O} = X_{Ca}X_{Ti}X_{Si}X_O^5$. Da sich jedoch die Substitution von F und OH ausschließlich auf die O1-Position bezieht, wurde von TROPFER et al. (2002) basierend auf den Untersuchungen von OBERTI et al. (1991), das ideale gekoppelte ionische Modell beschrieben. Im Gegensatz zum random mixing Modell berücksichtigt dieses Modell die Tatsache, dass die Substitution der Anionen ausschließlich auf der O1-Position auftritt. Für das Aktivitätsmodell gilt demnach $a_{CaTiSiO_4O} = X_{Ca}X_{Ti}X_{Si}X_O$. Davon ausgehend, dass in krustalen Gesteinen auf der Si- und Ca-Position keine signifikanten Substitutionen auftreten, reduziert sich dieses Modell auf $a_{CaTiSiO_4O} = X_{Ti}X_O$.

Nicht-ideale Titanit-Aktivitätsmodelle: Grundlage zur Erstellung dieser Aktivitätsmodelle stellen experimentelle Untersuchungen diverser Autoren dar. Dabei gilt vor allem den Arbeiten von TROITZSCH & ELLIS (2002) und TROPFER et al. (2002) besonderes Augenmerk. TROITZSCH & ELLIS (2002) und TROPFER et al. (2002) untersuchten in ihren Arbeiten nicht-ideale Mischungsmodelle entlang der Zusammensetzung $CaTiSiO_4O-CaAlSiO_4F$. Während TROITZSCH & ELLIS (2002) ein reguläres Aktivitätsmodell mit einem positiven Margules-parameter W_G bevorzugen, erstellten TROPFER et al. (2002) ein Modell dessen W_G Parameter einen negativen Wert annimmt. Durch diese zwei verschiedenen Ansätze ergeben sich unterschiedliche nicht-ideale Titanit-Aktivitäten. TROITZSCH & ELLIS (2002) verwendeten für ihre Berechnungen zwei Aktivitätsmodelle, ein Multi-site mixing Modell (MM) und ein local charge balance Modell (LCB). Das MM Modell erlaubt eine unabhängige Verteilung von F und Al auf den jeweiligen Positionen, während das LCB Modell von einer gekoppelten Al-F Substitution ausgeht. Daraus ergeben sich folgende Formulierungen:

$$\begin{aligned} \text{MM Modell: } a_{CaTiSiO_4O} &= (X_{Ti})^2 \gamma_{CaTiSiO_4O} \\ \text{LCB Modell: } a_{CaTiSiO_4O} &= (X_{Ti}) \gamma_{CaTiSiO_4O} \end{aligned}$$

In Abhängigkeit dieser Aktivitätsmodelle ergeben sich unterschiedliche Margules Parameter:

$$\begin{aligned} \text{MM Modell: } W_G &= 13.6 \text{ kJmol}^{-1} \\ \text{LCB Modell: } W_G &= -9.1 \text{ kJmol}^{-1} \end{aligned}$$

Von den Autoren wird das MM Modell und der daraus resultierende positive Margules Parameter bevorzugt. Die Untersuchung von TROPPER et al. (2002) stützt sich auf ein local charge balanced (LCB) Modell: $[a_{\text{CaTiSiO}_4} = (X_{\text{Ti}})\gamma_{\text{CaTiSiO}_4}]$. Der Margules Parameter zeigt, im Gegensatz zu den Ergebnissen von TROITZSCH et al. (2002), eine ausgeprägte T Abhängigkeit und nimmt mit steigender Temperatur einen kleineren, negativen Wert an. Bei Temperaturen von 1100°C beträgt der Margules Parameter $0.93 \pm 0.86 \text{ kJmol}^{-1}$. Beim Vergleich der diversen Titanit-Aktivitätsmodelle in Abbildung 03 wird deutlich dass das ideale molekulare Modell die Obergrenze der berechneten Aktivitäten darstellt während das gekoppelte Mischungsmodell nach OBERTI et al. (1991) das Aktivitätsminimum markiert. Das reguläre Mischungsmodell von TROPPER et al. (2002) ergibt Aktivitäten, welche zwischen diesen beiden Modellen liegen, wobei sich die Aktivitäten zwischen 0 und 0.4 X_{Ti} deutlich an das gekoppelte Mischungsmodell annähern. Das MM Modell, welches von TROITZSCH & ELLIS (2002) berechnet wurde, tendiert zwischen ca. 0.2 und 0.4 X_{Ti} in Richtung molekularem Modell. Während die Abweichung der Titanit-Aktivität des gekoppelten Mischungsmodells vom molekularen Mischungsmodell zwischen $X_{\text{Ti}}=0-1$ eine symmetrische Kurve beschreibt zeigen die regulären Aktivitätsmodelle einen asymmetrischen Verlauf (Abb. 04)

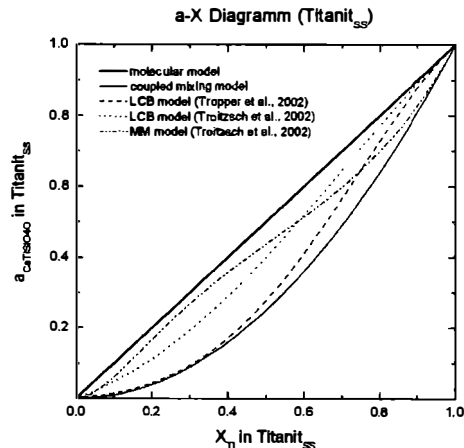


*Abb.03.:
Aktivitäten von a_{CaTiSiO_4} in $\text{Titanit}_{\text{ss}}$ unter Verwendung diverser Aktivitätsmodelle.*

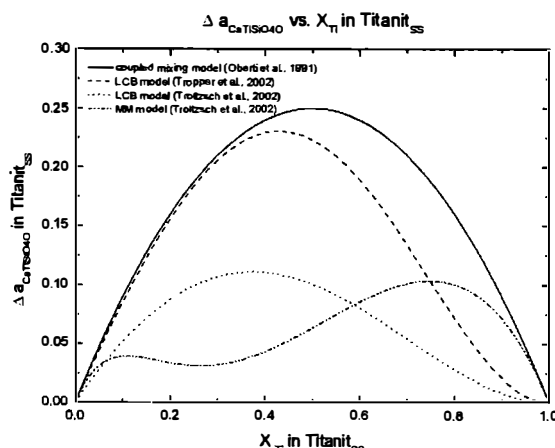


*Abb.04.:
Abweichung der verschiedenen idealen und realen Aktivitätsmodelle vom idealen molekularen Mischungsmodell (verläuft entlang der x-Achse bei $\Delta a_{\text{CaTiSiO}_4}$ in $\text{Titanit}_{\text{ss}} = 0$).*

Die größten Abweichungen vom molekularen Modell und die entsprechenden X_{Ti}-Gehalte sind in der nachfolgenden Tabelle aufgelistet:

	X _{Ti}	$\Delta a_{CaTiSiO_4}$ in Titanit _{ss}
Coupled mixing model (OBERTI et al., 1991)	0.500	0.2500
LCB model (TROPPER et al., 2002)	0.420	0.2304
LCB model (TROITZSCH et al., 2002)	0.380	0.0532
MM model (TROITZSCH et al., 2002)	0.740	0.1264

Die diversen Mischungsmodelle bilden die Grundlage zur Berechnung der Aktivität der Titanite in dieser Untersuchung. Allerdings beziehen sich diese Modelle auf das Fe- und OH-freie System. Somit spielt in diesen Modellen die Fe³⁺-Substitution, wie sie in natürlichen Titaniten auftritt, keine Rolle und wird nicht in die Berechnung des X_{Ti}-Gehaltes ($X_{Ti} = Ti/(Ti+Al^{[VI]})$) mit einbezogen. Auf der O1-Position tritt demnach ausschließlich die F-Substitution auf (O = 1-F). In natürlichen Titaniten erfolgt der Fe³⁺- und OH-Einbau entlang der gekoppelten Substitution $(Al, Fe^{3+}) + (F, OH) \leftrightarrow Ti + O$. Daher ergeben sich in natürlichen Titaniten für die oktaedrisch koordinierte und die O1-Position folgende Molenbrüche:

$$X_{Ti} = Ti/(Ti+Al^{[VI]}+Fe^{3+})$$

$$X_{Al} = 1-(X_{Ti}+X_{Fe^{3+}})$$

$$O \text{ auf O1} = 1-(F+OH)$$

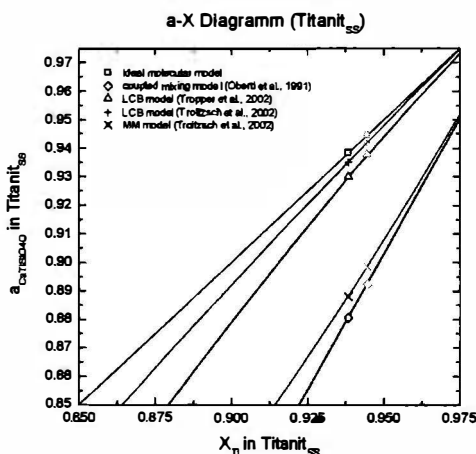


Abb.05.:

Ausschnitt aus dem a-X-Diagramm der Titanit_{ss} mit den aus den Proben berechneten minimalen X_{Ti}-Gehalt der Titanite in Abhängigkeit des Berechnungsmodus für X_{Ti}.
 $X_{Ti}=Ti/(Ti+Al^{[VI]}+Fe^{3+})$ (schwarze Punkte).
 $X_{Ti}=Ti/(Ti+Al^{[VI]})$ (graue Punkte).

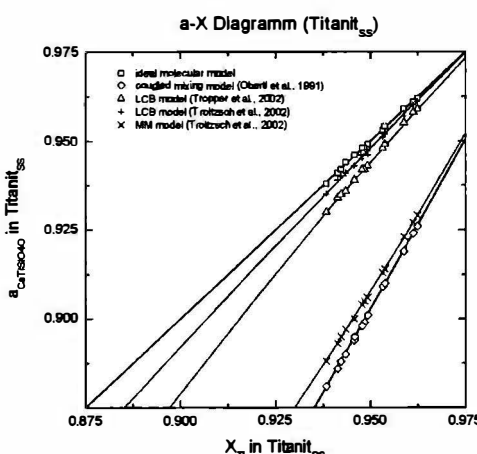


Abb.06.:

Ausschnitt aus dem a-X-Diagramm der Titanit_{ss} mit den aus den Proben berechneten X_{Ti}-Gehalten der Titanite.
Aktivitäten von $a_{CaTiSiO_4}$ in Titanit_{ss} unter Verwendung diverser Aktivitätsmodelle.

Um den Einfluß der verwendeten Molenbruchverrechnungsart (X_{Ti} ohne bzw. mit Fe^{3+}) darzustellen wurde jener Titanit mit dem höchsten und dem niedrigsten Al-Gehalt ($X_{Al} = 0.055$ und $X_{Al} = 0.031$) zum Vergleich der diversen Aktivitätsmodelle herangezogen. Durch das Ignorieren des Fe^{3+} -Anteils im Titanit wird die Verunreinigung relativ kleiner weshalb sich der X_{Ti} -Gehalt zu höheren Werten verschiebt (Abb. 05). Aufgrund des geringen Al- und Fe^{3+} -Einbaus ($\varnothing 0.041$ apfu Al, $\varnothing 0.008$ apfu Fe^{3+}) in den Titaniten aus den Proben handelt es sich um relativ reine Zusammensetzungen. Dies äußert sich auch in den X_{Ti} -Gehalten, welche einen durchschnittlichen Wert von 0.950 annehmen (Abb. 06).

Der Einfluß der idealen Titanit-Aktivität auf die Lage ausgewählter Reaktionskurven

Um den Einfluss des gewählten Titanit-Aktivitätsmodells, mit den daraus resultierenden diversen Aktivitäten, auf die Lage der Reaktionen im P-T Raum zu verdeutlichen, wurden folgende Modellreaktionen ausgewählt:

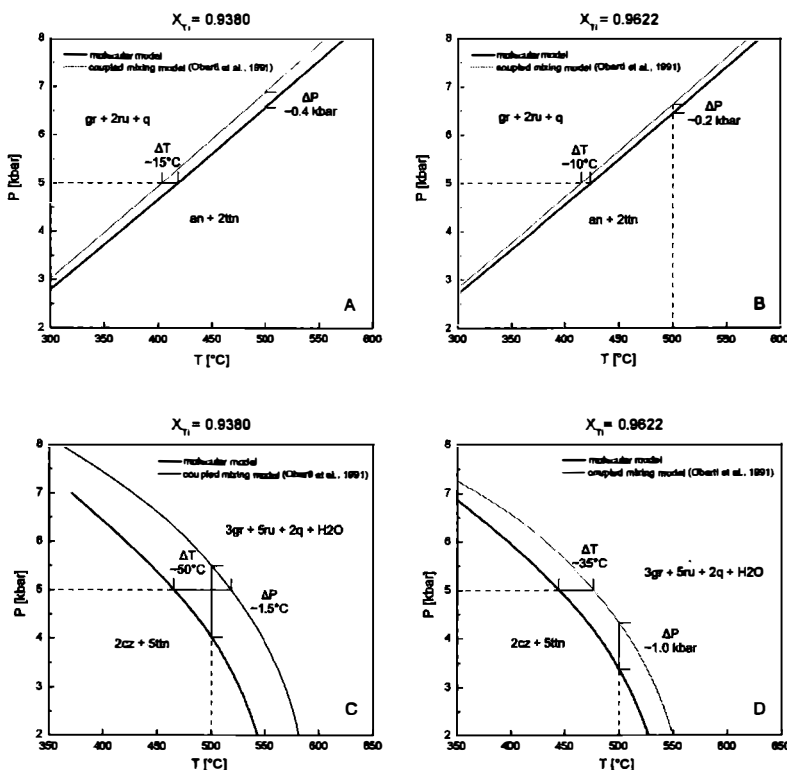
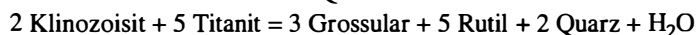


Abb.07.:

Lage ausgesuchter Reaktionen im P-T Raum in Abhängigkeit des gewählten Aktivitätsmodells.

Vergleich mit unterschiedlichen X_{Ti} -Gehalten.

Für die Berechnungen wurden jener Titanit mit dem höchsten und jener mit dem niedrigsten X_{Ti} herangezogen. Dabei wird deutlich, dass die dem molekularen Mischungsmodell zugrunde liegenden Reaktionskurven die P Untergrenze des Titanit-Stabilitätsfeldes markieren (Abb. 07). Dabei kommt es bei einem X_{Ti} von 0.9384 und einer Temperatur von 500°C zu einem Druckunterschied von ca. 0.4 kbar und bei 5 kbar zu einer Temperaturdifferenz von ca. 15°C (Abb. 07a). Die Reaktionskurven, welche mit einem X_{Ti} von 0.962 berechnet wurden, liegen näher beisammen, als jene mit einem kleineren X_{Ti} . Der Temperaturunterschied bei 5 kbar liegt bei ca. 10°C und die Druckdifferenz bei 500°C beträgt ca. 0.2 kbar (Abb. 07b). Um diesen Einfluss des gewählten Aktivitätsmodells auf die Lage der Reaktion im P - T Raum noch besser zu verdeutlichen, wurde eine Reaktion mit einem höheren Titanit-Koeffizienten gewählt (Abb. 08c, d). Bei einem Druck von 5 kbar und einem X_{Ti} von 0.938 bzw. 0.962 beträgt die Temperaturdifferenz ca. 50°C, bzw. 35°C und der entsprechende Druckunterschied bei 600°C liegt bei ca. 1.5 kbar, bzw. bei 1.0 kbar. Auch in dieser Abbildung wird wieder deutlich, dass die Reaktion berechnet mit dem molekularen Mischungsmodell die Untergrenze des Titanitstabilitätsfeldes markiert, und dass eine Verdünnung der Titanit-Komponente zu einer Stabilisierung des Minerals im P - T Raum führt.

Conclusio

Bei beiden Reaktionen fällt auf, dass die Kurven aus den zwei unterschiedlichen Aktivitätsmodellen mit einem höheren X_{Ti} also einer zunehmend „reineren“ Zusammensetzung des Titanits, konvergieren. Dies liegt daran, dass sich das gekoppelte Mischungsmodell in Richtung Endgliedzusammensetzung dem molekularen Modell sukzessive annähert (Abb. 08). Da die X_{Ti} in den Titaniten aus dem Sprontal Werte zwischen 0.938 und 0.962 annehmen, liegen die aus dem molekularen und gekoppelten Mischungsmodell berechneten Aktivitäten nahe aneinander. Allerdings zeigt diese Untersuchung, dass bereits diese geringfügigen Änderungen in den Titanit-Aktivitäten zu sichtbaren Verschiebungen der Reaktionskurven im P - T Raum führen. Daher sollte in Anbetracht der kontrastierenden bereits bestehenden Modelle die Berechnungen mit mehr als einem Aktivitätsmodell (ionisches Modell, reguläre Modelle) durchgeführt werden.

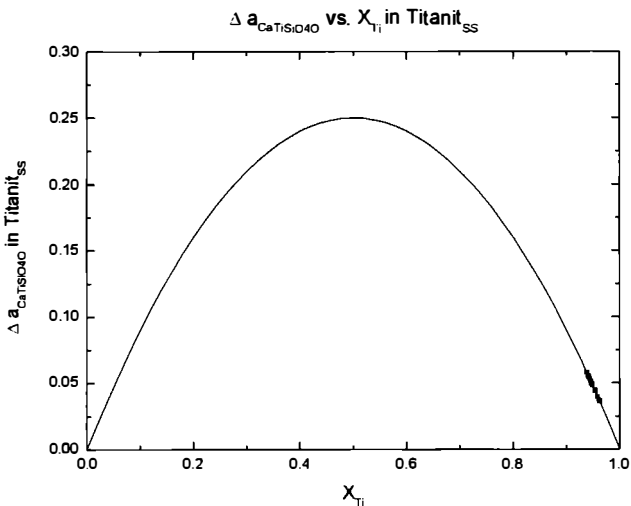


Abb.08.:
Abweichung des gekoppelten
Aktivitätsmodells nach OBERTI et al.
(1991) vom idealen molekularen
Mischungsmodell.

Literatur

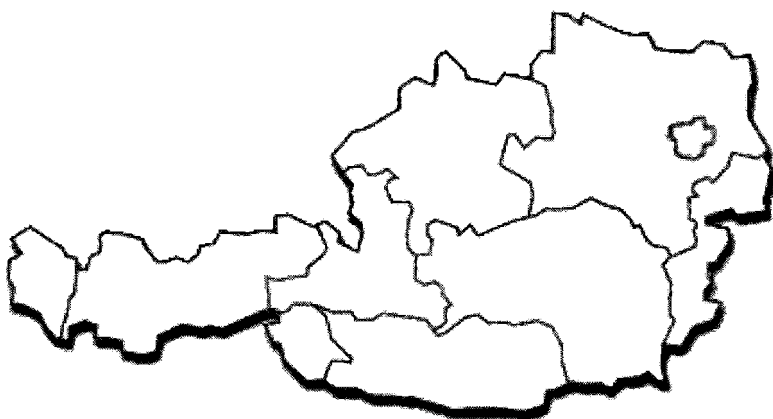
- DEER, W. A., HOWIE R. A. & ZUSSMAN J. (1992): An introduction to the rock-forming minerals, 2nd edition. - Pearson Education Limited, Harlow, Essex, England.
- ENAMI, M., SUZUKI, K., LIOU, J.G. & BIRD, D.K. (1993): Al-Fe³⁺ and F-OH substitutions in titanite and constraints on their P-T dependence. - Eur. J. Mineral. 5, 219-231
- HARLOV, D. et al. (2006): Formation of Al-rich titanite (CaTiSiO₄O - CaAlSiO₄OH) reaction rims on ilmenite in metamorphic rocks as a function of f_{H2O} and f_{O2}. - Lithos 88, 72-84.
- MANNING, C.E., BOHLEN, S.R. (1991): The reaction titanite+kyanite=anorthite+rutile and titanite-rutile barometry in eclogites. - Contributions to Mineralogy and Petrology 109, 1-9.
- OBERTI, R., SMITH, D.C., ROSSI, G., CAUCIA, F. (1991): The crystal chemistry of high-aluminum titanites. - European Journal of Mineralogy 3, 777-792.
- SPEAR, F.S. (1995): Metamorphic phase equilibria and pressure-temperature-time paths, 2nd printing. - BookCrafters, Inc., Chelsea, Michigan, USA.
- TRIBUS, M. (2009): Petrologische und thermobarometrische Untersuchungen des amphibolit/eklogitfaziellen eo-Alpinen Events in den Metabasiten des Texel Komplex. - Unveröffentlichte Diplomarbeit, Universität Innsbruck, 163 S.
- TROITZSCH, U. & ELLIS, D. J. (2002): Thermodynamic properties and stability of AlF-bearing titanite CaTiO₄ - Ca-AlFSiO₄. - Contrib. Mineral. Petrol. 142, 543-563
- TROPFER, P., MANNING, C. E. & ESSENE, E. J. (2002): The substitution of Al and F in titanite at high pressure and temperature: experimental constraints on phase relations and solid solution properties. - J. Petrol. 43, 1787-1814.

received: 26.06.2013.

accepted: 07.07.2013.

**DIPLOM / MASTERARBEITEN UND
DISSERTATIONEN
VON ÖSTERREICHISCHER UNIVERSITÄTEN**

**DIPLOMA / MASTER / PhD THESIS
OF AUSTRIAN UNIVERSITIES**



Liste der abgeschlossenen Arbeiten

Juli 2012 bis Juli 2013

Donjá Susanne Assbichler

„Eklogite des Tauernfensters und ihre Nebengesteine: Chemische Wechselwirkungen während der Metamorphose und Vergleich deer aufgezeichneten Metamorphosebedingungen“

Masterarbeit (Dezember 2012)

Institut für Erdwissenschaften

Bereich Mineralogie und Petrologie

Universität Graz

Supervisor: Alexander Proyer

Raphael Johannes Baumgartner

„Mineralogical and geochemical investigation of layered chromitites from the Bracco Gabbro Complex, Ligurian Ophiolite, Italy“

Masterarbeit (Oktober 2012)

Lehrstuhl Rohstoffmineralogie

Montanuniversität Leoben

Supervisor: Oskar A.R. Thalhammer

Udo Haefeker

„Raman-spektroskopische (Fe/Fe+Mg, CO₂, N₂) und strukturelle Untersuchungen an Mg-Fe-Cordieriten“

Dissertation (Mai 2013)

Institut für Mineralogie & Petrographie

Universität Innsbruck

Supervisor: Reinhart Kaindl

Thomas Leitner

„Gold in the historic copper deposits at Flatschach, Styria“

Masterarbeit (Oktober 2012)

Lehrstuhl Rohstoffmineralogie

Montanuniversität Leoben

Supervisor: Johann G. Raith

Magdalena Mandl

„Geochemical characteristics of garnets from Tanzanian kimberlites (Mwadui, Singida, Nyangwale and Galamba“

Masterarbeit (Februar 2013)

Institut für Erdwissenschaften

Bereich Mineralogie und Petrologie

Universität Graz

Supervisor: Christoph Hauzenberger

Prayath Nantasin

„Metamorphic evolution of the Thabsila metamorphic complex and the Sri Sawat contact aureole, Kanchanaburi Province“

Dissertation (März 2013)

Institut für Erdwissenschaften

Bereich Mineralogie und Petrologie

Universität Graz

Supervisor: Aberra Mogessie

Peter Onuk

„Petrology and mineralization of mafic-ultramafic rocks of the Las Aguilas-Las Pieras area, San Luis Province, Argentina“

Masterarbeit (August 2012)

Institut für Erdwissenschaften

Bereich Mineralogie und Petrologie

Universität Graz

Supervisor: Aberra Mogessie

Barbara Julia Puhr

„Metamorphic evolution and geochemistry of metacarbonate rocks of the Austroalpine Basement (Eastern Alps)“

Dissertation (Dezember 2012)

Institut für Erdwissenschaften

Bereich Mineralogie und Petrologie

Universität Graz

Supervisor: Georg Hoinkes

Daniela Schmidmair

„Thermische feuchteabhängige und strukturelle Untersuchungen an Kanemit“

Masterarbeit (Juli 2013)

Institut für Mineralogie & Petrographie

Universität Innsbruck

Supervisor: Volker Kahnenberg

VEREINSMITTEILUNGEN

TÄTIGKEITSBERICHT ÜBER DAS VEREINSJAHR 2012

1. Im Vereinsjahr 2012 fanden folgende Vorträge und Veranstaltungen statt:

(Zusammenstellung aller erdwissenschaftlich relevanten Vorträge im Rahmen von Vortragsveranstaltungsreihen der entsprechenden Institutionen an den universitären Standorten Graz, Innsbruck, Leoben, Salzburg und Wien)

Veranstaltungsort Wien

Mo 16. Jänner 2012: Volker Kahnenberg (Universität Innsbruck)

„*Polymorphie von kristallinen Festkörpern: Mineralogie trifft Pharmazie*“

Do 19. Jänner 2012: Angela Forchielli (Universität Wien)

„*The Chengjiang Fauna (SW China): overview and latest results from an Early Cambrian Burgess Shale-type fossil Lagerstätte*“

Do 19. Jänner 2012: Martin Schöpfer (Universität Wien)

„*Conceptual and mechanical models for evolution of the three-dimensional structure of fault zones*“

Mo 23. Jänner 2012: Falko Langenhorst (Bayreuth, Deutschland)

„*Microbes on the rocks*“

Do 8. März 2012: Alexander Nützel (Bayerische Staatssammlung für Paläontologie und Geologie)

„*Zwischen zwei Massenaussterben: Über die Evolution der Gastropoden in der Trias*“

Do 8. März 2012: Walter Kurz (Universität Graz)

„*Die tektonische Entwicklung der Ostalpen im Känozoikum: Störungen und die Exhumierung von Eklogiten*“

Do 15. März 2012: Gina Semprebon (Bay Path College, Massachusetts, USA)

„*Reconstructing ancient ecosystems by tracking dietary shifts in mammals*“

Do 15. März 2012: Greg Houseman (University of Leeds)

„*Collision and instability of the lithosphere and upper mantle beneath central and eastern Europe*“

Do 22. März 2012: Quinn Passey, Kevin Bohacs, Robert Klimentidis, William Esch, Somnath Sinha (ExxonMobil Upstream Research)

„My source rock is now my shale gas reservoir – geological and petrophysical characterization of organic-rich rocks“

Do 29. März 2012: Ulrike Exner (Universität Wien)

“Unravelling the evolution of deformation bands in the Matzen Reservoir from microstructural and stable isotope data”

Do 12. April 2012: Bernhard Grasemann (Universität Wien)

“Deformation mechanisms in continental low-angle normal faults”

Mo 16. April 2012: Richard Göd (Universität Wien)

„Lagerstätten des Lithiums - geologische, mineralogische und wirtschaftliche Aspekte“

Do 19. April 2012: Lukas Ackerman (Academy of Sciences of the Czech Republic)

“Upper mantle rocks from Kozakov and Horní Bory, Czech Republic: two distinct evolutions of the Bohemian Massif upper mantle”

Do 26. April 2012: Gabor Tari (OMV)

“Alpine tectonics of the broader Pannonian Basin: some new elements”

Do 3. Mai 2012: Franz Ottner (Wien)

„Am Anfang war der Wind, dann kam das Feuer – die Verknüpfung von Löss mit der Geschichte der Wiener Ziegel“

Do 10. Mai 2012: David Selby (University of Durham)

„Rhenium-osmium geochronology of sulphide mineralization: implications for ore system models“

Mo 21. Mai 2012: Festkolloquium „100 Jahre Paläobiologie an der Universität Wien“

Mo 21. Mai 2012: Christa Göpel (CNRS Paris)

„Meteorite – Zeugen frühen Sonnensystems“

Di 22. Mai 2012: Fritz F. Steininger (Eggenburg)

“Die Fossilienlagerstätte Grube Messel - Ein Fenster in die Evolution des Lebens vor 45 Millionen Jahren und das erste fast vollständig erhaltene Skelett eines Trockennasenaffen („Menschennasenaffen“) - „IDA“ (Darwinulus masillae)“

Do 24. Mai 2012: Florian Fußeis (Ruhr-Universität Bochum)

“3D characterization of porosity and its temporal changes in metamorphic rocks using synchrotron X-ray microtomography”

Do 31. Mai 2012: Joachim Reitner (Universität Göttingen)

“Resolving neoproterozoic early metazoa - assumptions and facts”

Mi 6. Juni 2012: Michel Cuney (Nancy, Frankreich)
„*Magma types and ore deposits with special reference to uranium and rare metal deposits*“

Do 18. Oktober 2012: Patrik Grunert (Graz)
„*IODP Expedition 339: Paleo-oceanographic and paleoclimatic significance of the Mediterranean outflow*“

Mi 24. Oktober 2012: Ralf Tappert (Institut für Mineralogie und Petrographie, Universität Innsbruck)
„*Diamanten und ihre Mineraleinschlüsse*“

Do 25. Oktober 2012: Robert Faber (Terramath Indonesia):
„*Animal Perception of Seismic Phonomena: Forschungs- und Medienkooperation RedBull MediaHouse – Boku/Terra Math Indonesia auf Nord Sumatra (Indonesien)*“

Mi 7. November 2012: Uwe Kolitsch (NHM Wien):
„*Seltene und vielfältige Sekundärminerale aus einer Wolfram-Lagerstätte in Frankreich*“ –
Mineralogische Untersuchungen, präsentiert anhand des neuen Rasterelektronenmikroskops“

Mi 14. November 2012: Christian Meyer (Naturhistorisches Museum Basel)
„*Im Westen nichts Neues Ein Blick auf die Trias der Westschweiz Sedimentologie und Palichnologie*“

Do 15. November 2012: Georg Dresen (GFZ Potsdam)
„*Erdbeben im Labor und im Gelände*“

So 18. November 2012: Ludovic Ferrière (Naturhistorisches Museum Wien)
„*What are meteorites ?*“

Mi 21. November 2012: Ludovic Ferrière (Naturhistorisches Museum Wien)
„*What do we do with our meteorite collection ?*“

Do 22. November 2012: Roman Aubrecht (Universität Bratislava)
„*Venezuelan sandstone caves: A new view on their genesis and speleothems*“

So 25. November 2012: Ludovic Ferrière (Naturhistorisches Museum Wien)
„*Meteorites and impacts on earth*“

Mo 26. November 2012: Urs Klötzli (Department für Lithosphärenforschung, Wien)
„*Absolute Altersbestimmung vom Einzelmineral zum Gestein*“

Di 27. November 2012: Jaroslaw Tyska (Akademie der Wissenschaften Krakow)
„*Modelling approach in understanding the foraminiferal morphogenesis*“

Mi 28. November 2012: Susan Ivy Ochs (ETH Zürich)
„*Dating landslides with cosmogenic nuclides*“

Mo 3. Dezember 2012: Ralf Tappert (Institut für Mineralogie und Petrographie, Universität Innsbruck)
„*The formation of diamonds in the Earth's mantle. What is the role of plate tectonics?*“

Di 4. Dezember 2012: Phillip Mitteroecker (Universität Wien)
„*The evolution of human cranial development: A morphometric approach*“

Do 6. Dezember 2012: Josep Anton Munoz de la Fuente (Universitat de Barcelona)
„*Structural styles resulting from the tectonic inversion of a rift to passive margin system: the Pyrenean orogen*“

Di 11. Dezember 2012: Michal Kováč (Universität Bratislava)
„*Neogene Geodynamics and Paleogeography of the Alpine - Carpathian - Pannonian Junction*“

Mi 12. Dezember 2012: Alfred Schreilechner (Mariapfarr)
„*Faszination Mineralien: Edelsteine im Schatten der Siebentausender Pakistans*“

So 13. Dezember 2012: Benjamin Sames (Universität Wien)
„*(Bio)-Stratigraphie in der nichtmarinen Unterkreide – Aufbrechen etablierter Vorstellungen*“

Veranstaltungsort Graz

Di 6. März 2012: Maria Perraki (Athen)
„*Raman spectroscopy: a useful tool in the study of mineral phases in HP/UHP rocks*“

Di 13. März 2012: Antonino Briguglio (Universität Wien)
„*Berechnete Röntgenstrahl-Tomographie: Neue Anwendungen für Paläontologen*“

Di 27. März 2012: Ralf Schuster (Wien)
„*Zur tektonischen und lithographischen Gliederung des ostalpinen Kristallins und dessen Fortsetzung gegen Osten*“

Di 8. Mai 2012: Richard Göd (Universität Wien)
„*Lagerstätten des Lithiums - geologische, mineralische und wirtschaftliche Aspekte*“

Di 13. November 2012: Ralf Brauchler (Geological Institute-Engineering Geology, ETH Zürich)
„*High resolution aquifer characterization based on hydraulic tomography inversion techniques: Numerical case studies and field examples*“

Di 20. November 2012: Urs Klötzli (Department für Lithosphärenforschung, Wien)
„*Absolute Altersbestimmung vom Einzelmineral zum Gestein*“

Di 27. November 2012: Deta Gasser (Department of Geosciences, Universität Oslo)
„*Migmatite, Mylonite und Moschusochsen: Eindrücke aus den Kaledoniden Ost-Grönlands*“

Di 4. Dezember 2012: Ralf Tappert (Institut für Mineralogie und Petrographie, Innsbruck)
"The formation of diamonds in the Earth's mantle. What is the role of plate tectonics?"

Veranstaltungsort Innsbruck

Do 12. Jänner 2012: Thomas Scheiber (Geologisches Institut, Universität Bern)
"Bildung von großmaßstäblichen Kristallindecken in einer Kollisionszone - Beispiele aus der Briançonnais Zone der Schweiz"

Do 26. Jänner 2012: Walter Kurz (Institut für Erdwissenschaften, Universität Graz):
"Hot Spots in den zentralen Ostalpen - Neue Hinweise zur tektonischen Entwicklung der Ostalpen im Miozän"

Do 8. März 2012: Christian Köberl (Department für Lithosphärenforschung der Universität Wien und Naturhistorisches Museum, Wien)
"Der El'gygytgyn Meteoritenkrater: Ein ICDP-Bohrprojekt in der russischen Arktis"

Do 15. März 2012: Erich Draganits (Department für Geodynamik und Sedimentologie, Universität Wien)
"Der Neusiedlersee: Entstehung, Seespiegelschwankungen und hydrologische Zusammenhänge"

Do 22. März 2012: Frank Melcher (Bundesanstalt für Geowissenschaften und Rohstoffe, Hannover)
"Mineralogie und Mineralchemie von Ta-Sn-W Lagerstätten in Afrika: Nachweis der Herkunft von Columbit-Tantalit-Erzen mit der Fingerprinting Methode"

Do 29. März 2012: Claudia Dojen (Abteilung für Geologie, Mineralogie, Paläontologie und Montanwesen, Landesmuseum Kärnten, Klagenfurt):
"Small and almost everywhere: Devonische Ostrakoden aus aller Welt und ihr Nutzen in der Biostratigraphie, Paläogeographie und Paläökologie"

Do 19. April 2012: Thomas Nagler / Helmut Rott (Enveo IT GmbH, Innsbruck / Institut für Meteorologie, Universität Innsbruck)
"Überwachung von Massenbewegungen mit satellitengetragenen Radarsensoren"

Do 3. Mai 2012: Thomas Scheiber (Geologisches Institut, Universität Bern)
"Bildung von großmaßstäblichen Kristallindecken in einer Kollisionszone - Beispiele aus der Briançonnais Zone der Schweiz"

Do 10. Mai 2012: Florian Fusseis (Institut für Geologie, Mineralogie und Geophysik, Ruhr-Universität Bochum)
"Die drei- und vierdimensionale Charakterisierung von Porosität in Gesteinen mittels Synchrotron Röntgentomographie, mit Fallbeispielen aus der metamorphen Geologie"

Do 24. Mai 2012: Magdalena Rogger (Institut für Wasserbau und Ingenieurhydrologie, TU Wien)
„*Verwendung geophysikalischer Daten für die hydrologische Abflussmodellierung am Beispiel Krumgampental (Ötztaler Alpen)*“

Do 31. Mai 2012: David Flöss (Faculty of Geosciences and Environment, Université de Lausanne)
“*Contact metamorphism and emplacement of the Western Adamello pluton*”

Do 18. Oktober 2012: Istvan Kovac (Eötvös Loránd Geophysical Institute of Hungary, Budapest)
„*Water in the shallow upper mantle and its geodynamic implications*“

Do 25. Oktober 2012: Ross Angel (Crystallography Laboratory, Virginia Tech, Blacksburg, USA, c/o Dipartimento di Science, Università degli studi di Padova, Italien)
“*Why are feldspars so anisotropic ?*”

Do 8. November 2012: Andrew Kos (Institut für Geotechnik, ETH Zürich, Schweiz)
“*The application of combined portable radar interferometry and laser scanning on rockslopes*”

Do 22. November 2012: Michael Sarnthein (Institut für Geowissenschaften, Universität Kiel und Institut für Geologie und Paläontologie, Universität Innsbruck)
„*Sustainable Earth*“: *Kohlenstoff-Aufnahme ozeanischer Tiefenwässer in Hoch- und Spätglazial - Hinweise aus 14C-Altern*“

Do 29. November 2012: James Connolly (Institut für Geochemie und Petrologie, ETH Zürich)
“*The mythology of metamorphic fluid flow*”

Do 6. Dezember 2012: Neven Gergiev (Department of Geology, Sofia University “St. Kliment Ohridski“ and c/o Institut für Geologie und Paläontologie, Universität Innsbruck)
“*Origin of the Rhodopes: permanent vs. change of the subduction polarity*”

Do 13. Dezember 2012: Jörg Hayer (Solexperts AG - Swiss Precision Geomonitoring, Mönchaltorf, Schweiz)
“*Hydrogeologische und geotechnische in-situ Bohrloch-Feldversuche im Locker- und Festgestein*”

Veranstaltungsort Leoben

Mi., 14./21./28. März 2012: Artur Deditius (Graz)
“*Nanogeoscience in ore deposits*”

Di 5. Juni 2012: Michel Cuney (Nancy, Frankreich)
“*Magma types and ore deposits with special reference to uranium and rare metal deposits*”

Mi 5. Dezember 2012: Ralf Tappert (Institut für Mineralogie und Petrographie, Innsbruck)
“*The formation of diamonds in the Earth's mantle. What is the role of plate tectonics?*”

Veranstaltungsort Salzburg

Di, 6. März 2012: Franz Neubauer (Universität Salzburg)

„*China auf dem Weg zur wissenschaftlichen Weltmacht ? – Persönliche Eindrücke*“

Di, 13. März 2012: Harry Fritz (Universität Graz):

„*Making Gondwana – Gebirgsbildungstypen der ostafrikanischen Orogenesen zwischen Ägypten und Madagaskar*“

Di, 29. Mai 2012: Hans Genser (Universität Salzburg)

„*Postvariszischer Magmatismus längs der Periadrischen Störung (Karawanken)*“

Di, 22. Mai 2012: Jörg Robl (Universität Graz / Universität Salzburg)

„*Das Entwässerungssystem in alpinotypen Gebirgen: Entwicklung und Auswirkung auf die Gebirgsbildung*“

Di, 6. Juni 2012: Björn Berning (Landesmuseum Oberösterreich Linz)

„*Bryozoen - Biologie und Paläontologie von Superorganismen*“

Di 20. November 2012: Sha Wali Faryad (Prag)

„*Variscan suture(s) and exhumation of HP-UHPM rocks in the Bohemian Massif*“

Di 18. Dezember 2012: Johannes Horner (Salzburg/Bergheim)

„*Die geotechnische Bohrkernaufnahme bei großen Bergbauprojekten – eine Herausforderung*“

2. Tagungen

Im Vereinsjahr 2012 fand die "First European Mineralogical Conference" - EMC²⁰¹² in Frankfurt statt (2. - 6. September 2012); veranstaltet wurde diese von den mineralogischen Gesellschaften aus Deutschland, Finnland, Frankreich, Großbritannien und Irland, Italien, Österreich, Polen, Rußland, Schweiz sowie Spanien und den lokalen Organisatoren Heidi Höfer und Gerhard Brey. Anlässlich dieser Tagung prämierte die ÖMG fünf Poster junger Wissenschaftler. Die Preisträger sind:

D. Aßbichler (KFU Graz, Institut für Erdwissenschaften):

„*Magnesite-bearing eclogite from the TauernWindow/Eastern Alps*“

M. Krismer (Universität Innsbruck, Institut für Mineralogie und Petrographie):

„*Polymetallic ores of the prehistoric copper mining area "Mauken Valley" (Brixlegg-Radfeld, Austria) as a possible source of Bronze Age Co-Ni bearing "fahlore-copper" metal artefacts in the Eastern Alps and the German Alpine Foreland*“

C. Lenz (Universität Wien, Institut für Mineralogie und Kristallographie):

„*A Nd³⁺ luminescence spectroscopic study on the structural disorder of monazite-(Ce)*“

B. Purgstaller (TU Graz, Institut für Angewandte Geowissenschaften):
„Uptake of CO₂ and precipitation of CaCO₃ in alkaline solutions - Mechanisms and Rates“

K.S. Scheidl (Universität Wien, Department für Lithosphärenforschung):
„Chemically induced fracturing in alkali feldspar“

3. Exkursionen

Im Vereinsjahr 2012 fanden keine Exkursionen statt

4. Vorstandssitzungen und Jahreshauptversammlung

Die Abwicklung der geschäftlichen Angelegenheiten erfolgte in zwei Vorstandssitzungen (Wien, 16. Jänner 2012 und Graz, 11. Juni 2012).

Die ordentliche Jahreshauptversammlung fand am 16. Jänner 2012 statt,

5. Der Vereinsvorstand

Bei der Jahreshauptversammlung am 16. Jänner 2012 wurde der Vorstand für das Vereinsjahr 2012 gewählt und folgende Ämterverteilung vorgenommen:

Präsident:	Prof. Dr. Volker Kahlenberg, Innsbruck
Vize-Präsident:	Prof. Mag. Dr. Aberra Mogessie, Graz
Kassier:	Prof. Dr. Christian L. Lengauer, Wien
Schriftführung:	Prof. Dr. Herta Effenberger
Vorstandsmitglieder:	Prof. Mag. Dr. Rainer Abart, Wien Mag. Dr. Hans-Peter Bojar, Graz Prof. Dipl.-Ing. Dr. Martin Dietzel, Graz Prof. Dr. Richard Göd, Wien Doz. Dipl.-Min. Dr. Uwe Kolitsch, Wien Prof. Dr. Friedrich Koller, Wien Msc. Helmut Pristacz, Jr., Wien Prof. Mag. Dr. Günther J. Redhammer, Salzburg Dr. Albert Schedl, Wien Mag. Andreas Thinschmidt, Krumbau am Kamp Prof. Dr. Ronald J. Bakker, Leoben Doz. Mag. Dr. Reinhard Kaindl, Leoben Dipl.-Ing. Dr. Roland Nilica, Leoben
Beirat:	Prof. Dr. Friedrich Koller, Wien Prof. Dr. Richard Tessadri, Innsbruck Prof. Mag. Dr. Eugen Libowitzky, Wien Prof. Mag. DR. Manfred Wildner, Wien
Schriftleitung:	Prof. Dr. Friedrich Koller, Wien Prof. Dr. Richard Tessadri, Innsbruck Prof. Mag. Dr. Eugen Libowitzky, Wien Prof. Mag. DR. Manfred Wildner, Wien
Rechnungsprüfer:	Prof. Dr. Friedrich Koller, Wien Prof. Dr. Richard Tessadri, Innsbruck Prof. Mag. Dr. Eugen Libowitzky, Wien Prof. Mag. DR. Manfred Wildner, Wien

Mitgliedsbeiträge:

Die Jahreshauptversammlung beschloß die Höhe der Mitgliedsbeiträge für 2013 mit € 30 für ordentliche Mitglieder und € 10 für studentische Mitglieder unverändert zu belassen. Insbesondere sei auf Artikel 5.6 der Satzung der ÖMG hingewiesen der vorsieht, daß fördernde Mitglieder der Gesellschaft ein Vielfaches des Jahresbeitrages entrichten.

Bankverbindung: Österreichische Postsparkasse, BLZ 60 000,
Kontonummer 7.807.220
IBAN = AT31 6000 0000 0780 7220, BIC = OPSKATWW

6. Schriftwerk

Band 158 der „Mitteilungen der Österreichischen Mineralogischen Gesellschaft“ wurde mit der Aussendung des Herbstprogramms an die Mitglieder versendet. Die Aussendung des Programms der ÖMG erfolgte (gemeinsam mit den Programmen der ÖGG, ÖPG und ÖVH als GEOPOST mittels e-mail (bei nicht bekannter e-mail-Adresse in gedruckter Form).

7. Ehrungen

Herr Dr. Walter Postl wurde zum Ehrenmitglied ernannt. Die Urkunde wird während der diesjährigen Tagung der ÖMG MinPet2013 (19.-23. September 2012) in Graz überreicht werden.

8. Mitgliederbewegung

Mitgliederstand zum 16.01.2012:

Mitglieder	272
Verstorben	1
Beigetreten	4
Ausgetreten	8
Ausgeschlossen	11

Ehrenpräsident:

Josef Zemann, A

† Friedrich Becke, A
† Josef Emanuel Hibsch, A
† Gustav Tschermak, A

Ehrenmitglieder:

Gerhard Niedermayr, A
Walter Postl, A
Anton Preisinger, A
Ekkehart Tillmanns, A
Josef Zemann, A

† Franz Angel, A
† Karl Franz Johann Chudoba, A
† Eberhard Clar, A
† Georg Gasser, A
† Viktor Mordechai Goldschmidt, D
† Haymo Heritsch, A
† Emilie Jäger, CH
† Hans Johann Ritter von Karabacek, A
† Alois Kieslinger, A
† Rudolf Koechlin, A
† Karl Kontrus, A
† Gero Kurat, A
† Fritz-Henning Emil Paul Laves, D
† Adolf Lechner, A
† Heinrich Hermann Meixner, A
† Ernst Niggli, CH
† Grigiriev Dimitry Pavlovic, RUS
† Walter Emil Petraschek, A
† Percy Dudgeon Quensel, S
† Otto Rotky, A
† Erich Schroll, A
† Herbert Schuhmann, D
† Vladimir Stephanovich Sololev, RUS
† Herbert Strunz, D
† Eugen Friedrich Stumpf, A
† Hermann Julius Tertsch, A
† Moklós Vendel, H
† Isidor Weinberger, A
† Hans Wieseneder A

Träger der Friedrich Becke-Medaille:

Petr Cerny, CDN
Dimitri P. Grigoriew, RUS
Wilhelm Heinrich, D
Klaus Langer, D
Dimitry Pushcharovsky, RUS
George R. Rossman, USA
Friedrich Seifert, D
Heinrich Waenke, D
Hans Wondratschek, D

† Helge Götrik Backlung, EST
† Carl Wilhelm Erich Correns, D
† Wolf v. Engelhardt, D
† Pentti Eelis Eskola, FIN

† Michael Fleischer, USA
† Clifford Frondel, USA
† Heinz Jagodzinski, D
† Felix Karl Ludwig Machatschki, A
† Adolf Papst, USA
† Paul Georg Karl Ramdohr, D
† Bruno Sander, A
† Waldemar Theodore Schaller, USA
† Karl Hermann Scheumann, D
† Werner Schreyer, D
† William Hodge Taylor, USA
† Herman Julius Tertsch, A
† Volkmar Trommsdorff, CH
† Helmut Gustav Franz Winkler, D

Felix-Machatschki-Preis:

Rainer Abart, A
Robert Krickl, A
Hannes Krüger, D
Ronald Miletich, A
Günther Redhammer, A
Peter Tropper, A

Mitglieder auf Lebenszeit:

W. Hollender, A
F. Marsch, A

Schriftentausch:

Biblioteka Główna AGH, Krakau, PL
Deutsche Nationalbibliothek in Leipzig, Ref. Auslandserwerbung, Leipzig, D
Exchange & Gifts, U. S. Geological Survey Library, Reston, Virginia, USA
Geologische Bundesanstalt, Bibliothek, Wien, A
Geozentrum Hannover - BGR/LBEG/GGA, Bibliothek, Hannover, D
Haus der Natur, Salzburg, A
Mineralogical Society of Finland, Helsinki, FIN
Nationale Natuurhistorisch Museum, Leiden, B
Natural History Museum, Dept. of Library and Inf. Services, London, GB
Naturwissenschaftlicher Verein f. Kärnten, Klagenfurt, A
NÖ Landesbibliothek, St. Pölten, A
Österreichische Geologische Gesellschaft, Wien, A
Universalmuseum Joanneum, Abt. f. Mineralogie, Graz, A
Universitätsbibliothek u. Techn. Informationsbibliothek, Hannover, D
Università di Bologna, Dipartimento di Scienze Della Terra, Bologna, I

Der Dank für Spenden ergeht an folgende Mitglieder:

Anton Beran, Michael Bergmair, Herta Effenberger, Eleonore Franz, Richard Göd, Michael Götzinger, Ewald Haidl, Friedrich Koller, Michael Kozlik, Gerhard Niedermayr, Wilhelm Niemetz, Anton Rauscher, Richard Tessadri, Ekkehart Tillmanns und Hans Wondratschek, sowie an die Firmen: Uni-Credit Bank Austria,-Graz, Tyrolit, Zeiss, Swarovski, Bartelt, Bruker, Jeol, Agilent, Incoatec, RHI, Fei Company und Stoe.

Wien, 18. 1. 2013

H. Effenberger
(Schriftführung)

Autorenhinweise

MITTEILUNGEN DER ÖSTERREICHISCHEN MINERALOGISCHEN GESELLSCHAFT

Manuskripte können via e-mail unter folgenden Adressen eingereicht werden:

Friedrich.Koller@univie.ac.at

(Department of Lithospheric Research, Universität Wien, Althanstr. 14. A-1090 Wien)

Peter.Tropper@uibk.ac.at

(Institut für Mineralogie und Petrographie, Universität Innsbruck, Innrain 52, A-6020 Innsbruck)

Texte, Abbildungen und Tabellen müssen getrennt gespeichert sein (Texte ausschließlich im WORD-Format, einfache Formatierung (linksbündig/Flattersatz), bevorzugter Font: Times 12, Abbildungen und Tabellen ausschließlich als hochauflöste JPG-, EPS-, TIFF- oder PDF-Dateien).

Zitierungen von Autoren im Text (Beispiel):

,.....(ALEKSANDROV et al., 1985).....“

Zitierungen von Autoren bei der Literaturzusammenstellung (Beispiel):

ALEKSANDROV, I. V., KRASOV, A. M. & KOCHNOVA, L. N. (1985): The effects of potassium, sodium and fluorine on rock-forming mineral assemblages and the formation of tantaloniobate mineralization in rare-metal granite pegmatites. - Geochem. Int., 22, 85-94.

Abgabetermin für eingereichte Arbeiten ist Ende Mai des jeweiligen Jahres.

Bei eingereichten Arbeiten in den Kategorien Originalarbeiten - Vorträge - Exkursionen werden generell 50 Sonderdrucke kostenlos hergestellt. Andere oder zusätzliche Sonderdrucke von Arbeiten, sowie Abbildungen in Farbe sind explizit zu bestellen und werden in Rechnung gestellt.

Zuständig für Kommunikation, Layout, Druck: **Richard.Tessadri@uibk.ac.at**

Die Zeitschrift erscheint einmal jährlich mit Ausgabe September/Oktobe.

Publikationen in den Kategorien Originalarbeiten - Vorträge - Exkursionen sind ab Band 142 (1997) auch als PDFs auf der MG-Homepage veröffentlicht:

**<http://www.univie.ac.at/Mineralogie/Oemg.htm>
[<http://www.uibk.ac.at/mineralogie/oemg/>]**



D2 PHASER

- Brings the XRD to your samples

- World's fastest tabletop X-ray diffraction
- LYNXEYE™ integrated PC and cooling unit
- "All-in-One" Solution for Phase Analysis
- Phase ID, Quantification and Degree of Crystallinity
- Crystal Structures, Crystallite Size & Strain

think forward

XRD

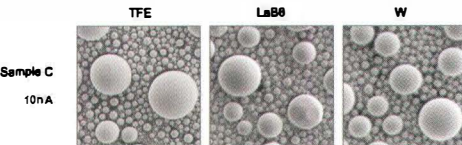
Your Partner In High Performance Analytics...

Electron microscope with:

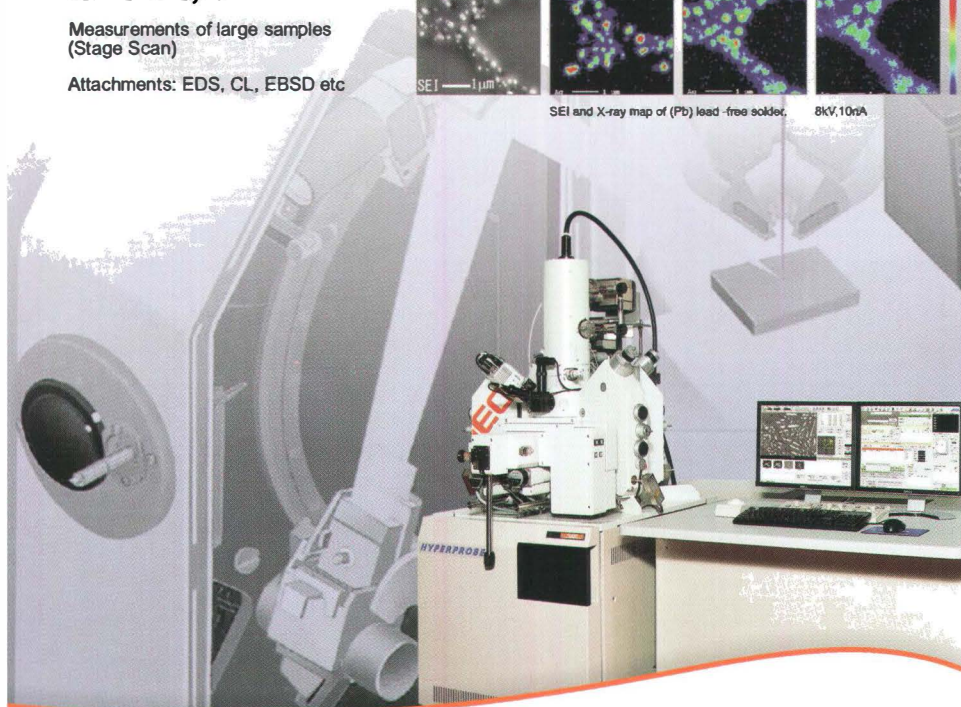
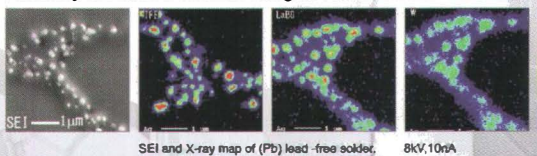
- Extreme high probe current stability
- Possibility of very high probe current
- Analysis of main and trace elements (down to 20ppm)
- Automatic Analysis

Measurements of large samples (Stage Scan)

Attachments: EDS, CL, EBSD etc



Extremely Small Probe Diameter at higher Probe Currents JXA-8530F



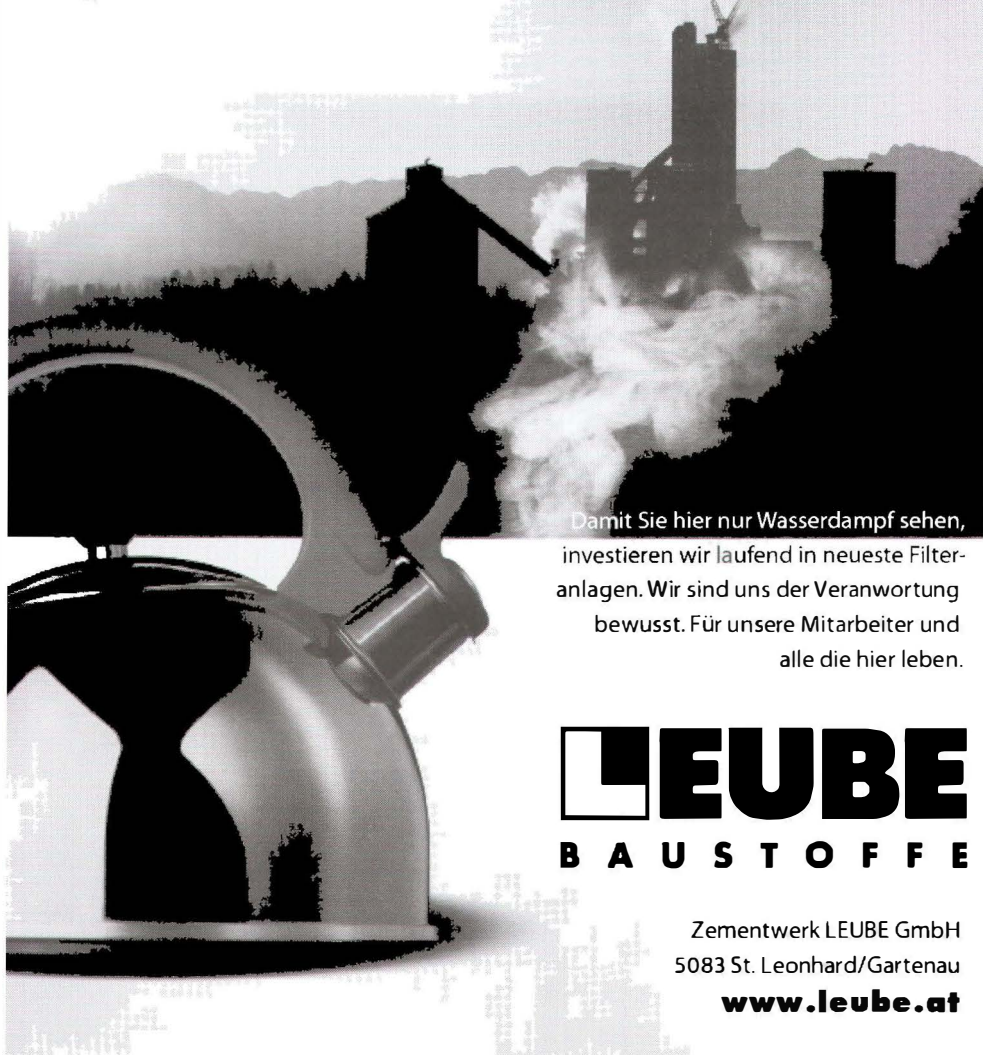
JEOL

Global Solutions Provider for Advanced Technology

www.jeol.de

JEOL (Germany) GmbH Oskar-v.-Miller-Straße 1A D-85386 Eching
Tel.: +49 (0)8165 77-346 · Fax: +49 (0)8165 77-512 · E-Mail: sales@jeol.de

WASSERDAMPF



Damit Sie hier nur Wasserdampf sehen,
investieren wir laufend in neueste Filter-
anlagen. Wir sind uns der Verantwortung
bewusst. Für unsere Mitarbeiter und
alle die hier leben.

LEUBE
B A U S T O F F E

Zementwerk LEUBE GmbH
5083 St. Leonhard/Gartenau
www.leube.at



Die BXiS Serie

Aufrechte Mikroskope zur Materialforschung und Qualitätsprüfung.

BXFM – Das flexible Forschungs- und Prüfungsmikroskop

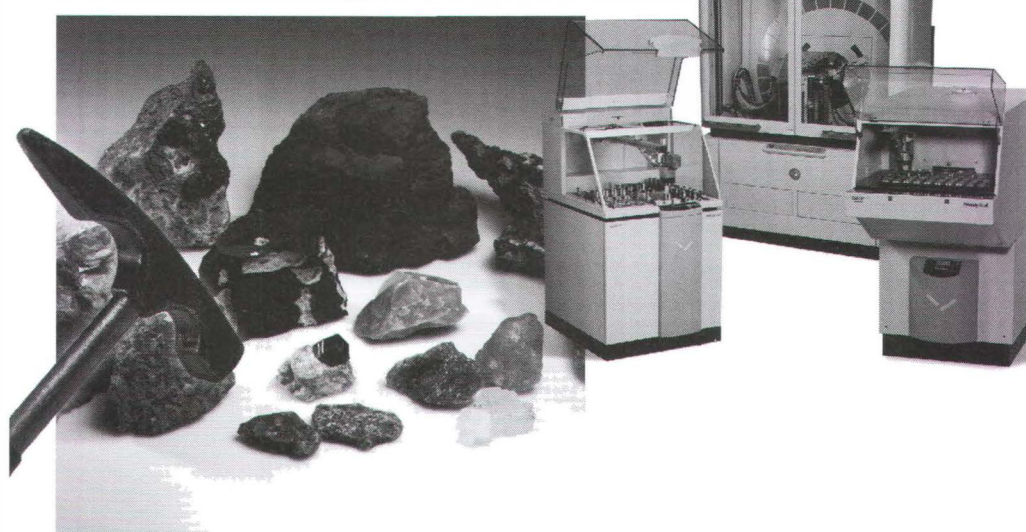
BX41M – Das lichtreflektierende aufrechte Mikroskop

BX51/BX51M – Das aufrechte Forschungs- und Prüfungsmikroskop

BX61 – Das motorisierte aufrechte Mikroskop

Für mehr Informationen besuchen Sie www.olympus-ims.com

Most advanced and versatile tools for mineralogical analysis



Axios^{MAX}-Minerals: offers a dedicated solution to the industry and includes a complete set of traceable standards.

CubiX3 Minerals: most accurate and fastest diffractometer for production and process control

Empyrean, the multipurpose X-ray diffractometer for phase identification and quantification

WROXI: a set of synthetic standards for fused beads major and minor elemental analysis

Pro-Trace: reliable trace element analysis in mineral beneficiation

HighScore Plus: software for analysis of crystalline phase composition



PANalytical B.V. - Branch Austria
Lemböckgasse 63
1230 Wien
www.panalytical.com
info@panalytical.com

The Analytical X-ray Company

 **PANalytical**

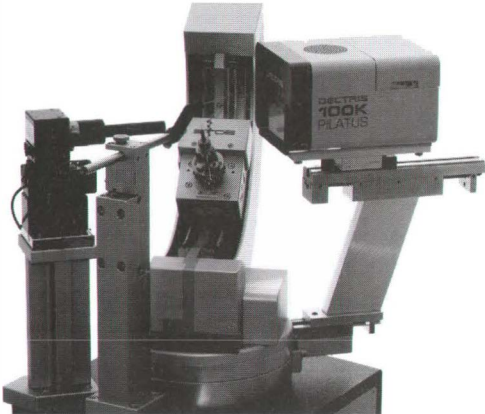


RHI: Ein Weltmarktführer in der Feuerfesttechnologie

Wir sind seit über 175 Jahren einer der führenden Hersteller von keramischen Feuerfestprodukten für industrielle Hochtemperaturprozesse.

Weltweit schätzen und vertrauen führende Stahl-, Glas-, Zement-, und Nichteisenmetalle-Produzenten auf die Qualität der Produkte und Serviceleistungen von RHI.

www.rhi-ag.com EXCELLENCE
IN REFRACTORIES **RHI**



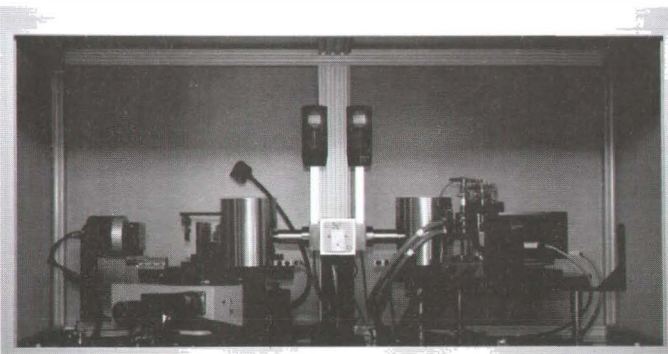
STOE STADI VARI PILATUS

single crystal diffractometer

- Four circle goniometer, open Eulerian cradle
- Ultra fast and sensitive Pixeldetectors Pilatus 100K und 300K
- Various sources possible:
standard sealed tube, Microfocus BDS,
- Fully integrated in the well known STOE X-Area Software

STOE STADI P powder diffractometer

- Pure $K\alpha 1$ radiation using Fe, Co, Cu, Mo **AND Ag** radiation
- **Ag RADIATION IDEAL FOR PDF INVESTIGATIONS**
- Transmission / Debye-Scherrer or Bragg-Brentano mode
- Various high- / low temperature systems and sample changers
- High throughput and combinatorial analysis
- Scintillation counter, position sensitive and imaging plate detectors, MYTHEN 1K strip detector for ultra high resolution



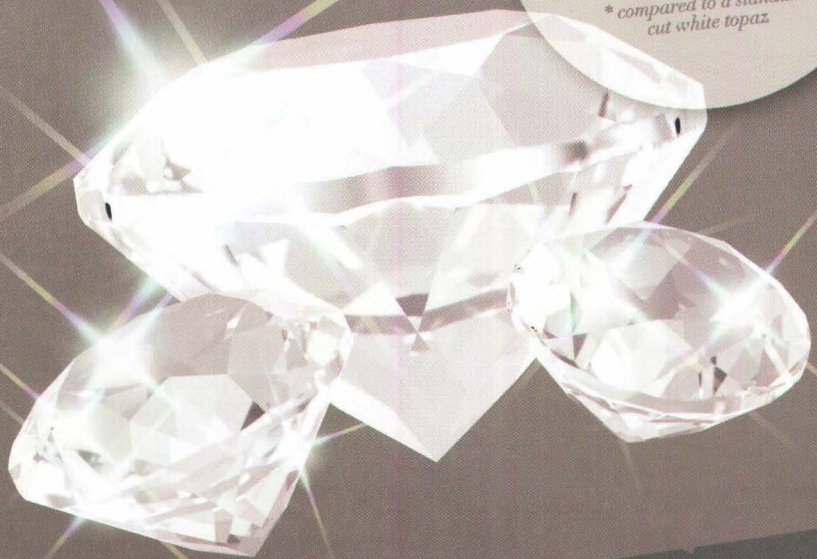
STOE & Cie GmbH P.O.Box 101302 D-64213 Darmstadt
Phone: (+49) 6151 / 98870 Fax: (+49) 6151 / 988788
E-mail: stoe@stoe.com Homepage: <http://www.stoe.com>

SWAROVSKI GEMS™

Swarovski GENUINE TOPAZ

+130%
*more brilliance**

* compared to a standard
cut white topaz



DISCOVER SWAROVSKI GEMS™ Interactive Contents.
Download the free DISCOVER SWAROVSKI GEMS™ app at the Apple app store –
Scan the image – Discover more

WWW.SWAROVSKI-GEMS.COM



Ein Unternehmen der SWAROVSKI Gruppe

TYROLIT